ANALYTICA CHIMICA ACTA

International monthly devoted to all branches of analytical chemistry
Revue mensuelle internationale consacrée à tous les domaines de la chimie analytique
Internationale Monatsschrift fur alle Gebiete der analytischen Chemie

ELSEVIER SCIENTIFIC PUBLISHING COMPANY

AMSTERDAM

Anal. Chim. Acta, Vol. 78, No. 2, 241–329, September 1975

Published monthly

Completing Volume 78

Publication Schedule for 1975

Vol. **74,** No. **1**	January 1975	
Vol. **74,** No. **2**	February 1975	**(completing Vol. 74)**
Vol. **75,** No. **1**	March 1975	
Vol. **75,** No. **2**	April 1975	**(completing Vol. 75)**
Vol. **76,** No. **1**	May 1975	
Vol. **76,** No. **2**	June 1975	**(completing Vol. 76)**
Vol. **77**	July 1975	**(complete in one issue)**
Vol. **78,** No. **1**	August 1975	
Vol. **78,** No. **2**	September 1975	**(completing Vol. 78)**
Vol. **79**	October 1975	**(complete in one issue)**
Vol. **80,** No. **1**	November 1975	
Vol. **80,** No. **2**	December 1975	**(completing Vol. 80)**

Subscription price for 1975 (covering Vols. 74–79): Dfl. 570.00 plus Dfl. 54.00 postage; US$ 265.53 inclusive of postage. Subscribers in the U.S.A. and Canada receive their copies by airmail. Additional charges for airmail to other countries are available on request. For advertising rates apply to the publishers.

Subscriptions should be sent to:
Elsevier Scientific Publishing Company, P.O. Box 211, Amsterdam, The Netherlands.

GENERAL INFORMATION

Languages

Papers will be published in English, French or German.

Detailed information

Authors should consult Vol. 73, p. 435 for detailed instructions. Reprints of this information are obtainable from Dr. MacDonald or from: Elsevier Editorial Services Ltd., Mayfield House, 256 Banbury Road, Oxford (Great Britain).

Submission of papers

Papers should be sent to:

PROF. PHILIP W. WEST,
Coates Chemical Laboratories,
College of Chemistry and Physics,
Louisiana State University,
Baton Rouge 3,
La. 70803 (U.S.A.)

or to:

DR. A. M. G. MACDONALD,
Department of Chemistry,
The University,
P.O. Box 363
Birmingham B15 2TT (Great Britain)

Reprints

Fifty reprints will be supplied free of charge. Additional reprints (minimum 100) can be ordered at quoted prices. They must be ordered on order forms which are sent together with the proofs.

PRINTED IN THE NETHERLANDS

Medicinal Chemistry IV

Proceedings of th 4th International Symposium on Medicinal Chemistry, Noordwijkerhout, The Netherlands, September 9-13, 1974

edited by **J. MAAS,** Gist Brocades, Haarlem, The Netherlands

1974. 384 pages. US $35.95 / Dfl. 90.00. ISBN 0-444-41296-4

Many new and exciting topics were discussed at the symposium, among them one of great contemporary interest and practical application: central transmitter substances and their antagonists.

The programme on 1,3-indandiones led, through a historical link, to a discussion of those agents which can prevent blood clots, and even those agents (so full of promise for clinical application), that can actually dissolve them. A number of the papers presented covered anti-parasitic agents.
The symposium concluded with a session on the connexions between structure and biological activity, as mediated by physical properties and kinetics.

CONTENTS: Inflammation – A biological and chemical outlook *(J. Oort and H. Mullink).* Potential ways of interference with the biosynthesis of central monoamine transmitters *(N. E. Andén).* Processes involved in the regulation of the functional activity of central monoamines *(D. E. Grahame-Smith).* Monoamine metabolic pathways: Interrelations and aberrations *(M. Sandler).* Medicinal chemistry related to the central regulation of blood pressure. I. Chemical part *(H. Stähle).* Medicinal chemistry related to the central regulation of blood pressure. II. Pharmacological part *(W. Kobinger).* Organic and physical chemistry of 1,3-indandiones and related compounds *(G. Duburs).* Biocidal activity of indandiones-1,3 and related compounds *(J. A. Durden Jr.).* The clinical use of anti-thrombotic drugs – Rationale and results *(D. P. Thomas).* The platelet as a point of attack for anti-thrombotic agents *(D. Mills).* Regulation and control of fibrinolysis *(P. Brakman).* New vistas for folate antagonists in the chemotherapy of parasitic infections *(E. F. Elslager).* Recent advances in the medicinal chemistry of anthelmintics *(H. Loewe).* Chemical structure and toxic action. Avoidance of toxicity by molecular manipulation *(E. J. Ariëns).* The relationship between chemical structure and drug absorption, distribution and excretion *(E. J. Lien).* The relationship between chemical structure and drug metabolism *(A. H. Beckett).* Concluding remarks *(A. Albert).*

Elsevier
P.O. BOX 211
AMSTERDAM - THE NETHERLANDS
1553E

AUTOMATIC AIR QUALITY MONITORING SYSTEMS

Proceedings of the Conference held at the National Institute of Public Health, Bilthoven, The Netherlands, 5-8 June, 1973.

edited by **T. SCHNEIDER,** National Institute of Public Health, Bilthoven, The Netherlands.

1974. 284 pages. Dfl. 42.00 (about US$15.30) ISBN 0-444-41202-6

This symposium was organized by the National Institute of Public Health in Bilthoven, The Netherlands. Its purpose was to set up an exchange of knowledge on existing and planned automated air quality monitoring systems and the analysis of the air pollution data. It comprised the following subjects: monitors for measurement of air pollution and their use in the systems approach; design and application of automatic systems; data handling and data evaluation in connection with large systems; use of models for the determination of dispersion of air pollution; and application of monitoring systems within the existing international cooperation. As a result of the symposium a plan has been developed for future international cooperation between national research institutes and governmental agencies in the field of monitoring of pollution with a systematic and harmonized approach.

CONTENTS:

Elsevier
P.O. BOX 211
AMSTERDAM, THE NETHERLANDS
1292E

Analytica Chimica Acta, 78 (1975) 241–249

COMPUTERIZED ELECTROANALYSIS

PART I. INSTRUMENTATION AND PROGRAMMING

LARS KRYGER, DANIEL JAGNER* and HANS J. SKOV

Department of Inorganic Chemistry, Aarhus University, DK-8000 Aarhus C (Denmark)

(Received 5th March 1975)

Electrochemical analysis has become very much more popular during the past few years[1,2]. Its increase in popularity is partly due to the improved performance of inexpensive electronic components which have made new techniques such as different wave and pulse modes feasible[3–7]. Such techniques have considerably enhanced both precision and accuracy and have, moreover, lowered the limits of detection. The development of new solid electrode materials, like glassy carbon[8–11], has considerably reduced the experimental difficulties associated with electrochemical analysis.

The high sensitivity which can be achieved with anodic stripping has found application in the analysis of natural waters[11–13]. With this technique it is, moreover, possible to obtain information on the degree of complexation of the various metals analysed. Voltammetric analysis thus acts as a complement to other methods of analysis, which normally yield total concentrations.

Electrochemical analysis is well suited to computer automation. Repeated potential scans can normally be carried out with only very short intervals of time between successive scans. This means that signal-averaging techniques can be used to achieve improved precision, accuracy, and sensitivity. Standard additions from syringe burets, the rate of flow of inert gas, stirrer motors, etc. can all be operated completely automatically by the computer. Since the flow of data is high, access to a computer is imperative for the storage of data and their subsequent evaluation. With a computer on-line, processing of data, *e.g.* measurement of peak heights or integration of peaks, can be performed rapidly and the results inspected continually during the analysis on a graphical screen. Even for routine work with a well tested method it is vital that the data can be inspected during the analysis. A graphical screen permitting direct visual inspection is probably the most convenient device for this purpose.

A general, completely automatic instrument for electrochemical analysis is described in this paper. The system is extremely flexible and can be programmed to suit almost any electrochemical application in which the experimental parameters are to be computer-controlled. The device can also be used in conjunction with analytical techniques other than voltammetry. Only minor changes in hard-ware and

* On leave from Department of Analytical Chemistry, University of Göteborg, Sweden.

soft-ware are necessary if the instrument is to be coupled to a modern computer other than that used in the present work.

HARD-WARE

A block diagram of the system is shown in Fig. 1.

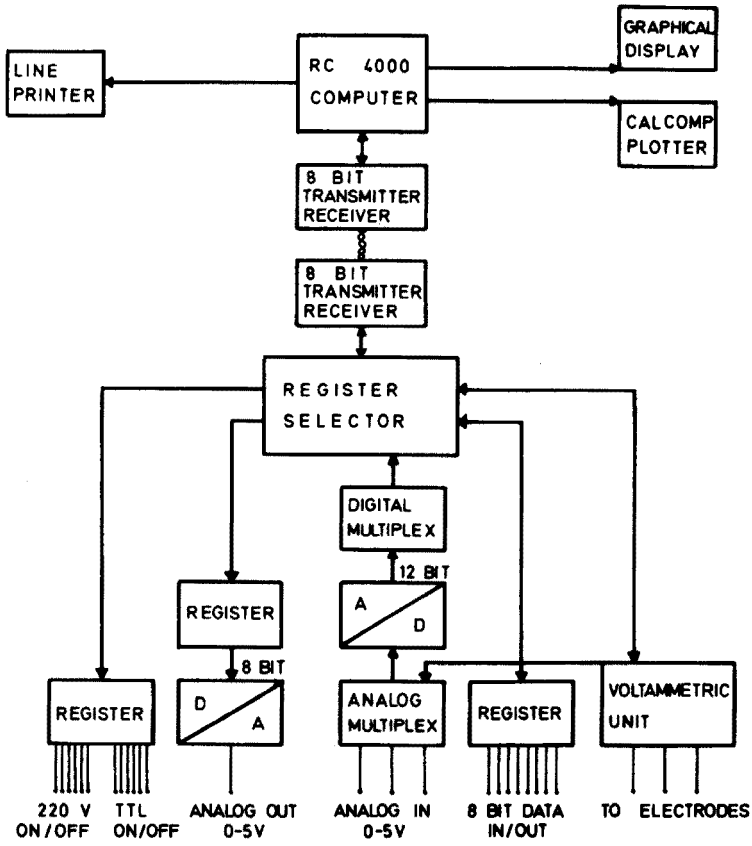

Fig. 1. Block diagram of the system.

The computer

The RC4000 computer is a general-purpose digital computer with an internal store of 48 K 24 bits words. Each word is extended by 3 protection bits. The cycle time is 1.5 μs. Direct addressing of the entire core is possible. The four first words of core are used as working registers; three of these also function as index registers. The computer is backed by a 2 Mwords disc. The I/O control comprises a low-speed data channel for transfer of single words between character-orientated devices and working registers, and a high-speed data channel for transfers between block-orientated devices and core memory, simultaneously with program execution. The RC4000 has a 24-level interruption system. In addition to the standard I/O media and a transmission system to a CDC6400, the computer controls several external units, *e.g.* x-ray diffractometers, and i.r. and e.s.r. spectrometers.

Terminals and displays

The Tektronix 4012 graphical screen also serves as an alphanumerical terminal. If the complete screen area is required for graphical display, the system can also be operated from a ASR 33 or a CDC alphanumerical terminal. Hard copies of the screen display are obtained on a Calcomp 563 plotter.

Communication

Communication with the computer is via nine twisted line-pairs, eight of which are for data transmission while the ninth is for clock pulses. The control system has been described elsewhere[15]. An output operation is initiated in two steps: a choice command and then, after 3 μs, a data code. The register selector decodes the choice command and opens the desired register in which the data are then stored. All registers are addressed individually in random mode. After the output initiation, the interrupt system is disabled for 50 μs. During this period the A/D converter converts the analogue signal to binary digital form. The eight most significant bits are then transferred to the computer. The four least significant bits cannot be transmitted to the computer until a new output/input operation has been initiated.

Control functions

The system contains all the functions normally required by a computer-controlled analytical procedure, *i.e.* analogue and digital input and output and 220 V and TTL on/off relays. The number of such relays is evident from Fig. 1. The computer clock, which has a resolution of 100 μs, is used for real-time measurements.

The voltammetric unit

The voltammetric unit, which is the most important part of the electro-analytical instrument, is illustrated in Fig. 2. The unit acts as a potentiostat, maintaining a constant potential between the reference and test electrodes. It can, moreover, generate a linear potential scan of given rate and direction between these electrodes, and it is possible to change both the speed and the direction several times during a single scan. In this way, linear scans of every conceivable form can be generated. The initial and final potentials can be varied throughout the region of electrochemical interest. Pulses of differing size and duration can be superimposed on the linear scans. The current between the counter and the test electrode is measured either continually or at given times during the pulse sequence. Complete computer control of all these parameters is achieved partly via digital information which the computer feeds into the registers A–D and partly via control of the solid-state switches Nos. 1–8 (*cf.* Fig. 2).

The desired constant potential between the test and reference electrodes is transmitted from the program to register B, which is part of the potentiostat, the digital information being converted to analogue form by the D/A converter B. After the desired value of the scan speed has been transmitted to register A by the program, a potential scan is initiated by closing switch No. 1. For practical reasons, it is easiest to insert the initial potential (register B), the final potential, and the total scan time as input data in the program. The computer then calculates the scan speed from these data and transmits it to register A. The

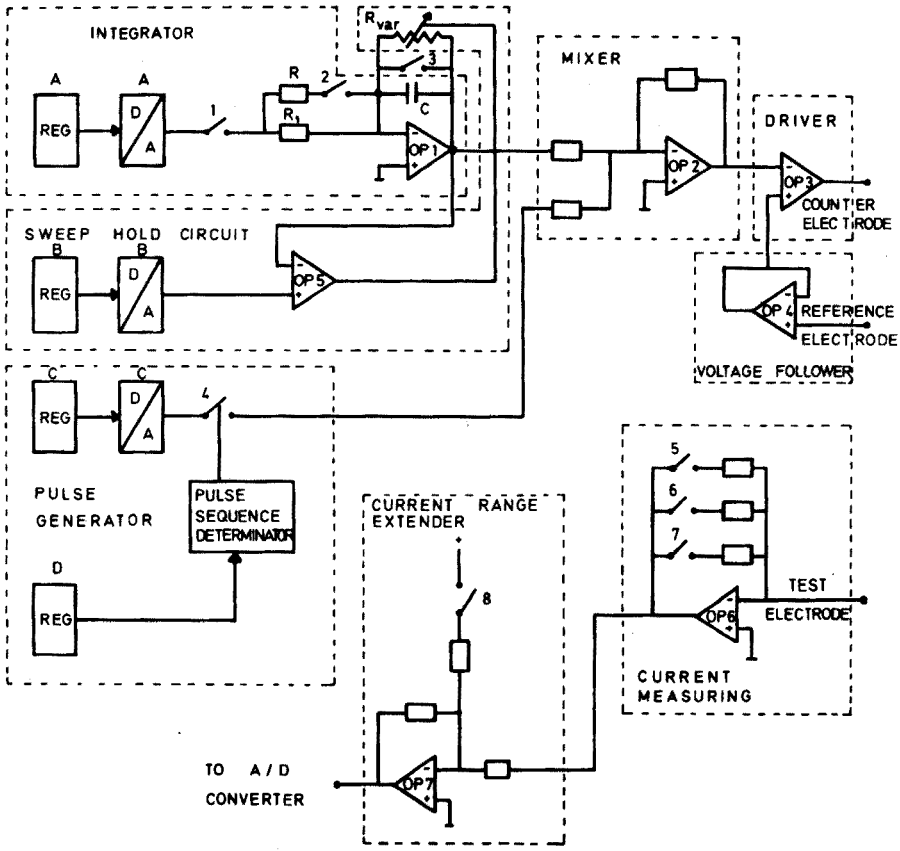

Fig. 2. The voltammetric unit.

scan is controlled by the operational amplifier OP1 whose output is $-(R_1C)^{-1}\int V_i dt$, where V_i is the value of the potential obtained from the D/A converter A.

The scan is terminated by the computer when the specified scan time is reached. Since the computer used sometimes works on a time-sharing basis, it has, however, been necessary to include a hard-ware device for stopping the scan. This is operated by a programmed instruction to register B. The scan speed can be varied from 1.5 mV s^{-1} to 20 V s^{-1} in steps of 1.5 mV s^{-1}. Switch No. 2 is closed during scans of high speed.

The desired pulse height and sign is transmitted to register C by the program. The pulse height can be varied in 127 equally large steps between 0 and a manually controlled upper limit ranging from 100 mV to 2 V. The duration of the pulse (4 bits) and the time between two successive pulses (4 bits) is transmitted to register D. The time between two successive pulses can be 20, 60, 100, 140, 180, 200, 600 or 1000 ms, etc. Multiples of 20 ms are, of course, only chosen if the line frequency is 50 Hz. The pulse is added to the linear scan in the mixer unit.

The current between the counter and the test electrode can be measured in three different ranges, *i.e.* 4, 40 and 400 μA, by closing switches Nos. 5–7, respectively. The current range extender changes its polarity according to the

direction of the current. In this way, the 12 bits resolution of the A/D converter can always be exploited.

SOFT-WARE

General

The RC4000 computer uses multi-programming techniques. This means that several programs can be loaded simultaneously into the disc memory of the computer. However, when it is resident in the disc memory, a program is not active. Only when it has been transferred to core memory and given access to the central processing unit (CPU), can a program be used for real-time data collection. Access to real-time operation is essential for most computer-processed analytical applications, for continuous data sampling at constant time intervals is almost always necessary at some stage during the execution of the analysis.

In the computer used, access to core memory is distributed to the different programs by means of a core-resident monitor program, BOSS[14]. This monitor allows two programs simultaneously in core memory provided that none of them is greater than 22 kwords, which is close to the total core size available for user programs. When two user programs are stored in core memory at the same time, real-time operation is not feasible because, at a specific time, only one of the programs has access to the CPU. In order to ensure sole excess to core memory for the program processing the electroanalytical device, dummy variables are inserted into the program, making its total size in excess of 22 kwords. Despite this, there is a possibility that the monitor program will transfer the processing program back to disc memory (swopping out) during real-time data sampling, thus destroying the experiment. This can be avoided by using the core-lock option available in the monitor program. By means of this option, a user can specify a time interval during which swopping out must not occur.

The monitor program also performs I/O operations and responds to interrupts. The low-speed channel (maximum 0.5 Mbaud) of the computer is used by the interface to the electroanalytical instrument.

Output/input sequence

The computer communicates with the interface of the electroanalytical instrument through an output/input sequence. Here output denotes information transferred from the computer to the interface, *e.g.* a request for data reading, and input denotes information transferred from the interface to the computer, *e.g.* a binary value of the current as measured by the A/D converter. All input information is accompanied by a real-time measurement of the computer clock.

An output/input sequence requires four words in the computer program. The contents of these words when used for output or input are as follows:

	Output	*Input*
Word (1)	Channel address, to be decoded by register selector (*cf.* Fig. 1)	Pulse on/off status

Word (2)	Output data, to be stored in *e.g.* registers A–D (*cf.* Fig. 1)	A/D converter reading
Word (3)	0	Clock reading
Word (4)	0	Clock reading.

The monitor program transmits word (1) as the choice command and word (2) as the data code.

The reading of the hard-ware clock occurs immediately after an output instruction has been started. After 50 μs the A/D converter has finished reading the relevant channel. The value of the A/D converter, and information concerning pulse status is then transmitted to the computer via an input instruction. During A/D conversion the monitor driver senses the hard-ware clock and updates internal time. The real-time accuracy is thus 100 μs.

Since the transmission system contains only eight bits, two O/I instructions are required to transfer the twelve bits of the A/D converter. These operations are performed consecutively with the interrupt system of the computer disabled. The maximum sampling rate is 700 Hz.

Programming languages

The executive program is written[14] in ALGOL 6. By using a high-level language it is possible to construct complicated executive and evaluation subroutines in a short space of time. This is, of course, a great advantage if the instrument is to be used for several different analytical applications.

Since rapid input and output processes cannot be written in a high-level language, these subroutines have been written in the assembler language SLANG[14]. All assembler routines can, however, be called from the ALGOL programs.

Basic processing subroutines

The executive program for a particular analytical procedure is composed of processing and evaluation subroutines. The processing subroutines control the switches, the ramp generator, the measurement of the current, and the display of the experimental data. Examples of such subroutines are given in Table I. All the subroutines can be called from the main program by giving the names and the relevant values of the various parameters as input.

Example of an implemented analytical procedure

When combined in a suitable way, the subroutines specified in Table I yield a complete analytical procedure. The procedure MULTI for example, is used for stripping analysis, either with or without pulses. The statement: MULTI 4, 0.90, 0.35, 15, 2, 2, 0, 0, 0.0, 1.0, 0.9, 5 causes the instrument to perform four potential scans between -0.90 V and -0.35 V (*vs.* SCE) each with a total scan time of 15 s. Before each potential scan there is to be a pre-electrolysis of 2-min duration. Measurement range No. 2 (40 μA) is to be used. The first zero in the input statement indicates that the pulse is not to be used, while the next three instructions require that the complete potential range be displayed on the graphical screen. Finally, the last two instructions require that the pre-electrolysis be carried out

TABLE I

BASIC PROCESSING SUBROUTINES

Command	*Process*	*Parameters*
On/off	Switch (i) on/off	Switch No.
Ramp	Starts ramp generator from preset potential value	Ramp on/off or reset, ramp rate and direction, current range and direction, maximum or minimum ramp potential
Pulse	Pulse train added to the ramp potential	Pulse on/off, pulse height and duration, interval between pulses, time interval between pulse on and start of current measurement, time interval between pulse off and start of current measurement
Add	Add reagent from automatic syringe buret	Volume of increment
Input	Read digital data from voltammetric unit at specified rate and time	Reading rate, total reading time
Insp	Display primary data on graphical screen	—
Disp	Display reduced primary data on graphical screen	Fraction of data to be displayed, data reduction mode
Wait	Delay program execution, process remains in core	Delay time
Swop	Delay program execution, process on disc memory	Delay time
Lock	Lock process in core	Core-lock time

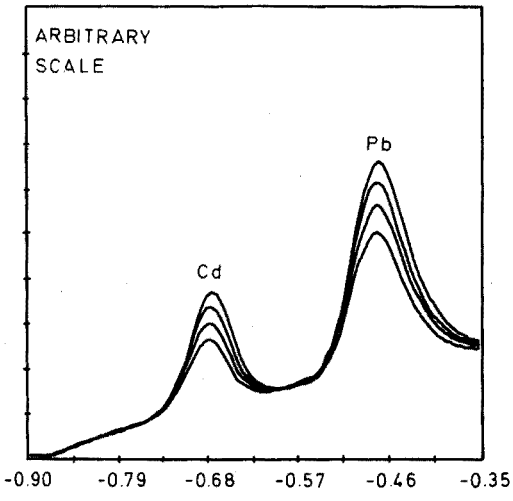

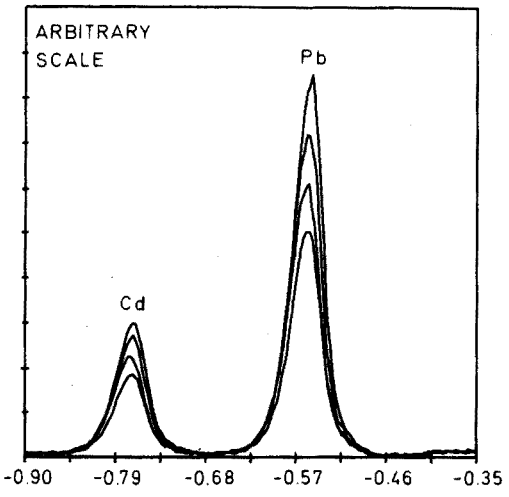

Fig. 3. Anodic stripping analysis of a 0.2 M potassium nitrate solution containing 7.5 p.p.b. cadmium and 16.5 p.p.b. lead. Increments of 1.5 p.p.b. cadmium and 3.9 p.p.b. lead.

Fig. 4. Pulse anodic stripping analysis of a 0.2 M potassium nitrate solution containing 7.5 p.p.b. cadmium and 16.5 p.p.b. lead. Increments of 1.5 p.p.b. cadmium and 3.9 p.p.b. lead.

at 0.9 V and that five increments of 0.1 ml be added from the buret after each potential scan.

The results of an analysis with the procedure MULTI, using the input parameters mentioned above, are shown in Fig. 3. The sample is a 0.2 *M* solution of potassium nitrate containing 7.5 p.p.b. cadmium and 16.5 p.p.b. lead. Five buret increments of 0.1 ml each correspond to an addition of 1.5 p.p.b. Cd and 3.9 p.p.b. Pb. The test electrode is a glassy carbon electrode covered with a thin film of mercury.

The same experiment in the pulse-stripping mode is illustrated in Fig. 4. MULTI is here preceeded by a pulse command (*cf.* Table I). The scan time is 120 s, the pulse height 100 mV, and the duration of the pulse 60 ms. The interval between successive pulses is 600 ms, and the current is measured only during the last third of each interval during which the pulse is on or off.

Different applications of this instrument will be dealt with in future papers.

DISCUSSION

The instrument described in this paper has been designed primarily in order to investigate and develop new electroanalytical techniques and to attempt to improve existing techniques with the aid of a computer. Obviously, the use of a computer such as that described in this work would make a routine electroanalytical procedure unnecessarily expensive. Nevertheless, it seems likely that, within a few years, micro- and mini-process computers will be included as standard parts of all types of commercial analytical instrument, for only slight additional costs. These computers must, however, be programmed in machine code and are not therefore suited to the development and improvement of analytical procedures. Before a micro- or mini-process computer can be incorporated into an analytical instrument, the analytical procedure and numerical evaluation method must be worked out in detail, by means of a larger computer. The advantages gained by using a larger computer for this purpose are access to disc-resident compilers for high-level languages, to editor programs and to rapid input and output processes for alphanumerical and graphical information. Owing to the large storage capacity on the disc, it is, moreover, possible to collect a large number of data without unnecessary interruptions for data reduction.

The use of a large computer can, however, be problematic as far as real-time measurements are concerned, because of time-sharing. Although core-lock options lock a program in the core memory, thus preventing other programs from having access to the core, they do not solve the more serious problem of sharing CPU time with, for example, the operating system.

In extreme circumstances, this can lead to the loss of important information. Nor is this problem solved by direct memory access (DMA). For electroanalytical applications, where the same experiment is often repeated several times, the problem can be circumvented by allowing the executive program to inspect the real-time measurements and reject those sets of data which have been seriously affected by time-sharing.

A guest professorship (D.J.) provided by the Danish Natural Science Research Council is gratefully acknowledged.

SUMMARY

The electronic circuit of a computerized electroanalytical instrument is described. The computer is programmed in a high-level language. The instrument can generate linear potential scans of any conceivable form within a wide range of scan rates. Pulses of varying height and duration can be superimposed on the linear scans. Stirrer motors, inert gas flow and addition of standard reagent are under computer control, thus permitting completely automatic analytical procedures. Data are displayed on a graphical screen. Results from anodic stripping experiments are given.

REFERENCES

1 J. B. Flato, *Anal. Chem.*, 44 (1972) 75A.
2 T. R. Copeland and R. K. Skogerboe, *Anal. Chem.*, 46 (1974) 1257A.
3 H. Siegerman and G. O'Dom, *Amer. Lab.*, 61 (1972) 116.
4 M. A. Brooks, J. A. F. de Silva and M. R. Hackman, *Amer. Lab.*, 12 (1973) 126.
5 *Princeton Applied Research Corporation, Application Notes Nos. 107, 108, 117, 119 and 120*, Princeton, N.J.
6 H. Blutstein and A. M. Bond, *Anal. Chem.*, 46 (1974) 1531, 1934.
7 M. R. Hackman, M. A. Brooks, J. A. F. de Silva and T. S. Ma, *Anal. Chem.*, 46 (1974) 1075.
8 W. J. Blaedel and R. A. Jenkins, *Anal. Chem.*, 36 (1974) 1952.
9 A. M. Bond, T. A. O'Donnell and R. J. Taylor, *Anal. Chem.*, 46 (1974) 1063.
10 R. A. Osteryoung and J. H. Christie, *Anal. Chem.*, 46 (1974) 351.
11 T. M. Florence, *J. Electroanal. Chem., Interfacial Electrochem.*, 35 (1972) 237; 49 (1974) 255; 51 (1974) 191.
12 M. I. Abdullah and L. G. Royle, *Anal. Chim. Acta*, 58 (1972) 283.
13 A. H. Miguel and C. M. Jankowski, *Anal. Chem.*, 46 (1974) 1832.
14 *Regnecentralen*, Hard-ware/Soft-ware System Library, Copenhagen.
15 G. Thirup and Hans J. Skov, to be published.

Analytica Chimica Acta, 78 (1975) 251–260

COMPUTERIZED ELECTROANALYSIS

PART II[1]. MULTIPLE SCANNING AND BACKGROUND SUBTRACTION. A NEW TECHNIQUE FOR STRIPPING ANALYSIS

LARS KRYGER and DANIEL JAGNER*

Department of Inorganic Chemstry, Aarhus University, DK-8000 Aarhus C (Denmark)

(Received 5th March 1975)

Owing to its extremely high sensitivity, anodic stripping has begun to be used more frequently for the analysis of toxic metals[2]. The development of new electrodes[3] and instruments has made the technique more reliable and easier to execute. The most promising electrode for ultra-sensitive analyses for trace metals is the glassy carbon electrode, plated *in situ* with mercury[4].

Although high sensitivity and low background can be achieved with differential pulse anodic stripping (DPAS)[5], results obtained with a computer-controlled electroanalytical instrument[1] indicate that this technique has several draw-backs. The potential scan must be carried out very slowly, *i.e.* over a period of several minutes, and, despite the long scan time, very few data can be obtained from each scan. Only a small fraction of the information available in the scan is thus exploited. This is because only one measurement can be obtained per superimposed pulse and because the pulse length must be a multiple of the line frequency.

A new technique, suitable for both anodic and cathodic stripping, is described in this paper. After pre-electrolysis, several rapid potential scans are performed in swift succession and the signals, each comprising the analytical signal and the background currents, are added by the computer. The background is then registered with a number of rapid scans, after the deposited material has been removed at a suitable high potential. The analytical (Faradaic) signal is obtained by subtracting the normalized total background from the normalized total signal. The method is completely automatic, the flow of inert gas, the stirrers, the standard additions and the evaluation of the results all being controlled by the computer.

Principle of the method

During anodic stripping analysis on a mercury film electrode, the metals are first reduced into the mercury film at a suitable potential by pre-electrolysis. The half-wave potentials of these metals are then passed by means of an anodic potential scan. If this anodic potential scan is carried out sufficiently rapidly, *e.g.* with a duration of less than 1 s, it is reasonable to assume that most of the oxidized

* On leave from Department of Analytical Chemistry, University of Göteborg, Sweden.

metal ions will remain within the diffusion layer surrounding the electrode. This means that, if the potential is reduced to the electrolysis value immediately after the termination of the scan, some of these ions will again be reduced into the mercury film. A subsequent scan would therefore still yield an analytical signal. By rapidly forcing the metal ions in and out of the mercury film in this way, and adding the signals from the different scans with the aid of a computer, it ought to be possible to achieve a very favourable signal/noise ratio.

The signals obtained during these scans are each composed of the analytical signal and the background arising from capacitance currents. Since the surface of the electrode changes continually, the background currents are not reproducible from one sample to the next. The background therefore cannot be calculated according to a numerical model, nor can it be compensated for electronically. The background can, however, be determined experimentally for each sample. After the series of analytical scans has been completed, all metals other than mercury are oxidized by applying a sufficiently high potential to the working electrode. This potential is maintained for a few seconds while the electrode is rotated, the metal ions thus being removed from the immediate vicinity of the electrode. Since the ions are present in very small amounts in comparison to the amount of mercury, the surface properties of the electrode should be little affected. The background is then measured by adding the signals from a number of scans of the same speed and over the same potential range as the scans used to register the analytical signals. The analytical signal is obtained by subtracting the normalized sum of the background scans from the normalized sum of the analytical scans.

EXPERIMENTAL

Chemicals

All reagents were of analytical grade. Standard metal solutions in the concentration range 0.1–5 p.p.m. were prepared by diluting 1000-p.p.m. stock solutions. Distilled water was purified by passage through an organic adsorbent, an ion-exchanger and a Millipore filter. Argon, purified with active charcoal, was used as inert gas.

Instrumentation

The computerized electroanalytical instrumentation and displays have been described in Part I[1]. The motor syringe buret (Metrohm Dosimat E 415) had a total volume of 5 ml. The test electrode was rotated by means of a Radiometer synchronized motor (type M 22) at about 1000 r.p.m. The argon flow was controlled by a Radiometer magnetic valve (type MNV 1C).

The reference electrode was a Radiometer K 410 saturated calomel electrode and the counter electrode was a platinum wire. The working electrode was made from a new type of glassy carbon ("Ringsdorff Glassartiger Kohle"; Ringsdorff-Werke GmbH, 53 Bonn-Bad Godesberg 10, Germany). The electrode was polished with emery paper and diamond paste down to a particle size of 0.25 μm. Beakers (100 ml) were used as sample vessels.

General procedure

Samples (50 ml) were deaerated separately. Mercury(II) nitrate was added

to the samples, before deaeration, to a total concentration of 20 p.p.m. During electrolysis, a stream of argon was passed through the sample solution and during scanning an argon stream was passed over the sample surface. The working electrode surface was cleaned in methanol with paper tissue between analyses.

Multiple scanning

In order to investigate whether or not it was possible to force metal ions into and out of the mercury film by means of rapid consecutive scans, the following experiment was performed.

A 0.2 *M* solution of potassium nitrate, containing 25 p.p.b. zinc, 10 p.p.b. cadmium and 25 p.p.b. lead, was plated at −1.30 V for 2 min. A potential scan up to −0.20 V was then applied during 0.3 s, after which the potential was immediately reduced to the plating potential. This potential was maintained for 1 s, in order to allow the decay of capacitance currents, during which time the data were processed by the computer. A new scan was then started. The results from twenty such consecutive scans are shown in Fig. 1. A background scan, which was registered after the electrode had been maintained at 0 V for 10 s is also indicated.

It is apparent from Fig. 1 that the analytical signal decreases by roughly 25% from the first scan to the second, the zinc signal decreasing more than the lead and cadmium signals. This is undoubtedly because, during a potential scan, the working electrode is held above the oxidation potential for zinc for a much longer time than it is held over the potentials for cadmium or lead. The zinc ions thus have a longer time during which they can migrate in the diffusion layer. It is also apparent from Fig. 1 that the decrease in the analytical signal is much less marked after four or five scans. The cadmium signal, for example, decreases by only 25% between the tenth and the twentieth scan.

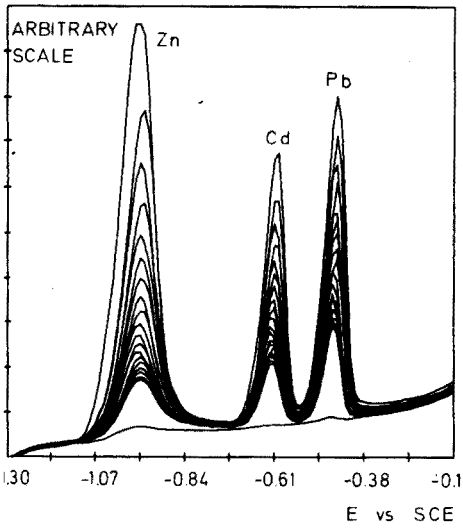

Fig. 1. Current from twenty multiple scans and one background scan plotted against potential. Plating for 2 min; scan time, 0.3 s.

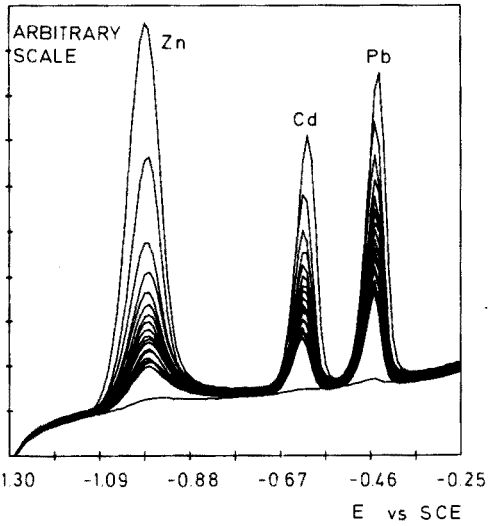

Fig. 2. Current from twenty multiple scans and one background scan plotted against potential. Plating for 2 min; scan time, 0.9 s.

It has been shown experimentally that, for the same scan interval and rate, the relative decrease in the analytical signal is almost independent of the total amount of metal reduced. This means that the relative decrease in signal for a sample with standard reagent added is the same as for the sample alone.

It would seem reasonable to predict that the decrease in the analytical signal between consecutive scans would increase with increasing scan time, since the ions have a longer time in which to migrate from the immediate vicinity of the working electrode. Although this is true, it appears that the effect of increased scan time is not as large as might have been expected. This is illustrated by a comparison of Fig. 1 with Fig. 2, which shows the results obtained when the experiment was repeated with a trebled scan time.

Both Figs. 1 and 2 show that multiple scanning is very favourable analytically. The analytical signals for cadmium and lead are increased by a factor of approximately ten while that for zinc is increased by a factor of five. A greatly improved signal/noise ratio is obtained by signal averaging of the analytical signal and of the background.

Cyclic scanning

It has been demonstrated that the stripping scan can be repeated several times, only a fraction of the signal being lost between successive scans. It is not, however, clear whether this is because the metal ions are forced into and out of the mercury film or because only a fraction of the amalgamated metals leaves the mercury film during each scan.

In order to investigate this further, a 0.2 *M* potassium nitrate solution, containing 50 p.p.b. zinc, 20 p.p.b. cadmium, 20 p.p.b. lead and 20 p.p.b. copper, was pre-electrolysed at -1.3 V for 2 min. Fifteen cyclic scans from -1.3 V up to -0.25 V and immediately down to -1.3 V were then registered. The scan rate was the same in both directions and the total scan time was 0.5 s. The signals from the different scans were added by the computer.

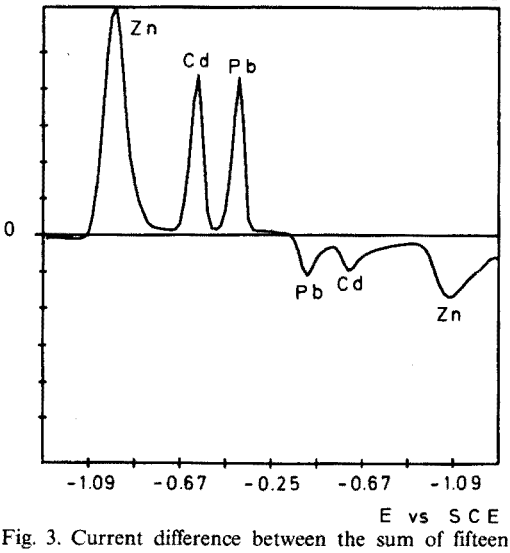

Fig. 3. Current difference between the sum of fifteen analytical scans and fifteen background scans plotted against potential during cyclic scanning.

The electrode was then rotated at −0.01 V for 10 s, and the background was registered with fifteen new cyclic scans under the same conditions. The total background signal was then subtracted from the total analytical signal. The results are shown in Fig. 3. It can be seen that some of the metal ions are indeed forced back and forth during multiple scanning. It is, however, also evident that the total amount of stripped metal cannot be re-reduced, which is consistent with the results shown in Figs. 1 and 2. The increased analytical signal obtained with multiple scanning can therefore be attributed partly to re-reduction of the metal ions and partly to the fact that only a fraction of the amalgamated metal is oxidized during a single scan.

Since the current in the reducing direction is only about 25% of that in the oxidizing direction, little is to be won by registering the current in both directions during multiple scanning. The contribution from the reducing current would only slightly enhance the precision of the analysis, and its inclusion would make the experimental procedure far more complicated. Moreover, as is apparent from Fig. 3, the peak width is larger for oxidation than for reduction.

Proposed analytical procedure

A block diagram for the proposed analytical procedure is shown in Fig. 4. The buffers 1–4 each comprise 100 words. At the end of a potential scan, (i) of buffer 1

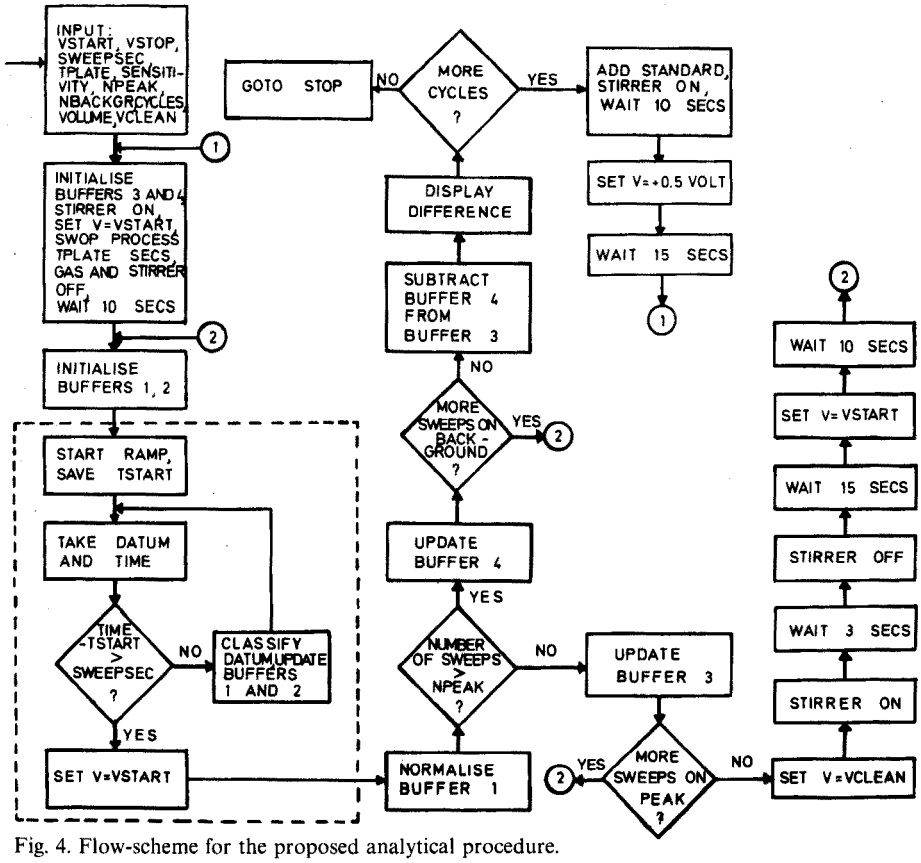

Fig. 4. Flow-scheme for the proposed analytical procedure.

contains the sum of the data acquired during the ith time (potential) interval of that particular scan. Word (i) of buffer 2 contains the total number of data stored in word (i) of buffer 1.

After the npeak and nbackgr scans have been completed, the buffers 3 and 4 represent the total analytical signal and the total background signal, respectively.

In order to achieve rapid data acquisition, part of the procedure has been implemented in assembler language. This part is framed by dotted lines. The times required for the different stages and the order in which the stirrer motor and the gas flow are operated, are apparent from the diagram.

TABLE I

INPUT DATA TO THE EXECUTIVE PROGRAM FOR THE PROPOSED ANALYTICAL PROCEDURE

Parameters	*Significance*
vstart, vstop	The limits for the potential scan
sweepsec	Total scan time
tplate	Plating time
sensitivity	Measuring range
npeak	Number of scan over the analytical signal
nbackgr	Number of scans over the background
cycles	Number of standard additions
vol	Volume of each addition
vclean	Potential for removing amalgamated metals before background measurements

The input data from the terminal are specified in Table I. If different values are given to npeak and nbackgr, the program normalizes the total signals before subtraction.

After the plating, the stirrer and the gas flow are stopped and the desired number of analytical scans is carried out. The amalgamated metals are then completely removed by rotating the electrode for 15 s at the potential vclean, and the background is measured. A standard increment is added and the potential is raised to 0.5 V for a few seconds in order to remove most of the plated mercury. This is in order to ensure a mercury film of approximately the same thickness during analysis of the sample plus standard addition as during analysis of the sample alone.

RESULTS AND DISCUSSION

Background subtraction

The relevance of the background correction was investigated by electrolysing a 0.2 M solution of potassium nitrate, containing 7 p.p.b. cadmium and 18 p.p.b. lead at -1.25 V for 1 min. Forty potential scans between -0.9 V and -0.25 V, each with a scan time of 1 s, were then carried out and the signals added. The electrode was held at -0.01 V for a few seconds after which forty background scans were carried out and added. The total analytical scan (curve 1), the total background scan (curve 2) and the difference (curve 3) are shown in Fig. 5. It is

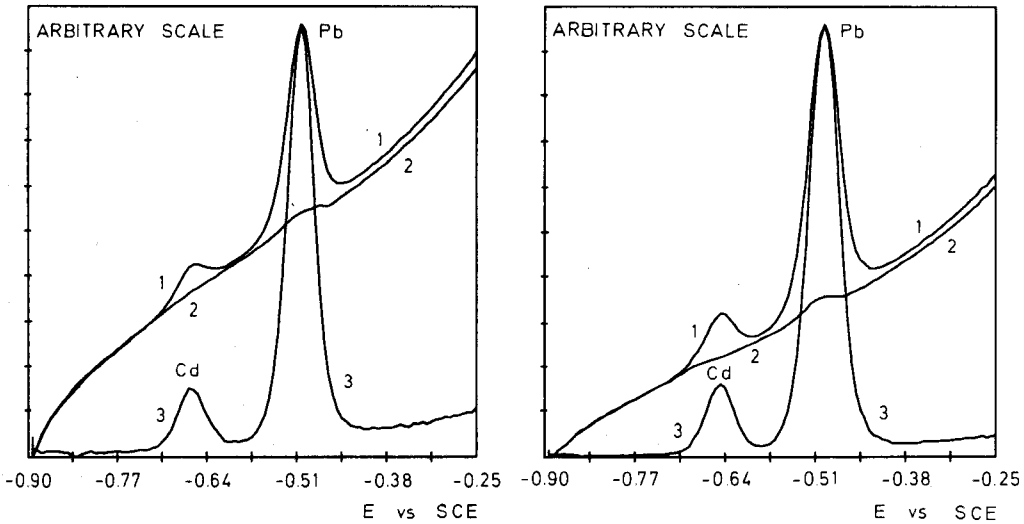

Fig. 5. The sum of the currents from forty analytical scans (curve 1) and from forty background scans (curve 2), and the difference between these sums (curve 3). Scan time, 1 s.

Fig. 6. The sum of the currents from forty analytical scans (curve 1) and from forty background scans (curve 2), and the difference between these sums (curve 3). Scan time, 0.2 s.

apparent that curve 2 follows curve 1 until the first peak—for cadmium—commences. After this peak there is a slight difference between the curves. The discrepancy can be attributed to a Faradaic current caused by the oxidation of an additional amount of cadmium. The same effect can be seen after the lead peak.

Subtraction of the measured background would thus appear to yield the true analytical, *i.e.* Faradaic, signal. This signal is usually not obtained experimentally by other anodic stripping techniques.

The results of an experiment carried out with a scan rate five times greater than that in the previous experiment are shown in Fig. 6. As expected, the signal/background ratio increases for the analytical can (curve 1). After subtraction of the background (curve 2), a curve is obtained (curve 3) which is almost identical with curve 3 of Fig. 5.

Standard addition

A standard addition method was examined for a sample containing 0.1 p.p.b. cadmium and 2.5 p.p.b. lead. The supporting electrolyte was 0.2 *M* potassium nitrate which also contained 20 p.p.m. mercury for *in situ* plating of the electrode. After plating for 2 min, twenty analytical scans were recorded between -0.90 and -0.35 V, the scan time being 0.3 s. After cleaning at 0 V, the background was recorded with the same number of scans. The volume of each standard addition increment was 0.5 ml, which corresponds to an increase in the cadmium and lead concentrations of 0.4 and 1 p.p.b., respectively. Duplicate plating and scanning cycles were performed on the original sample and after each standard addition in order to test the reproduciblity. The result is shown in Fig. 7.

Since the base lines are linear before and after a peak, a simple gradient

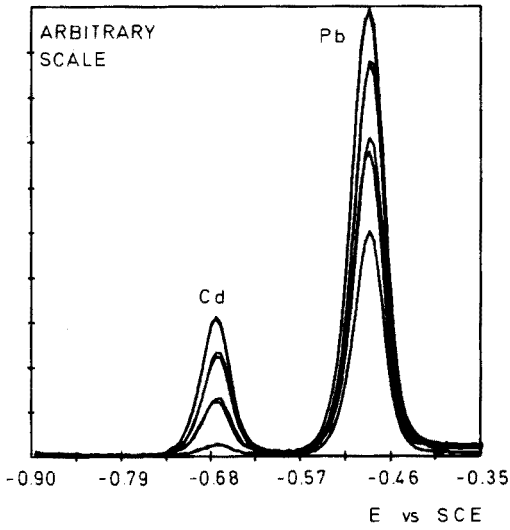

Fig. 7. Standard addition method for 0.1 p.p.b. cadmium and 2.5 p.p.b. lead. Increments of 0.4 p.p.b. cadmium and 1 p.p.b. lead were added. Duplicate analyses were performed for each concentration (*cf.* Figs. 8 and 9).

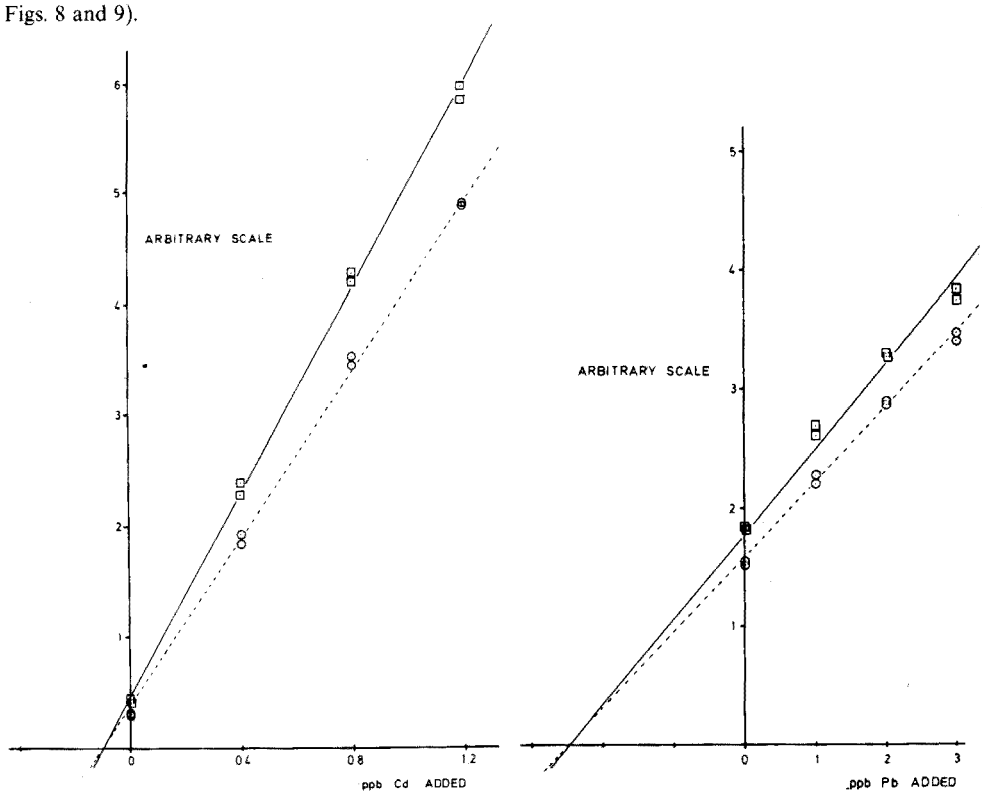

Fig. 8. Peak height (□) and peak area (○) in the standard addition method for 0.1 p.p.b. cadmium. Increments of 0.4 p.p.b. cadmium were added; duplicate analyses were performed for each concentration (*cf.* Fig. 7).

Fig. 9. Peak height (□) and peak area (○) in the standard addition method for 2.5 p.p.b. lead. Increments of 1 p.p.b. lead were added; duplicate analyses were performed for each concentration (*cf.* Fig. 7).

criterion for finding the peak limits could be exploited in the evaluation program. More elaborate methods, such as the standard deviation method proposed by Lehmann and Larsen[6] were also investigated but were not found to yield improved results. A straight line between the peak limits provided the base line under the peak and was used in evaluating peak height and peak area. In Figs. 8 and 9 peak heights and areas are plotted against the concentrations of cadmium and lead added.

Precision, accuracy and sensitivity

The experimental points shown in Figs. 8 and 9 show that the average deviation between duplicate measurements is less than 2%. It is also evident that the precision of measurement of peak height and peak area is almost the same. This was always found to be the case for solutions of high ionic conductivity. For solutions with ionic strengths less than 0.05 *M*, peak area measurements were found to be superior.

The linear increase in signal between standard additions confirms the accuracy of the method. Only metal-containing species which can be reduced at the relevant plating potential can, of course, contribute to the signal.

The sensitivity of the method is verified by the fact that signals well above the detection limits were obtained for less than p.p.b. concentrations of cadmium and lead after only 2 min of plating and at a moderate stirring rate.

Integration of the plating current

During plating the mercury used for *in situ* plating and the trace metals are deposited on the rotating electrode causing an electrolysis current to flow. If it is assumed that these are the only species which contribute to the electrolysis current, integration of this current during the period of pre-electrolysis should give a more accurate measurement of the total amount of metal plated than a measurement of the total plating time. Current integration would, for example, compensate for changes in the speed of the stirring motor and for changes in the surface area of the electrode during plating. Even though mercury contributes far more to the electrolysis current than do the trace metals to be determined, it can safely be assumed that the plated amount of a particular metal is proportional to the amount of mercury plated.

Integration of the electrolysis current, by means of the computer, was attempted. It was, however, found that integration caused a slight decrease in the precision of duplicate analysis. This can presumably be attributed to the capacitance currents flowing during electrolysis. These currents, which are caused by, for example, irregular variations in the geometry of the diffusion layer, are, of course, by no means proportional to the amount of metal plated.

Aspects of the electrode

In situ plating. The multiple scanning technique has proved to be applicable to many kinds of working electrode, such as the hanging mercury drop and pre-plated mercury thin-film electrodes. The hanging mercury drop electrode has the disadvantage that it cannot be rotated during plating and, moreover, reproducible renewal of mercury drops is not easy to automate by means of a computer. Thin-film electrodes, pre-plated separately outside the sample solution, were found to give

reproducible results. The best results were, however, obtained with a combination of pre-plating and *in situ* plating of mercury, the latter permitting a constant renewal of the mercury surface. Before the commencement of analysis, the working electrode was immersed in a mercury-containing sample for a couple of minutes at a potential sufficiently high to allow mercury only to be plated. The draw-backs caused by working with very thin mercury films were thus avoided. Before each new addition of standard solution the electrode was held at +0.5 V for a couple of seconds in order to remove most of the mercury plated during the previous plating. In this way the thickness of the mercury film could be kept reasonably constant.

Electrode material. Different kinds of electrode materials were investigated. Wax-impregnated graphite electrodes sometimes yielded irreproducible results probably owing to cracks in the wax. The glassy carbon used in this investigation, which has not previously been tested in electrochemical applications, has a high density and is easily polished to give a high lustre. It did not contain any craters as do many other similar products. The electrode kept its high polish for several weeks provided that it was not exposed to high oxidizing potentials.

Electrode shape. Since the suggested technique permits measurement of the background capacitance currents, it should be possible to use working electrodes of practically any shape, *e.g.* electrodes with large surface areas allowing large amounts of metals to be deposited in the mercury film during a short time. This might lead to increased sensitivity. It was found that electrodes with large surfaces can, indeed, be used for this technique. The full advantages of such electrodes have, however, yet to be investigated.

The electrode used in this investigation consisted of a L-shaped glass tube, the length of the "leg" being 100 mm and that of the "foot" 15 mm. A glassy carbon cylinder, 15 mm in length and 3 mm in diameter, was inserted in the "foot". Electrical conductance was achieved by means of mercury. When rotated around the "leg" axis, this arrangement minimized the diffusion layer around the working electrode allowing a high plating rate of the metals.

A guest professorship (D.J.) provided by the Danish Natural Science Research Council is gratefully acknowledged.

SUMMARY

A method of registering the pure Faradaic current in anodic stripping voltammetry is described. A computer-controlled voltammetric unit is used. The chemical significance of the voltammograms obtained is discussed. Details of the computer algorithm and results from anodic stripping analysis of metal solutions are given. The design of a mercury-plated glassy carbon electrode is discussed.

REFERENCES

1 For Part I see L. Kryger, D. Jagner and H. J. Skov, *Anal. Chim. Acta*, 78 (1975) 241.
2 T. R. Copeland and R. K. Skogerboe, *Anal. Chem.*, 46 (1974) 1257A.
3 H. E. Zittel and F. J. Miller, *Anal. Chem.*, 37 (1965) 200.
4 T. M. Florence, *J. Electroanal. Chem. Interfacial Electrochem.*, 27 (1970) 273.
5 H. Siegerman and G. O'Dom, *Amer. Lab.*, 6 (1972) 116.
6 M. S. Lehmann and F. K. Larsen, *Acta Crystallogr., Sect. A*, 30 (1974) 580.

Analytica Chimica Acta, 78 (1975) 261–270

SELECTIVITY COEFFICIENT CHANGES FOR LIQUID-MEMBRANE ELECTRODES

ADAM HULANICKI and ZOFIA AUGUSTOWSKA

Institute of Fundamental Problems in Chemistry, University, Warsaw (Poland)

(Received 2nd January 1975)

A principal factor which affects the application of membrane electrodes is their selectivity for the primary ion in the presence of interfering ions. A qualitative measure of the selectivity is given by the values of selectivity coefficient, K_{ij}; the variability of these selectivity coefficients is well recognized and is reflected in the abandonment of the term selectivity constants. There are not sufficient data about the factors which play the most important roles in changes in the selectivity coefficients. The numerical values of selectivity coefficients for identical electrodes evaluated by different authors show significant discrepancies. As an example, for the Orion calcium electrode (92-20), the published selectivity coefficients for sodium ions lie in the range 10^{-4}–0.42 (Table I). Less abundant data with less spectacular but still significant differences, can also be quoted for the Orion 92-32 divalent cation electrode (Table II).

The most important parameters affecting the selectivity coefficients are the activity level of the primary ion, the activity levels of the interfering ions and the limit of sensitivity of the electrode. To some extent, the different methods of evaluation of selectivity coefficients which have been proposed by various authors, may —under real conditions as opposed to theoretical ones—also introduce errors in selectivity coefficients. Because systematic studies of such parameters do not seem to be available, an elucidation of the effects of at least some of these factors is attempted in this paper. The selectivity coefficients used were determined by the method of Srinivasan and Rechnitz[9] (Method I). The K_{ij} values were also compared with measurements carried out as suggested by the manufacturer[10] (Method II).

EXPERIMENTAL

All cation solutions were prepared from the nitrate salts (analytical reagent grade) and twice-distilled water. Measurements were made with a Radelkis (OP-205) potentiometer. The reference electrode was a saturated calomel electrode connected through a KCl bridge. The indicator electrodes—the Orion 92-20 calcium electrode and the Orion 92-32 divalent ion electrode—were placed about 1 cm under the surface of the solution, which was stirred magnetically at a constant rate. The calcium(II) solutions were added from a Radiometer automatic burette (ABU-13). All measurements were carried out at 25 ± 0.5°C.

TABLE I

SELECTIVITY COEFFICIENTS FOR THE ORION CALCIUM ELECTRODE DETERMINED BY VARIOUS AUTHORS

Interfering ions					*Conditions*	*Ref.*
Li^+	Na^+	K^+	Rb^+	NH_4^+		
—	0.003	0.0001	—	0.0001	10^{-1} *M* Me^+ in 10^{-3} *M* Ca^{2+}	1
	0.0016					
—	0.001	0.001	—	—	pH = 9.2; I = 0.01	2
0.156	0.010	0.006	—	—	Flow conditions (142 ml min^{-1})	3
0.33 ± 0.03	⩽0.006	⩽0.006	⩽0.006	⩽0.006	Mole ratio $MeCl/CaCl_2$ of 0.5–100; I = 0.03–0.3	4
0.33 ± 0.03	0.07 ± 0.01	0.02 ± 0.01	—	—	I = 0.6	
—	0.039	—	—	—	I = 2	5
	0.011				I = 0.75	
	0.0001				I < 0.1	
—	0.024	0.013	—	0.15	Method of intersection of extrapolated lines[a]	6
	0.011	0.0083	—	0.066	Method: $\Delta E = 18/z_i$	
—	0.0058–0.42	0.002–0.37	—	—	$a_{Ca^{2+}} = a_{Me^+}$[a]	7
—	0.005–0.006	0.0013–0.0016	—	—	$E_{Ca^{2+}} = E_{Me^+}$[b]	
—	0.00053	0.00066	—	—	Method of intersection of extrapolated lines[a]	
—	0.00011	0.00011	—	—	Method $\Delta E = 18/z_{ib}$	

[a] Method of separated solutions; $C_{Ca} = 1.9 \cdot 10^{-2} - 9.7 \cdot 10^{-6}$ *M*. $C_{Me} = 10^{-1} - 10^{-2}$ *M*.
[b] Method of mixed solutions; $C_{Ca^{2+}} = 5 \cdot 10^{-3} - 4.3 \cdot 10^{-5}$ *M*.

TABLE II

SELECTIVITY COEFFICIENTS FOR THE ORION DIVALENT CATION ELECTRODE DETERMINED BY VARIOUS AUTHORS

Interfering ions				*Conditions*	*Ref.*
Li^+	Na^+	K^+	NH_4^+		
—	0.015	<0.015	—		8
	0.010				
0.124	0.025	0.018	—	Flow conditions (142 ml min^{-1})	3
—	0.033	0.015	0.12	Method of intersection of extrapolated lines	6
—	0.021	0.008	0.035	Method: $\Delta E = 18/z_i$	

RESULTS AND DISCUSSION

The effects of the various above-mentioned factors on the selectivity coefficients are quite different; this follows from the rather involved form of the Nicolsky equation used in the calculations:

$$a_i^* \ln\left[\frac{(E'-E^*)z_iF}{RT}\right] - a_i' = K_{ij}\left\{a_j'^{z_i/z_j} - a_j^{*\,z_i/z_j} \ln\left[\frac{(E'-E^*)z_iF}{RT}\right]\right\} \quad (1)$$

where activities are represented by a, potentials by E, valencies by z, the selectivity coefficient by K, and i and j indicate the measured ion and the interfering ion, respectively. The asterisked activities a^* correspond to the potential values E^*, measured in the initial solution containing a known activity of interfering ion and an indicator activity of the main ion. The primed activities and potentials refer to values after each addition of the main ion.

In this equation, when the electrode limit, L, which corresponds to the activity level below which the electrode is no longer sensitive to changes in activity, is added as a third term, the situation becomes even more complicated:

$$-a_i^* \ln\left[\frac{(E'-E^*)z_i}{S}\right] - a_i' + L\left\{\ln\left[\frac{(E'-E^*)z_i}{S}\right] - 1\right\}$$

$$= K_{ij}\left\{a_j'^{z_i/z_j} - a_j^{*\,z_i/z_j} \ln\left[\frac{(E'-E^*)z_i}{S}\right]\right\} \quad (2)$$

where $S = RTF^{-1}$.

The effects of variables were traced by evaluation of K_{CaNa} values at different activity levels of both ions of interest.

The effect of the activity level of the main ion

For a series of measurements, $\Delta E = E' - E^*$ is positive and a_j decreases because of dilution on addition of the solution of the main ion. Therefore, the expression on the right-hand side in eqn. (1) is negative. To obtain a positive value for the selectivity coefficient, it is necessary that:

$$a_i^* \exp\left(\frac{\Delta E \cdot z_i}{S}\right) < a_i' \tag{3}$$

and

$$\Delta E < \frac{S}{z_i} \ln \frac{a_i'}{a_i^*} \tag{4}$$

When the potential difference ΔE approaches the value of the right-hand side of eqn. (4), *i.e.* when the potential response is close to the Nernstian value, the error in the determination of the selectivity coefficient for a given precision of measurement is large. This corresponds to conditions where the contribution of the $K_{ij}a_j^{z_i/z_j}$ term in the Nikolsky equation is small compared to the first term a_i.

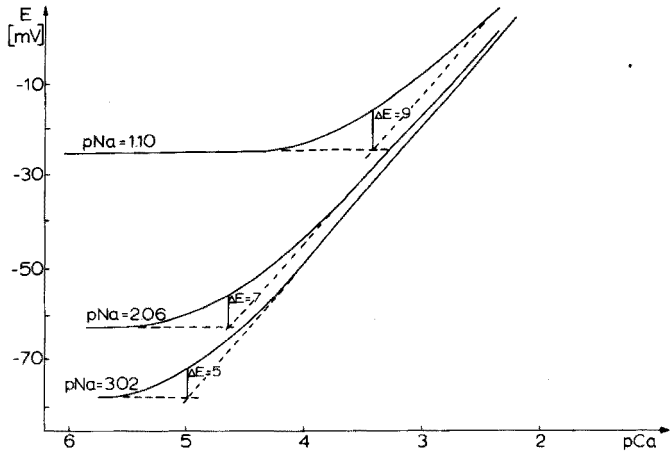

Fig. 1. Potential, *p*Ca, diagram for the divalent cation electrode at various activity levels of sodium as interfering ion.

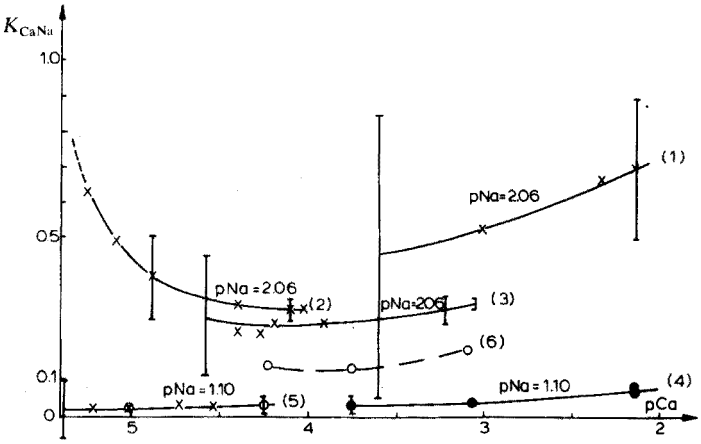

Fig. 2. Selectivity coefficients K_{CaNa} of the divalent cation electrode calculated at various ion activities on the basis of eqn. (1)—solid lines, and on the basis of eqn. (2)—dashed line. The lines parallel to the *K*-axis indicate the uncertainty connected with the potential reading (± 1 mV). See text for curve numbering.

Figure 1 shows the changes in the potential of the divalent cation electrode at various levels of sodium ions. When the sodium ion level corresponds to pNa 3.0, the calcium ion activity at which the selectivity coefficient can be determined is approximately pCa 5.0. For pNa 2.0 and pNa 1.0, the corresponding levels of calcium are approximately pCa 4.6 and pCa 3.4.

Equation (1) was used to calculate the selectivity coefficients for various ranges of calcium activity for the divalent cation electrode (Fig. 2). The results obtained for one series of measurements (fixed value of E') are connected with a solid line.

For pNa values of about 2.0, the selectivity coefficients determined for pCa values less than 3.6 (curve 1) have a very significant error; this is indicated on Fig. 2 by the line parallel to the K-axis, and corresponds to an uncertainty of 1 mV in the potential measurement. These determinations were carried out in the range where the activity of the main ion in the Nikolsky equation plays a dominating role. When the activity of the main ion decreases, the error also decreases, and the values obtained describe the behaviour of the electrode in a much more realistic manner (curve 3). The difference in the errors indicated on curves (1) and (3) at the same levels of pCa and pNa is a consequence of the different reference values a_i^* and E^*. When these correspond to the potential range where the interference is small, the error is greater (curve 1) than in the case when the sodium effect is more significant (curve 3). However, if the calcium activity is significantly smaller (pCa >4.0), the limit of the electrode contributes to a large extent both to the increase in the calculated selectivity coefficient and to an increase in the error (curve 2). This behaviour is in accordance with eqn. (2) because the positive value of the L-containing term increases the absolute value of the left-hand side of this equation.

For greater activities of sodium ion (about pNa 1.0; curves 4 and 5), the results seem to be reasonable and the error of these results is small over the whole range except for low limiting activities of calcium, where the contribution of the electrode limit again starts to be significant.

The effect of the electrode limit

As was mentioned above, the contribution of the electrode limit is not very important in those measurements which correspond to high activities of the main ion. However, when the contribution increases, the effect should be calculated, at least using an approximate numerical value of the limit. On Fig. 2, curve 6 was calculated for conditions corresponding to those for curve 3, and the values of the selectivity coefficients obtained are indicated by the dashed line. In these calculations, the electrode limit was arbitrarily taken as 10^{-5} M.

The electrode limit also affects the graphical procedure recommended by Orion Research[10]. In this procedure, the intersection of the two extrapolated parts of the calibration curve should be found at a potential value $18/z_i$ mV below the curved part of the calibration curve (Fig. 1). However, this value cannot be obtained in the range where the electrode limit starts to contribute to the potential readings. At a pNa level of 1.10, the theoretically predicted value $18/z_i = 9$ mV is obtained, whereas for pNa levels of 2.06 and 3.02, lower values—7 and 5 mV, respectively—are produced by extrapolation.

The effect of time after electrode preparation

During the time between the preparation of the liquid membrane electrode and the end of its correct functioning, the absolute values of the potential response, as well as the relative sensitivity to various ions, change significantly (Fig. 3). The changes in the absolute potentials are usually quite easily corrected by calibration before a series of measurements, but the second effect may have much more practical significance. It is obvious that such changes affect the selectivity coefficients which are determined experimentally. To evaluate the extent of ageing of the electrode, the selectivity coefficients for the divalent cation electrode were determined during the first 3 days after electrode preparation and again 8 weeks later (Fig. 4). The electrode was kept in a 10^{-3} M solution of calcium nitrate during its lifetime, and during the whole period the slope of the calibration curve was 27 ± 1 mV per decade.

In the first period of the electrode life, the selectivity coefficients for alkali metals are generally higher than those obtained at a later stage, and more dependent

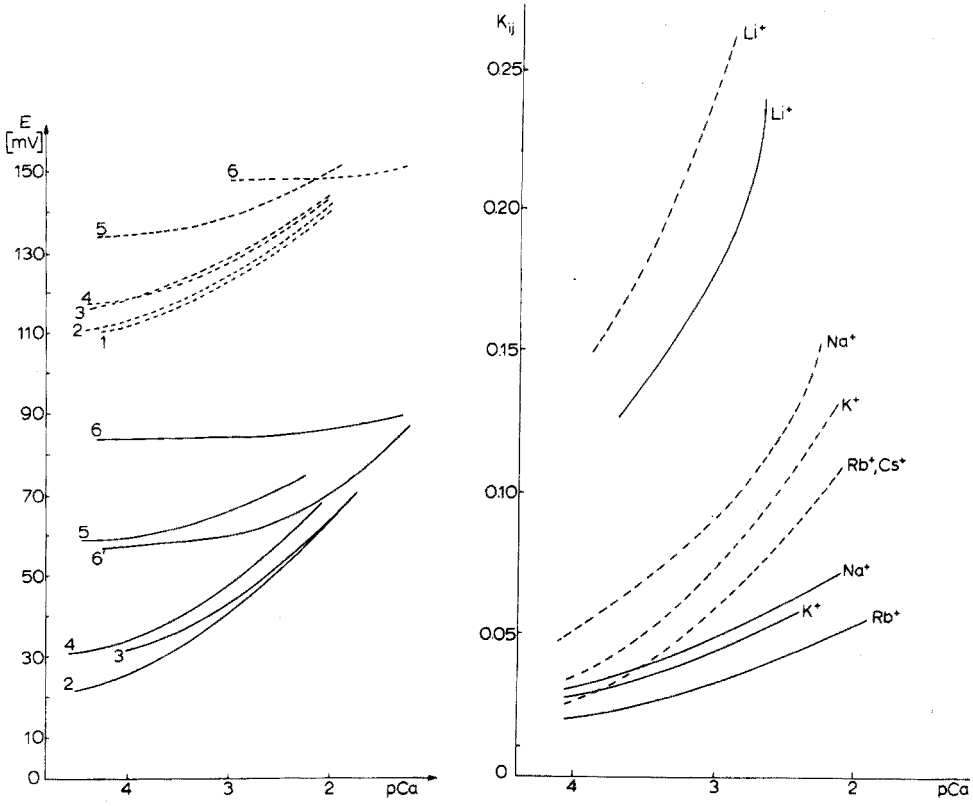

Fig. 3. Calibration curves obtained with the divalent cation electrode for calcium ions in the presence of 10^{-1} M solutions of interfering ions: 1, $CsNO_3$; 2, $RbNO_3$; 3, KNO_3; 4, $NaNO_3$; 5, $LiNO_3$; 6, $Mg(NO_3)_2$; 6′, 10^{-2} M $Mg(NO_3)_2$. The dashed lines correspond to the results obtained 3 days after the electrode preparation, and the solid lines to the results obtained 8 weeks later.

Fig. 4. The selectivity coefficients of the divalent cation electrode calculated on the basis of measurements taken 3 days (dashed lines) after electrode preparation, and 8 weeks later (solid lines).

on the activity of the main ion at which they were determined. These changes can probably be attributed to equilibration of the organic phase with the aqueous solutions, and elution of the organic solvent by the external solution, so that the dielectric constant of the membrane phase changes.

At present it seems that any exact evaluation of the ageing process is difficult, if possible at all; therefore, the values given should be used rather to stress the importance of the problem than to give strict numerical descriptions of the electrode behaviour.

The values of the selectivity coefficients of the calcium and divalent cation electrodes

On the basis of the study of the parameters that influence the values of the selectivity coefficients, it was possible to calculate the coefficients under carefully defined optimal conditions. In these measurements, both the main and the interfering ions were present in the solution, so that the conditions approached those found in analytical measurements.

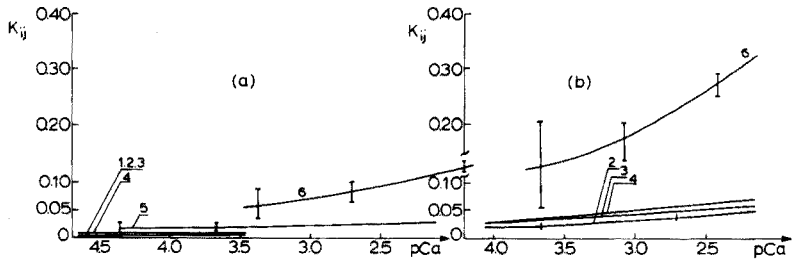

Fig. 5. Comparison of selectivity coefficients for the calcium electrode (a) and the divalent cation electrode (b). The activity levels of the interfering ions were 10^{-1} *M*. 1, K_{CaCs}; 2, K_{CaRb}; 3, K_{CaK}; 4, K_{CaNa}; 5, K_{CaNH_4}; 6, K_{CaLi}.

TABLE III

SELECTIVITY COEFFICIENTS FOR SOME MONOVALENT INTERFERING IONS (pM = 1.10) WITH THE CALCIUM ELECTRODE

Interfering ion	*Method I*	*Method II*
Cs^+	0.0049 ± 0.002	0.0049
Rb^+	0.0051 ± 0.002	0.0052
K^+	0.0050 ± 0.002	0.0064
Na^+	0.0070 ± 0.002	0.0083
NH_4^+, pH = 7.5	0.02 ± 0.01 to 0.03 ± 0.007	0.037
Li^+	0.06 ± 0.03 to 0.13 ± 0.01	0.083

Calcium electrode—Orion 92-20. Caesium, rubidium, potassium and sodium interfere only to a very small extent with calcium ion measurements (Fig. 5). The selectivity coefficients are nearly independent of the activity level of the main ion, and the error of determination is relatively small. Ammonium and lithium interfere much more, and selectivity coefficients towards those ions increase with the activity level of calcium.

The calculated data are shown in Table III. When the change in the selectivity

coefficient with calcium activity is small, the numerical values obtained by Methods I and II are in good agreement. When the selectivity coefficient varies with calcium the activity level at which the measurements were made, led to an apparent decrease Obviously, comparison of the two methods should be carried out for the same activity level of the main ion.

Divalent cation electrode—Orion 92-32. Because in general the response of this electrode is more affected by alkali metal interferences than the response of the calcium electrode, the selectivity coefficients are more influenced by the activity level of the main ion, calcium (Fig. 5).

TABLE IV

SELECTIVITY COEFFICIENTS FOR THE DIVALENT CATION ELECTRODE WITH CALCIUM AS THE MAIN ION

Interfering ion	*Method I*	*Method II*
Rb^+	0.020 ± 0.005 to 0.050 ± 0.003	0.051
K^+	0.030 ± 0.005 to 0.050 ± 0.003	0.055
Na^+	0.040 ± 0.007 to 0.070 ± 0.005	0.065
Li^+	0.15 ± 0.06 to 0.30 ± 0.03	0.30

For rubidium, potassium and sodium, the interferences are similar when determined at the 10^{-1} *M* level of interfering ion (Table IV). Under similar conditions the lithium ion shows a much greater interference.

The selectivity coefficients for a constant level of calcium (pCa 3.0) and different levels of sodium were found to be 0.30 ± 0.02 (Method I) or 0.32 (Method II) for a pNa value of 2.05, and 0.05 ± 0.005 (Method I) or 0.065 (Method II) for a pNa value of 1.10. These values, as well as Fig. 2, indicate that decreasing the sodium activity makes the selectivity for calcium worse. This is in agreement with the observations for PVC matrix anion-selective electrodes[11], where a decrease in the activity level at which the measurements were made, led to an apparent decrease in selectivity when the selectivity coefficient was less than 1.

The general conclusion following from this study is that selectivity coefficients are analytically meaningful only when the conditions of their measurement are strictly defined. Unless the activity levels of the main and interfering ions are quoted, as well as a description of the method, or unless the potential response curves are given their values seem of little practical value.

The conditions of measurement of the selectivity coefficients which provide the best results were chosen as follows:

(i) the liquid-state electrode should not be used until potential readings are sufficiently stable (not less than 1 week after preparation);

(ii) the ionic strength should be such that it is practical to adjust it in measurements, but it should not approach the value 1.0, where the calculation of activity coefficients is doubtful, and, because of the necessary high level of the interfering ion, 0.1 is the best compromise;

(iii) the level of the interfering ion should be relatively high, especially when the selectivity coefficients are small, because this provides a reasonable contribution

of the interfering ion to the measured potential: in the present systems where the selectivity coefficients do not exceed 0.5, the concentration of interfering ion should not be less than 0.1;

(iv) the activity of the main ion should be varied over the required range, but the initial value used for calculations should be located in the range where the curvature of the potential response curve for a given (0.1) concentration of interfering ion is greatest.

SUMMARY

The effects of the activity levels of the measured ion and interfering ions, and of the detection limit of the electrode on the values of selectivity coefficients for liquid-membrane ion-selective electrodes are discussed. The coefficients were determined by the mixed-ion solution method. Depending on the activity of the interfering ion, the activity of the main ion for which the selectivity coefficient is determined may differ. The best conditions of measurement are those which involve the largest contribution from the term containing the selectivity coefficient in the Nikolsky equation; the measurements are then most precise, and the values of the selectivity coefficients describe the electrode behaviour most consistently. When the limit of detection of the electrode is comparable with the other terms, it must be taken into account in calculations. Under the optimal conditions, selectivity coefficients were calculated for the Orion calcium and divalent cation electrodes, with calcium as the main ion and alkali metal ions as interfering ions.

REFERENCES

1 *Orion Calcium Specific Ion Electrode, Model 92-20, Instruction manual.*
2 G. A. Rechnitz and Z. F. Lin, *Anal. Chem.*, 40 (1968) 696.
3 B. Fleet and G. A. Rechnitz, *Anal. Chem.*, 42 (1970) 690.
4 J. Bagg, O. Nicholson and R. Vinen, *J. Phys. Chem.*, 75 (1971) 2138.
5 M. Whitfield and J. V. Leyendekkers, *Anal. Chem.*, 42 (1970) 444.
6 M. Trojanowicz, Doctoral Thesis, University of Warsaw, 1973.
7 G. J. Moody and J. D. R. Thomas, *Analyst (London)*, 95 (1970) 910.
8 *Orion Divalent Specific Ion Electrode, Model 92-32, Instruction manual.*
9 K. Srinivasan and G. A. Rechnitz, *Anal. Chem.*, 41 (1969) 1203.
10 Orion Research Inc., *Newslett.*, 1 (1969) 5.
11 A. Hulanicki and R. Lewandowski, *Chem. Anal.*, 19 (1974) 53.

Analytica Chimica Acta, 78 (1975) 271–276

VOLTAMMETRIC MEASUREMENT OF REDUCED NICOTINAMIDE–ADENINE NUCLEOTIDES AND APPLICATION TO AMPEROMETRIC MEASUREMENT OF ENZYME REACTIONS*

LAWRENCE C. THOMAS and GARY D. CHRISTIAN

Department of Chemistry, University of Washington, Seattle, Washington 98195 (U.S.A.)

(Received 12th March 1975)

Nicotinamide–adenine dinucleotide (NAD) and nicotinamide–adenine dinucleotide phosphate (NADP) oxidoreductase reactions are important in biochemistry and clinical chemistry laboratories[1,2]. The electrochemical reduction of NAD and NADP has been well characterized[3–5]. However, the electrochemical oxidation of their reduced forms, NADH and NADPH, is less well understood. Burnett and Underwood[6] reported that NADH gives a poorly defined oxidation wave on platinum but that it can be quantitatively electrolyzed to NAD at an applied potential of +1.05 V *vs.* SCE. NADPH has been electrolyzed to NADP at +0.62 V *vs.* SCE[7]. An electrochemical oxidation mechanism for reduced pyridine nucleotide analogs has been proposed by Blaedel and Haas[8], and the effect of bases and dissolved oxygen were studied. Blaedel and Jenkins[9] have recently reported on the oxidation of NADH by steady-state voltammetry.

Few amperometric methods have been described for the measurement of dehydrogenase enzyme reactions. Smith[10] reacted Bindschedler's Green with the NADH produced in enzymatic dehydrogenation and measured the reduced form of Bindschedler's Green at a tubular carbon electrode and a rotating platinum electrode. All solutions were deaerated in this method. Williams *et al.*[11] determined lactic dehydrogenase (LDH) activity at a platinum electrode by amperometric measurement of cyanoferrate(III) reacted with lactate in the presence of LDH.

In the present paper, conditions are reported for obtaining well defined voltammetric oxidation waves for NADH and NADPH, at a carbon paste or a stationary glassy carbon electrode. A linear relationship is found between the peak current and the NADH or NADPH concentration. These voltammetric waves were investigated for the direct amperometric monitoring of dehydrogenase enzyme reactions. Ethanol in serum was measured by integrating, over a preset time, the amperometric current from NADH in the presence of NAD and alcohol dehydrogenase (alcohol:NAD oxidoreductase; ADH). Lactic dehydrogenase (L-lactate:NAD oxidoreductase; LDH) in serum was measured by recording fixed-time differences in the amperometric current from the NADH produced in the presence of NAD and D,L-lactate.

* Presented in part at the "Symposium on Electrochemical Techniques in Bioanalytical Chemistry", 166th National Meeting of the American Chemical Society, August 26–31, 1973; Chicago and the International Workshop on Ion Selective Electrodes and on Enzyme Electrodes in Biology and Medicine, September 15–18, 1974, Schloss Reisensburg, Germany.

EXPERIMENTAL

Apparatus

Current–voltage (d.c.) curves were recorded on a Princeton Applied Research Model 174 Polarographic Analyzer, in the three-electrode mode. A saturated calomel electrode (SCE) was used with a platinum gauze auxiliary electrode. The working electrode was either a carbon paste electrode constructed as described before[12] according to the directions of Adams[13], a glassy carbon electrode obtained from Chemtrix, Inc., or a platinum wire electrode. The carbon paste electrode had a surface area of 0.07 cm^2 and the glassy carbon electrode had a surface area of 0.38 cm^2. Amperometric measurements were made with the amperometric integrator/potentiostat previously described[12].

Reagents

NAD (DPNR 2HA), reduced NAD (DPNH 2KA), and ADH (ADHL 2EB at 325 I.U./mg) were obtained from Worthington Biochemical Corporation. LDH (lot 220068; Calbiochem) and reduced NADP (lot 361002; P-L Biochemicals Inc.) were also used. All other chemicals were reagent-grade quality. All solutions were prepared with deionized, distilled water.

Procedure

Current–voltage curves were recorded by scanning toward more positive potentials in quiet solutions of the reduced nucleotides in 0.1 *M* disodium hydrogen phosphate adjusted to pH 8.3 with sodium hydroxide, unless otherwise stated. Current–voltage curves for $3.16 \cdot 10^{-4}$ *M* solutions of NADH at a glassy carbon electrode were run at pH values of 5.6, 6.0, 6.5, 7.0, 7.4, 8.0, and 8.3 in 0.1 *M* disodium hydrogen phosphate. Constant-potential amperometric measurements were used to monitor enzyme reactions. Serum ethanol analyses employed the current-integrating capability of the integrator/potentiostat instrument, and serum LDH assays utilized its current-following recorder output[12].

Alcohol measurements were made with samples of pooled serum to which known quantities of ethanol and water had been added. The serum was diluted (10+1) in all cases. The diluted serum sample (100 μl) was added to 8 ml of a solution of 0.1 mg ADH ml^{-1} in 0.1 *M* phosphate at pH 8.3, in a 10-ml beaker, stirred at a constant rate by a 0.5-in. magnetic stirring bar. After stabilization of the glassy carbon electrode current, at +0.75 V *vs.* SCE, the current was integrated for 8 s to obtain the integrated residual current. Then 250 μl of 0.0125 *M* NAD in 0.1 *M* phosphate buffer, pH 7.3, was added; 8 s after the NAD addition, another 8-s current integration was performed. The difference between these two integrations was displayed by the instrument.

Serum LDH measurements were made with samples of pooled serum to which known quantities of LDH and water had been added so that all samples were diluted (10+1). The serum sample (100 μl) was added to 6 ml of 0.115 *M* D,L-lactate solution in 0.1 *M* phosphate, pH 7.3, in a 10-ml beaker, stirred at a constant rate by a 0.5-in. magnetic stirring bar. After the current at the glassy carbon electrode at +0.75 V *vs.* SCE had stabilized, 250 μl of 0.014 *M* NAD in 0.1 *M* phosphate, pH 7.3, was added. The change in amperometric current, over a

fixed 5-min interval, was recorded.

RESULTS AND DISCUSSION

Current–voltage curves for NADH in TRIS buffer, pH 8.0, on platinum and carbon paste electrodes are shown in Fig. 1. On platinum, a diffuse voltammetric wave was observed, in agreement with previous reports[6]. On the carbon paste electrode, however, the residual current was much smaller and a well defined anodic wave was obtained for NADH with a half-peak potential of +0.60 V *vs.* SCE. A linear calibration curve of peak height *versus* concentration was obtained over a range of 0–0.4 mg NADH ml^{-1} and 0–150 nA current. Successful amperometric monitoring of enzyme reactions at +0.75 V *vs.* SCE with the carbon paste electrodes was achieved. One must be careful, however, to avoid exposing the electrode to air while the high positive potential is still applied; otherwise high and erratic residual currents are obtained. When this occurs, satisfactory results are again obtained after rebuilding the electrode, an easy and reproducible process.

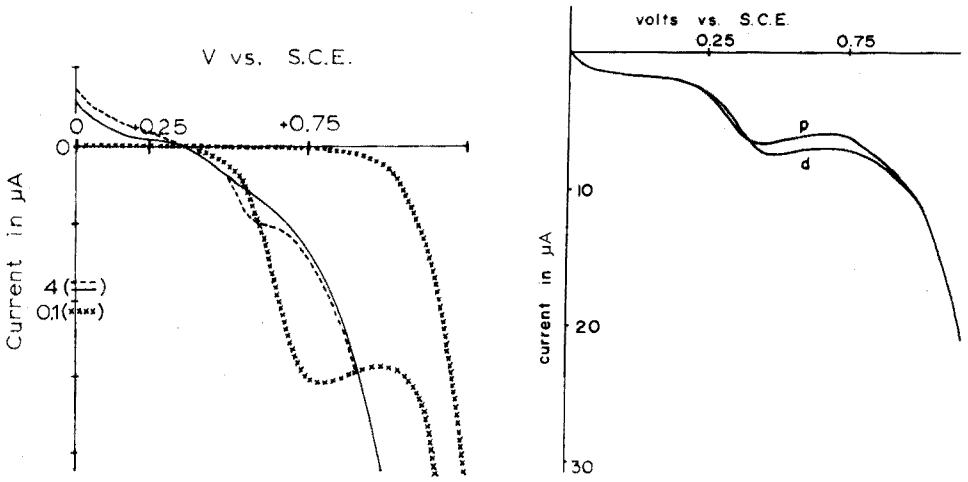

Fig. 1. Current–voltage curves for NADH on platinum and carbon paste electrodes in 0.1 *M* TRIS buffer at pH 8.0. Current scale for platinum is 40-fold greater than for carbon paste. Scan rate was 5 mV s^{-1}. $[NADH]_{Pt} = 5.7 \cdot 10^{-4}$ *M*, $[NADH]_c = 5.2 \cdot 10^{-4}$ *M*. (——) Blank on Pt, (– – –) NADH on Pt, (× × ×) blank and NADH on carbon paste.

Fig. 2. Current–voltage curves for NADH(d) and NADPH(p) on glassy carbon in 0.1 *M* sodium phosphate, pH 7.3, at a scan rate of 50 mV s^{-1}. $[NADH] = 0.89 \cdot 10^{-3}$ *M*, $[NADPH] = 0.71 \cdot 10^{-3}$ *M*.

The glassy carbon electrode is more stable than is the carbon paste electrode and current–voltage curves were recorded using this electrode. Voltammetric curves on glassy carbon for NADH and NADPH in 0.1 *M* phosphate buffer, pH 7.3, are shown in Fig. 2. The waves are similar and show half-peak potentials at *ca.* +0.32 V *vs.* SCE, at a scan rate of 50 mV s^{-1}, for $8.9 \cdot 10^{-4}$ *M* NADH and $7.1 \cdot 10^{-4}$ *M* NADPH. The waves could not be resolved when recorded together. They are well defined and do not have the large residual current contribution found in their oxidation on platinum. The difference between the half-peak

potentials on glassy carbon and carbon paste, *i.e.* +0.64 V and +0.32 V, may be due to the formation and subsequent dissolution of NADH dimers at the carbon paste electrode surface[3]. The half-peak potential of the NADH voltammetric oxidation wave showed no pH-dependence between pH 5.5 and 8.3, at a scan rate of 20 mV s^{-1}. In addition, no clear change in the NADH anodic peak current, with changing pH, was apparent. A linear calibration curve of peak height *versus* concentration was obtained at pH 7.3 for NADH and NADPH over a range of 0–$5 \cdot 10^{-4}$ mole l^{-1} and 0–3 μA; the plots for the two compounds were the same. The linearity of the amperometric response is desirable, although not necessary, for kinetic analyses[14].

The feasibility of direct amperometric monitoring of enzyme reactions was investigated by following the production of NADH at the glassy carbon electrode. It has been suggested that interferences by oxidation of endogenous amines preclude the use of bare electrode amperometry in serum samples at high positive potentials[10,15]. Park *et al.*[16], however, have successfully determined uric acid in undiluted serum by amperometry with a carbon paste electrode at +0.64 V *vs.* Ag/AgCl. Figure 3 compares the residual current and voltammetric response of serum diluted (1+60) with 0.1 *M* phosphate, pH 7.3, and of serum diluted (1+60) containing added NADH in 0.1 *M* phosphate, pH 7.3, at a glassy carbon electrode. This illustrates the ability to detect the anodic oxidation of NADH in the presence of serum on glassy carbon. Oxidation of endogenous species occurs both slightly negative and positive to the NADH wave. Changes in current can be measured in their presence (*e.g.*, during enzyme reactions) since the current from these species is constant.

With an untreated electrode (carbon paste or glassy carbon), the current decays exponentially, slowly approaching an equilibrium value. The time-constant for this current decay is of the order of several minutes. A pre-treatment by constant potential electrolysis of a dilute serum solution at +0.75 V *vs.* SCE for several minutes may be performed. This results in a shorter current-decay time constant, of the order of 1 min or less, and decreases the time necessary for current stabilization preceding the subsequent enzymatic assays.

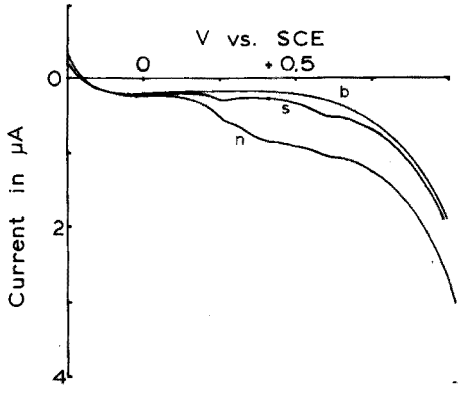

Fig. 3. Current–voltage curves for blank (b), serum diluted (1+60) (s), and serum diluted (1+60) plus NADH at $1.6 \cdot 10^{-4}$ *M* (n). Diluent is 0.1 *M* sodium phosphate, pH 7.3; the scan rate is 5 mV s^{-1}.

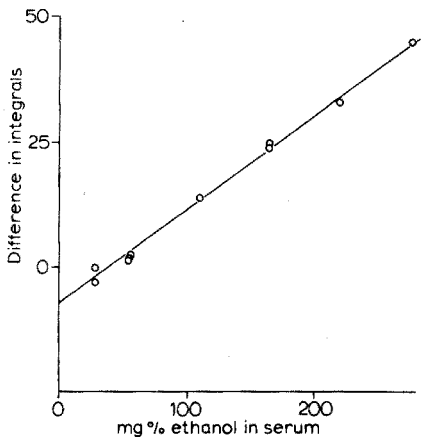

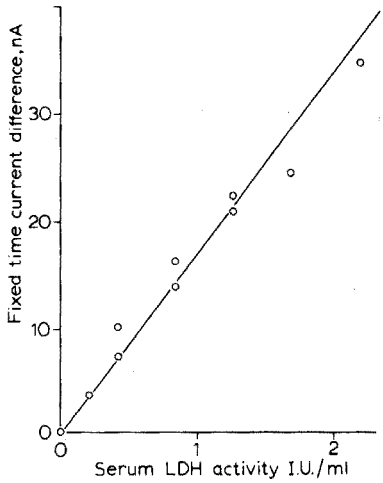

Fig. 4. Difference integral–concentration curve for ethanol in serum. Integral units are arbitrary.

Fig. 5. Fixed-time current difference–activity curve for LDH in serum.

Figure 4 shows a linear relationship between serum ethanol concentrations and the integrated amperometric current from the NADH produced by the enzymatic oxidation of ethanol:

$$CH_3CH_2OH + NAD^+ \xrightarrow{ADH} CH_3CHO + NADH + H^+$$

The calibration curve is in the range of physiological levels of blood ethanol expected after ingestion of alcoholic beverages[17], and was obtained by the described procedure (serum diluted *ca.* 1+80). The non-zero intercept is the result of a slight residual negative drift in the current at the electrode during the integration periods (see above).

Figure 5 shows the relationship between physiological levels of LDH in serum and a fixed-time change in NADH oxidation current resulting from the reaction:

$$\text{L-lactate} + NAD^+ \xrightarrow{LDH} \text{pyruvate} + NADH + H^+$$

Normal LDH levels in serum range from 20 to 100 I.U./l and high values usually range between 200 and 1000 I.U./l. These ranges were spanned by the experiment, with the serum samples diluted approximately (1+60). The precision of the technique, under conditions of a large stirring noise contribution, needs improvement. Experiments are underway in cell design to decrease stirring noise. In addition, Fig. 3 suggests that with a glassy carbon electrode in serum, the signal-to-noise ratio should be improved by using a somewhat less positive potential than +0.75 V *vs.* SCE. This direct amperometric monitoring of enzyme reactions is unique and demonstrates the feasibility of measuring reduced nicotinamide–adenine nucleotides in serum dehydrogenase assays.

Elevated ascorbic acid and uric acid levels in serum would be expected to contribute to the residual current[16], but these would be constant and would not

contribute to the net current changes in the present methods. The methods are simple, rapid, and could be readily automated.

SUMMARY

The electrochemical oxidations of reduced nicotinamide–adenine dinucleotide and reduced nicotinamide–adenine dinucleotide phosphate on platinum and carbon electrodes are described. Well defined voltammetric anodic waves are observed on carbon electrodes, with a linear relationship between peak height and concentration for 0–0.5 *mM* NADH and NADPH. Amperometric methods for NAD oxidoreductase analyses by direct electrochemical oxidation of the reduced nucleotide have been developed for lactic dehydrogenase and ethanol in serum.

REFERENCES

1 G. Sims, *Clinical Enzyme Primer*, Beckman Instruments, Fullerton, California, 1973.
2 *Manual of Clinical Enzyme Measurements*, Worthington Biochemical Corporation, Freehold, New Jersey, 1972.
3 P. J. Elving, J. E. O'Reilly and C. O. Schmakel in D. Glick (Ed.), *Methods of Biochemical Analysis, Vol. 21*, Interscience, New York, 1973, pp. 287–465.
4 D. Thevenot and R. Buvet, *J. Electroanal. Chem. Interfacial Electrochem.*, 39 (1972) 429.
5 D. Thevenot and R. Buvet, *J. Electroanal. Chem. Interfacial Electrochem.*, 40 (1972) 197.
6 J. N. Burnett and A. L. Underwood, *Biochemistry*, 4 (1965) 2060.
7 J. A. Cunningham and A. L. Underwood, *Arch. Biochem. Biophys.*, 117 (1966) 88.
8 W. J. Blaedel and R. G. Haas, *Anal. Chem.*, 42 (1970) 918.
9 W. J. Blaedel and R. A. Jenkins, *Anal. Chem.*, 46 (1974) 1952.
10 M. D. Smith, Ph.D. Thesis, Ohio State University, 1972.
11 D. L. Williams, A. R. Doig and A. Korosi, *Anal. Chem.*, 42 (1970) 118.
12 L. C. Thomas, G. D. Christian and J. D. S. Danielson, *Anal. Chim. Acta*, 77 (1975) 163.
13 R. N. Adams, *Electrochemistry at Solid Electrodes*, M. Dekker, New York, 1969.
14 S. R. Crouch in J. S. Mattson, H. B. Mark and H. C. MacDonald (Eds.), *Computers in Chemistry and Instrumentation, Vol. 3*, Dekker, New York, 1963, pp. 119–131.
15 R. I. Porterfield, Thesis, Ohio State University, 1972.
16 G. Park, R. N. Adams and W. R. White, *Anal. Lett.*, 5 (1972) 887.
17 W. S. Lovell, *Science*, 178 (1972) 264.

Analytica Chimica Acta, 78 (1975) 277–283

PHOTOCHEMICAL REDUCTION OF PHENOSAFRANINE BY EDTA AND ITS USE IN AMPEROMETRIC TITRATIONS

F. SIERRA, C. SANCHEZ-PEDREÑO, T. PEREZ, C. MARTINEZ and M. HERNANDEZ
Department of Analytical Chemistry, Faculty of Science, University of Murcia, Murcia (Spain)
(Received 24th January 1975)

The oxidation of aminopolycarboxylates by certain groups of dyes, *e.g.* thiazines and xanthines, under the excitation of light has been utilized in several ways since Merckel and Nickerson[1] presented their theoretical study of the photoreduction of methylene blue by EDTA[2,3]. The reducing character of EDTA in these photochemical reactions is unexpected, for, under oridinary conditions, oxidation of such organic materials requires the use of vigorous oxidants, strongly acidic media, and in some cases heating[4–7]. The mechanisms of these oxidation processes involving the thiazine dyes under the action of light are complicated and have not been completely clarified, despite several studies. Many investigators think that these photochemical reactions occur through a series of collisions between the protonated forms of the dyes in an excited triplet state with particular forms of the aminopolycarboxylate anion[7–11]. The total reaction is irreversible, yielding the leuco form of the dye and several products of oxidation of the polyaminopolycarboxylate.

In the present paper, some kinetic studies of the photochemical reaction between EDTA and 3,7-diamino-5-phenylphenazinium chloride (phenosafranine) are described; the dye belongs to the phenazine group which has known photosensitive properties. The research was then orientated towards different analytical applications. In this paper, the use of phenosafranine as a electrometric indicator in amperometric titrations of metal ions with EDTA is discussed.

EXPERIMENTAL

Reagents

Aqueous phenosafranine solutions (K and K) and standard EDTA solutions (dry primary standard disodium ethylenediaminetetraacetate dihydrate, Merck) were prepared.

Standard solutions of lead(II), zinc(II) and copper(II), were prepared from lead nitrate (Merck), electrolytic zinc (99.99%) dissolved in sulfuric acid, and copper sulfate pentahydrate standardized by electrogravimetry, respectively.

Buffer solutions were prepared by mixing a solution which was 0.1 *M* in phosphoric, acetic and boric acids with appropriate amounts of 1 *M* sodium hydroxide. The pH values were always checked with a Radiometer glass electrode pH-meter, model PHM63.

In amperometric titrations, a 1 *M* acetate buffer pH 5.5 was used.

All solutions were prepared from analytical reagent-grade chemicals with distilled–deionized water.

Apparatus

For kinetic measurements, a precision chronometer was used with a specially designed illumination device (built by Arrosu Electromedidas, Murcia). In this device (Fig. 1), the optical axis remained steady, and the light source (B) could be shifted along the optical path in order to obtain different light intensities. The light produced was passed through a small water-cooled chamber which was arranged so that several interference filters could be used. The reaction cell was thermostated at 30 ± 0.5°C. The photoelectric cell for the measurement of light intensity was connected to an electronic universal digital read-out.

The bleaching process of the phenosafranine was followed with a photometric titration unit (EEL-Unigalvo 200), a 604 filter being used.

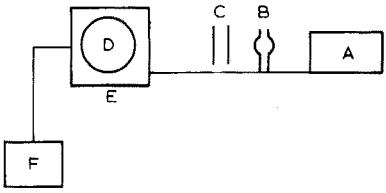

Fig. 1. Illumination device. A, d.c. source. B, Halogen lamp (24 V, 150 W bulb; Sylvania). C, Cooling system. D, Reaction cell. E, Filter support and thermostated stirrer. F, Selenium cell.

To obtain the voltammograms, a Radiometer rotating platinum wire-electrode was used. Amperometric titrations were carried out with a platinum electrode with an area of about 1 cm^2; a saturated calomel electrode was used as reference.

Procedure for photoreduction measurements

For the absorbance measurements, suitable volumes of phenosafranine, EDTA and buffer solution were placed in the reaction cell, and oxygen was removed by bubbling pure nitrogen (99.9997%) for 20 min through it. The sample was then illuminated and the decoloration time was measured with the photometric system outlined above.

The phenosafranine was considered colourless when its absorbance was reduced to 1/10 of its initial value.

Procedure for amperometric titrations

The sample of Pb(II), Zn(II) or Cu(II) was placed in a 100–150-ml reaction cell; 2–6 ml of buffer solution (pH 5.5) and 2 ml of 0.001 *M* phenosafranine solution were added, and the mixture was diluted with water to 40–50 ml. A constant stream of nitrogen was maintained through the solution during the titration. After some minutes, the sample was illuminated with a 300-watt halogen or tungsten lamp placed at a distance of *ca.* 30 cm. The rotating platinum anode was held at a constant potential of 100 mV against the SCE. The titrant (0.1–0.001 *M* EDTA) was added from a microburette in increments of 0.5 ml as long as the current

remained constant and in 0.05-ml in the vicinity of the equivalence point, when the current began to increase.

The measured current corresponds to the anodic oxidation of the phenosafranine reduced by excess of EDTA. The current was read at regular intervals of time, usually 2 min. In titrations of very dilute solutions (10^{-3}–10^{-4} *M*) with 0.001 *M* EDTA, the titrant was added in 0.1-ml increments at 3-min intervals.

THE PHOTOREDUCTION OF PHENOSAFRANINE

When a solution containing phenosafranine and EDTA, at suitable pH and in the absence of oxygen, is illuminated with white light, photoreduction of the dye occurs, and the pink colour disappears. The total reaction is:

$$\underset{\text{(pink)}}{\text{Phenosafranine}_{ox.}} + \text{EDTA} \xrightarrow{\text{light}} \underset{\text{(colourless)}}{\text{Phenosafranine}_{red}} + \text{Oxidation products of EDTA} \quad (1)$$

The reaction proceeds at an adequate rate only if the light is sufficiently intense. If air is passed through the colourless solution, the dye is oxidized very quickly, returning to its original pink colour. Figure 2 shows the absorption spectra of the dye before reduction and then after the oxidation with hydrogen peroxide of the leucophenosafranine formed by photoreduction.

Effect of experimental variables

To study the influence of pH on the rate of the photochemical reaction, several samples which were 10^{-5} *M* in phenosafranine and 10^{-3} *M* in EDTA,

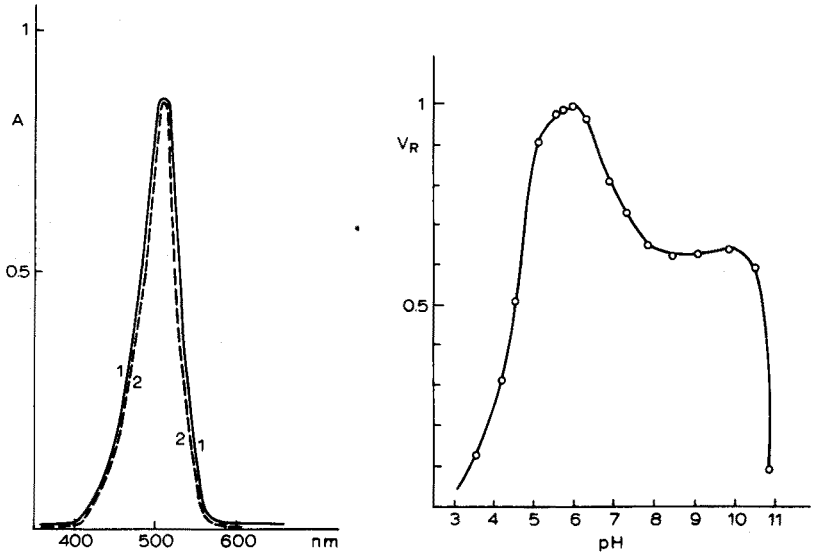

Fig. 2. Absorption spectrum for a solution containing $2 \cdot 10^{-4}$ *M* phenosafranine, $2 \cdot 10^{-3}$ *M* EDTA and acetate buffer. Curve 1: Before the photochemical process. Curve 2: After the photochemical process and reoxidation with hydrogen peroxide.

Fig. 3. Rate of photoreduction as a function of pH.

were adjusted to different pH values in the range 3.5–11. Figure 3 shows the result obtained by plotting the rate of photoreduction (expressed in relation to its maximum value) as a function of pH. The reaction rate is at a maximum at about pH 6 and becomes practically zero below pH 3 or above pH 11.

The photoreduction rate of phenosafranine was studied at different values of light intensity, for solutions which were 10^{-5} *M* in phenosafranine and $4 \cdot 10^{-3}$ *M* in EDTA, buffered at pH 6. Between 3000 and 17000 lux, the decoloration rate is directly proportional to the illumination. The reaction rate is maximal when the wavelength of the radiation corresponds to the wavelength of maximum absorbance of the dye, *i.e.* 510 nm.

Variations in temperature between 18 and 80°C have little influence on the rate of the photochemical process.

To study the influence of the dye concentration, the time necessary to complete definite fractions of reaction was measured in samples which contained $4 \cdot 10^{-3}$ *M* EDTA at pH 6 and different concentrations of phenosafranine between $4 \cdot 10^{-5}$ *M* and 10^{-6} *M*. The rate of the process was found to be proportional to the square root of the dye concentration.

Inhibitors of the photochemical process

As indicated above, the photooxidation of EDTA by phenosafranine does not occur—at least with any appreciable speed—in very acidic (pH < 3) or alkaline (pH > 11) media.

EDTA is not photooxidized by phenosafranine if metal–EDTA chelates which are sufficiently stable under the conditions used have been formed.

It is interesting to note that substances such as *p*-phenylenediamine and iodide, even in small amounts, considerably decrease the rate of the photochemical reaction. This effect can be used for the determination of traces of iodide[12].

Mechanism of the reaction

As has been stated, the reaction between EDTA and phenosafranine is irreversible, yielding as final substances oxidation products of EDTA (probably amine oxides) and leucophenosafranine. The different variables that affect this photochemical process indicate that the kinetic behaviour is similar to that found in the reaction between EDTA and thiazine dyes, especially with regard to the close relationship existing between the reaction rate and the pH, and the inhibitory effect of substances such as iodide and *p*-phenylenediamine, which are typical deactivators of excited triplet states.

The mechanism of the reaction between phenosafranine and EDTA is probably analogous to that suggested by several investigators[8–11,13] for the photochemical reaction between EDTA and methylene blue or thionine. In these, the process is thought to be initiated by protonated molecules of the dye which are promoted to the excited triplet state, followed by collisions with the anionic forms YH^{3-} and Y^{4-} of EDTA, which do not possess protonated nitrogen atoms.

AMPEROMETRIC TITRATIONS

The titration with EDTA of a metal ion at a suitable pH in the presence

of a small amount of phenosafranine, under irradiation in an inert atmosphere, takes place in two steps. First, the metal–EDTA chelate is formed, and when all the metal ion has been complexed, the photochemical reaction proceeds according to eqn. (1). The end point can be detected by the amperometric method which conveniently shows the appearance of the reduced form of phenosafranine.

Electrochemical behaviour of phenosafranine at a platinum rotating electrode

The voltammograms were recorded for solutions containing 0.01 *M* EDTA, acetate buffer pH 5.5 and 0.1 *M* potassium chloride as supporting electrolyte; the scan rate was 0.1 V min^{-1}. Figure 4 shows the current–potential curves for the supporting electrolyte (curves 1 and 2) and for solutions of $5 \cdot 10^{-4}$ *M* phenosafranine in its oxidized (curve 3) and reduced (curve 4) forms. The voltammogram corresponding to a mixture which was approximately equimolecular in the two forms of phenosafranine is shown in Fig. 4(b). The equilibrium potential was found to be −0.55 V *vs.* SCE, which agrees with the literature values[14,15]. As can be observed in Fig. 4(b) phenosafranine acts as an almost ideally reversible system under the experimental conditions used.

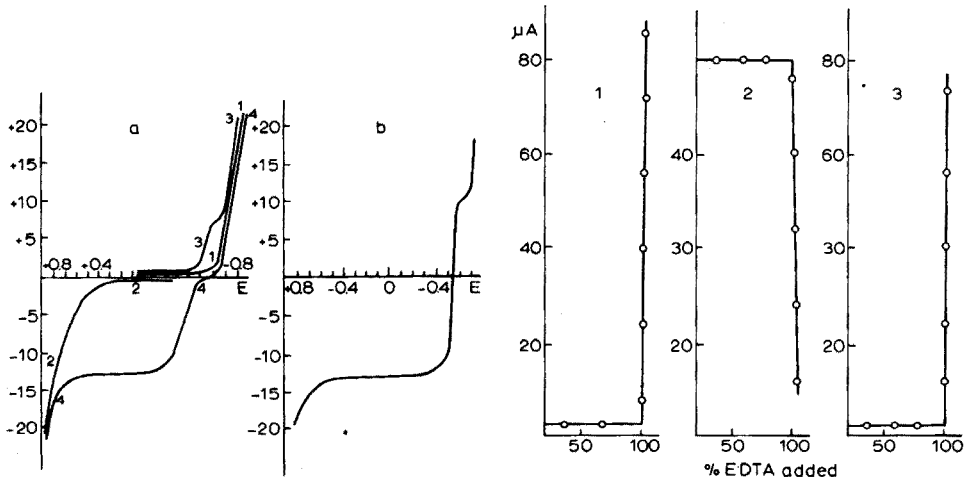

Fig. 4. Current–potential curves. (a) Curves 1 and 2: supporting electrolyte. Curve 3: phenosafranine$_{ox}$. Curve 4: phenosafranine$_{red}$. (b) The curve for an equimolecular mixture of the two forms of the dye.

Fig. 5. Amperometric titration curves of zinc(II) with 0.01 *M* EDTA as amperometric indicator. 1, Applied potential. +100 mV (*vs.* S.C.E.). 2, Applied potential. −580 mV (*vs.* S.C.E.). 3, With two indicator electrodes at an applied potential of 100 mV.

Phenosafranine as a photoredox indicator in amperometry

From the current–potential curves obtained, the optimal conditions for amperometric titrations with this indicator system can be established. Thus, for titrations with an indicator platinum electrode at an applied potential between −0.2 V and +0.50 V (*vs.* SCE), the titration curve will have a reversed L-shape; at applied potentials between −0.55 V and −0.60 V (*vs.* SCE), the titration

curve will have an inverted L-shape. When titrations are done with two indicator platinum electrodes at an applied potential of 100 mV, a reversed L-curve is obtained. In all cases, the current changes only after the equivalence point when free EDTA is present to start the photochemical process; the current is directly proportional to the excess of titrant.

Figure 5 shows the curves obtained for the titration of zinc(II) with EDTA in the presence of phenosafranine as an amperometric indicator under the above conditions.

The best results were obtained when the applied potential lay between −0.2 V and +0.50 V, the single indicator electrode acting as anode. The current then corresponds to the oxidation process of leucophenosafranine after the equivalence point. A potential of 0.1 V *vs.* SCE was preferred.

The general method for the titration of metal ions was applied to the determinations of Zn(II), Pb(II) and Cu(II) in a buffered medium at pH 5.5; at this pH the photochemical reaction between phenosafranine and EDTA is sufficiently fast. Typical results are shown in Table I.

TABLE I

AMPEROMETRIC TITRATION OF LEAD, ZINC AND COPPER IN 0.02 *M* ACETATE BUFFER (pH 5.5) WITH EDTA

Pb taken (mg)	*Pb found (mg)*	*Error (%)*	*Zn taken (mg)*	*Zn found (mg)*	*Error (%)*	*Cu taken (mg)*	*Cu found (mg)*	*Error (%)*
207.2	208.2	+0.50	65.38	65.90	+0.80	31.77	31.68	−0.30
103.6	103.1	−0.45	32.69	32.49	−0.60	15.88	15.95	+0.45
51.80	52.41	+0.75	16.34	16.40	+0.35	12.71	12.65	−0.45
20.72	20.76	+0.20	6.538	6.512	−0.40	6.354	6.298	−0.50
10.36	10.40	+0.40	3.269	3.243	−0.80	3.177	3.182	+0.15
2.072	2.063	−0.45	1.308	1.305	−0.23	1.271	1.268	−0.25
1.036	1.042	+0.60	0.327	0.325	−0.60	0.635	0.630	−0.80
0.414	0.416	+0.50	0.131	0.130	−0.50	0.127	0.128	+0.45

SUMMARY

Phenosafranine in the presence of ethylenediaminetetraacetic acid is reduced to the leuco dye form on illumination with white light. The rate of photoreduction is strongly pH-dependent and exhibits a maximum at about pH 6. Variables such as wavelength and intensity of the light and the concentration of reactants have been studied. The photoreduction involves a long-lived excited state of the dye and is retarded by small amounts of *p*-phenylenediamine and iodide. The dye is used as an amperometric indicator in titrations of Pb(II), Zn(II) and Cu(II) with EDTA; the method is applicable in the range 0.02–0.0005 *M*. The current is caused by anodic oxidation of the phenosafranine reduced in the photochemical reaction with EDTA.

REFERENCES

1 J. R. Merckel and W. J. Nickerson, *Biochim. Biophys. Acta*, 14 (1954) 303.
2 J. Joussot-Dubien and G. Oster, *Bull. Soc. Chim. Fr.*, 67 (1960) 343.
3 F. Sierra, C. Sánchez-Pedreño, C. Martinez and T. Pérez, *An. R. Soc. Esp. Fis. Quim.*, 68 (1972) 1091; *Inform. Quim. Anal.*, 25 (1971) 73; 27 (1973) 93; *An. R. Soc. Esp. Fis. Quim.*, 70 (1974) 595.
4 F. Bermejo Martinez and R. Rey Mendoza, *An. R. Soc. Esp. Fis. Quim.*, 55B (1954) 309.
5 M. T. Beck, *Chem. Anal.*, 50 (1961) 14.
6 M. T. Beck and O. Kling, *Acta Chem. Scand.*, 15 (1961) 433.
7 P. N. Palei and V. N. Udaltoova, *Zh. Anal. Khim.*, 16 (1961) 649.
8 G. Oster and N. Wotherspoon, *J. Amer. Chem. Soc.*, 79 (1957) 4836.
9 J. Joussot-Dubien and J. Faure, *J. Chim. Phys.*, 91 (1963) 1214.
10 J. Faure and J. Joussot-Dubien, *J. Chim. Phys.*, 63 (1966) 621.
11 M. Nemoto, K. Hiroshi and M. Kuizumi, *Bull. Chem. Soc. Jap.*, 42 (1969) 2464.
12 F. Sierra, C. Sánchez-Pedreño, T. Pérez, C. Martinez and M. Hernández, *Anal. Chim. Acta*, in press.
13 H. G. Langer, *Inorg. Chem.*, 2 (1963) 1080.
14 W. L. Hall, P. W. Priesler and B. Cohen, *Public Health Reports (U.S.), Suppl.* (1928) 71.
15 M. Brezina and P. Zuman, *Polarography in Medicine, Biochemistry and Pharmacy*, Interscience, London, 1958.

Analytica Chimica Acta, 78 (1975) 285–292

DIRECT ANALYSIS OF BLOOD, URINE, SEA WATER, FILTER PAPER, AND POLYETHYLENE BY ATOMIC ABSORPTION SPECTROMETRY WITH THE "HOLLOW-T" ATOMIZER

JAMES W. ROBINSON, DUANE K. WOLCOTT and LARRY RHODES

Chemistry Department, Louisiana State University, Baton Rouge, Louisiana 70803 (U.S.A.)

(Received 20th November 1974)

In recent years numerous atomization devices for atomic spectrometry have been developed[1–5]. They are all electrically heated and atomize by rapid heating to temperatures up to 2800°C. Unfortunately the absorption signals generated by such electrothermal atomizers are subject to both chemical and spectral interferences. Different chemical forms of the sample decompose at different rates and cause significant chemical interference effects. West and co-workers[6] have carried out at least one extensive study of this effect. Spectral interferences are due to overlap of molecular absorption bands with atomic absorption lines of interest[7]. Scattering by salt particles, "smoke", and other partially decomposed matrix materials also contributes to broad-band spectral scattering[8]. In a few cases, corrections can be made for broad-band spectral interference[9–11] but the broad-band absorption is usually too strong for correction.

Under these conditions, the molecular background can be reduced by utilizing a three-stage atomization process to remove solvent and matrix material. Such a three-step technique has been shown to result in loss of some of the more volatile sample elements during the drying and ashing steps[12,13]. An excellent study of the problems caused by heavy matrix effects has been made by Cruz and Van Loon[14].

In 1970, Robinson *et al.*[15] reported on the development of a radiofrequency carbon bed atomizer which was used for the direct analysis of air for metals. The carbon bed atomizer was shown greatly to reduce molecular absorption interference by organic solvents[16] and to be suitable for the direct analysis of liquids[13]. Unfortunately, the atomizer used quartz tubing which softens at 1650°C, hence the temperature attainable in the carbon bed was limited to *ca.* 1600°C, which was too low for atomization of many less volatile elements.

To overcome the temperature limitations of the carbon bed atomizer, the "hollow-T" atomizer was designed[17]. Use of this atomizer reduced spectral interference from molecular absorption, reduced chemical interference from different volatility rates of different chemical forms, and increased the analytical sensitivity. In addition, it was easy to determine metals with low volatility with this atomizer.

The design and operation of the hollow-T in the continuous-flow mode has been previously discussed[17]. This paper reports on a new "stop-flow" mode of operation which results in the virtually complete elimination of molecular absorption interference, and removes the necessity for a three-stage atomization process as in

other flameless atomizer designs.

EXPERIMENTAL

Equipment

The following items were used: Barnes demountable hollow cathode and cathode elements, hollow-cathode power supply (Barnes GPS-1), deuterium lamp, deuterium lamp power supply, Jarrell-Ash 0.5-m Ebert monochromator with variable slit, photomultiplier power supply (Hewlett Packard 6515A), Heathkit photometric readout, Beckman 10-in. potentiometric recorder, hollow-T atomizer, Signal Transformer Co. Model 12–500 step-down transformer, and solid-state power control.

Chemicals and supplies

Metal standard solutions (1000 p.p.m.) were diluted as required. Filter paper discs (Whatman 44, 6 mm dia.) and polyethylene tubes (Intramedic, 1.5 mm dia. × 4 mm) were used. The organic solvents used were 2-propanol, formic acid, ethyl propionate, hexane, and benzene.

Modification of hollow-T atomizer to allow stop-flow operation

The atomizer design was the same as that previously reported, except for the addition of a three-way valve in the exhaust line (Fig. 1). Initially, only a ball valve (2-way on–off) was used, but it was found to be unsatisfactory. As the exhaust flow pump was in continuous operation, when the ball valve was closed, the entire line between pump and valve was pumped out producing a volume under relatively low pressure. When the valve was opened, this vacuum caused the sample to be drawn through the atomizer at an increased rate which the readout system could not record accurately. The three-way valve eliminated the problem by preventing a build-up of vacuum in the exhaust line.

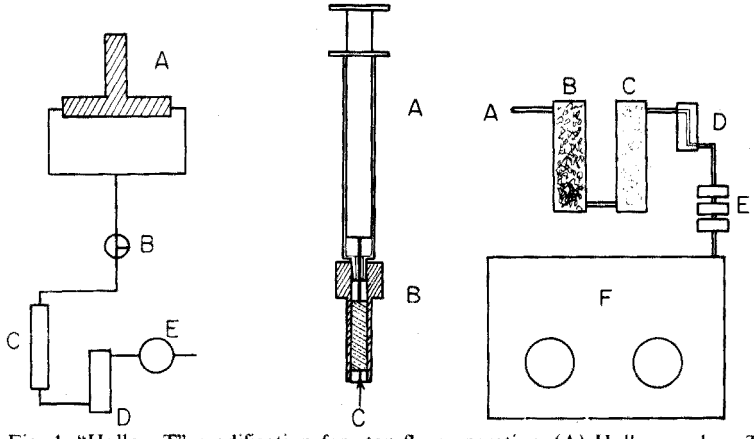

Fig. 1. "Hollow-T" modification for stop-flow operation. (A) Hollow carbon T, (B) three-way valve, (C) scrubber, (D) flowmeter, (E) diaphragm vacuum flow pump.

Fig. 2. Solid injector for "Hollow-T". (A) Modified tuberculin syringe, (B) teflon barrel, (C) teflon plunger.

Fig. 3. "Clean box" for handling ultra-trace samples. (A) Air inlet, (B) silica gel (12 in.), (C) activated charcoal (12 in.), (D) flowmeter, (E) particulate filters (2 μm), (0.45 μm), (0.1 μm).

Sample injection

Liquids. Liquid samples were introduced into the atomizer with the modified Drummond Micropipette that has been previously described[17]. Samples were injected directly into the hot stem of the atomizer without any pretreatment.

Solids. Solid samples were introduced into the atomizer with a specially constructed solid injector (Fig. 2). By using different sizes of Teflon barrels different sample media (*e.g.* filter paper or polyethylene tubes) could be handled. In practice, solid samples were injected directly into the hot stem of the T atomizer without any type of pretreatment.

Sample handling

All samples were transferred, pipetted, loaded, etc. inside a Plexiglas clean-box, which was maintained under a positive pressure of clean air (Fig. 3).

Most liquid samples were handled and stored in snap-cap polyethylene vials of the type utilized for neutron activation. An exception was the blood sample which was stored in a standard vacuum blood collection tube (Pyrex). Glass barrels were used in the modified micropipettes.

Solid samples were handled with stainless-steel forceps and FEP teflon sample trays. Paper disc samples were punched out of a 47-mm disc with a stainless-steel office punch and stored in a snap-cap polyethylene vial.

Atomizer operation—the stop-flow process

The flowing gas was argon. First, the flow was stopped and the samples were introduced directly into the stem of the T-shaped atomizer, which was maintained at 2700°C throughout the analysis. After the sample was introduced, stop-flow conditions were maintained for a period of time ranging from 2 to 10 s. During this period, decomposition of the metal compound and decomposition and combustion of the solvent took place. The time varied with the solvent used, but was long enough to permit complete breakdown and complete atomization. The delay period was timed with a stopwatch. At the end of the delay time the gas flow was resumed, and the decomposed sample was swept into the cross-bar of the T; the latter was in the light path of the instrument, and atomic absorption measurements were made.

RESULTS

Reduction of molecular background

A study of molecular background absorption was undertaken. The solvents were injected directly into the atomizer T and held under conditions of stopped flow for varying lengths of time. The results (Fig. 4) indicated that molecular absorption spectral interference was reduced to less than 2% absorption after a delay period of 5 s or less for all except the most persistent matrix materials. The materials causing the greatest molecular interference were benzene and polyethylene, since they decompose directly to hydrogen and free carbon. However, even for these materials, molecular absorption was reduced to negligible levels after a delay time of about 10 s.

Analysis of aqueous solutions

Sea water. Samples of sea water (2 μl) were injected directly into the stem of

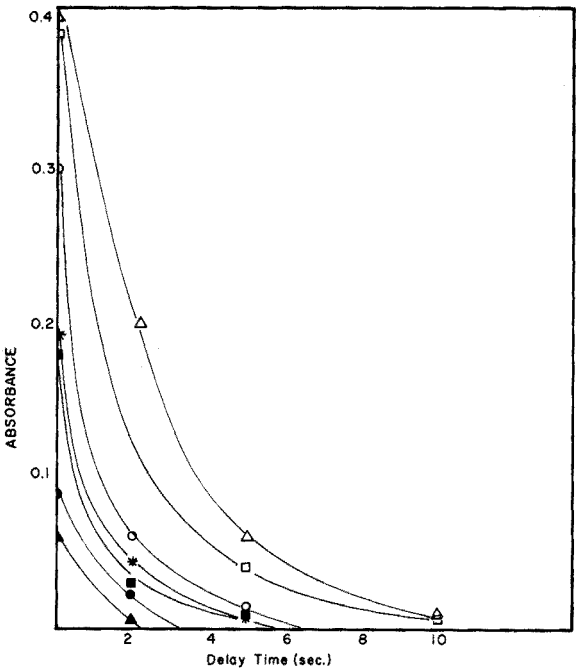

Fig. 4. Reduction of molecular background by "stop-flow" technique. (●) 2-Propanol. (▲) Formic acid. (■) Ethyl propionate. (○) Hexane. (△) Benzene. (□) Polyethylene. (*) Filter paper + blood.

TABLE I

ANALYSIS FOR LEAD IN SEA WATER AND URINE

(In all analyses, the monochromator slitwidth was 50 μm, the lamp current was 50 mA and the argon flow rate was 50 ml min^{-1}.)

	Sea-water samples		*Urine sample*
Analytical wavelength (nm)	283.3	217.0	217.0
Photomultiplier voltage (V)	450	600	600
Atomic signal (A.U.)	0.015 ± 0.004	0.097 ± 0.008	0.044 ± 0.003
Molecular background	0.004 ± 0.002	0.010 ± 0.008	0.010 ± 0.003
Lead concentration ($\mu g\ ml^{-1}$)	0.11	0.12	0.05

the atomizer without any pretreatment, and the lead content was determined at the 283.3-nm or 217.0-nm resonance lines. The molecular absorption was measured at these wavelengths with a deuterium lamp. A summary of the analytical conditions and results is given in Table I. The sea-water samples contained 0.12 μg Pb ml^{-1}. Molecular absorption at 283.3 nm was less than 0.004 absorbance units, but was higher at 217.0 nm. After decomposition of organic material, hydrogen is formed which absorbs at shorter wavelengths. The increase at 217.0 nm can be attributed to the greater absorptivity of hydrogen at these wavelengths.

Urine. Urine samples were analyzed in the same manner as sea water (*e.g.*, direct injection of the sample into the atomizer with no pretreatment). The results

of analysis of urine for lead content are also given in Table I. These data indicated a lead level in urine of 0.05 μg ml^{-1}, which was in good agreement with the range of levels given by Christian and Feldman[18]. Molecular absorption was also measured with results similar to those obtained in the sea-water analysis. The spectral interference was less than 1% at 283.3 nm. and somewhat greater (3%) at 217.0 nm.

Analysis of solid samples

Polyethylene. Samples of polyethylene tubing were analyzed for copper and lead by direct injection into the stem of the hot atomizer T. The stop-flow method was used to eliminate molecular absorption. Results of the analyses for copper and lead in polyethylene are given in Table II.

TABLE II

DIRECT ANALYSIS FOR COPPER AND LEAD IN POLYETHYLENE

	Copper	*Lead*
Analytical wavelength (nm)	324.7	217.0
Monochromator slitwidth (μm)	25	50
Photomultiplier voltage (V)	400	600
Lamp current (mA)	35	50
Atomizer argon flow (ml min^{-1})	50	50
Wt. of polyethylene (mg)	22.2 ± 0.09	22.2 ± 0.09
Atomic signal (Absorbance unit)	0.098 ± 0.008	0.53 ± 0.04
Molecular signal (Absorbance unit)	0.007 ± 0.002	0.022 ± 0.003
Metal concentration (μg g^{-1})	9.0 ± 0.5	0.36 ± 0.04

Polyethylene was chosen for analysis for a number of reasons: (a) it is widely used for containers for trace analysis, (b) it has been previously shown that polyethylene can be cleaned of trace metals[19], and (c) it would be convenient if powder samples could be loaded into polyethylene and injected directly into the atomizer for analysis.

Filter paper. Filter paper was chosen as a sample for a number of reasons: (a) in pollution analysis, particulate samples are collected on filter papers; (b) filter paper is a convenient material for use in immobilizing trace metals in liquid samples for storage and transport; (c) if filter paper could be used as a sample transport medium, almost any desired degree of preconcentration could be obtained by multiple application and drying steps of liquid samples to a filter-paper disc; (d) filter paper can be used for direct analysis of blood samples. In each case it is important to know the blank level of the filter paper.

Filter-paper discs (6-mm dia.) were cut from typical filter papers and were injected directly into the hot atomizer stem, using the solids injector (Fig. 2). Both the copper and lead contents were determined. The results are given in Table III. Calibration was carried out by standard addition; a typical curve is shown in Fig. 5. Molecular absorption interference was reduced to less than 1% absorption at both the 324.7-nm and the 217.0-nm bandpasses.

The manufacturer's literature for the filter paper gave values of <0.1 ng 6 mm disc for lead and 5 ng/6 mm disc for copper. Values were obtained by flame a.a.s.

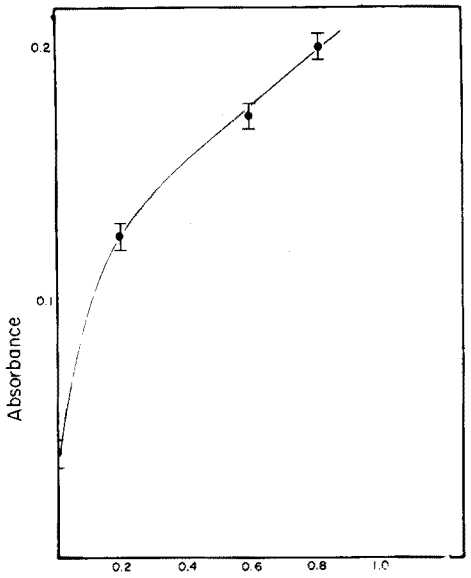

Fig. 5. Lead in filter paper. Standard addition curve.

TABLE III

DIRECT ANALYSIS FOR COPPER AND LEAD IN FILTER PAPER

(Analytical parameters were the same as those in Table II.)

	Copper	*Lead*
Weight of paper (mg)	2.6±0.3	2.6±0.3
Atomic signal (A.U.)	0.046±0.007	0.037±0.007
Molecular signal (A.U.)	0.003±0.001	0.004±0.002
Metal concentration (ng/disc)	4.9±0.2	0.096±0.009
Manufacturer's value (ng/disc)	5	<0.1

for lead and spectrophotometry for copper. These values were in good agreement with those obtained in this study.

Analysis of whole blood

Analysis for trace metals in blood is extremely important for an understanding of many branches of medicine. For elemental analyses, atomic absorption has become the method of choice, especially for the determination of lead in blood[20–23]. Attempts have been made to determine lead in blood directly[24,25] but have met with difficulty owing to the large and variable amount of molecular absorption arising from the complex organic and inorganic matrix of whole blood.

It has been demonstrated that the hollow T atomizer virtually eliminates molecular absorption, hence direct blood analysis should be feasible. However, initial attempts to inject liquid whole blood directly into the atomizer failed. It was difficult to eject reproducibly the viscous whole blood from the liquid sampler and this caused

high imprecision in the results. To overcome these difficulties, it was decided to immobilize the blood sample on a filter paper disc and eject the entire disc plus blood into the atomizer. The results obtained for lead in blood are given in Table IV.

TABLE IV

DIRECT ANALYSIS FOR LEAD IN WHOLE BLOOD

(Analytical parameters were the same as those in Table II.)

Atomic absorbance (paper + blood)	0.108 ± 0.004
Atomic absorbance (paper only)	0.044 ± 0.004
Molecular absorbance	0.008 ± 0.002
Lead concentration	15 μg/100 ml

Initial results on the fresh blood sample gave a blood lead level of 25 μg/100 ml. This level is in good agreement with those given for "typical" blood lead levels[26]. It should be noted however, that after the blood sample had been stored in a glass container at room temperature for a week the analytical results indicated a blood lead level of 15 μg/100 ml, thus indicating a loss of lead from the blood sample to the walls of the container. However, no special precautions had been taken to prevent such losses. The only treatment given the sample was the addition of 40 mg of Ca_2EDTA to prevent coagulation. Immediate transfer of blood to the paper disc after withdrawal should immobilize the trace metals and prevent such absorptive losses to container walls.

The molecular absorption interference of the blood–paper samples was reduced to the level of 0.008 absorbance unit by the stop-flow technique and thus presented no difficulty in the analysis.

DISCUSSION

The hollow T atomizer has been shown to be suitable for the direct analysis of paper, polyethylene, blood, urine, and sea water. Molecular absorption has been greatly reduced by the stop-flow methods. It should be noted that the sensitivities obtained for analysis of these samples were less than those obtained by direct injection in a flowing system[18]. This discrepancy was due to the fact that an optimum flow rate was used for maximum absorption signal, but the objective of the stop-flow method was to minimize molecular absorption. The delay used to create optimum conditions for elimination of background resulted in a loss in free atoms, presumably by diffusion through the cell walls. A loss in analytical sensitivity resulted. It is necessary to determine optimum conditions to complete atomization as quickly as possible and reduce sample loss by diffusion through the cell walls. These conditions will probably vary slightly from sample to sample, depending on the principal anion present and the predominant solvent in the sample.

L'Vov, using his flameless atomizer, stated that diffusion was the only mechanism of loss of free atoms from the light path[1]. Since the delay times were as high as 15 s, it is not surprising that some sample losses occur during the stop-flow

delay period. Loss of sensitivity also indicated increased porosity, as the atomizer carbon became porous after long periods of operation. Such a loss in sensitivity was not noted in the continuous-flow mode of operation. Various techniques are available for prevention of sample diffusion[26,27]. In particular, the use of pyrolytic graphite has been suggested[28]. The grade of carbon chosen for atomizer construction was chosen for low trace metal contamination rather than minimum diffusion. Plans are underway to utilize a less porous graphite to eliminate the problem.

The authors would like to thank Dr. Joe A. Bowden of the LSU-BR Biochemistry Department for his assistance in obtaining the blood samples used.

SUMMARY

The hollow-T atomizer developed for atomic absorption spectrometry greatly reduces chemical interferences and background absorption. The widespread utility of the atomizer has been demonstrated by carrying out direct analyses on untreated samples of blood, urine, polyethylene, filter paper, and sea water.

REFERENCES

1 B. V. L'Vov, *Spectrochim. Acta*, 17 (1961) 761.
2 T. S. West and X. K. Williams, *Anal. Chim. Acta*, 45 (1969) 27.
3 R. Woodriff and G. Ramelow, *Spectrochim. Acta*, 2313 (1968) 665.
4 J. Y. Hwang, P. A. Ulucci, S. B. Smith and A. L. Malenfant, *Anal. Chem.*, 43 (1971) 1319.
5 H. Massmann, *Anal. Chem.*, 225 (1967) 203.
6 L. Ebdon, G. F. Kirkbright and T. S. West, *Anal. Chim. Acta*, 58 (1972) 39.
7 J. R. Koirtyohann and E. E. Pickett, *Anal. Chem.*, 37 (1965) 601.
8 H. L. Kahn, *At. Absorption Newslett.*, 7 (1968) 40.
9 B. V. L'Vov, *Atomic Absorption Spectrochemical Analysis*, Elsevier, New York, 1970.
10 J. W. Robinson, *Atomic Absorption*, Dekker, New York, 1960.
11 T. Hadeishi, D. A. Church, R. D. Mehaughlin, B. D. Zak and M. Nakamura, *USAEC Bulletin LBL-1593*, February 1973.
12 C. W. Fuller, *Anal. Chim. Acta*, 62 (1972) 442.
13 J. W. Robinson, D. J. Slevin, D. K. Wolcott and G. D. Hindman, *Anal. Chim. Acta*, 66 (1973) 13.
14 R. B. Cruz and J. C. Van Loon, *Anal. Chim. Acta*, 72 (1974) 231.
15 H. P. Loftin, G. M. Christian and J. W. Robinson, *Spectrosc. Lett.*, 3 (7) (1970) 161.
16 J. W. Robinson, P. J. Slevin and G. D. Hindman, *Anal. Chim. Acta*, 66 (1973) 165.
17 J. W. Robinson and D. K. Wolcott, *Anal. Chim. Acta*, 74 (1975) 43.
18 G. D. Christian and F. J. Feldman, *Atomic Absorption Spectroscopy*, Wiley–Interscience, New York, 1970, p. 408.
19 Duane K. Wolcott, Ph.D. Dissertation, Louisiana State University, Baton Rouge, 1972.
20 P. P. Donovan and D. T. Feely, *Analyst (London)*, 94 (1969) 879.
21 H. T. Delves, G. Shepherd and P. Vinter, *Analyst (London)*, 96 (1971) 260.
22 H. L. Kahn and J. S. Sebestyen, *At. Absorption Newslett.*, 9 (1970) 33.
23 E. Norval and L. R. P. Butler, *Anal. Chim. Acta*, 58 (1972) 47.
24 T. R. Hauser, T. A. Hinners and J. L. Kent, *Anal. Chem.*, 44 (1972) 1819.
25 J. Y. Hwang, P. A. Ulucci and C. J. Mokeler, *Anal. Chem.*, 45 (1973) 795.
26 D. A. Boyland, *G.E.C. Atomic Energy Review*, 2 (1) (1959) 44.
27 W. Watt, R. L. Bickerdike, A. R. G. Brown, W. Johnson and G. Hughes, *Nuclear Power*, February (1959) 86.
28 C. L. Chakrabarti, R. Pal and M. Katyal, *Anal. Chem.*, 43 (1971) 1704.

Analytica Chimica Acta, 78 (1975) 293–298

THE DETERMINATION OF TITANIUM IN IRON AND STEEL BY ATOMIC ABSORPTION SPECTROMETRY

W. D. COBB, W. W. FOSTER and T. S. HARRISON

Group Chemical Laboratories, British Steel Corporation, Scunthorpe DN16 1BP (England).

(Received 8th January 1975)

The application of atomic absorption spectrometry to the determination of titanium in iron and steel has been limited by the lack of sensitivity. Amos and Willis[1] reported enhancement of the titanium absorption in the presence of hydrochloric acid and iron, whilst Headridge and Hubbard[2] reported enhancement with hydrofluoric acid and ethanol. Kirkbright *et al.*[3] developed an amplification procedure in which molybdotitanophosphate is extracted into butanol, and the absorbance of molybdenum is measured. Nakahara *et al.*[4] reported enhancement of titanium absorption and suppression of interferences in the presence of 5000 p.p.m. aluminium.

Attempts to determine titanium in this laboratory showed interfering effects —usually enhancements—from other elements such as chromium, nickel and aluminium. The effects of lanthanum and aluminium on the titanium absorption and on the interferences shown by other elements in irons and steels were therefore studied further.

Preliminary tests

Since a fusion is needed to recover any insoluble titanium oxide, titanium cannot be included in the general scheme of analysis[5]. However, if the hydrochloric acid–nitric acid solution[5] is filtered, and any residue is fused with a (3+1) mixture of sodium carbonate and boric acid, extracted and added to the main solution, total aluminium may be determined in the same initial sample solution before aliquots are taken for determination of titanium.

The following tests were based on a titanium concentration of 16 p.p.m. (*ca.* 0.16%). The acid, flux and iron concentrations were maintained at the levels given in the recommended method. For the atomic absorption spectrometry, maximal absorbance was obtained with a fuel-rich slightly luminous flame with a red feather 20–25 mm high. Some carbon build-up made it necessary to scrape the burner slot after every two or three readings. For higher concentrations of titanium when maximal sensitivity is not required, a less fuel-rich flame may be used to minimize this problem. For each batch of tests the instrument was set against the reference solution containing 16 p.p.m. titanium, the scale expansion being adjusted to give a reading of 40 scale divisions.

The effects of diverse elements, in concentrations relevant to steel analysis, were examined in the presence of the recommended concentrations of acid, flux and iron without a spectroscopic buffer. Enhancements were observed for nickel, chromium, molybdenum, aluminium and vanadium, and suppressions for phosphorus,

TABLE I

THE EFFECTS OF OTHER ELEMENTS

(The synthetic solution contained the equivalent of 0.16% Ti in a sample. The amounts of the other elements correspond to their percentages in samples.)

Composition of synthetic solution											*Ti found (%)*	
Ni	*Cr*	*Mo*	*Co*	*Cu*	*Al*	*Al*	*Mn*	*V*	*P*	*Fe*	*Al present*	
											Nil	*500 p.p.m.*
—	—	—	—	—	—	—	—	—	—	100	0.160	0.160
20	—	—	—	—	—	—	—	—	—	80	0.196	0.166
—	25	—	—	—	—	—	—	—	—	75	0.202	0.158
—	—	3	—	—	—	—	—	—	—	97	0.174	0.164
—	—	—	25	—	—	—	—	—	—	75	0.146	0.169
—	—	—	—	5	—	—	—	—	—	95	0.146	0.159
—	—	—	—	—	1	—	—	—	—	99	0.250	0.159
—	—	—	—	—	—	8	—	—	—	92	0.266	0.141
—	—	—	—	—	—	—	12.5	—	—	87.5	0.156	0.164
—	—	—	—	—	—	—	—	2	—	98	0.168	0.167
—	—	—	—	—	—	—	—	—	2	98	0.126	0.158
20	—	—	25	5	—	—	—	2	—	48	0.172	0.158
20	25	3	—	—	—	—	—	—	—	52	0.198	0.154

copper and cobalt (Table I). Enhancement effects can be attributed to a change in the ionization equilibrium between the element concerned and titanium, and suppression effects to compound formation.

Effects of spectroscopic buffers

The use of lanthanum or aluminium to overcome these interferences was then studied. Figure 1 shows the effects of increasing concentrations of lanthanum and aluminium on the absorption of 16 p.p.m. titanium. Lanthanum enhances the absorption by 75%, with a plateau region between 1000 and 5000 p.p.m. La. Aluminium gives an initial enhancement of 100%, which then decreases with increasing concentrations of aluminium.

The effect of increasing concentrations of lanthanum on the absorption of titanium in the presence of 100% iron and of 20% nickel plus 80% iron is shown in Fig. 2(b). (These % values refer to a supposed sample.) In the presence of 20% nickel, an initial enhancement of the titanium absorption eventually becomes a suppression as the concentration of lanthanum is increased. As there is no plateau region, lanthanum is unsuitable for overcoming nickel interference. Since the initial tests with aluminium (Fig. 1) showed a peak enhancement at the 500-p.p.m. concentration, a closer study was made at this level. Figure 2(a) shows that in solutions corresponding to samples essentially 100% iron, there is a plateau region from 400 to 600 p.p.m., where maximum enhancement is observed. When 80% iron and 20% nickel are present, the nickel enhancement on the titanium absorption is overcome within the same range of aluminium (Fig. 2(a), curve B).

A comparison of the results found for the interferences of diverse elements in

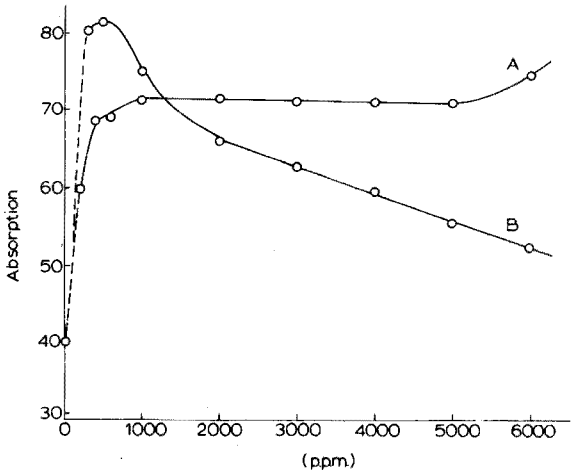

Fig. 1. The effect of spectroscopic buffers on the absorption of 16 p.p.m. titanium. The solutions contained 10% HCl + 1% HNO_3 and 1% iron, with 0.1% boric acid and 0.3% sodium carbonate. A, Lanthanum added as chloride. B, Aluminium added as chloride.

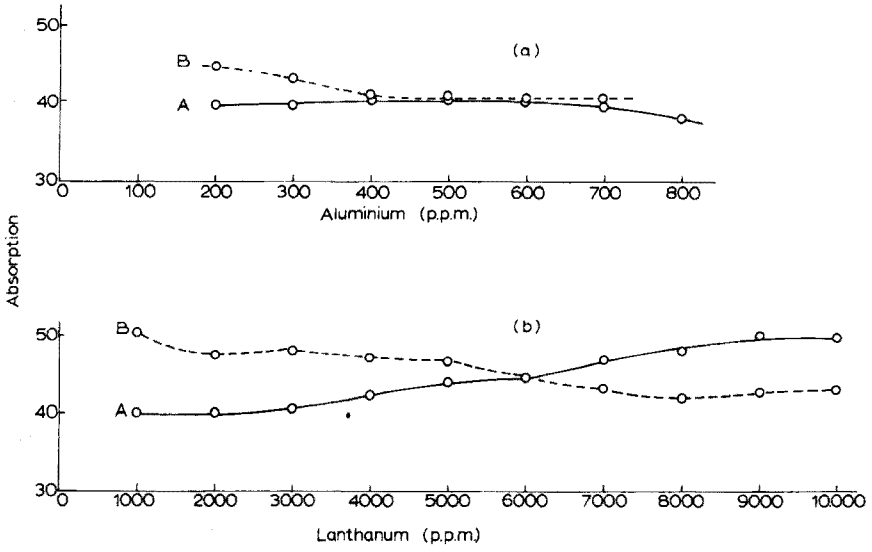

Fig. 2. The effect of spectroscopic buffers on the absorption of 0.16% titanium on a 1% (w/v) sample basis for A, 100% iron, and B, 80% iron + 20% nickel.

the presence of 500 p.p.m. Al with those found earlier in the absence of aluminium is given in Table I. Interferences are effectively overcome, with the exception of the test containing additional aluminium equivalent to 8% in a sample (B.C.S. steel 365 contains 8.15% Al). Concentrations of aluminium above the equivalent of 1% in a sample bring the final concentration outside the plateau region indicated in Fig. 2(a) and result in low values.

It was found that 2% of silica at the fusion stage had no effect on the

absorption of titanium; consequently, for steels containing 1% silicon it is not necessary to voltatilize the silica as fluoride.

These tests led to the development of the following method for iron and mild and alloy steels containing less than 1% aluminium. The range of the method is 0–0.80% titanium.

EXPERIMENTAL

Apparatus

A Techtron model AA5 instrument, fitted with an AA5 readout unit and a high-solids nitrous oxide–acetylene burner, was used under the following conditions:

Wavelength	364.3 nm
Lamp current	20 mA
Slit width	50 μm
Burner	Nitrous oxide–acetylene
Observation height	1 mm (Note 1)
Fuel setting	Acetylene pressure 10 p.s.i.; fuel flow 10 (see above).
Support setting	Nitrous oxide pressure 36 p.s.i.; gauge reading 20 p.s.i.
Damping	B
Scale expansion	0–0.16% ≃ × 10
	0–0.80% ≃ × 2

Reagents

All solutions were stored in polythene bottles

Stock iron solution. Transfer 50 g of pure iron to a 1.5–1 beaker and add 300 ml of hydrochloric acid (d. 1.16–1.18). When the iron has dissolved, cautiously oxidize with nitric acid (d. 1.42). Replace any loss in bulk with hydrochloric acid (d. 1.16–1.18). Boil to expel the brown fumes and add a further 200 ml of hydrochloric acid. Cool and dilute to 1 l with water. (20 ml = 1 g Fe, 10 ml HCl, 1 ml HNO_3.)

Sodium carbonate–boric acid solution. Dissolve 30 g of sodium carbonate and 10 g of boric acid in 300 ml of water and 100 ml of hydrochloric acid (d. 1.18). Dilute to 500 ml with water.

Aluminium solution (0.025 g Al ml^{-1}). Dissolve 44.75 g of aluminium chloride hexahydrate in water and dilute to 200 ml.

Standard titanium solution. (800 μg Ti ml^{-1}). Dissolve 0.8 g of pure titanium sponge in 50 ml of hydrochloric acid (d. 1.16–1.18). Add a further 150 ml of hydrochloric acid and dilute to 1 l in a calibrated flask.

Preparation of sample solution

Transfer 2.0 g of sample to a 150-ml conical beaker and add 40 ml of hydrochloric acid (50% v/v). Cover and digest until the sample has dissolved, oxidize with the minimum amount of nitric acid (d. 1.42) and boil to expel nitrous fumes. Filter through a small ashless paper pulp pad, washing with water. Reserve the filtrate and transfer the residue to a platinum capsule. Ignite (Note 2) and then fuse with 0.6 g of sodium carbonate and 0.2 g of boric acid. Moisten the fused melt with 2 ml of water, add 4 ml of hydrochloric acid (50% v/v) and allow to dissolve.

Combine with the reserved filtrate and dilute to 100 ml in a calibrated flask.

Transfer a 25-ml aliquot to a 50-ml calibrated flask, add 1 ml of aluminium solution, dilute to the mark and mix.

Preparation of calibrated solutions

To each of a series of 100-ml calibrated flasks, transfer 20 ml of stock iron solution, 5 ml of sodium carbonate-boric acid solution and 2 ml of aluminium solution. Add aliquots of 0, 0.5, 1.0, 2.0, 3.0, 4.0, 5.0, 7.5 and 10.0 ml of the standard titanium solution, dilute to the calibration mark and mix well.

These solutions correspond to 0–80 p.p.m. titanium, or to 0–0.80% titanium in the original sample.

Determination

Set the instrumental conditions as described above. Spray the appropriate calibration solutions followed by the sample solution. Spray water between each test and set the zero whilst spraying water. (Repeat this operation). Plot the mean absorbances against the titanium concentrations, construct a calibration curve and read off the percentage titanium (Note 3) in the sample.

Notes. (1) The optimal position for the burner height is found by raising the burner until it just begins to obstruct the light path. Then lower the burner 1 mm. (2) For samples containing 1% silicon treat the residue with 2 ml of sulphuric acid (20%, v/v) and 5 ml of hydrofluoric acid (40%, v/v), evaporate to dryness and ignite cautiously at 900°C. (3) For the greatest accuracy, spray each sample solution between calibration solutions containing concentrations of titanium above and below that present in the sample, and relate the mean absorbance reading to percentage titanium.

RESULTS

Application and reproducibility tests

A series of British Chemical Standard samples, including mild and stainless

TABLE II

DETERMINATION OF TITANIUM IN STEEL AND CAST IRON

B.C.S. no.	*Type*	*Other elements present (%)*		*Titanium (%)*		
				Certificate value		*Found*
		Ni	*Cr*	*Range*	*Mean*	
320	Mild steel	—	—	0.018–0.024	0.021	0.017, 0.0175
321	Mild steel	—	—	0.127–0.139	0.13	0.137, 0.136
322	Mild steel	—	—	0.037–0.046	0.042	0.042, 0.041
323	Mild steel	—	—	0.016–0.020	0.018	0.0165, 0.017
324	Mild steel	—	—	0.029–0.036	0.033	0.032, 0.0315
325	Mild steel	—	—	0.011–0.016	0.013	0.011, 0.0115
235/2	Alloy steel	9.38	18.6	0.31 –0.33	0.32	0.30, 0.305
335	Alloy steel	9.47	18.4	0.44 –0.47	0.46	0.46, 0.455
236/3	Cast iron	—	—	0.049–0.057	0.052	0.050, 0. 051

steel and a cast iron, was analysed by the recommended procedure. The results obtained (Table II) compare well with the certificate values, confirming the accuracy of the procedure.

TABLE III

REPRODUCIBILITY TESTS

Sample no.	*Titanium (%)*		
	B.C.S. 236/3	*B.C.S. 321*	*B.C.S. 335*
Type	Cast iron	Mild steel	Alloy steel
Certificate value	0.052	0.13	0.46
Mean value[a]	0.050	0.136	0.455
Reproducibility 95% ± 2s	0.0016	0.0036	0.014

[a] Mean of 10 determinations on separate days.

Reproducibility tests were carried out on three different types of samples containing varying levels of titanium. In each case, determinations were made on ten separate occasions. The results (Table III) show good reproducibility.

Analysis time

Determinations of titanium in a batch of 6 samples may be completed in 2.5 h by this method compared with about 5 h for the diantipyrylmethane photometric method.

An added advantage is that aluminium may be determined in the range 0.002–0.100% on the initial 2% (w/v) sample solution.

The authors thank the management of the Scunthorpe Group, British Steel Corporation, for permission to publish this paper.

SUMMARY

A method has been developed for the determination of titanium by atomic absorption spectrometry in a wide range of iron and steels containing <1% aluminium. Interferences are overcome by the addition of aluminium to sample and standard solutions. The accuracy and reproducibility of the method have been established at the 0.05, 0.15 and 0.50% levels with British Chemical Standard samples. The procedure is time-saving, particularly as aluminium may be determined on the same initial 2% (w/v) sample solution.

REFERENCES

1 M. D. Amos and J. B. Willis, *Spectrochim. Acta*, 22 (1966) 1325, 2128.
2 J. B. Headridge and D. P. Hubbard, *Anal. Chim. Acta*, 37 (1967) 151.
3 G. F. Kirkbright, A. M. Smith, T. S. West and R. Wood, *Analyst*, 94 (1969) 754.
4 T. Nakahara, M. Munemori and S. Musha, *Bull. Chem. Soc. Jap.*, 46 (1973) 1172.
5 T. S. Harrison, W. W. Foster and W. D. Cobb, *Metallurgia Metal Form.*, 40 (1973) 361.

Analytica Chimica Acta, 78 (1975) 299–306

THE USE OF FLAME PROCEDURES IN METALLURGICAL ANALYSIS

PART II. DETERMINATION OF ALUMINUM IN SULPHIDE AND SILICATE MINERALS AND IN ORES AND SLAGS

R. J. GUEST and D. R. MacPHERSON

Chemical Analysis Section, Extraction Metallurgy Division, Mines Branch, Department of Energy, Mines and Resources, Ottawa (Canada)*

(Received 3rd February 1975)

In process control work the need for rapid analyses makes the use of flame procedures for aluminum especially attractive because of their speed and simplicity compared to most other methods. This paper describes the use of flame emission and atomic absorption procedures for the rapid determination of aluminum in sulphide and silicate minerals and in complex sample materials from hydrometallurgical and pyrometallurgical process work. The dissolution procedures used were the same as those described previously[1] for the atomic absorption determination of silicon, but some sample materials were dissolved by multi-acid attack.

EXPERIMENTAL

Apparatus and reagents

The apparatus and reagents used were essentially as described previously[1] except for the preparation of standard aluminum solutions with and without concomitants.

Standard aluminum solutions. Weigh 1.0016 g of aluminum metal (British Chemical Standard 195F, 99.84% Al) into a beaker and dissolve with dilute hydrochloric acid, warming if necessary. Make the solution up to 1 l, with the final acidity being 1% in hydrochloric acid. This is the standard aluminum stock solution (1000 p.p.m. Al).

Prepare working solutions by suitable dilution; in each case add enough acid to ensure that the final solution will be acidic after sufficient sodium solution has been added to give a final concentration of 3000–6000 p.p.m. sodium. If solutions of aluminum plus concomitants are required, add the concomitants to the diluted aluminum standard just before making up the standard to the mark in the volumetric flask.

Dissolution of sample

Weigh out 0.5–2 g of sample if sodium peroxide fusion is to be done, or

* Since 1st January 1975: Solution Chemistry Section, Mineral Sciences Laboratories, Canada Centre for Mineral and Energy Technology (Canmet).

0.2–0.5 g if Teflon bomb dissolution is to be used, and follow the procedure described previously[1].

For multi-acid dissolution, treat 1–5 g of sample with nitric, hydrochloric, hydrofluoric, and perchloric acids, finally taking to perchloric fumes before dissolving the salts and diluting to volume in a volumetric flask.

Flame procedure

Take an aliquot of the main sample solution and place it in an appropriate volumetric flask. Add enough of the sodium solution so that the final solution for atomization contains about 6000 p.p.m. of sodium; ensure that the sample solution remains acidic by adding hydrochloric acid if necessary. Dilute to the mark with water. This solution should contain between 0.02 and 200 p.p.m. of aluminum. As a precaution run a blank with each new reagent batch or with new equipment.

Emission mode. If the aluminum in the final dilution is very low (0.02–5 p.p.m. Al), use the emission mode, making a background correction at nearby points on both sides of the peak by scanning the area to determine suitable "shoulders" and making appropriate corrections. When the aluminum peak at 396.5 nm is used, there are suitable "shoulders" at about 396.1 nm and 396.8 nm. Compare readings against aluminum standards which contain approximately the same amount of aluminum as the sample. If the sample is complex or if optimal accuracy is desired, add appropriate amounts of the major concomitants in the sample to the comparison standard. In either case, make a background correction on the comparison standard in the same manner as on the sample.

Absorption mode. If the aluminum present is greater than 5 p.p.m., use the absorption mode, reading the sample against comparison standards of aluminum alone or with added concomitants to match the samples.

Instrumental parameters

In both the flame emission and absorption modes, a 3-mm "feather" nitrous oxide-acetylene flame is recommended with three burner systems: Hetco total-consumption with laminar-flow head (used with the Jarrell-Ash, Model 82-300); pre-mix with laminar-flow head (used with the Jarrell-Ash, Model 810); and Techtron grooved-head (used with a Techtron, Model AA3).

RESULTS

Preliminary studies

Investigative work on the effect of concomitants on aluminum determination has been reported more extensively for atomic absorption than for flame emission spectrometry[2–9]. Reported interference effects are sometimes contradictory, probably because of variations in flame and instrumental parameters, and of the salt matrix present, all of which can seriously affect results[10]. Therefore, the effects of the major concomitants were measured for the conditions found here after typical sample dissolution, in the emission mode with a background correction, and in the absorption mode. Concomitant ions in the following ratios to aluminum were used: Fe (100:1 for f.e.s.; 100 and 200:1 for a.a.s.), Ti (40:1), Si (50:1 for f.e.s.; 10:1 for a.a.s.), Mg (6:1), Ca (15:1), Mn (30:1), K (10:1) and Cu (20:1).

In the emission mode after fusion dissolution, or after Teflon bomb dissolution if 6000 p.p.m. of sodium was added, little or no interference ($< \pm 5\%$) was found from any of these concomitants. However, after bomb dissolution if sodium was not added, solutions containing the following elements gave positive deviations: Fe (19%), Mg (10%), Mn (7%), and K (10%).

In the absorption mode after fusion dissolution, silicon and manganese gave deviations of -13% and $+9\%$, respectively. After bomb dissolution, provided that sodium was added, only manganese interfered ($+6\%$), if sodium was not added, potassium and manganese interfered giving deviations of $+9\%$ and $+7\%$, respectively. Little or no interference was caused by Fe, Ti, Ca, and Mg in pure mineral acid solution provided that sodium was added; but without sodium, large errors were caused by Fe ($+15\%$), Ti ($+13\%$), Ca ($+23\%$), and Mg ($+20\%$). Clearly, it is desirable to add a large amount of an easily ionized salt to the sample solution.

Analysis of sulphide and silicate minerals and their mixtures

Flame emission and atomic absorption procedures for aluminum were used on seven hand-picked minerals and six mixtures of the minerals, and results were compared with those found by chemical methods (Tables I and II). Both peroxide fusion and Teflon bomb dissolution procedures were used in all cases; also, multi-acid dissolution was used before the atomic absorption finish.

TABLE I

COMPARISON OF RESULTS FOR PURE MINERALS

Sample[a]	*Al*[b] *found chemically (%)*	*Flame emission*[c]		*Atomic absorption*[d]	
		Al found (%)	*Deviation*[e] *(%)*	*Al found (%)*	*Deviation*[e] *(%)*
Amphibole	4.74	4.51	−4.85	4.52	−4.64
Biotite	5.48	5.76	+5.11	5.71	+4.20
Feldspar (Labradorite)	14.35	14.05	−2.09	14.13	−1.53
Oligoclase	11.72	11.6	−1.02	11.63	−0.77
Feldspar (Albite)	10.79	10.65	−1.30	10.48	−2.87
Feldspar (Microcline)	9.73	9.93	+2.06	9.95	+2.26
Muscovite	15.86	15.95	+0.57	16.17	+1.95

[a] See Part I[1], p. 240 for the mineral composition.
[b] Titrimetric procedure[11,12].
[c] Average result for fusion and Teflon bomb dissolution.
[d] Average result for fusion, Teflon bomb, and acid dissolution procedures.
[e] Deviation from chemical result.

With the individual minerals the average deviation was found to be $\pm 2.4\%$ with flame emission, and $\pm 2.6\%$ with atomic absorption. Good agreement was found between flame results obtained after each of fusion, Teflon bomb and multi-

TABLE II

COMPARISON OF RESULTS FOR MINERAL MIXTURES

Mineral mixture no.[a]	*Al*[b] *found chemically (%)*	*Flame emission*		*Atomic absorption*	
		Al found (%)	*Deviation*[c] *(%)*	*Al found (%)*	*Deviation*[c] *(%)*
1	2.29	2.38	+3.93	2.34	+2.18
2	5.93	6.125	+3.29	5.985	+0.93
3	2.58	2.64	+2.52	2.595	+0.97
4	2.96	3.16	+6.76	3.02	+2.20
5	1.01	1.055	+3.48	1.00	−0.50
6	9.84	10.1	+2.44	9.96	+1.63

[a] See Part I[1], p. 243 for composition of the mineral mixtures.
[b] Calculated from the average results found on the individual minerals used in the mineral mixtures by chemical methods.
[c] Deviation from chemical result.

acid dissolution, and chemical results; the solution media from each dissolution procedure was therefore considered to be satisfactory for flame determination.

The precision of the flame emission procedure, expressed as the relative standard deviation, after fusion dissolution was $\pm 2.5\%$ compared to $\pm 1.5\%$ after Teflon bomb dissolution. The atomic absorption procedure showed a relative standard deviation of $\pm 1.0\%$ on solutions from both fusion and bomb dissolution.

With the mineral mixtures, the percentage deviation obtained on each sample, between chemical and atomic absorption values, was less than that between chemical and flame emission results; the average deviation was $\pm 1.4\%$ for atomic absorption compared to $\pm 3.7\%$ for the emission mode. In no case did the deviation with the mineral mixtures exceed significantly that for the individual minerals used in their composition.

It was concluded, therefore, that the decomposition methods described were effective in liberating aluminum from all the minerals in the simulated mixture, and that the interaction of elements and compounds arising from different minerals was successfully overcome in both the emission and absorption modes.

Effects of some experimental variables in flame emission

The effects on emission results of three variables were studied for some typical sample material as follows.

Background correction. The necessity of making a background correction is shown in Table III for each of the three dissolution methods. In all cases, the comparison standards matched the acidity and sodium contents found in the samples, but no sample concomitants were added.

Variation of the flame type. The effect of using more oxidizing and more luminous flames rather than the 3-mm "feather" flame recommended in the Procedure, is shown in Table IV. The samples analysed were five high-temperature furnace slags from iron ore and ilmenite smelting, four ilmenite samples (both treated and untreated), and Certified Standard samples of iron ore (BCS 302) and

ferrotitanium (NBS 116a). A background correction was made in each case.

TABLE III

EFFECT OF BACKGROUND CORRECTION ON EMISSION RESULTS AFTER DIFFERENT DISSOLUTION PROCEDURES

(All results are given as % Al. Columns A give results without background correction and columns B with background correction.)

Sample	*Al[a] present*	*Multi-acid[b]*		*Multi-acid[c]*		*Na_2O_2 fusion*		*Teflon bomb*	
		A	*B*	*A*	*B*	*A*	*B*	*A*	*B*
EMP1561, Slag from Smelting	6.18	6.64	6.28	—	—	—	6.15	7.77	6.20
EMP2846, Slag from Ilmenite Smelting	1.99	—	1.90[d]	2.26[d]	1.86[d]	2.67	1.93	2.38	1.87
EMP3009, Ilmenite	1.05	—	0.68[d]	1.18[d]	0.94[d]	1.49	1.00	1.22	0.82
BCS302, Certified Iron Ore	3.83	3.78	3.83	—	—	—	3.78	4.56	3.92
NBS116a, Ferrotitanium	3.25	—	—	3.42	3.15	—	3.22	3.94	3.15
BCS174/1, Basic Slag	0.91	1.41	0.93	—	—	—	—	1.84	0.95

[a] Certified results, or analysed chemically in EMD Laboratory (EMP numbers).
[b] Nitric, hydrochloric, hydrofluoric, and perchloric acids.
[c] Nitric, hydrochloric, hydrofluoric, and sulphuric acids.
[d] Incomplete dissolution of sample.

TABLE IV

EFFECT OF VARIATION OF FLAME TYPE AND COMPOSITION OF THE COMPARISON STANDARDS

(The results given are the average % deviations of the flame emission values from the chemical values. Comparison standards were used in all cases.)

	Flame type ("Red feather" size)					
	6 mm		*3 mm*		*1.5 mm*	
	Al	*Al plus concomitants*	*Al*	*Al plus concomitants*	*Al*	*Al plus concomitants*
All samples	7.70	3.56	2.27	1.65	2.96	2.18
Slags only	8.92	4.20	2.64	1.92	3.18	2.24
Certified samples	2.20	1.01	0.59	0.59	1.95	1.95

Flame emission results obtained with each of the flame types showed good agreement with values for Certified Standard samples. Results obtained with a 3-mm "feather" flame were satisfactory for all the samples, and burner problems were minimal. With a more oxidizing flame, burner problems caused by salt build-up were encountered; with a more luminous flame, carbonization problems were frequent, and there was less satisfactory agreement between emission and chemical results for slags and ores.

Variation of composition of the comparison standard

Emission results obtained with comparison standards of aluminum plus major concomitants, showed better agreement with the results of other procedures than those obtained by comparison with pure aluminum standards (Table IV). This finding was more pronounced with regular slag and ore samples than for the Certified sample materials tried, especially when a more luminous flame was used.

Precision

The precision obtainable in the emission mode for an optimum flame type and comparison standards, with and without added concomitants, was calculated for two slag and one ilmenite sample after sodium peroxide fusion. The relative standard deviation for six sets of readings was $\pm 1.0\%$ with aluminum comparison standards, and $\pm 1.7\%$ with aluminum plus concomitants.

Comparison of flame and chemical results

Typical samples were analysed by the recommended emission and absorption flame procedures and the results obtained were compared with the available chemical results. Sodium peroxide fusion was chosen because some of the sample materials (*i.e.* chromite, fly ash) could not be dissolved by the Teflon bomb or multi-acid procedure. Also, for reasons not clearly understood, erratic results were found for the Elliott Lake ore samples in the hydrofluoric–boric medium after bomb dissolution. The results (Table V) gave an average deviation of $\pm 3.7\%$ between flame and chemical procedures, equal or similar deviations being found for the emission and absorption modes.

DISCUSSION

Although the results obtained by flame emission and atomic absorption are in good agreement with the chemical results, the more sensitive emission mode would be the choice when the aluminum content is small and when large amounts of manganese or silicon are present. The absorption mode is preferred in the presence of large amounts of calcium because of line interference with the 396.5-nm aluminum emission line.

Sodium peroxide fusion provides the most satisfactory combination of speed, effectiveness and convenience for flame determination. When Teflon bomb or multi-acid dissolution procedures are used, a large amount of an easily ionized salt such as sodium should be added.

In the emission mode the use of a 3-mm "feather" flame and background correction are recommended. The addition of major sample concomitants to the

TABLE V

COMPARISON OF RESULTS FOR TYPICAL SAMPLES

Sample	*Al found[a] chemically (%)*	*Flame emission*		*Atomic absorption*	
		Al found (%)	*Deviation[b] (%)*	*Al found (%)*	*Deviation[b] (%)*
Ilmenite (EMP2715)	0.75	0.74	−1.33	0.72	−4.00
Slag from Ilmenite Smelting (EMP2958)	2.65	2.50	−5.66	2.59	−2.26
Slag from Iron Ore Smelting (EMP1552)	7.92	7.77	−1.89	7.79	−1.64
Synthetic Slag[c] (EMS2779)	1.26	1.22	−3.17	1.21	−3.97
Ferromanganese Slag (EMQ2931)	9.83	9.89	+0.61	—	—
Furnace Concentrate (EMQ2879)	4.27	4.28	+0.23	—	—
Furnace Concentrate, Reduced (EMQ3055)	5.17	4.97	−3.87	—	—
Elliot Lake Uranium[d] Ore (EMQ2035)	4.78	5.13	+7.32	5.28	+10.5
Elliot Lake Uranium[e] Ore (EMQ2030)	2.37	2.09	−11.8	2.28	−3.80
Beaverlodge Uranium[e] Ore (EMQ3012)	7.07	7.00	−0.99	7.04	−0.42
Chromite (EMQ2856)	14.2	14.4	+1.41	—	—
Fly Ash (EMQ3437)	1.63	1.53	−6.13	—	—
Russian Ore (EMQ2872)	0.91	0.93	+2.20	—	—
Iron Ore Pellets (EMT1372)	—	0.13	—	0.13	—

[a] Solvent extraction–titrimetric procedure[11,12].
[b] Deviation from chemical result.
[c] Made from Certified Standard samples: 8 parts NBS 88 (dolomite), 2 parts NBS 99 (soda feldspar), and 2 parts BCS 301 (iron ore).
[d] Canadian Radioactive Ore Standard DL.
[e] Canadian Radioactive Ore Standard DH.
[f] Canadian Radioactive Ore Standard BL-4.

comparison standards is also recommended when accuracy requirements are stringent and the sample is complex.

The usable ranges of the two procedures are complementary to each other and permit aluminum determinations between at least 0.01% and 15%. The emission procedure is sufficiently sensitive to allow its application to samples containing amounts of aluminum as low as 0.001%, with a corresponding decrease in precision.

SUMMARY

Flame emission and atomic absorption procedures are described for determination of aluminum in typical sulphide and silicate minerals and in representative ores and slags. Sodium peroxide fusion was the most satisfactory of three dissolution procedures used. Optimum flame types, background correction, and the addition of sample concomitants to the comparison standards are discussed.

REFERENCES

1 R. J. Guest and D. R. MacPherson, *Anal. Chim. Acta*, 71 (1974) 233.
2 V. A. Fassel, R. W. Slack and R. N. Kniseley, *Anal. Chem.*, 42 (1971) 186.
3 B. Bernas, *Anal. Chem.*, 40 (1968) 1682.
4 T. V. Ramakrishna, P. W. West and J. W. Robinson, *Anal. Chim. Acta*, 39 (1967) 81.
5 A. P. Ferris, W. B. Jepson and R. C. Shapland, *Analyst (London)*, 95 (1970) 574.
6 S. R. Koirtyohann and E. E. Pickett, *Anal. Chem.*, 40 (1968) 2068.
7 C. Thulborne and P. H. Scholes, *B.I.S.R.A., Open Report, MG/D/676/70*, 1970.
8 D. M. Dagnall, G. F. Kirkbright, T. S. West and R. Wood, *Anal. Chem.*, 42 (1970) 1029.
9 A. C. West, R. N. Kniseley and V. A. Fassel, *Anal. Chem.*, 42 (1971) 186.
10 J. Y. Marks and G. G. Welcher, *Anal. Chem.*, 42 (1970) 1033.
11 A. Hitchen, *Mines Branch Technical Bulletin TB 168*, Canada Dept. of Energy, Mines and Resources, Ottawa, 1973.
12 A. Hitchen, *Mines Branch Technical Bulletin TB 169*, Canada Dept. of Energy, Mines and Resources, Ottawa, 1973.

Analytica Chimica Acta, 78 (1975) 307–315

A TWO-GROUP SEPARATION SCHEME FOR THE DETERMINATION OF ELEVEN TRACE ELEMENTS IN BIOLOGICAL MATERIAL BY NEUTRON ACTIVATION ANALYSIS

E. STEINNES

Institute for Atomenergi, Isotope Laboratories, Kjeller (Norway)

(Received 6h March 1975)

Although purely instrumental activation analysis with Ge(Li) detectors can be used in a number of cases for the determination of minor and trace elements in biological material[1–4], radiochemical separations are necessary in most cases when a considerable number of elements must be determined simultaneously, or when very low concentrations are encountered. Various multielement separation schemes have been developed for use in neutron activation analysis of biological materials[5–13]. In most cases, such methods have been based on wet-ashing of the irradiated samples, followed by removal of volatile elements by distillation and subsequent chemical fractionation of the residual elements, most frequently by anion-exchange separations. Recently, applications of high-temperature distillation after dry-ashing of the sample have been reported[14,15], but this technique has not yet found widespread application in activation analysis of biological tissue.

Since the advent of Ge(Li) detectors, simple chemical group separations which permit the elimination of major activities in the sample, may often facilitate the determination of a large number of elements in cases where splitting into many groups was previously necessary. A good example is the removal of ^{24}Na from strong hydrochloric acid solutions by means of hydrated antimony pentoxide[9,16]. The technique of solvent extraction, which is being extensively used elsewhere in analytical and separation chemistry, has found very limited application in the multi-element neutron activation schemes developed for biological materials, although there are many extraction systems that might be useful for group separations. In particular, systems that can be applied for a number of elements with high yield from strongly acidic solutions, such as tri-n-butyl phosphate (TBP), tri-iso-octyl-amine (TIOA), and tri-n-octylphosphine oxide (TOPO), could be successfully applied after wet-ashing. In this laboratory, it was shown that TOPO could be advantageously used for the separation of radioisotopes of Cu, Zn, Mo and Cd from the major activities in irradiated biological material[17]. More recently, it was found that various other elements can also be successfully separated by this extraction method, and attempts were made to construct a general scheme[18].

In the present paper, some solvent extraction experiments carried out to extend the scope of the TOPO group separations are described. A method for the simultaneous determination of 11 or more minor and trace elements in biological tissue, based on combination of the TOPO separation with a distillation step, is proposed.

Solvent extraction experiments with TOPO

Trioctylphosphine oxide can be used for the extraction of many elements from solutions of various mineral acids[19]. Cyclohexane has most often been preferred as a diluent, and a TOPO concentration of 0.1 *M* (5% w/w) has frequently been used. In general, the highest extraction is obtained from strong hydrochloric acid solutions, and distribution ratios for most elements in the system 5% TOPO–HCl have been determined in the range 1–12 *M* HCl[20]. For several elements, extraction is maximal in the concentration region around 6 *M* hydrochloric acid. This concentration therefore seemed to be the optimal choice for group separations. Elements which are appreciably extracted under these conditions include Sc, Fe(III), Co, Cu, Zn, Ga, As(III), Zr, Mo, Cd, In, Sn, Sb(III), W, Au, Hg, Th, Pa, U and Np. From this list, Sc, Fe, Co, Cu, Zn, Mo, Cd, W and Au seemed to be the most interesting elements for study in connection with a neutron activation scheme for biological materials based on medium- and long-lived radionuclides. The study of scandium would also serve as the basis for the determination of calcium via the ^{47}Ca–^{47}Sc reaction.

The most favourable conditions for group separation cannot be established by considering only the distribution ratios given in the literature for the 5% TOPO/HCl system, and the residual acid phase from the wet-ashing process must also be taken into account. In this laboratory, wet-ashing of biological material is most often carried out with a few ml of nitric acid or hydrogen peroxide as the oxidizing agent, in the presence of 2 ml of sulphuric acid and 0.5 ml of phosphoric acid. Batch extractions with radiotracers of the elements of interest were therefore undertaken with a mixture of 10 ml of 6 *M* HCl, 2 ml of concentrated H_2SO_4 and 0.5 ml of concentrated H_3PO_4 as the aqueous phase, and 25 ml of 5% TOPO in cyclohexane as the organic phase.

The amount of carrier to be used must also be considered, as the extraction coefficient varies with the amount of element in the aqueous phase. With molybdenum(VI), for example, 99.8% was found to be extracted from 5 *M* HCl with 20 mg present, whereas the figure dropped to 80% with 30 mg Mo present in the aqueous phase[19]. Extractions were therefore carried out with varying amounts (0.2–20 mg) of each element, and the results are illustrated in Fig. 1. For most elements the extraction increases slowly with an increasing amount of the element, up to a certain level (of the order of 5–10 mg) where extraction starts to drop; for iron or cobalt, the drop is quite substantial. If carriers of all elements were added simultaneously, the decreased extraction would occur for lower amounts of each particular element. Moreover, difficulty with the separation of the two phases was encountered with 10 mg of zinc and 20 mg of cobalt. It was therefore decided to use as small an amount as 0.5 mg of each element as carrier. With this mixture, tracer experiments showed the following results for the unextracted fraction of each element (the corresponding value from Fig. 1 is given in brackets): Sc, 1.7% (1.7); Fe, 0.37% (0.22); Co, 10.7% (19); Cu, 27% (32); Zn, 3.5% (4.0); Mo, 0.20% (0.17); Cd, 1.7% (2.1); W, 1.6% (1.7); Au, 0.20% (0.85).

The presence of the other elements at the 0.5-mg level does not seem to affect the extraction of any element appreciably, except in the case of cobalt, where there seems to be a certain improvement.

For all the elements studied, except cobalt and copper, very little of the

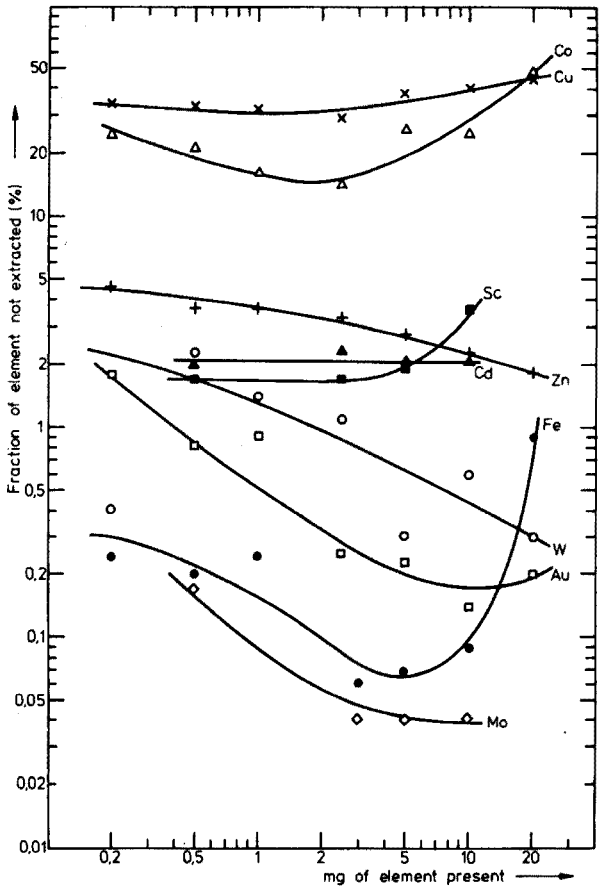

Fig. 1. Extraction as a function of quantity of 9 elements. For conditions, see text.

element should be lost in two subsequent extractions (extraction and washing step), and the recovered amount should be highly reproducible. For these elements, a separate chemical yield determination was therefore deemed unnecessary. In the case of cobalt, for which a loss of about 25% is likely, the reproducibility should still be satisfactory, considering the very low concentration levels at which this element is usually found in biological tissue. For copper, the chemical yield should be determined, *e.g.* by re-activation after back-extraction into 6 *M* nitric acid[17]. In the analytical work described here, copper was not considered.

It should be noted that the distribution ratios observed in the present system sometimes show considerable deviations from the literature values given for the 5% TOPO/6 *M* HCl system[20]. For iron(III) and cadmium, the distribution ratios are more than 10 times higher in the present work; extractions of Co, Cu, and W are also considerably higher in the present system. For the remaining elements, there are no great differences.

Distillation subgroup

Distillation of the volatile chlorides of Hg(II), As(III) and Se(IV) from hydrochloric acid–hydrobromic acid mixtures has been frequently used in activation analysis. In some of the multielement methods developed for biological materials, the determination of these elements is based on the assumption of a chemical yield close to 100%, and no chemical yield determination is carried out[8,12,13]. In routine work, it is often difficult to obtain a nearly quantitative chemical yield, especially for mercury and repeated distillation may be required. If the distillation flask is heated excessively during the distillation process, difficulties may be caused by the precipitation of sparingly soluble sulfates. In the present work it was found advantageous to use only one distillation and to avoid excessive heating of the sulfuric–phosphoric acid residue, although this sacrificed the high chemical yield for mercury. The mercury, arsenic and selenium are then separated from the distillate by precipitation of mixed sulfides. After the precipitate has been collected on a membrane filter and sealed between two sheets of polyethylene, the sample is counted and subsequently re-irradiated for chemical yield determination. It is advantageous to treat a mixture of standards in the same manner, otherwise neutron-shielding effects in the re-activation may affect the results.

EXPERIMENTAL

Reagents

Tri-n-octyl phosphine oxide (TOPO; Eastman Organic Chemicals) was of unspecified grade. The TOPO solution used was 5% (w/w) in cyclohexane. The other reagents used were of analytical grade.

Samples and standards

In order to test the feasibility of the method, the following international biological reference materials were analyzed: Bowen's kale[21], National Bureau of Standards Bovine liver (SRM 1577), and six samples from the International Atomic Energy Agency, namely A-3/1 Animal bone, A-8 Milk powder, V-4 Dried potatoes, and V-2/1 Wheat flour. Samples of about 250 mg were weighed into quartz ampoules for irradiation; for Animal bone, about 100 mg was used.

Standards were usually prepared by evaporating 100-μl aliquots of appropriate standard solutions on separate 3×3 cm squares of aluminium foil. However, for calcium and iron, 10 mg of $CaCO_3$ and 10 mg of Fe metal, respectively, were wrapped in aluminium foil; and for mercury, 250 μl of a 100 p.p.m. standard solution in 0.1 *M* nitric acid was sealed in a quartz ampoule. The following approximate amounts of elements were used to make the standards on Al foil: Se, 20 μg; As, 10 μg; Mo, 10 μg; Cd, 50 μg; W, 10 μg; Sc, 2 μg; Zn, 200 μg; Co, 10 μg.

Irradiation

Samples and standards were irradiated for 5 days in the JEEP II reactor (Kjeller, Norway) at a thermal neutron flux of $5 \cdot 10^{12}$ n cm^{-2} s^{-1}. The samples were left for 3 days before the chemical separation was started.

Radiochemical separation procedure

The quartz ampoule with its contents, after external cleaning and breaking,

was transferred to a distillation flask containing 2 ml of concentrated sulfuric acid, 0.5 ml of concentrated phosphoric acid, 5 ml of concentrated nitric acid, and the following carriers: Se, 5 mg; As, 1 mg; Hg, 5 mg; Mo, Ca, Cd, Zn, Sc, Fe, Co, 0.5 mg. In order to avoid possible loss of tungsten by precipitation of WO_3 during the distillation step, no tungsten carrier was added. The mixture was heated with an electrothermal burner until white fumes of SO_3 appeared. If necessary, more nitric acid was added portionwise. The distillate was discarded.

After cooling, 5 ml of concentrated hydrochloric acid and 5 ml of concentrated hydrobromic acid were added, and distillation was carried out until strong fumes of SO_3 appeared. The distillate was then diluted to 150 ml with water, and the mixed sulfides were precipitated with an aqueous 5.0% (w/w) solution of thioacetamide by heating on a hot plate. If the dark colour of HgS did not appear, more water was added. After 30 min, the precipitate was filtered onto a 0.45 μm membrane filter, washed with water, and sealed between two sheets of polyethylene foil.

The residue in the distillation flask was boiled gently for 10 min with 15 ml of 6 *M* hydrochloric acid under reflux. The solution was then decanted into a separatory funnel. The residual pieces of quartz were washed with two 5-ml portions of 6 *M* HCl, and the solutions were transferred to the separatory funnel. Extraction was then carried out for 2 min with 25 ml of TOPO solution. The organic phase was washed with 5 ml of 6 *M* HCl. The aqueous phases were discarded. (The combined aqueous phases may be retained for the determination of elements such as alkali elements, alkaline earths, chromium, and rare earths.) The organic phase was transferred to a 100-ml plastic screwcap bottle for activity measurements.

Post-irradiation treatment of standards

Standards evaporated on aluminium foils were released from the unfolded foils with 10 ml of hot 7.5 *M* nitric acid and diluted to 25 ml with water. Solids were dissolved in strong hydrochloric acid and subsequently diluted to 25 ml. From the mercury solution 0.100 ml was withdrawn and diluted in the same manner. Two aliquots of mixed standards were run through the radiochemical separation procedure. During the distillation step, the presence of some pieces of crushed quartz ampoule was found necessary in order to prevent adhesion of sulfate precipitate to the inner wall of the flask. The following amounts of standards were taken: As, 0.4 μg; Ca, 1000 μg; Cd, 3 μg; Co, 0.4 μg; Fe, 200 μg; Hg, 0.2 μg; Mo, 1.2 μg; Sc. 0.02 μg; Se, 0.8 μg; W, 0.4 μg; Zn, 20 μg.

Comparison of the γ-activities of the TOPO fraction of a standard aliquot with those of a corresponding untreated aliquot showed chemical yields of the order of 93–98% for the elements Cd, Fe, Mo, Sc, W, and Zn. For cobalt, about 70% was found; this is slightly lower than would be expected from the initial extraction experiments, and the difference is probably caused mainly by mechanical losses.

Activity measurements

After a delay of 1 day to permit the radioactive equilibria ^{99}Mo–^{99m}Tc and ^{115}Cd–^{115m}In to be approached, γ-spectrometric measurements were made with a 35-cm^3 Ge(Li) detector (2.5 keV FWHM for ^{60}Co, 1332 keV) with associated electronics, connected to a 1700-channel pulse-height analyzer based on a NORD-1 digital computer. Peak areas were calculated by the Covell[22] and Sterlinski[23]

TABLE I

RESULTS OBTAINED BY NEUTRON ACTIVATION ANALYSIS OF SIX BIOLOGICAL REFERENCE MATERIALS BY THE TWO-GROUP SEPARATION SCHEME

(All results are given in p.p.m.)

	As	*Hg*	*Se*	*Ca*	*Cd*	*Co*	*Fe*	*Mo*	*Sc*	*W*	*Zn*
NBS Bovine liver (SRM 1577)	0.059	0.0149	1.08	138	0.31	0.200	254	3.39	< 0.001	0.018	122
	0.058	0.0144	1.06	124	0.31	0.206	244	3.26		0.012	128
Bowen's kale[a]	0.130	0.182	0.113	43000	0.83	0.060	111	2.00	0.0121	0.052	30.8
	0.132	0.181	0.115	39000	0.79	0.048	112	2.11	0.0105	0.055	32.5
IAEA A-3/1 Animal bone	1.33	0.0183	0.156	N.D.[b]	< 0.1	0.42	1520	1.52	< 0.005	0.61	182
	1.26	0.0198	0.136			0.51	1680	1.40		0.61	174
IAEA A-8 Milk powder	0.014	0.0025	0.039	12600	0.026	0.028	70	0.128	< 0.001	< 0.01	40
	0.018	0.0023	0.035	12200	0.032	0.017	89	0.125			37
IAEA V-4 Dried potatoes	0.028	0.0035	0.016	370	0.22	0.032	18.1	0.26	< 0.001	< 0.01	11.6
	0.026	0.0040	0.025	450	0.24	0.025	17.5	0.24			11.8
IAEA V-2/1 Wheat flour	0.022	0.0036	0.227	570	0.090	0.036	88	0.38	0.0015	< 0.01	32.7
	0.026	0.0046	0.249	540	0.081	0.020	104	0.37	0.0018		30.2
Radionuclide used	^{76}As	^{197}Hg	^{75}Se	^{47}Sc	^{115}Cd–^{115m}In	^{60}Co	^{59}Fe	^{99m}Tc	^{46}Sc	^{187}W	^{65}Zn
γ-Rays measured (keV)	558	69,77	265	160	336,528	1173,1332	1099,1292	140	889	479,684	1115

[a] Corrected for 5.5% drying loss.
[b] Not determined.

TABLE II

COMPARISON OF THE PRESENT RESULTS WITH REFERENCE DATA

(All results are given in p.p.m.)

		As	*Hg*	*Se*	*Ca*	*Cd*	*Co*	*Fe*	*Mo*	*Sc*	*W*	*Zn*
Bovine liver	This work	0.059	0.0147	1.07	131	0.31	0.203	249	3.33	< 0.001	0.015	125
	NBS values[a]	(0.055)	0.016	1.1	(123)	0.27	(0.18)	270	(3.2)	—	—	130
Kale	This work	0.131	0.182	0.114	41000	0.81	0.054	112	2.06	0.0113	0.054	31.7
	Bowen[24], "best mean value"	0.141	0.167	0.121	40850	0.80	0.0581	118.3	2.28	0.0083	0.0605	33.2
Animal bone	This work	1.30	0.0191	0.146	—	< 0.1	0.47	1600	1.46	< 0.005	0.61	178
	IAEA[25]	1.16	(0.021)	—	—	(1.7)	0.463	1520	—	—	—	183
Milk powder	This work	0.016	0.0024	0.037	12400	0.029	0.023	80	0.127	< 0.001	< 0.01	38.5
	IAEA[25]	—	(0.0039)	—	—	(0.030)	0.0166	41.4	—	—	—	38.7
Dried potatoes	This work	0.027	0.0038	0.021	410	0.23	0.029	17.8	0.25	< 0.001	< 0.01	11.7
	IAEA[25]	0.026	(0.0037)	—	—	0.227	0.0205	18.6	—	—	—	11.9
Wheat flour	This work	0.024	0.0041	0.238	560	0.086	0.028	96	0.38	0.0017	< 0.01	31.5
	IAEA[25]	0.022	0.0035	—	—	(0.080)	0.0368	84.3	—	—	—	33.2

[a] Values in brackets are not certified.

methods. The radionuclides and γ-ray energies involved are listed in Table I.

Chemical yield determination

When the ^{197}Hg and ^{76}As activities in the sulfide precipitates from the distillation group had decayed to a negligible level, the chemical yields of As, Se, and Hg were determined by reactivation. An irradiation time of 30 s was used. After a 30-min delay for the decay of 3.9-min ^{79m}Se, the samples were subjected to γ-spectrometry for the ^{81m}Se (103 keV), ^{76}As, and ^{197}Hg peaks. Typical chemical yields were as follows: As, 70–90%; Se, 85–95%; Hg, 40–60%.

RESULTS AND DISCUSSION

The biological standards mentioned above were analyzed in duplicate by the proposed method, and the results are listed in Table I. For most elements concerned, the reproducibility is good down to very low concentration levels. In Table II the present mean values are compared with data from the issuing organizations. In the case of the now well established standards Bovine liver and Bowen's kale, the mean values of this work in most cases show a deviation of less than 10% from the reference values. The four IAEA standards were first distributed in 1973 in connection with a laboratory intercomparison test[25]. Among the elements for which data were requested, were As, Hg, Cd, Co, Fe, and Zn. The author's laboratory participated with the data presented in this paper for the elements mentioned. The IAEA reference values listed in Table II are so-called "overall mean of accepted laboratory averages", which were obtained after the rejection of some outlying results. Values in brackets are the medians of all returned values, which were used in some cases where the results were so widely spread that a statistical interpretation was impossible[25]. Again the results of the present work appear to be in good agreement with the reference values in most cases. As the six samples studied represent a broad spectrum of biological tissue, the evidence in Table II suggests that the proposed method is capable of producing data of good accuracy on a wide variety of biological samples.

As indicated in Table I, the 11 elements concerned could be determined readily down to very low levels in five of the six samples. In the case of Animal bone, the high total activity, mainly from ^{47}Sc, involved less favourable limits of detection for other elements, but the trace element levels were such that most of the elements could be determined in any case. In blood samples[17], a similar problem is associated with the high level of ^{59}Fe. With regard to the sulfide group, experience with other types of samples has shown that for samples high in arsenic it may be necessary to wait several days before the ^{75}Se activity can be measured.

Spectral interferences do not seem very significant in most cases, but the following possibilities should be mentioned. (1) Interference from ^{46}Sc (1120 keV) on the measurement of ^{65}Zn (1115 keV). Owing to the comparatively high level of zinc in biological tissue, this correction would usually be insignificant, unless the sample has been contaminated with soil. In any case, this source of error is easily checked by the 889-keV peak of ^{46}Sc. (2) Interference from ^{59}Fe (142 keV) on the measurement of ^{99m}Tc. This interference may prevent determination of molybdenum in blood by the present method. (3) Interference from ^{59}Fe (335 keV) on the measurement of ^{115m}In (336 keV), which is likely to hamper the determination

of cadmium in blood.

As has been shown[17], copper may be included in the TOPO extraction group. As the copper extraction is only 65–70% complete (Fig. 1), a chemical yield determination would be necessary. Moreover, the short half-life (12.8 h) would involve an earlier start for the radiochemical separation after the end of the irradiation, which would mean a significantly higher radiation level from the samples during the analytical work.

SUMMARY

The applicability of solvent extraction with tri-n-octylphosphine oxide (TOPO) in the neutron activation analysis of biological material has been studied. A two-group radiochemical separation scheme is presented. After wet oxidation, As, Se, and Hg are removed by distillation and subsequent sulfide precipitation; Ca, Cd, Co, Fe, Mo, Sc, W, and Zn are then determined after extraction with TOPO. Chemical yield is determined for the volatile group by re-irradiation of the sulfide precipitate. No chemical yield determination is performed for the TOPO group. Results for six international biological standards are presented. The method is applicable to a wide variety of biological samples.

REFERENCES

1 R. W. Perkins and W. A. Haller, *Nuclear Activation Techniques in the Life Sciences*, I.A.E.A., Vienna, 1967, p. 557.
2 R. A. Nadkarni and W. D. Ehmann, *J. Radioanal. Chem.*, 3 (1969) 175.
3 R. A. Nadkarni and G. H. Morrison, *Anal. Chem.*, 45 (1973) 1957.
4 N. M. Spyrou, M. E. Fricker, R. Robertson and W. B. Gilboy, *Comparative Studies of Food and Environmental Contamination*, I.A.E.A., Vienna, 1974, p. 471.
5 F. Girardi, M. Merlini, J. Pauly and R. Pietra, *Radiochemical Methods of Analysis, Vol. 2*, I.A.E.A., Vienna, 1965, p. 3.
6 R. E. Jervis and K. Y. Wong, *Nuclear Activation Techniques in the Life Sciences*, I.A.E.A., Vienna, 1967, p. 137.
7 P. Van den Winkel, A. Speecke and J. Hoste, *Nuclear Activation Techniques in the Life Sciences*, I.A.E.A., Vienna, 1967, p. 159.
8 K. Samsahl, P. O. Wester and O. Landström, *Anal. Chem.*, 40 (1968) 181.
9 W. A. Haller, R. H. Filby and L. A. Rancitelli, *Nucl. Appl. Technol.*, 6 (1969) 365.
10 K. Samsahl, *Sci. Total Environ.*, 1 (1972) 65.
11 G. H. Morrison and N. M. Potter, *Anal. Chem.*, 44 (1972) 839.
12 J. Schumacher and W. Maier-Borst, *Kerntechnik*, 14 (1972) 165.
13 L. O. Plantin, *Nuclear Activation Techniques in the Life Sciences*, I.A.E.A., Vienna, 1972, p. 73.
14 A. R. Byrne and L. Kosta, *Talanta*, 21 (1974) 1083.
15 E. Orvini, T. E. Gills and P. D. LaFleur, *Anal. Chem.*, 46 (1974) 1294.
16 F. Girardi and E. Sabbioni, *J. Radioanal. Chem.*, 1 (1968) 169.
17 E. Steinnes, O. R. Birkelund and O. Johansen, *J. Radioanal. Chem.*, 9 (1971) 267.
18 E. Steinnes, *Technical Report IAEA-157*, 1973, p. 149.
19 J. C. White and W. J. Ross, *NAS-NS 3102*, 1961.
20 T. Ishimori and E. Nakamura (Eds.), *Data of Inorganic Solvent Extraction (1), JAERI-1047*, 1963.
21 H. J. M. Bowen, *Analyst (London)*, 92 (1967) 124.
22 D. F. Covell, *Anal. Chem.*, 31 (1959) 1785.
23 S. Sterlinski, *Anal. Chem.*, 40 (1968) 1995.
24 H. J. M. Bowen, *J. Radioanal. Chem.*, 19 (1974) 215.
25 L. Górski, J. Heinonen and O. Suschny, *IAEA/RL/25*, 1974.

Analytica Chimica Acta, 78 (1975) 317–327

NEUTRON ACTIVATION ANALYSIS FOR BULK AND TRACE ELEMENTS IN URINE

R. CORNELIS*, A. SPEECKE and J. HOSTE

Institute for Nuclear Sciences, Rijksuniversiteit Gent, Proeftuinstraat 86, B-9000 Gent (Belgium)

(Received 24th February 1975)

The elemental composition of urine reflects the performance of the kidneys in regulating the electrolyte and water metabolism of the body; with the faeces urine also removes superfluous and toxic substances. Research in this field has shown that each mode of excretion deals specifically with certain waste products: urine removes the bulk of Na, Cl, F, P, As, K, Rb, Ca, Mg, Co, Br, etc., whereas the intestine eliminates most of the Mn, Cu, Zn, etc.[1–4]. A knowledge of irregularities in the mode of excretion may indicate renal disorders and may be helpful in establishing suitable medication. Therefore it seems worthwhile to compare the amounts of elements in urine of normal healthy individuals with those of pathological cases.

Determination of the bulk elements Na, Cl, K, Ca, Mg, Br, etc. can be done either by n.a.a. or by any other suitable analytical technique. Trace elements, however, need much more refined analytical methods. A survey of the values reported in the literature is given in Table I; it can be seen that the so-called normal values for some very low trace contents vary considerably, depending on the laboratory performing the analyses. It is obvious that some results have been obtained by inadequate procedures or after inaccurate sampling[39], particularly in the cases of Mn, Cr and Co. In 1966 Schroeder and Nason[4] published values of 225 mg Mn per day, but Moav[33] determined 7.7–16.7 μg per day in 1965 and Kanabrocki *et al.*[18], also in 1965, reported 0.09–2.3 μg Mn per day. Van Ormer and Purdy[32] give a range of 3.0–6.1 μg Mn.

Chromium is another element for which the results are open to discussion. The highest values are reported by Schroeder and Nason[4], namely 15–60 μg per day; but fractions of a microgram up to several micrograms have been claimed as normal contents[12–16]. Similarly, for cobalt, the high values of 150–260 μg Co[4] are too different from the *ca.* 1 μg per day currently reported[5,12].

Arsenic and mercury also exhibit wide ranges, but since these elements are toxic and not essential, the divergent values may be correct.

For the purpose of this study, urine can be described as a solution with high ionic strength, containing gram amounts of Na, K, Cl, PO_4^{3-} and SO_4^{2-} per day, as well as trace elements. The latter may be ionically or organically bound, or both. Neutron activation analysis is beyond doubt the most suitable technique for determining some of the bulk elements as well as nearly all of the trace elements.

The first problem however, is how to obtain a representative urine sample

* Research Associate, Interuniversity Institute for Nuclear Sciences.

TABLE I

THE AMOUNTS OF BULK AND TRACE ELEMENTS PRESENT IN A 24-h URINE COLLECTION

Element	*Amounts per day (lit. ref. in parentheses)*						
Ag, μg	0.55 (5)						
Al, μg	100 (4)						
As, μg	180 (5)	25 (6)	255[a] (4)				
Au, μg	0.011 (5)						
B, mg	1 (4)						
Be, μg	1.6[a] (4)						
Ba, μg		8.3–38.6 (7)	0.03[a] (4)				
Br, mg	3.7 (5)	3–8[a] (8)	7.0 (4)				
Ca, mg	130–340 (7)						
Cd, μg	2.1 (5)	0.98 (9)	18–66[a] (4)	0.6–5.6[a] (10)			
Cl, g	5.6–7.3 (11)						
Co, μg	0.73 (5)	0.75[a] (12)		260 (4)			
Cr, μg	0.6[a] (12)	1.15[a] (13)	3.9–15.9[a] (14)	0–18 (15)	4.5–57 (16)	15–60[a] (4)	
Cs, μg	13 (5)						
Cu, μg	50 (5)	10–50 (17)	15–130 (18)	10–114 (19)	5–25 (20)	35 (21)	60 (4)
F, mg	3.1[a] (22)	0.45–20[a] (23)	1.6 (4)				
Fe, μg	131 (5)	92–204 (24)	250 (4)				
Hg, μg	1.0 (5)	7.2–26 (25)	4.3 (26)	7.6 (27)	15[a] (4)		
I, μg	150–360[a] (22)	126–246[a] (28)	150–1100 (29)	175 (4)			
K, g	3.5 (11)						
Li, μg	855[a] (4)						
Mg, mg	246[a] (30)						
Mn, μg	1–4 (31)	3–6.1[a] (32)	0.09–2.9 (18)	7.7–16.7 (33)	225 (4)		
Mo, μg	81 (5)	150 (4)					
Na, g	3.6–4.7 (11)						
Nb, μg	360 (4)						
Ni, μg	11 (4)						
P, g	0.47–1.39 (7)						
Pb, μg	30–180[a] (34)	54[a] (4)					
Rb, mg	2.4 (5)	2.3[a] (36)	1.1 (4)				
Sb, μg	1.5 (5)						

Sc, μg	0.073 (5)			
Se, μg	30 (5)	15–240[a] (37)	40 (4)	
Sr, μg	144–358 (7)	200 (4)		
Ti, μg	333 (4)			
Th, μg	3.6[a] (38)			
V, μg	8–46 (35)	15 (4)		
W, μg	32 (5)			
Zn, μg	520 (5)	141–779 (19)	141–415 (31)	500 (4)
Zr, μg	140 (4)			

[a] Assuming 1.5 l per day.

which is suitable for trace element analysis.

COLLECTION AND PREPARATION OF SAMPLES

Representative samples can only be obtained by a twenty-four hour urine collection. Avoidance of any contamination during collection is a very difficult task. The first requirement is a very clean collection vessel. For this purpose, a high-density polythene container is thoroughly cleaned with H_2O_2, detergent, water, suprapure (1 + 10) HNO_3 and (1 + 10) H_2SO_4, and double-distilled water, and then steam-cleaned with triple quartz-distilled–deionized water. Nevertheless, dust falling into the container remains a hazard, as the cover must be removed several times during one day, usually not in dust-free rooms. Transfer of the urine from the body into the vessel again introduces some major risks of contamination, *e.g.* from clothes or skin.

Storage

Other errors can arise from the transfer of elements from the vessel wall into the urine, or a loss of trace elements by adsorption on to the wall. These errors depend on the choice of the container material and on the length of time the urine as a liquid remains in contact with it. As a "metal-free" container, polythene proves very convenient. Unbreakable, it is supposed to become "ultra-clean" by the profound cleansing procedure already mentioned.

An attempt was made to study the influence of storage in polythene on the stability of the trace elements in the solution.

Detection of possible losses. To 1 l of fresh urine, collected from different individuals, 1 ml of a radioactive stock solution in 6 *M* HNO_3–HCl was added, containing ^{56}Mn, ^{122}Sb, ^{64}Cu, ^{69m}Zn, ^{76}As, ^{134}Cs, ^{75}Se, ^{86}Rb, ^{51}Cr, ^{60}Co and ^{203}Hg. Reference samples of 10 ml were immediately pipetted. The rest was divided between several polythene containers, stored at room temperature and in the light.

It should be kept in mind that the chemical form of the elements added was purely ionic and cannot be strictly compared with the actual chemical form in urine. Moreover, as the tracers were not carrier-free, the concentration of all elements was markedly raised, which would counteract possible losses by adsorption. Sampling varied from 2 h up to 5 days. The duration of study varied according to the radioactive half-life: for ^{56}Mn ($T_{\frac{1}{2}}$ 2.58 h) this was one day; for ^{76}As ($T_{\frac{1}{2}}$ 26.3 h), ^{64}Cu ($T_{\frac{1}{2}}$ 12.8 h), ^{122}Sb ($T_{\frac{1}{2}}$ 2.75 d) two days; and for the other isotopes five days. The vessels remained undisturbed till sampling. Then a first 10-ml aliquot was taken from the clear supernatant solution solely, followed by another 10-ml sample from the suspension created by vigorously shaking the urine.

The results can be summarized as follows. After 2 h no losses could be found for any element. The elements which remained in the clear solution throughout storage were Mn, Co, Cs and Rb. The elements which were greatly enriched in the sediments, but were eventually brought into the suspension by vigorous shaking, were As, Cu, Sb, Cr, Hg, Se and Zn.

It therefore seems advisable to sample the urine as soon as possible (*e.g.* within 24 h after the end of the collection period), after vigorous shaking.

TABLE II

TRACE AND BULK ELEMENT CONTENT IN URINE SAMPLES, TAKEN AFTER VIGOROUS SHAKING IMMEDIATELY AT THE END OF THE 24 HOUR COLLECTION AND AFTER 3 DAYS STORAGE

Element	*Mean amounts per day*[a]	
	Immediate sampling	*Three days storage*
As, μg	24.1 ±1.2	20.6 ±1.0
Br, mg	5.4 ±0.5	5.3 ±0.5
Ca, g	0.24±0.04	0.24±0.04
Cl, g	6.5 ±0.4	6.5 ±0.4
Co, μg	2.2 ±0.6	2.3 ±0.6
Cr, μg	0.6 ±0.4	0.6 ±0.4
Cs, μg	9.9 ±0.8	9.6 ±0.8
Cu, μg	18.9 ±2.0	16.4 ±1.8
I, μg	117 ±6	108 ±5
K, g	3.0 ±0.3	3.1 ±0.3
Mn, μg	0.22±0.04	0.22±0.4
Na, g	4.2 ±0.5	4.2 ±0.5
Rb, mg	2.4 ±0.1	2.4 ±0.1
Se, μg	187 ±47	189 ±47
Zn, μg	403 ±40	389 ±39

[a] The errors given are twice the standard deviation for a single determination.

An adequate proof that this procedure of collecting and sampling suffices was given by the n.a.a. results for fifteen elements in a given urine, sampled immediately at the end of the collection and again after three days storage at room temperature (Table II). No significant differences were found for Br, Ca, Cl, Co, Cr, Sc, Cu, I, K, Mn, Na, Rb, Se and Zn, so that neither adsorption nor desorption could be traced. The small loss of arsenic is in agreement with the tracer experiments. Anyway, direct deep-freezing and lyophilization solves this problem almost completely.

Sample preparation

This manipulation is performed in a specially designed dust-free hood, in which a slight over-pressure is maintained by means of compressed air discharged through filters. The pipettes must be rinsed at least five times with the urine under study. For the determination of Br, Cl, K and Na, 1-ml fractions are pipetted into polythene vials. Samples of 5 or 10 ml are pipetted into ultra-pure polythene bags for the other elements. All plastic materials are cleaned by the procedure described above.

The samples are immediately frozen in liquid nitrogen and lyophilized. Lyophilization lasts for two days and at the end dry nitrogen is passed into the drying chamber. The bags containing the lyophilized material are then carefully sealed and considered fit for irradiation.

CONTAMINATION HAZARDS DURING IRRADIATION

Transfer of traces from the polythene bags to the urine during the neutron bombardment, could invalidate the results. Indeed, some irradiation damage to the polythene occurs, as can be derived from a visual inspection of the bags. Measuring the γ-activities of the plastic material shows the presence of ^{110m}Ag, ^{198}Au, ^{82}Br, ^{51}Cr, ^{59}Fe, $^{122+124}$Sb, ^{46}Sc and ^{65}Zn. Recoil of these radioactive elements could contaminate the urine as it is washed out of the bags after irradiation.

Possible contaminations were checked in the following way: three empty "ultra-clean" polythene bags were sealed and irradiated for 14 h at a flux of $2 \cdot 10^{12}$ n cm^{-2} s^{-1}. After irradiation the bags were opened, and 10 ml of urine were pipetted into each of them, frozen in liquid nitrogen and lyophilized. Afterwards the urine was carefully washed out and measured for possible γ-activity. As expected, transfer of radioactivity occurred. When conversion to 1 l of urine was made, blank values of an apparent chromium content of 0.31 μg were detected (counting statistics 30%); this means a 5.8% apparent transfer of chromium from the bag ($\pm$55 ng Cr). An apparent transfer of 7.5% of the gold content of the bag and a 0.4% transfer of its antimony content were also observed.

Thus the n.a.a. determinations of chromium in the urine of healthy persons are seriously jeopardized by the high blank value, the normal levels being about 1 μg a day. The gold and antimony transfers are no problem, because their concentration in urine appears to be so low that their detection is impossible in the complex γ-spectra obtained by the analytical procedure outlined in this paper. In contrast, the zinc content of urine is high (*ca.* 500 μg per day) so that no significant contamination from the bag can occur (*ca.* 200 ng Zn is present in a bag).

Among the short-lived isotopes, manganese is the most difficult one to deal with from the point of view of avoidance of contamination. Its concentration in urine is minute, being as little as 0.1 μg l^{-1}. Owing to the short half-life of ^{56}Mn ($T_{\frac{1}{2}}$ 2.58 h), possible contamination during neutron irradiation was ascertained as follows. Three bags which had been irradiated for about 3 h at $2 \cdot 10^{12}$ n cm^{-2} s^{-1}, were filled with 5 ml of urine each, emptied immediately and rinsed with nitric acid. After addition of manganese carrier, the element was precipitated as manganese oxinate. Apparent manganese levels of 0.012 μg, 0.015 μg and 0.020 μg l^{-1} of urine were calculated (overall error on each determination $\pm$ 11%). The poor reproducibility of the results already indicates fortuitous contaminations.

In conclusion, it can be said that, mainly because of recoil of activated atoms during irradiation, polythene is not entirely ideal as a packing material. Nevertheless, it still offers considerable advantages. Sampling, lyophilization and irradiation are possible in a single container, thus minimizing manipulations and contamination hazards.

However, the highly hygroscopic and electrostatic nature of lyophilized urine does not allow a simple, quantitative emptying of the containers. Sample adhesion to the vessel wall is so important that complete recovery from the bag needs a thorough rinse, and this enhances contamination hazards. The use of strong nitric acid for this purpose is compulsory. It serves as a preservative and keeps the traces in solution during the prolonged storage time required for instrumental n.a.a., for which the first measurement is made one week after irradiation

and the second one two weeks after the first measurement.

ANALYTICAL METHOD

Three different sizes of urine samples were prepared, depending on the concentrations and the nuclear properties of the elements to be determined. For this purpose, suitable multielement-doped urine standards were used. Their preparation and evaluation are similar to those of the multielement serum standard[40].

The 1-ml samples

Na, Cl, K and Br. These elements occur in large concentrations and are determined by instrumental neutron activation analysis. Lyophilized urine (from a 1-ml original liquid sample) and a standard are irradiated together for 15 min at $1.73 \cdot 10^{11}$ n cm^{-2} s^{-1}; a cooling time of 5 min is allowed. The γ-rays of ^{38}Cl and ^{24}Na are detected with a Ge–Li detector (FWHM of 2.1 keV for the 1.33-MeV of ^{60}Co) and a dead-time stabilizer[41] built into the circuit. If detectable, ^{27}Mg is also determined. After allowing for the decay of ^{38}Cl ($T_{\frac{1}{2}}$ 37.3 min), the samples are suitable for measurements of ^{24}Na, ^{42}K and ^{82}Br activities.

Iodine. One week later, the same samples are submitted to a 30-min irradiation at $2.56 \cdot 10^{12}$ n cm^{-2} s^{-1}. This allows iodine to be determined by a Schöniger combustion followed by precipitation of silver iodide in strongly alkaline medium[42].

As, Cu, Mn and Zn

These elements are determined on a 5-ml urine sample which has been lyophilized. The sample is irradiated, together with a suitable standard, for 3 h at $1.80 \cdot 10^{12}$ n cm^{-2} s^{-1}. After a 2-h cooling period, the samples undergo a wet digestion with nitric and sulfuric acids in the presence of carriers, followed by precipitation of the elements either as sulphides or as oxinates. The ^{56}Mn and ^{69m}Zn activities are measured as soon as possible on a Ge–Li detector; the ^{76}As and ^{64}Cu are measured the day after irradiation.

Br, Ca, Co, Cr, Cs, Hg, Rb, Se and Zn

These elements are determined on the lyophilization residue of a 10-ml liquid sample. Irradiation, in the presence of a suitable doped standard, lasts 14 h at a neutron flux of $1.8 \cdot 10^{12}$ n cm^{-2} s^{-1}. After a cooling period of one week, to allow for the decay of ^{24}Na, the samples are measured for the first time to determine the ^{82}Br and ^{47}Ca–^{47}Sc activities, if detectable. A second measurement is done a fortnight later to determine the long-lived γ-activities of ^{60}Co, ^{134}Cs, ^{86}Rb, ^{75}Se and ^{65}Zn.

Because of their extremely low concentrations and the high ^{32}P Bremmstrahlung, ^{51}Cr and ^{203}Hg must be isolated. The distillation of chromium as CrO_2Cl_2 in the presence of Cr-carrier proved to be very suitable. It so happens that mercury is also distilled, which provides a separation from the bulk of the ^{75}Se, whose 279.6-keV γ-ray coincides with the 279.1-keV γ-ray of ^{203}Hg. Post-irradiation of part of the distillate provides an excellent method for the necessary yield determination.

RESULTS AND DISCUSSION

Trace and major elements were determined in urine from a normal, healthy male subject. Six 24-h collections were spread over a period of nine months. The results are summarized in Table III and are expressed in amounts per day; the total volume collected per day and the amount of solid residue after lyophilization are also mentioned.

TABLE III

TOTAL AMOUNTS OF BULK AND TRACE ELEMENTS IN URINE OF A MALE SUBJECT ON SIX 24-h COLLECTIONS

	Date					
	Volume/day (l)					
	Solid residue (g)					
	3-10-73	*14-2-74*	*10-3-74*	*19-3-74*	*18-4-74*	*6-6-74*
	1.5	*1.0*	*1.0*	*0.9*	*0.8*	*0.8*
	90.0	*61.1*	*66.9*	*53.1*	*50.9*	*57.5*
As, μg	1650	24.1	715	160	165	77.3
Br, mg	10.5	5.5	7.0	5.0	3.5	3.6
Ca, mg	N.d.[a]	242	N.d.	140	152	N.d.
Cl, g	11.1	6.49	5.48	6.00	3.41	4.37
Co, μg	0.5	2.2	0.9	0.8	0.8	0.6
Cr, μg	N.d.	0.6	0.3	1.2	0.6	0.7
Cs, μg	9.9	9.8	9.7	7.4	6.7	8.0
Cu, μg	N.d.	18.9	16.8	12.7	11.5	16.6
Hg, μg	N.d.	N.d.	5.9	11.4	9.8	2.3
I, μg	N.d.	117	612	125	96	102
K, g	N.d.	2.83	4.20	2.38	2.27	3.42
Mn, μg	0.64	0.22	0.15	0.10	0.11	0.11
Na, g	8.4	4.2	3.3	3.7	2.1	2.5
Rb, mg	2.1	2.3	1.1	1.8	1.8	2.6
Se, μg	36.9	184	49.0	45.2	43.8	39.2
Zn, μg	750	393	515	370	342	404

[a] Not determined.

TABLE IV

CLASSIFICATION OF THE ELEMENTS ACCORDING TO THE TOTAL AMOUNTS PRESENT IN A 24-h URINE COLLECTION

Range	*Elements*	
>1 g	Cl, K, Na	
1 mg–1 g	Br, Ca, Rb	As
1 μg–1 mg	Cs, Cu, Hg, I, Se, Zn	
<10 μg	Co, Cr, Mn	

The first comment concerns the remarkable drop in the sodium chloride

content and in the total volume of urine per day after the first collection. This coincides with a deliberate change to a low NaCl diet by the donor.

Table IV shows a classification by magnitude of the elements present in the 24-h urine outputs. Of all the elements determined cesium shows the best constancy (*s.d.* 16%). In contrast, arsenic varies wildly, up to a factor 70, reaching the very high value of 1.7 mg per day. The Co, Cr and Mn values are very low compared to some of the values reported in the literature. The extreme attention paid to the method of collection, the use of "ultra-clean" vials and the work in a dust-free room explain beyond doubt the present low manganese values. For cobalt and chromium, the careful metal-free manipulations probably explain the low values obtained.

The trace and major element pattern of urine from a healthy female subject on two different occasions, and the data for another male subject, are given in Table V. Classification of the elements according to the order of magnitude, completely coincides with the one already made in Table IV.

TABLE V

TOTAL AMOUNTS OF BULK AND TRACE ELEMENTS IN URINE OF A FEMALE SUBJECT AND A MALE SUBJECT FOR 24-h COLLECTIONS

	Female subject		*Male subject*
	Date		
	Volume/day (l)		
	Solid residue (g)		
	6-12-73	*3-10-74*	*14-2-73*
	1.1	*1.3*	*2.35*
	46.1	*49.9*	*93.2*
As, μg	480	21.8	1190
Br, mg	4.39	5.30	4.2
Cl, g	2.91	3.80	8.6
Co, μg	0.6	0.9	2.7
Cr, μg	N.d.[a]	1.1	N.d.
Cs, μg	10.4	12.4	20
Cu, μg	26	13	34
Hg, μg	6	2.5	N.d.
I, μg	921	255	501
K, g	1.78	3.15	5.9
Mg, mg	N.d.	N.d.	225
Mn, μg	0.67	0.093	0.37
Na, g	2.17	2.30	5.6
Rb, mg	1.57	2.61	4.0
Se, μg	27	19.5	90
Zn, μg	85	177	506

[a] Not determined.

In conclusion, it can be said that the careful analytical method outlined in this paper ensures reliable results. The necessity of avoiding any possible contamination must continuously be kept in mind, and pursued by strict discipline and appropriate storage. In studying the amounts of traces in urine of one person over

a period of one year and of two other persons on different occasions, no "high" results for Mn, Co and Cu were ever detected. An elaborate survey can therefore be started to determine the distribution of trace and macro elements in urine of normal healthy individuals in comparison with those of pathological ones.

The authors acknowledge with gratitude the valuable technical assistance of Mr. L. Mees. The work was supported by the Inter-University Institute for Nuclear Sciences.

SUMMARY

Problems in sampling urine for trace element analysis by neutron activation are systematically examined. Collection, storage, sample preparation and contamination hazards during irradiation are studied in detail. Three different sizes of urine samples are prepared for analysis, depending on the concentration and nuclear properties of the elements, and suitable multielement doped urine standards are used. As, Br, Ca, Cl, Co, Cr, Cs, Cu, Hg, I, K, Mg, Mn, Na, Rb, Se and Zn are determined. The extreme care given to sample collection, use of "ultra-clean" vials, and work in a dust-free room, allows consistent values to be obtained over long periods of time. A literature review of the amounts of forty elements present in urine per day is also given.

REFERENCES

1 H. J. M. Bowen, *Trace Elements in Biochemistry*, Academic Press, New York, 1966, pp. 98–101.
2 L. S. Maynard and S. Fink, *J. Clin. Invest.*, 35 (1956) 831.
3 G. C. Cotzias, *Physiol. Rev.*, 38 (1953) 503.
4 H. A. Schroeder and A. P. Nason, *Clin. Chem.*, 17 (1971) 461.
5 P. O. Wester, *Acta Med. Scand.*, 194 (1973) 505.
6 D. Brune, K. Samsahl and P. O. Wester, *Clin. Chim. Acta*, 13 (1966) 285.
7 T. E. F. Carr and A. Sutton, *Nuclear Activation Techniques in the Life Sciences, IAEA-SM 91/12*, Amsterdam, 1967, p. 445.
8 S. Ohno, *Analyst (London)*, 96 (1971) 423.
9 G. Lehnert, K. H. Schaller and Th. Haas, *Z. Klin. Chem. Klin. Biochem.*, 6 (1968) 174.
10 R. T. Ross and J. G. Gonzalez, *Anal. Chim. Acta*, 70 (1974) 443.
11 W. S. Spector, *Handbook of Biological Data*, Saunders, Philadelphia 1956.
12 R. F. Coleman, J. Herrington and J. T. Scales, *Brit. Med. J.*, 1 (1973) 527.
13 K. Beyermann, H. J. Rose and R. P. Christian, *Anal. Chim. Acta*, 45 (1969) 51.
14 I. W. F. Davidson and W. L. Secrest, *Anal. Chem.*, 44 (1972) 1808.
15 K. M. Hambidge, *Anal. Chem.*, 43 (1971) 103.
16 R. T. Ross, J. G. Gonzalez and D. A. Segar, *Anal. Chim. Acta*, 63 (1973) 205.
17 C. J. Gubler, H. Brown, H. Markowitz, G. E. Cartwright and M. M. Wintrobe, *J. Clin. Invest.*, 36 (1957) 1208.
18 E. L. Kanabrocki, L. F. Case, Th. Fields, L. Graham, E. B. Miller, Y. T. Oester and E. Kaplan, *J. Nucl. Med.*, 6 (1965) 780.
19 S. Meret and R. I. Henkin, *Clin. Chem.*, 17 (1971) 369.
20 G. E. Cartwright and M. M. Wintrobe, *Amer. J. Clin. Nutr.*, 14 (1964) 224.
21 G. T. Strickland, W. M. Becker, M. L. Leu and S. O'Reilley, *Clin. Sci.*, 43 (1972) 605.
22 S. Ohno, M. Suzuki, K. Sasajima and S. Iwata, *Analyst (London)*, 95 (1970) 260.
23 J. D. Neefus, J. Cholak and B. E. Saltzman, *Amer. Ind. Hyg. Ass., J.*, 31 (1970) 96.
24 M. Brodnova, Vosteck and Hoenig, *Scand. J. Gastroenterol.*, 1 (1968) 167.

25 K. J. Rohm and W. C. Purdy, *Anal. Chim. Acta*, 72 (1974) 177.
26 K. M. Schaller, P. Strasser, R. Woitowitz and D. Szadkowski, *Z. Anal. Chem.*, 256 (1971) 123.
27 O. S. Gibbs, *J. Pharmacol. Exp. Ther.*, 72 (1941) 16.
28 M. Heurtebise and W. J. Ross, *Anal. Chem.*, 43 (1971) 1438.
29 A. J. Blotcky, D. M. Duven, W. M. Grauer and E. P. Rack, *Anal. Chem.*, 46 (1974) 838.
30 C. K. Kim and W. W. Meinke, *2nd Modern Trends in Activation Analysis, Texas*, I.A.E.A., 1965, p. 316.
31 E. D. Bird, W. H. Ellis and W. C. Thomas, Jr., *2nd Modern Trends in Activation Analysis, Texas*, I.A.E.A., 1965, p. 216.
32 D. G. Van Ormer and W. C. Purdy, *Anal. Chim. Acta*, 64 (1973) 93.
33 B. Moav, *Int. J. Appl. Radiat. Isotopes*, 16 (1965) 365.
34 G. A. Rechnitz and N. C. Kenny, *Anal. Lett.*, 3 (1970) 259.
35 G. D. Christian, *Anal. Lett.*, 4 (1971) 187.
36 O. L. Wood, *Biochem. Med.*, 3 (1970) 458.
37 G. J. Patriarche, *Anal. Lett.*, 5 (1972) 45.
38 B. L. Twitty and M. W. Boback, *Anal. Chim. Acta*, 49 (1970) 19.
39 A. Speecke, J. Hoste and J. Versieck, *7th Materials Research Symposium: Accuracy in Trace Analysis*, NBS, Gaithersburg, 1974.
40 R. Cornelis, A. Speecke and J. Hoste, *Anal. Chim. Acta*, 68 (1973) 1.
41 J. Bartošek, F. Adams and J. Hoste, *Nucl. Instr. Methods*, 103 (1972) 45.
42 R. Cornelis and J. Hoste, *J. Radioanal. Chem.*, 13 (1973) 419.

Analytica Chimica Acta, 78 (1975) 329–341

SIMULTANEOUS DETERMINATION OF ALUMINA AND SILICA IN BAUXITE BY INSTRUMENTAL NEUTRON ACTIVATION ANALYSIS WITH THE AID OF A ^{227}Ac–Be ISOTOPIC NEUTRON SOURCE

L. ALAERTS*, J. P. OP DE BEECK and J. HOSTE

Institute for Nuclear Sciences, Rijksuniversiteit Gent, Proeftuinstraat 86, B-9000 Gent (Belgium)

(Received 16th February 1975)

Apart from the tedious decomposition of bauxites by digestion with strong mineral acids, the gravimetric determination of the aluminium content is subject to interferences by many other elements that are usually present in the ore. Especially the oxides of iron, titanium, phosphorus, chromium, vanadium and zirconium may coprecipitate with the alumina. As a result, corrections by other time-consuming chemical determinations[1] are necessary.

In view of the great industrial importance of bauxite for the aluminium industry, several authors have investigated the determination of silica and alumina by means of fast nuclear methods with isotopic neutron sources.

Aluminium can be determined by means of the reaction ^{27}Al(n,γ)^{28}Al without interference from the reaction ^{28}Si(n,p)^{28}Al, by using low-energy isotopic neutron sources such as ^{210}Po–B (ref. 2) and ^{124}Sb–Be (ref. 3). The simultaneous determination of Al and Si by a double irradiation technique, with and without a cadmium cover, has been reported by Ivanov *et al.*[4], Tatar and Shiklosh[5] and Dugain and Tatar[6,7]. For the industrial analysis of large series of samples, completely automatic systems[5,8] and on-stream analyzers[9] have been described. In all of these industrial methods, speed and simplicity are mainly emphasized, whereas the precision of the aluminium determination is usually not very high.

In this paper, it is shown that the method published earlier[10] for the simultaneous determination of aluminium and silicon in ferrosilicon, with the aid of an annular ^{227}Ac–Be isotopic neutron source, can be applied to bauxite analysis and that the results obtained for aluminium are precise to better than 1%, without the use of a cadmium neutron absorber.

THE ANALYTICAL METHOD

The neutron source and counting equipment

The irradiation facility and counting equipment have been described in earlier publications[10–12]. As has already been stated, the annular construction of the ^{227}Ac–Be source results in well separated fast and thermal fluxes, so that irradiation can be done at two positions with quite different $\phi_{fast}/\phi_{thermal}$ flux ratios (10.8 and 1.5, respectively) without the use of cadmium covers[10].

* Aspirant of the N.F.W.O.

Principle of the method

Typical compositions of some bauxites are given in Table I. Only a few of the reactions listed in Table II give rise to measurable activities when bauxite is exposed to a flux of both fast and thermal neutrons. As can be seen, corrections for Fe, Mn, Ti, V and P might be required. The correction for ^{56}Mn represents only 0.1–1.0% of the ^{28}Al+^{27}Mg count, depending on the amount of iron and manganese present in the bauxite. This correction can be made by a measurement after the complete decay of ^{28}Al, ^{29}Al (negligible for the silicon concentrations present) and ^{27}Mg, but this measurement includes the long-lived ^{24}Na activity formed by an (n, α) reaction on ^{27}Al. This ^{24}Na contribution was determined precisely, from the decay curves of a pure (99.99%) aluminium sample of 6.8 g after irradiation in positions 1 and 2. After a first estimate of the aluminium content, over-corrected for the ^{56}Mn activity, the ^{24}Na activity can be approximated and used for correction of the manganese measurement. This allows a more accurate aluminium concentration estimate, resulting in a better ^{24}Na correction for manganese, etc. Since the ^{24}Na activity does not exceed 0.3% of the ^{28}Al+^{27}Mg count, only one iteration is needed. The more or less constant concentration of titanium (*ca.* 2.70%) in all of the samples (except BX 27) made it possible to calculate the interference of the ^{51}Ti short-lived activity during the measurement of the ^{28}Al, ^{27}Mg and ^{24}Na activity, immediately after irradiation. The interference is negligible ($<0.1\%$) for both irradiation positions.

The presence of phosphorus in the ore could lead to a positive error for the silicon content, because of the reaction ^{31}P(n, α) ^{28}Al; but the low cross-section for the reaction and the low content of P_2O_5 (0.1–0.2%) in bauxites make this interference almost negligible. Irradiation of analytical grade P_2O_5 and SiO_2 showed that 1 g of P_2O_5 gives approximately the same activity as 0.5 g of SiO_2. Finally vanadium (up to 0.12% in bauxite ores) leads to a significant activity through the thermal neutron reaction ^{51}V(n, γ) ^{52}V ($T_{\frac{1}{2}}=3.755$ min). Since this short-lived interference with a γ-energy of 1434.4 keV cannot be corrected for by a separate measurement, such as that for the ^{56}Mn interference, a correction by calculation, as described below, is necessary.

Mathematically the method (without ^{52}V correction) can be described as follows

$$A_{1\ net} = a \cdot W_{Si} + b \cdot W_{Al} \tag{1a}$$

$$A_{2\ net} = c \cdot W_{Si} + d \cdot W_{Al} \tag{2a}$$

for

$$A'_{1\ net} = \frac{(A_1 - B.G.) - (A'_1 - B.G.) \times k}{W_b} \tag{3}$$

$$A'_{2\ net} = \frac{(A_2 - B.G.) - (A'_2 - B.G.) \times k}{W_b} \tag{4}$$

where A_1, A_2 = total activity during 1st measurement after irradiation at position 1 or 2; A'_1, A'_2 = total activity during 2nd measurement after irradiation at position 1 or 2; *B.G.* = background including the detector background as well as the natural radioactivity in the bauxite; k = decay factor of the ^{56}Mn between the 1st and 2nd measurement [$\exp(0.693 \times 108/154.9)$]; *a.c.* = "silica coefficients", *i.e.* total specific

TABLE I

CONCENTRATIONS IN PERCENT OF THE MOST IMPORTANT ELEMENTS PRESENT IN BAUXITE ORES

	NBS 69A	*BX 11*	*BX 13*	*BX 19*	*BX 22*	*BX 23*	*BX 27*	*BX 29*	*BX 44*	*BX 48*	*BX-N*
Al_2O_3	55.0	49.45	52.30	54.10	40.71	42.65	46.60	60.90	35.12	42.67	54.30
SiO_2	6.01	10.14	5.71	3.57	18.12	11.47	20.58	0.53	13.03	2.10	7.36
Loss on ignition	29.55	11.37	11.41	13.33	12.55	16.47	24.42	31.88	20.28	11.90	11.54
Fe_2O_3	5.82	25.75	26.65	22.40	24.90	23.25	7.10	4.27	27.80	40.20	22.89
TiO_2	2.78	2.82	2.92	2.76	2.34	2.47	0.86	2.47	2.91	2.70	2.40
CaO	0.29	0.25	0.60	2.35	0.32	2.60	0.02	0.01	0.00	0.05	0.25
ZrO_2	0.18	—	—	—	—	—	—	—	—	—	—
P_2O_5	0.08	—	—	—	—	—	—	—	—	—	0.13
V_2O_5	0.03	—	—	—	—	—	—	—	—	—	—
Cr_2O_3	0.05	—	—	—	—	—	—	—	—	—	—
BaO	0.01	—	—	—	—	—	—	—	—	—	—
MgO	0.02	—	—	—	—	—	—	—	—	—	0.13
MnO	<0.01	—	—	—	—	—	—	—	—	—	0.04
Na_2O	<0.01	—	—	—	—	—	—	—	—	—	0.09
K_2O	<0.01	—	—	—	—	—	—	—	—	—	0.07
SO_3	0.04	—	—	—	—	—	—	—	—	—	—

activity caused by silica only, after irradiation at position 1 or 2; b,d= "alumina coefficients", *i.e.* total specific acitivity caused by alumina only, after irradiation at position 1 or 2; W_{Si}=weight of SiO_2 per g of bauxite in the sample; W_{Al}=weight of Al_2O_3 per g of bauxite in the sample; W_b=weight of bauxite in the pellet.

Positions 1 and 2 are the irradiation positions described earlier[10].

First estimates of W_{Si} and W_{Al} are obtained by solving eqns. (1a) and (2a), by means of eqns. (3) and (4) for $A_{1,net}$ and $A_{2,net}$. A better estimate for $A_{1\ net}$ and $A_{2\ net}$ can then be calculated which takes into account the ^{24}Na contribution to the ^{56}Mn measurement:

$$A^{II}_{1\ net} = \frac{(A_1 - B.G.) - [(A'_1 - B.G.) - A''_1 \times W_{Al}] \times k}{W_b} \tag{5}$$

$$A^{II}_{2\ net} = \frac{(A_2 - B.G.) - [(A'_2 - B.G.) - A''_2 \times W_{Al}] \times k}{W_b} \tag{6}$$

where A''_1 and A''_2=^{24}Na activity per g of alumina during the second measurement after irradiation at position 1 or 2 determined from the decay curves of a pure Al sample. ($A''_1 = 110 \pm 5$; $A''_2 = 25 \pm 7$).

Solution of eqns. (1a) and (2a) by means of eqns. (5) and (6) gives more accurate values for W_{Si} and W_{Al}.

TABLE II

NUCLEAR REACTIONS AND DATA

Reaction	*Abundance of parent isotope (%)*	*Cross-section (mb)*[13,14]	*Half-life*[14]	*γ-Energies (keV)*[15]
(1) $^{28}Si(n,p)^{28}Al$	92.21	2.0	2.240 min	1778.8
(2) $^{29}Si(n,p)^{29}Al$	4.7	0.6	6.52 min	1273.3
(3) $^{30}Si(n,\alpha)^{27}Mg$	3.09	0.1	9.45 min	843.8; 1014.4
(4) $^{27}Al(n,\gamma)^{28}Al$	100	231	2.240 min	1778.8
(5) $^{27}Al(n,p)^{27}Mg$	100	4.3	9.45 min	843.8; 1014.4
(6) $^{27}Al(n,\alpha)^{24}Na$	100	0.65	15.02 h	1368.5; 2754.0
(7) $^{56}Fe(n,p)^{56}Mn$	91.7	0.9	2.582 h	846.8; 1811.0;
(8) $^{55}Mn(n,\gamma)^{56}Mn$	100	$13.3 \cdot 10^3$	2.582 h	2112.8
(9) $^{50}Ti(n,\gamma)^{51}Ti$	5.3	0.179	5.78 min	320.1; 928.5; 608.4
(10) $^{51}V(n,\gamma)^{52}V$	99.75	$4.88 \cdot 10^3$	3.755 min	1434.5
(11) $^{31}P(n,\alpha)^{28}Al$	100	1.3	2.240 min	1778.8

Determination of the coefficients

Two synthetic samples were prepared for determination of the coefficients a, b, c and d of eqns. (1a) and (2a). A pellet was pressed from each one with the same dimensions and approximately the same weight as the bauxite pellets of the unknown samples. The first pellet was pressed from a mixture of high-purity semiconductor silicon, carbonyl iron and wax (Hoechst, wachs C pulver) as a pelleting agent. This standard has been described for the determination of silicon in ferrosilicon[10]. A second pellet was pressed from a mixture of finely powdered high-

purity silica, high-purity alumina, analytical-grade TiO_2, carbonyl iron and wax, which resulted in a standard very similar to a typical bauxite. The silica coefficients were determined by means of pellet 1 after a small correction for ^{56}Mn (reaction 7, Table II). The pellet was irradiated four times in each irradiation position, so that four replicates were obtained for each of the "silica coefficients". In the same way, and from the mean coefficients a and c, the "alumina coefficients" were determined by irradiating the second pellet. For the actual irradiation and counting conditions, the means of the coefficients obtained and the experimental standard deviation on that mean were as follows: (in counts per 300 s g^{-1} for a 8.5 mm thick pellet containing *ca.* 4.5 g of bauxite):

$$a = 35710 \pm 90 \qquad b = 49476 \pm 130$$

$$c = 6092 \pm 10 \qquad d = 41994 \pm 90$$

Sequence of analysis

Samples were prepared from finely powdered bauxite, by the method described for ferrosilicon[10].

The sequence of analysis used for the determination of silicon and aluminium in ferrosilicon[10], in which the same pellet was irradiated at the two irradiation positions with a delay of 1 h 48 min, and measured twice after each irradiation in order to obtain a correction for ^{56}Mn can no longer be used. Indeed, the high concentration of aluminium in bauxite compared to ferrosilicon, results in a considerable ^{24}Na activity (reaction 6, Table II), which appreciably complicates the method of two irradiations and four measurements. Furthermore, in the case of bauxite, a decay time of 54 min between the first and the second counting of the same pellet after each irradiation, is no longer sufficient to reduce the ^{27}Mg activity (reaction 5, Table II) to a negligible level. The sequence of analysis was therefore modified, as shown in Fig. 1.

At position 1 each pellet of a first series of nine pellets (*e.g.* 3 pellets for 3 different bauxites) is irradiated for 200 s and then transferred from the irradiation

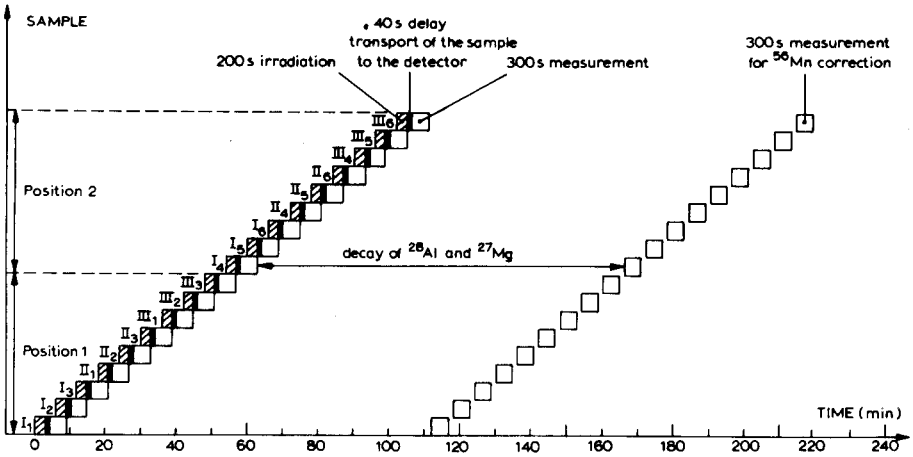

Fig. 1. Sequence of analysis for 6 pellets (1–3) of each of 3 samples (I–III).

container to the detector. A counting time of 300 s starts exactly 40 s after he end of the irradiation. The second pellet is irradiated while the first is counted. Subsequently, at position 2, a similar sequence of analysis is carried out, with a second series of nine pellets. After the last pellet has been counted, all of the pellets are counted a second time in order to provide a correction for ^{56}Mn activity, the ^{24}Na activity being taken into account as described above.

Corrections

A correction for ^{56}Mn is included in the sequence of analysis, and corrections for the decay of the ^{227}Ac (0.0088% per day) and for geometrical errors during irradiation (pellet thicknesses between 8.3 and 9.3 mm) have been described in connection with the ferrosilicon analysis[10].However, as the position of the source had been changed since the ferrosilicon experiments, the correction curves for differences in pellet thickness were accurately redetermined. Figure 2 shows the four correction curves (one for each coefficient) normalized for a 8.5-mm thick pellet.

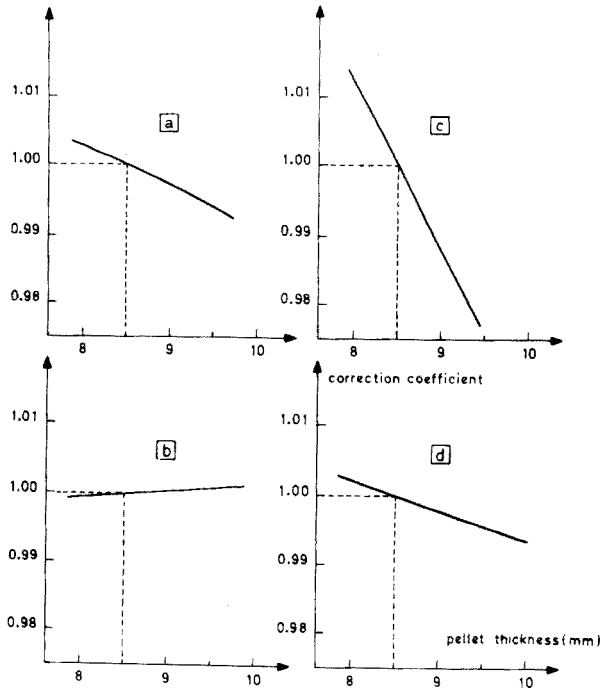

Fig. 2. Correction factors for the coefficients of eqns. (1a) and (2a) as a function of pellet thickness.

After these curves have been established for a given irradiation set-up, the correction can be read from a graph or can be taken into account by calculation as shown in eqns. (1b) and (2b):

$$A_{1\ \mathrm{net}} = a_h \cdot W_{\mathrm{Si}} + b_h \cdot W_{\mathrm{Al}} \tag{1b}$$

$$A_{2\ \mathrm{net}} = c_h \cdot W_{\mathrm{Si}} + d_h \cdot W_{\mathrm{Al}} \tag{2b}$$

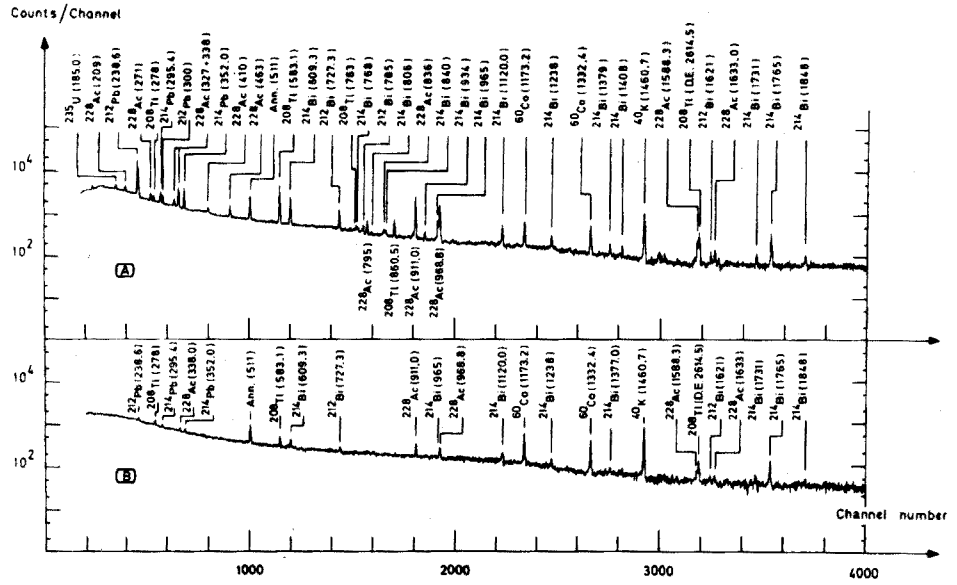

Fig. 3. Ge(Li) spectrum of 500 g of unirradiated bauxite (A) and the normal detector background (B) over the same period (64 h).

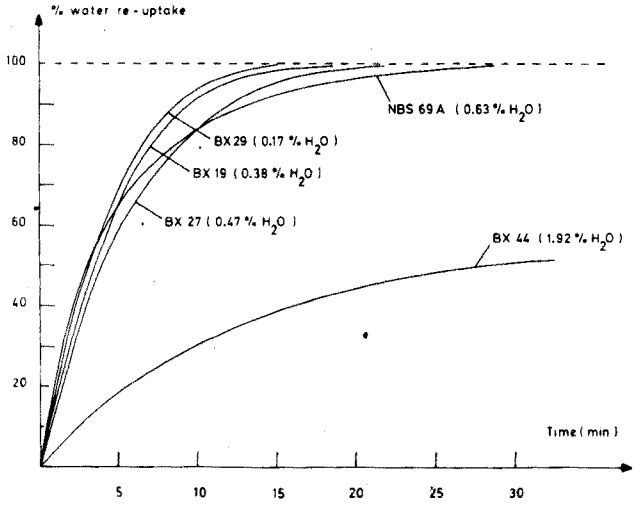

Fig. 4. Percent water re-uptake of some bauxites after drying for 2 h at 140°C.

where $a_h = a[1+(8.5-h)0.006]$
$b_h = b[1-(8.5-h)0.0008]$
$c_h = c[1+(8.5-h)0.024]$
$d_h = d[1+(8.5-h)0.004]$
h = pellet thickness in mm.

Ignoring this correction leads to a maximum relative error of *ca.* 0.4% on the alumina

determination. For samples with a low silica content, the induced error can be as large as 15% on the silica determination.

Natural radioactivity in bauxites. In Fig. 3 a Ge(Li) spectrum is shown of 500 g of an unirradiated bauxite (A). together with the normal background (B) of the same detector over the same counting period (64 h). The main activity of the bauxite is due to ^{212}Pb, ^{208}Tl, ^{228}Ac and ^{212}Bi, members of the ^{232}Th series, and ^{214}Bi and ^{214}Pb, which are both members of the ^{238}U series. Under the actual counting conditions, the integral net natural activity of the pellets varied from $\pm$350 to 1200 counts per pellet and per 300 s, corresponding to a maximum of 1.4% of the total activity measured in integral counting mode. This blank value was determined for each bauxite sample and taken into account together with the normal NaI(Tl) detector background.

Moisture of the sample. The moisture of the samples, determined by drying for 2 h at 140°C, varied from 0.17% to 1.92%. The water released by drying is taken up again very rapidly and almost completely (Fig. 4). Only one sample (BX 44), having lost 1.92% water, did not take up again all of the released water within 30 min. Since the water re-uptake is fast, drying of the samples before weighing and pellet preparation could result in errors. Therefore the humidity of the ores was determined separately and taken into account in the final results.

Vanadium correction. Because of the large cross-section (4.88 barn) of ^{51}V for thermal neutrons, in comparison with ^{27}Al, the small concentration of vanadium in bauxite (0–0.07%) leads to serious interference by the reaction ^{51}V(n,γ) ^{52}V. Although at first sight this reaction only influences the determination of alumina, the silica determination also needs a vanadium correction because of the method of analysis and calculation described above.

By irradiating analytical-grade V_2O_5 and specpure Al_2O_3, it was determined that 1 g of V_2O_5 gave 12.4 times more ^{52}V activity in the actual irradiating and measuring conditions than ^{28}Al from 1 g of Al_2O_3. Although the V_2O_5 actually used was not stoichiometric[16] ($V_2O_{4.89}$), the same compound was used as a standard for the determination of the vanadium concentrations in bauxite, so that the final correction was accurate. By solving eqns. (1b) and (2b) one obtains only approximate values for W_{Si} and W_{Al}, *i.e.* values uncorrected for ^{52}V interference ($(W_{Si})_{app}$ and $(W_{Al})_{app}$). The exact values for W_{Si} and W_{Al} can be calculated from the following set of equations:

$$A_{1\ net} = a_h W_{Si} + b_h W_{Al} + b_h(12.4 \times 0.71) W_V \tag{1c}$$

$$A_{2\ net} = c_h W_{Si} + d_h W_{Al} + d_h(12.4 \times 0.94) W_V \tag{2c}$$

where W_V = weight of $V_2O_{4.89}$ per g of bauxite.

Equations (1c) and (2c) take into account that in the irradiation positions 1 and 2, only 71% and 94% respectively, of the activity obtained from aluminium is due to ^{28}Al.

From eqns. (1b), (1c), (2b) and (2c), it can be calculated that,

$$\frac{W_{Si}}{(W_{Si})_{app}} = 1 + \frac{11.66 d_h b_h W_V - 8.8 b_h d_h W_V}{A_{1\ net} d_h - A_{2\ net} b_h} \tag{7}$$

and

$$\frac{W_{Al}}{(W_{Al})_{app}} = 1 - \frac{11.66 a_h d_h W_V - 8.8 b_h c_h W_V}{A_{2\ net} a_h - A_{1\ net} c_h} \tag{8}$$

where $(W_{Si})_{app}$ and $(W_{Al})_{app}$ are the approximate weights of SiO_2 and Al_2O_3 per g of bauxite calculated from eqns. (1b) and (2b).

After the actual values for the coefficients a_h, b_h, c_h and d_h (at 8.5 mm) have been inserted, the equations become:

$$W_{Si} = (W_{Si})_{app} + 5.15\ W_V \quad (9)$$

$$W_{Al} = (W_{Al})_{app} - 8.96\ W_V \quad (10)$$

The influence of the pellet thickness on the correction coefficients can be neglected. The precision for the correction coefficients is mainly influenced by the precision for the determination of the coefficient 12.4 described above and the percentages of thermal activation from aluminium in positions 1 and 2. As a result the following precision for the correction coefficients was calculated: 5.15 ± 0.65 and 8.96 ± 1.13.

TABLE III

V_2O_5 CONCENTRATIONS IN BAUXITE ORES

Ore code	*V_2O_5 (%)*		
	^{227}Ac–Be irradiation	*Reactor irradiation*	*Weighted mean*
BX 11	0.042 ± 0.019	0.090 ± 0.013	0.075 ± 0.011
BX 13	0.066 ± 0.022	0.074 ± 0.012	0.072 ± 0.011
BX 19	0.067 ± 0.018	0.055 ± 0.010	0.058 ± 0.009
BX 22	0.067 ± 0.023	0.082 ± 0.012	0.079 ± 0.011
BX 23	0.059 ± 0.019	0.090 ± 0.011	0.082 ± 0.010
BX 27	n.d.[a]	n.d.	—
BX 29	n.d.	0.017 ± 0.008	—
BX 44	0.096 ± 0.021	0.123 ± 0.010	0.118 ± 0.009
BX 48	0.116 ± 0.020	0.123 ± 0.013	0.121 ± 0.011
BXN	0.071 ± 0.023	0.068 ± 0.010	0.082 ± 0.009
NBS 69A	n.d.	0.038 ± 0.010	—
	Detection limit: 0.05 -0.06%	Detection limit: 0.02 -0.03%	

[a] Not detected.

The vanadium concentrations in the ores were determined by n.a.a.; samples were irradiated once with the ^{227}Ac–Be source and once in the Thetis reactor of the Institute for Nuclear Sciences. As a standard, BX 27 doped with $V_2O_{4\ 89}$ was used, and concentrations were calculated from the area of the 1434.4-keV peak of ^{52}V in a Ge(Li) spectrum. Table III shows the results for both determinations as well as the weighted mean. It can be seen that the ores can be divided into 3 classes: the first (BX 27, BX 29 and NBS 69A) contains V_2O_5 concentrations in the neighbourhood or lower than the detection limit of the analytical method; the second (BX 11, BX 13, BX 19, BX 22, BX 23 and BXN) contains *ca.* 0.075% of V_2O_5; and the third (BX 44 and BX 48) contains *ca.* 0.12% of V_2O_5. These results indicate that it should be possible to know the approximate V_2O_5 concentration of an ore if one knows its origin. The correction described above can then be estimated without a V_2O_5 determination.

TABLE IV

COMPARISON OF CHEMICAL AND N.A.A. RESULTS

	Al_2O_3 (%)				SiO_2 (%)		
	Chem.	*N.a.a.*	*N.a.a.* + V_2O_5 *correction*	*N.a.a. diff.*[a]	*Chem.*	*N.a.a.*	*N.a.a.* + V_2O_5 *correction*
REFR 1.69	60.05 ± 0.38	60.39 ± 0.27	60.39 ± 0.27	60.41 ± 0.29	36.66	36.42 ± 0.36	36.42 ± 0.36
SYNTH 4	27.73	27.91 ± 0.32	27.91 ± 0.32	—	51.52 (% Si)	51.49 ± 0.36 (% Si)	51.49 ± 0.36 (% Si)
BXN	54.30 ± 1.89[b]	54.99 ± 0.40	54.26 ± 0.42	53.53 ± 0.23	7.36 ± 0.49[b]	7.97 ± 0.40	8.39 ± 0.41
DTN	59.03 ± 1.47[b]	59.62 ± 0.40	59.62 ± 0.40	59.44 ± 0.29	36.45 ± 1.99[b]	38.03 ± 0.38	38.03 ± 0.38
NBS 69A	55.0	56.30 ± 0.43	55.96 ± 0.45	56.30 ± 0.23	6.01	5.98 ± 0.50	6.18 ± 0.50
BX 11	49.45	49.23 ± 0.31	48.56 ± 0.34	49.26 ± 0.22	10.14	11.21 ± 0.54	11.60 ± 0.54
BX 13	52.30	52.04 ± 0.32	51.39 ± 0.34	51.37 ± 0.23	5.71	6.55 ± 0.50	6.92 ± 0.50
BX 19	54.10	54.47 ± 0.43	53.95 ± 0.44	53.42 ± 0.19	3.57	3.79 ± 0.83	4.09 ± 0.83
BX 22	40.71	41.11 ± 0.23	40.40 ± 0.26	40.34 ± 0.19	18.12	18.78 ± 0.30	19.19 ± 0.31
BX 23	42.65	43.52 ± 0.32	42.78 ± 0.34	42.42 ± 0.17	11.47	11.91 ± 0.44	12.33 ± 0.45
BX 27	46.60	47.00 ± 0.27	47.00 ± 0.27	47.41 ± 0.16	20.58	20.44 ± 0.46	20.44 ± 0.46
BX 29	60.90	61.32 ± 0.33	61.17 ± 0.34	61.83 ± 0.22	0.53	0.93 ± 0.42	1.02 ± 0.42
BX 44	35.12	37.57 ± 0.24	36.51 ± 0.29	36.41 ± 0.20	13.03	14.07 ± 0.30	14.68 ± 0.32
BX 48	42.67	42.93 ± 0.25	41.85 ± 0.30	41.58 ± 0.20	2.10	3.04 ± 0.28	3.66 ± 0.30

[a] Weighted mean of 3 determinations with baseline setting at 1570 keV. 3 determinations by differential counting of the ^{28}Al peak ± the standard deviation on the mean of the six results (confidence level 70%).

[b] Standard deviation on 1 determination.

In order to check the validity of the calculated ^{52}V correction, the alumina concentrations were determined again with the measuring conditions changed so as to exclude the ^{52}V activity. Integral measurement with a baseline setting at *ca.* 1570 keV and differential counting of the 1778.9-keV peak of ^{28}Al were used.

The alumina concentrations were derived from a single measurement after correction for silica interference based on the synthetic standards, and the silica concentrations determined as described above. The results are included in Table IV; as can be seen, the two values confirm each other within the standard deviation for the determinations.

RESULTS AND DISCUSSION

Five standard samples of different origin and 9 industrial bauxite ores were used to test the method of analysis. Standard NBS 69A is certified by the U.S. National Bureau of Standards. BXN and DTN—a bauxite and a disthene (Kyanite), respectively—were subjected by the "Association Nationale de la recherche technique (France)" to a cooperative study by 21 laboratories[17]. REFR 1.69 is a refractory material with high alumina content on the basis of sillimanite, certified by the "Groupement des Utilisateurs de Matériaux Réfractaires". Finally, a synthetic standard (SYNTH 4) made in this laboratory and containing a much larger amount of silicon than typical bauxites, was used as a control; this standard pellet was pressed from a mixture of high-purity semiconductor silicon, spectrographically pure alumina, carbonyl iron and wax.

Table IV shows the results obtained by neutron activation analysis and classical methods. The standard deviations indicated for the n.a.a. results were obtained as follows: from the three counting results, corrected for ^{56}Mn, that were obtained at each irradiation position for each of the samples, the mean and the standard deviation on that mean were calculated, taking into account Student's t-factor for a 70% confidence level. With these net results, eqns. (1b) and (2b) were solved, and the standard deviations on the alumina and silica contents were calculated by means of the error propagation equations, the standard deviations on the activities as well as on the coefficients being considered. For the standard deviation on the n.a.a. results corrected for the ^{52}V contribution, the precisions of the V_2O_5 determination and of the determination of the ^{52}V correction coefficients were taken into account.

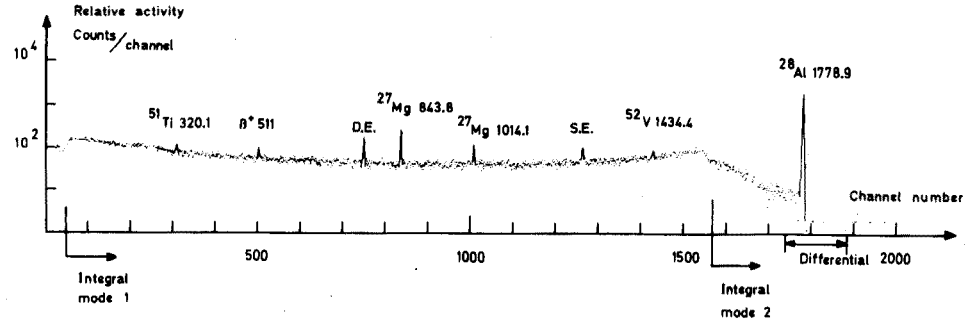

Fig. 5. Ge(Li) Spectrum of an NBS 69A sample irradiated at position 2 together with the various measuring conditions.

Table IV shows that the chemical and n.a.a. results for alumina in all the standard materials, except NBS 69A, are in very good agreement, when the indicated standard deviations are considered. In order to check whether other interfering activities than those mentioned above could influence the alumina determination, the measuring conditions were changed to exclude the contribution of ^{52}V (see above). All counting conditions, however, confirmed the high alumina value of the NBS reference material within the standard deviation on the determinations. Figure 5 shows a Ge(Li) spectrum of an irradiated NBS 69A sample; apart from the small ^{52}V contribution and a negligible ^{51}Ti peak this spectrum corresponds to a pure $^{28}Al + ^{27}Mg$ spectrum. No ^{56}Mn can be observed because this ore has a low manganese content compared to typical bauxites. For the industrial samples, the differences between chemical and n.a.a. results can be considered random with a small tendency to lower n.a.a. values.

With regard to the silica contents, for three of the standards the agreement is very good (REFR 16.9, SYNTH 4 and NBS 69A), although their origins and compositions are completely different. The high n.a.a. value for DTN was confirmed by 14-MeV activation analysis[18]. For the industrial samples, high results for silica were found by n.a.a. This systematic deviation was observed previously during the analysis of ferrosilicon[10] and may be due to the fact that gravimetric silica determinations are subject to negative errors[19].

The relative precision obtained for the alumina determination was $\pm 0.7\%$ for triplicate analysis. For the silica determination the relative precision depends strongly on the magnitude of the silica content.

Conclusions

Because of the similarity of the analytical method discussed here, to the determination of aluminium and silicon in ferrosilicon[10], essentially the same conclusions can be reached. Thus the method developed for the simultaneous determination of alumina and silica possesses high precision and accuracy, and is based on commercially available, inherently safe and relatively inexpensive irradiation facilities and measuring equipment.

The higher concentrations of aluminium in bauxite and the presence of vanadium compared to ferrosilicon, make the necessary calibrations and corrections slightly more complicated. The vanadium concentration must be determined separately or estimated from the origin of the ore; if this is not possible, the real alumina content can be calculated from an additional discriminative measurement excluding the ^{52}V activity with only a slight loss of precision.

Since all calibrations can be carried out once and for all, and since the remaining corrections are either numerically simple or are reduced to readings from graphs, the n.a.a. method is suitable for adaptation to an industrial environment for routine but precise and accurate analysis.

Both the precision and accuracy of this n.a.a. method are believed to be superior to those of similar techniques published hitherto and even to classical wet chemical analysis.

Thanks are due to the "Nationaal Fonds voor Wetenschappelijk Onderzoek" for partial financial support, to Dr. F. Dugain (Péchiney) for providing the

industrial bauxite samples, and to H. de la Roche (Assoc. Nat. de la Recherche Technique) and M. Govindaraju (Centre de Recherche Pétrographiques et Géochimiques) for providing the BXN and DTN standards.

SUMMARY

A method is described for the accurate and precise determination of alumina and silica in bauxites with the aid of a ^{227}Ac–Be isotopic neutron source with a total neutron output of 10^8 n s^{-1}. Three ores can be analysed in triplicate within 4 h, including the determination of the natural radioactivity of the ores. Samples are pellets pressed from a mixture of 4.5 g of powdered bauxite and 0.9 g of a wax as pelleting agent. The special flux distributions of the source allow irradiations at very different fast-to-thermal flux ratios without cadmium neutron absorbers. The drying and water re-uptake of bauxite and the natural radioactivity in these ores are discussed. The method was tested with several certified standards. A relative precision of 0.7% for the alumina determination was obtained for triplicate analyses. Vanadium is the only interfering element, the concentration of which should be determined separately or estimated; a correction procedure is given.

REFERENCES

1 N. H. Furman (Ed.), *Scott's Standard Methods of Chemical Analysis, Vol. II*, Van Nostrand, Princeton, 6th, edn., 1962, p. 69.
2 I. N. Plaksin, E. V. Ancheskii and M. A. Belyakov, *Dokl. Akad. Nauk SSSR*, 163 (1965) 1202.
3 R. W. Tolmie and C. J. Thompson, *Nuclear Techniques and Mineral Resources*, Vienna, I.A.E.A., 1969, 484.
4 I. N. Ivanov, N. Yu. Markun and A. S. Shtan, *Tr., Vses. Nauch.-Issled, Inst. Radiat. Tekhnol.*, 4 (1970) 186.
5 Ya. Tatar and A. Shiklosh, *Scientific and Technical Conference on Instrumentation in Activation Analysis, Budapest, 1968*, pp. 114–125.
6 F. Dugain and J. Tatar, *Ann. Inst. Geol. Publici Hung.*, 54 (1970) 375.
7 F. Dugain, *Eurisotop Report no. 61*, Eurisotop Office, Brussels, 1972.
8 A. Lundan, *Use of a Radioisotope Neutron Activation Analyzer for Process Control, 3rd Symp. on Recent Developments in N.A.A., Cambridge 2–4 July, 1973.*
9 J. R. Rhodes, *Isotop. Radiat. Technol.*, 6 (1969) 359.
10 L. Alaerts, J. P. Op de Beeck and J. Hoste, *Anal. Chim. Acta*, 70 (1974) 253.
11 L. Alaerts, J. P. Op de Beeck and J. Hoste, *Anal. Chim. Acta*, 69 (1974) 1.
12 L. Alaerts, J. P. Op de Beeck and J. Hoste, *J. Radioanal. Chem.*, 25 (1975) 155.
13 J. C. Roy and J. J. Hawton, *Report AECL-1181 (CRC-1003)*, 1960.
14 N. E. Holden and F. W. Walker, *Chart of the Nuclides*, General Electric Company, Schenectady, N.Y., 1972.
15 R. Dams and F. Adams, *J. Radioanal. Chem.*, 7 (1971) 127.
16 P. Lievens, A. Speecke and J. Hoste, *Anal. Chim. Acta*, 67 (1973) 269.
17 H. de la Roche and K. Govindaraju, *Bull. Soc. Fr. Céram.*, 90 (1971) 3.
18 K. Huysmans, Ph.D. Thesis, University of Ghent, Belgium, 1974.
19 I. M. Kolthoff and P. J. Elving, *Treatise on Analytical Chemistry, Part II, Vol. 2*, Wiley, New York, 1962, p. 156.

Analytica Chimica Acta, 78 (1975) 343–358

FLOW *VERSUS* BATCH DETECTION OF RADIOACTIVITY IN COLUMN LIQUID CHROMATOGRAPHY

G. B. SIESWERDA, H. POPPE and J. F. K. HUBER

Laboratory for Analytical Chemistry, University of Amsterdam, Nieuwe Achtergracht 166, Amsterdam (The Netherlands)

(Received 2nd December 1974)

In analytical applications, separation methods have to be combined with physical measurements. One of the most advanced combinations is column chromatography followed by measurement of a suitable physical quantity of the column effluent in a flow-through mode. Many flow-through detectors have been developed for chromatographic applications. Coupling of the detector to the separation system requires a mutual adaptation of the dynamic behaviour of both modules in order to minimize peak-broadening effects.

Radiometric flow-through detectors are a special class because of the statistical nature of the radioactive decay. The fluctuations in the number of counts measured in a given time are described by a Poisson distribution function, the relative standard deviation of which is inversely proportional to the square root of the number of counts and thus to the counting time. The precision of measurement of other physical quantities such as light absorption, electrical and thermal conductivity, or refractive index appears to increase much less with time than the precision of the measurement of radioactivity.

In this paper, the special nature of radiometric flow detectors is discussed. Conditions are derived which allow decisions to be made on the choice of flow-through or batchwise counting.

THEORETICAL

Sources of error

Each step in a chemical analysis contributes to the variations in value that appear in the final results. The following processes occur in chemical analysis and can contribute to the error: (1) sampling; (2) chemical conversion; (3) separation; (4) physical measurement.

The variance σ^2 in the final result is the sum of the variances of the single analytical steps:

$$\sigma^2 = \sum_{i=1}^{n} \sigma_i^2 \qquad (1)$$

It is necessary to estimate the different contributions to the total variance in order to improve the most pertinent steps, *viz.* those causing the greatest variation in the results.

In order to study detector effects in chromatography the other terms in eqn. (1) must be negligibly small. The contribution from the sampling process can be reduced by analysing aliquot parts from the same sample and the contribution from the chromatographic separation is not significant in most cases. Under these circumstances the variance caused by the measurement predominates. It is determined by contributions from different origins. If measurement of radioactivity is involved, the variations caused by the statistical nature of the radioactive decay become important. By taking precautions all the other possible contributions can be made negligibly small compared with that of the statistics of the radioactive decay.

Precision of counting

The influence of the statistical nature of the radioactive decay on the precision is considered here. The precision, defined as the signal-to-noise ratio, is the reciprocal of the relative standard deviation of the measurement. Counting a radioactive sample i during a time t_i results in a total number of counts N_c, which is determined by the activity of the sample, the background intensity, and the efficiency of the counting device. The background contribution to the number of counts is estimated by $t_i N_{c0}/t_0$, in which N_{c0} represents the background counts measured during counting time t_0. The nett number of counts N_{ci} originating from the radioactivity is estimated by:

$$N_{ci} = N_c - \frac{t_i}{t_0} \cdot N_{c0} \tag{2}$$

The variance of N_{ci} therefore includes contributions from N_c and N_{c0}. If the contributions from other sources such as the variation in the counting efficiency, are neglected the standard deviation of N_{ci} is determined by the statistics of radioactive decay and is given by:

$$\sigma_{N_{ci}} = \left(N_c + \frac{t_i^2}{t_0^2} \cdot N_{c0}\right)^{\frac{1}{2}} \tag{3}$$

From eqn. (3) an expression for the relative standard deviation can be derived:

$$\frac{\sigma_{N_{ci}}}{N_{ci}} = \left\{\frac{1}{N_{ci}}\left[1 + \frac{N_{c0}}{N_{ci}} \cdot \frac{t_i}{t_0}\left(1 + \frac{t_i}{t_0}\right)\right]\right\}^{\frac{1}{2}} \tag{4}$$

With the counting rate of the radioactive sample $R_{ci} = N_{ci}/t_i$ and the background intensity $R_{c0} = N_{c0}/t_0$, an expression which relates the relative standard deviation to the counting rates and times can be derived from eqn. (4):

$$\frac{\sigma_{N_{ci}}}{N_{ci}} = \left\{\frac{1}{R_{ci} t_i}\left[1 + \frac{R_{c0}}{R_{ci}}\left(1 + \frac{t_i}{t_0}\right)\right]\right\}^{\frac{1}{2}} \tag{5}$$

Figure 1 gives a graphical representation of eqn. (5). The relative standard deviation normalized with respect to the relative standard deviation $(1/R_{ci} t_i)^{\frac{1}{2}}$ caused by the radioactive sample alone is plotted as a function of the ratio of the counting times t_i/t_0 of the sample and of the background, respectively, for different background-activity ratios R_{c0}/R_{ci}. Figure 1 shows that the relative standard deviation approaches the minimum value $\{(1+R_{c0}/R_{ci})/R_{ci} t\}^{\frac{1}{2}}$ at decreasing values of t_i/t_0.

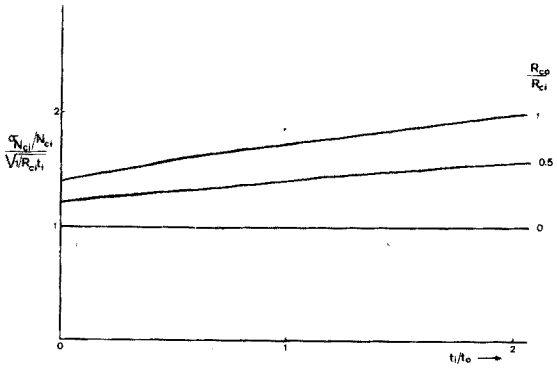

Fig. 1. Relative standard deviation caused by the statistics of the radioactive decay as a function of the counting time ratio of the sample and the background for different activity ratios of background and sample according to eqn. (5).

In order to retain a given precision, the ratio t_i/t_0 must be decreased by increasing t_0 if the ratio R_{c0}/R_{ci} increases.

In radio-column chromatography, the peak area of an eluted compound is composed of counts originating from the radioactive sample and the background. The nett number of counts N_{ci} is given by:

$$N_{ci} = N_c - \frac{t_w}{t_0} \cdot N_{c0} \tag{6}$$

in which t_w represents the peak width, which corresponds to the counting time of the elution peak; t_w has to be chosen so that the amount of radioactivity is measured as completely as possible in order to obtain high accuracy. From eqn. (6) an expression for the relative standard deviation can be obtained analogously to eqn. (4):

$$\frac{\sigma_{N_{ci}}}{N_{ci}} = \left\{\frac{1}{N_{ci}}\left[1 + \frac{N_{c0}\,t_w}{N_{ci}\,t_0}\left(1 + \frac{t_w}{t_0}\right)\right]\right\}^{\frac{1}{2}} \tag{7}$$

The counting rate R_{ci} of a radioactive sample is proportional to the number of radioactive atoms n_i (moles):

$$R_{ci} = Sn_i \tag{8}$$

where S is the sensitivity determined by the decay rate constant and the counting efficiency. During the elution of a radioactive compound, the momentary counting rate $R_{cid}(t)$ is determined by the number of radioactive atoms $n_{id}(t)$ present in the detector at a given time:

$$R_{cid}(t) = Sn_{id}(t) \tag{9}$$

The value of $n_{id}(t)$ is determined by the momentary concentration $c_{id}(V)$ of the compound in the detector, which is described by the elution function:

$$n_{id}(t) = \int_{V}^{V+V_d} c_{id}(V)\mathrm{d}V \tag{10}$$

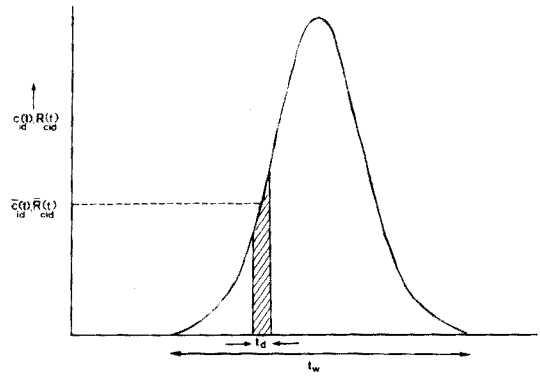

Fig. 2. Schematic representation of the passage of the elution peak through the detector; $\bar{c}_{id}(t)$ and $\bar{R}_{cid}(t)$ are the average activity concentration and counting rate at time t in the detector; t_d and t_w are the mean residence time in the detector and the peak width corresponding to the integration, respectively.

in which V_d is the detector volume and V is the eluant volume passing through the detector in time t. Combination of eqns. (9) and (10), and substitution of $dV = w dt$, in which w represents the flow rate, gives:

$$R_{cid}(t) = Sw \int_{t}^{t+t_d} c_{id}(t)dt \tag{11}$$

where t_d is the mean residence time of the radioactive atoms in the detector. The total nett number of counts is obtained by integration of eqn. (11) between $t_{Ri} - \frac{1}{2}t_w$ and $t_{Ri} + \frac{1}{2}t_w$, where t_{Ri} represents the retention time:

$$N_{ci} = Sw \int_{t_{Ri}-\frac{1}{2}t_w}^{t_{Ri}+\frac{1}{2}t_w} \int_{t}^{t+t_d} c_{id}(t)dt\,dt \tag{12}$$

Figure 2 gives a schematic representation of the situation outlined above. The integral of eqn. (11) is represented by the hatched area and can be replaced by the product $\bar{c}_{id}(t)$, in which $\bar{c}_{id}(t)$ is the average concentration in the detector:

$$\int_{t}^{t+t_d} c_{id}(t)dt = \bar{c}_{id}(t)t_d \tag{13}$$

Substitution of eqns. (8) and (13) in eqn. (12) gives an expression which relates the total nett number of counts N_{ci} to the mean residence time t_d in the detector and to the counting rate R_{ci} of the total radioactive sample:

$$N_{ci} = Swt_d \int_{t_{Ri}-\frac{1}{2}t_w}^{t_{Ri}+\frac{1}{2}t_w} \bar{c}_{id}(t)dt = t_d S n_i = t_d R_{ci} \tag{14}$$

From eqns. (7) and (14) the relationship between the relative standard deviation, the counting rates R_{ci} and R_{c0}, and the counting times t_d and t_0 can be derived:

$$\frac{\sigma_{N_{ci}}}{N_{ci}} = \left\{\frac{1}{R_{ci}t_d}\left[1 + \frac{R_{c0}}{R_{ci}} \cdot \frac{t_w}{t_d}\left(1 + \frac{t_w}{t_0}\right)\right]\right\}^{\frac{1}{2}} \tag{15}$$

In contrast to eqn. (5), the limiting value of eqn. (15) for $t_0 \gg t_w$ is determined

both by the ratio R_{c0}/R_{ci} and by the ratio t_w/t_d. An increase in t_d decreases the contribution of the radioactive sample as well as the contribution of the background. An increase in t_d can be effected either by extension of the detector volume V_d or by decrease of the flow rate w. These possibilities will be discussed in the following sections. The ratios t_i/t_0 in eqn. (5) and t_w/t_0 in eqn. (15) can be made negligibly small by the choice of a long background counting time. A simple expression for the ratio of the relative standard deviations in flow-through and batch counting can then be obtained:

$$\frac{(\sigma_{N_{ci}}/N_{ci})_{\text{flow}}}{(\sigma_{N_{ci}}/N_{ci})_{\text{batch}}} = \left\{\frac{t_i(1+R_{c0}t_w/R_{ci}t_d)}{t_d(1+R_{c0}/R_{ci})}\right\}^{\frac{1}{2}} \tag{16}$$

For $R_{ci}t_d \gg R_{c0}t_w$ and $R_{ci} \gg R_{c0}$, eqn. (16) approaches the minimum value $(t_i/t_d)^{\frac{1}{2}}$; the precision of flow counting therefore approaches a maximum compared with batch counting under these circumstances.

In eqn. (16) the counting efficiencies of flow-through and batch measurement are supposed to be equal. Flow-through counting, however, will in general be performed less efficiently. Thus in addition to the counting time ratios t_i/t_d and t_w/t_0, the ratio of the relative standard deviations in flow and batch counting is determined by the relative counting efficiency.

Precision versus resolution

From the chromatographic point of view, a small detector volume is essential for a true representation of the elution function. A smaller detector volume, however, corresponds to a smaller value of t_d and thus a larger standard deviation of the results, according to eqn. (15). A larger detector volume improves the precision of flow detection, but the chromatographic resolution of the sample components deteriorates. Good dynamic behaviour of a flow-through detector requires a cell volume not larger than $0.3\ \sigma_v^1$, where σ_v is the volume standard deviation of the elution peak. If mixing phenomena in the detector are neglected, the effect of a change of the cell volume on the measured resolution as well as on the precision of the counting can be calculated simply.

The measured resolution R'_{ji} between two sample components i and j can be defined as the difference in the measured retention times t'_{Rj} and t'_{Ri} divided by the measured standard deviation σ'_{ti} of the first component eluted:

$$R'_{ji} = \frac{t'_{Rj} - t'_{Ri}}{\sigma'_{ti}} \quad (t'_{Rj} > t'_{Ri}) \tag{17}$$

The measured values are derived from the signal function obtained from the detector as a representation of the elution function of the column. The total variance $(\sigma'_t)^2$ of the apparent elution curve represented by the detector is given by:

$$(\sigma'_t)^2 = \sigma_t^2 + \Delta\sigma_{td}^2 = \sigma_t^2\left(1 + \frac{\Delta\sigma_{td}^2}{\sigma_t^2}\right) \tag{18}$$

where σ_t^2 is the variance of the true elution function and $\Delta\sigma_{td}^2$ is the contribution of the detector to the total apparent variance. Assuming $t'_{Rj} - t'_{Ri} = t_{Rj} - t_{Ri}$, and considering the definition of the true resolution $R_{ji} = (t_{Rj} - t_{Ri})/\sigma_{ti}$, combination of

eqns. (17) and (18) gives an expression which shows the dependence of the measured resolution on the speed of the detector response $\Delta\sigma_{td}^2$:

$$R'_{ji} = R_{ji}\left(1 + \frac{\Delta\sigma_{td}^2}{\sigma_t^2}\right)^{-\frac{1}{2}} \tag{19}$$

According to eqn. (19), the apparent value of R'_{ji} approaches the true value R_{ji} for $\sigma_t^2 \gg \Delta\sigma_{td}^2$.

If mixing phenomena are neglected, the impulse response of the detector is described by a block function of width t_d. The contribution of the detector to the apparent peak variance is therefore given by:

$$\Delta\sigma_{td}^2 = t_d^2/12 \tag{20}$$

In order to obtain high accuracy (*i.e.* low systematic error) in the determination of a single component by flow-through detection, it is necessary to integrate the detector signal over a time period which corresponds to a certain width t'_w of the signal peak. This time can be expressed as a multiple α of the standard deviation σ'_t of the signal peak:

$$t'_w = \alpha\sigma'_t \tag{21}$$

Substitution of eqns. (18), (20) and (21) in eqn. (19) relates the apparent resolution R'_{ji} derived from the signal curve of the detector to the parameters α, r'_w and t_d:

$$\frac{R'_{ji}}{R_{ji}} = \left\{1 + \frac{1}{\left(\frac{12}{\alpha^2} \cdot \frac{t'^2_w}{t_d^2} - 1\right)}\right\}^{-\frac{1}{2}} \tag{22}$$

According to eqn. (19), the apparent elution function shown by the detector approaches the true elution function from the column, which has a gaussian shape, if $\sigma_t^2 \gg \Delta\sigma_{td}^2$. For this case, 99.9% of the total amount of radioactivity is measured if $\alpha = 6$. For $\sigma_t^2 \ll \Delta\sigma_{td}^2$, however, the shape of the response peak will be determined by the detector; it approaches the impulse response of the detector, which is a rectangular peak (block function) of width t_d, if mixing phenomena in the detector cell and the influence of the detector electronics can be neglected. In this case α has the value $\sqrt{12}$ according to eqn. (20). Thus the factor α can have a value between the limits $\sqrt{12}$ (determined by the detector) and 6 (determined by the column).

According to eqn. (15), t'_w and t_d also influence the relative standard deviation in quantitative analysis caused by the radioactive decay. Assuming $t_0 \gg t'_w$ and $R_{ci}t_d \gg R_{c0}t'_w$, the relative standard deviation in N_{ci} is given by:

$$\frac{\sigma_{N_{ci}}}{N_{ci}} = (R_{ci}t_d)^{-\frac{1}{2}} \tag{23}$$

The ratio of the relative standard deviations of the flow-through measurements of the same activity with different cell volumes is therefore determined by the ratio of the mean residence times in both cells. Figure 3 illustrates the meaning of eqns. (22) and (23); the resolution and relative standard deviation decrease with increasing t_d as the result of increasing detector volume. Figure 3(a) is constructed from two parts. Starting from high t'_w/t_d ratios, a value of 6 is taken for α until the apparent

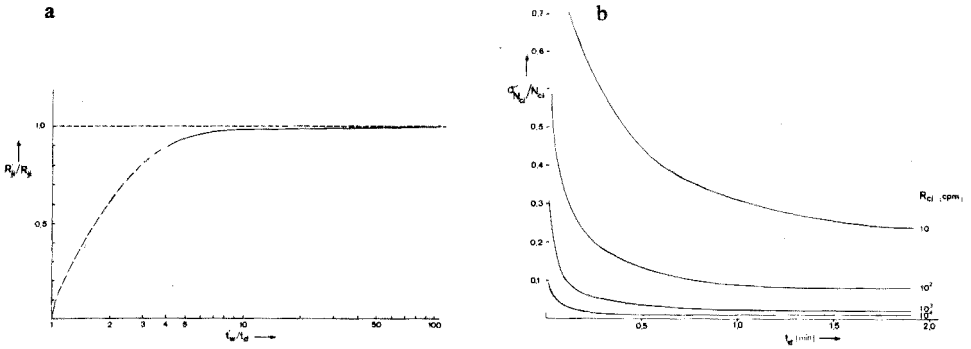

Fig. 3a. Ratio of the apparent and true resolution as a function of the ratio of the integration time and the residence time in the detector according to eqn. (22); $\alpha=6$ for $R'_{ji}/R_{ji}=1.0$ to 0.9; $\alpha=\sqrt{12}$ for $R'_{ji}/R_{ji}=0$ to 0.1; (– – –) extrapolated.
3b. Relative standard deviation caused by the statistics of radioactive decay as a function of the mean residence time in the detector for different counting rates of the test compound according to eqn. (23).

value of the resolution has decreased to 90% of the true value. It is assumed that the measured elution curve in this range is determined mainly by the column and described approximately by a gaussian function. Starting from low t'_w/t_d ratios, a value of $\sqrt{12}$ is taken for α until the apparent value of the resolution reaches 10% of the true value. It is assumed that the measured elution curve in this range is determined mainly by the detector and described approximately by a rectangular function of width t_d. Flow counting is therefore equivalent to batch counting in this case, since both the radioactivity of the sample and the background are counted for nearly the same time. The intermediate part of the curve can be constructed by interpolation. From Fig. 3(b), it is obvious that high precision cannot be expected in flow counting for counting rates smaller than 100 c.p.m. At high counting rates, a high precision can be achieved with a sufficiently large detector volume and low flow rates, respectively. For a detector volume of 10 μl and a flow rate of 0.2 ml min^{-1}, for example, the mean residence time is equal to $5 \cdot 10^{-2}$ min, which results in relative standard deviations of 13.9% and 4.5% for counting rates of 10^3 and 10^4 c.p.m., respectively.

If $t'_w/t_d=20$ under these circumstances, a 5-fold increase in the detector volume causes the apparent resolution to decrease by about 10%, as shown by Fig. 3(a). The precision, however, increases by a factor of 2.2, as shown in Fig. 3(b). Depending on the admissible decrease in the resolution, the detector volume can be increased to achieve better precision.

Precision versus retention time

The relationship between the chromatographic retention time and the precision of the radioactivity measurement is now considered. In batch counting, the counting time can be chosen arbitrarily. In flow-through measurements, the counting time equals the mean residence time in the detector, as determined by the cell volume and the flow rate, which is an important parameter in the separation process. The flow rate affects the speed of analysis, which is determined by the total time necessary for separation and detection together.

In radio column chromatography with batch counting, an effort is made to collect fractions of the column effluent containing the total amount of a single component. The counting time of the fractions can be chosen independently of the separation time. Therefore the counting time of each fraction can be adjusted to the amount of radioactivity present in the fraction in order to obtain the desired precision. The counting of the fractions can start immediately after elution of the first component, and can be continued as long as is necessary. A high precision or low detection limit can therefore be obtained at the expense of time. Batch counting should be chosen as the method of detection in chromatography at extremely low levels of trace analysis; the analysis time is determined by the counting time, which depends on the desired precision.

In radio chromatography with flow counting at the column outlet, the counting time, which equals the mean residence time in the detector, and the separation time are interdependent. Therefore the counting precision is limited by the speed of separation and the analysis time is determined by the time of separation. The speed of separation is related to the retention time of the final component. The chromatographic retention time t_{Ri} of any component i can be given as a function of its retention volume V_{Ri} and the flow rate w:

$$t_{Ri} = V_{Ri}/w \tag{24}$$

If $t_0 \gg t_w$, the introduction of $t_d = V_d/w$ and $t_w = 6\ V_{Ri}/w\ (N_{pi})^{\frac{1}{2}}$, in which N_{pi} is the theoretical plate number in eqn. (15), leads to an expression which relates the relative standard deviation of the radioactivity measurement of the flow rate, the chromatographic retention volume, and the detector volume:

$$\frac{\sigma_{N_{ci}}}{N_{ci}} = \left\{\frac{w}{R_{ci} V_d}\left(1 + \frac{R_{c0}\, 6\ V_{Ri}}{R_{ci}(N_{pi})^{\frac{1}{2}} V_d}\right)\right\}^{\frac{1}{2}} \tag{25}$$

In the interpretation of eqn. (25), it must be considered that the retention volume V_{Ri} is independent of the flow rate; the only variable dependent on flow rate is N_{pi}. The relationship between the theoretical plate number and the flow rate is rather complicated. It can be shown[2] that the theoretical plate number has a maximum at a very low flow rate in liquid chromatography. Above this value a decrease in the flow rate results in an increase in the theoretical plate number. Consequently, the first and second factors both decrease in eqn. (25) with decreasing flow rate. Equations (24) and (25) jointly allow discussion of the relationship between retention time and relative standard deviation; the flow rate is the crucial parameter in finding an optimum with respect to speed and precision in quantitative analysis by radio column chromatography with flow-through detection.

EXPERIMENTAL

Apparatus

Different types of radiometric flow detectors were used in order to test their performance. The continuous flow detector with a G.M. counter (Philips 18510) has been described previously[3]. The flow cell consists of teflon tubing (i.d. 0.6 mm) connected to the column outlet, which leads through the G.M. counter. The detector cell volume is 10 μl. The counter is used in combination with a high-voltage

power supply (Philips PW 4220) and a rate-meter (Philips PW 4242). The output signal is fed to a potentiometric recorder with ball and disc integrator (Servogor RE 512).

In another flow-through system a NaI(Tl) crystal, 2 × 2 in. well-type, was used with a photomultiplier (Nuclear Enterprises). The teflon tube (i.d. 0.6 mm) forming the detector cell is coiled up in the well. The detector cell volume can be adapted as required. In addition to the counting equipment described above, a pulse-height analyser (Philips PW 4280) was used.

The third type of detector used was described earlier[4]. Its flow cell is suitable for the measurement of weak β-emitters (^{14}C) and consists of a quartz U-pipe (i.d. 2 mm) packed with the scintillator 2,2'-phenylene-bis-(5-phenyloxazole) (POPOP; Nuclear Enterprises). The effective cell volume is about 100 μl. The detector is mounted in the counting chamber of the photomultiplier housing (Tracerlab Coruflow). The radioactivity is recorded by a rate-meter spectrometer (Tracerlab).

The chromatographic system has been described in detail previously[5] and is resistant to highly corrosive media. Two types of chromatographic columns, 480 × 5 mm and 500 × 2 mm, were used. The samples were injected with precision syringes (Hamilton, 701N, 702N, 705N) through the self-sealing membrane of the injection port.

Procedures

The samples were dissolved in the eluant before injection. The chromatographic procedures used have been described[4,5].

To determine the standard deviation caused by the sampling procedure, a sample containing a single radioactive species was injected into the column and collected in counting vials. The radioactivity was measured batchwise.

To study the effect of the detector volume on the resolution, the same amount of sample was injected, and the injection repeated after a given time interval.

Irradiations of sodium and potassium samples were carried out in the high-flux reactor (MTR-HFR) at Petten (Reactor Centre of the Netherlands).

Chemicals

^{24}NaCl, ^{42}KCl (Radiochemical Centre, Amersham), ^{86}RbCl, ^{137}CsCl (Philips Duphar, Petten), ^{14}C-labelled aspartic acid, glutamic acid, proline and serine (Radiochemical Centre, Amersham) were used as test compounds. Sodium nitrate and potassium nitrate (Merck Suprapur) were used for neutron activation.

A cation exchanger (Aminex Q-150S; BioRad Laboratories), spherical beads of diameter 20–35 μm, was used as column packing material. Separation of the alkali metals was carried out with hydrochloric acid as eluant. Separation of the amino acids was performed with a citrate buffer (pH 3.25).

RESULTS AND DISCUSSION

Influence on the precision of effects other than the statistics of radioactive decay

To determine the contribution of effects other than the statistics of radioactive decay to the standard deviation in quantitative analysis, 10-μl samples of a

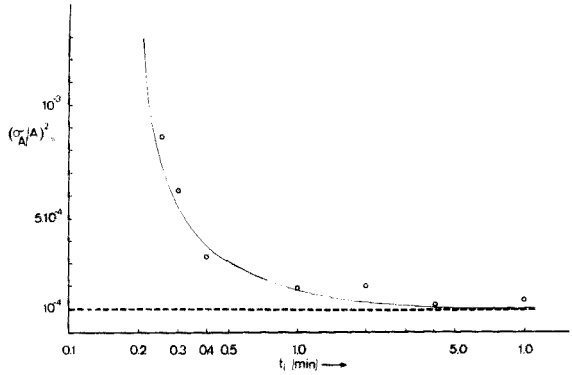

Fig. 4. Influence of other effects than statistics of radioactive decay. The average relative variance of the analytical result is plotted as a function of the counting time.

solution of ^{86}Rb in eluant were injected into the chromatographic column packed with cation exchanger. The flow rate (1 ml min^{-1}) and the composition of the eluant (4 *M* HCl) were adjusted in order to collect the total amount of the eluted sample within a volume of 4 ml. The radioactivity of the collected fraction was measured batchwise at different counting times. The experiment was repeated ten times; the average relative variance of the analytical result $(\sigma_A/A)^2$ was calculated for each counting time. Figure 4 shows the results.

As expected $(\sigma_A/A)^2$ approaches a limiting value at increasing counting times, since the relative standard deviation caused by the radioactive decay alone, $\sigma_{N_{ci}}/N_{ci}$, is inversely proportional to the square root of the counting time according to eqn. (5). From Fig. 4 it can be seen that σ_A/A approaches a limiting value of 1%, which is determined mainly by the sampling procedure. The relative standard deviation caused by the sampling has been found to be about 1%. If the contribution of $\sigma_{N_{ci}}/N_{ci}$ from the statistics of radioactive decay is not to influence significantly the result in quantitative analysis, $\sigma_{N_{ci}}/N_{ci}$ should be smaller than 1%. This demand determines the counting time required and therefore the residence time in the detector, and limits the value of R_{ci}, which can be determined, at best, with a precision of 1%. This limiting precision can only be improved if the sampling procedure is improved, or by the use of an internal standard.

Precision of flow-through counting

Three types of flow-through detectors were compared. For this purpose chromatographic separations were performed which were typical for the conditions with respect to resolution and speed. In order to facilitate the comparison of the flow-through detector, and to eliminate differences in the counting efficiencies, the samples were also counted batchwise for 1 min in the flow counting devices. For this purpose the total sample was placed in the counting chamber of the flow detector. Samples with a counting rate of about $4 \cdot 10^4$ c.p.m. per component in the corresponding flow counting device were chosen. Under these circumstances

the precision of batchwise counting was 0.5% for all flow detectors tested, which agrees with eqn. (5) with a proper choice of the counting time of the background. Subsequently, the overall relative standard deviation (σ/N_{ci}) for flow counting was determined experimentally. A total counting time of $t'_w = 6\sigma'_t$ was chosen from the chromatograms for each component. The values found were compared with the theoretical values calculated by means of eqn. (15).

The G.M. flow detector

The chromatogram of sodium, potassium, rubidium and caesium is shown in Fig. 5(a); a high precision cannot be expected for the determination of caesium, because of the marked tailing of its elution peak, and this component was therefore not included in the comparison. The detector volume was 10 μl. The results of the measurements and the calculations are compiled in Table I.

The differences between the theoretical and experimental values of the relative standard deviations, if significant, indicate effects which influence the precision in addition to the statistics of radioactive decay. Table I confirms that the statistics of the radioactive decay contribute predominantly to the overall standard deviation. The chromatographic resolution is not affected by the representation of the elution function by the detector, in agreement with eqn. (22).

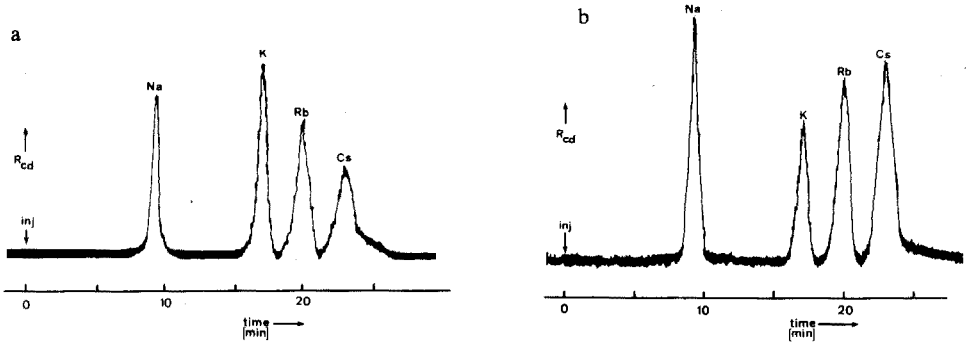

Fig. 5. Chromatogram of alkali metals ^{24}Na, ^{42}K, ^{86}Rb, ^{137}Cs. Sample dissolved in eluant; injection volume 50 μl (a), 30 μl (b). Column (480 × 5 mm) packed with cation exchanger (20–35-μm Aminex Q-150S); eluant 1.5 *M* HCl; flow rate 2 ml min^{-1}. Detection: (a) G.M. flow detector, volume 10 μl; (b) NaI(Tl) flow detector, volume 150 μl.

The NaI(Tl) flow detector

Figure 5(b) shows the chromatogram of the alkali metals; the chromatographic conditions were as in Fig. 5(a). The detector volume was 150 μl. No significant peak broadening occurred compared with detection by means of the G.M. counter. The results of the measurements and calculations are given in Table I. The data show an improvement with respect to the precision owing to the longer residence time in the detector. The theoretical and experimental values of the relative standard deviation show good agreement considering the precision of the sampling, but the value of the overall standard deviation is not completely satisfactory; it could be improved by increasing the detector volume at least 4-fold. From the chromatographic point of view, however, the detector has reached its maximum

TABLE I

PRECISION OF FLOW COUNTING

	$\sigma_v(\mu l)$	$(\sigma_{N_{ci}}/N_{ci})$ calc. (%)	$(\sigma/N_{ci})^b$ measured (%)
G.M. detector[a]			
Na	440	7.5	8.0
K	600	7.7	8.1
Rb	900	8.0	8.4
NaI(Tl) detector[c]			
Na	440	2.0	2.3
K	600	2.1	2.3
Rb	900	2.2	2.4
Scintillator detector[d]			
Aspartic acid	145	0.9	1.4
Threonine	165	1.0	1.4
Glutamic acid	200	1.0	1.5
Proline	220	1.1	1.5

[a] $V_d = 10\ \mu l$; $w = 2.0$ ml min^{-1}; $R_{c0} = 20$ c.p.m.; $R_{ci} = 4 \cdot 10^4$ c.p.m. Experimental conditions as in Fig. 5.
[b] Calculated from 5 measurements for each component; average number of counts: G.M. detector, 205, NaI(Tl) detector, 2790, scintillator detector, 20560.
[c] $V_d = 150\ \mu l$; $w = 2.0$ ml min^{-1}; $R_{c0} = 300$ c.p.m.; $R_{ci} = 4 \cdot 10^4$ c.p.m. Experimental conditions as in Fig. 5.
[d] $V_d = 100\ \mu l$; $w = 0.2$ ml min^{-1}; $R_{c0} = 350$ c.p.m.; $R_{ci} = 4 \cdot 10^4$ c.p.m. Experimental conditions as in Fig. 7.

allowable volume; any increase will decrease the resolution. The shielding of the NaI(Tl) crystal also causes difficulty. The penetrating power of the γ-radiation and the sensitivity to it makes a lead shield necessary to overcome artificial peak broadening.

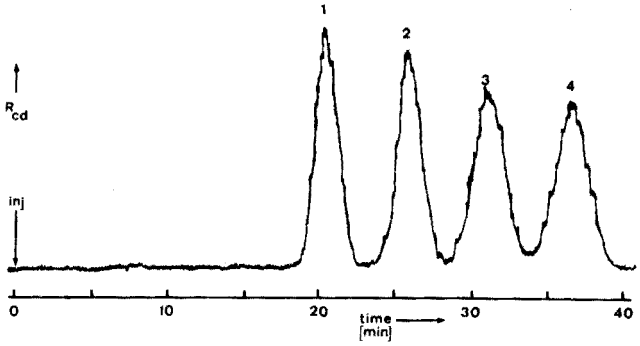

Fig. 6. Chromatogram of amino acids. Sample: aspartic acid (1), threonine (2), glutamic acid (3), proline (4); dissolved in eluant; injection volume: 40 μl. Column (500 × 2 mm) packed with cation exchanger (20–35-μm Aminex Q-150S); eluant citrate buffer (pH 3.25); flow rate 0.2 ml min^{-1}. Detector: scintillator flow detector; volume 100 μl.

The scintillator detector

The chromatogram of four amino acids is shown in Fig. 6. The detector volume was about 100 μl. Table I gives the results of the measurements and

calculations. The data show that the contribution of the statistics of the radioactive decay to the overall standard deviation has further decreased. The special construction of the detector[3], however, contributes considerably to the peak broadening, as indicated by the value of V_d expressed in terms of σ_v. This involves a considerable decrease in the resolution of two peaks at the beginning of a chromatogram obtained from a short column with a high number of theoretical plates.

Precision versus resolution

The effect on the resolution of increasing the detector volume was investigated by injecting the same amount of ^{24}Na twice, with a certain time difference between, so that two peaks of the same width and shape were produced in a given distance to simulate a given resolution. A time interval of 1 min between injections was chosen, resulting in a true resolution of 3.1. The experiments were carried out with differing detector volumes; the volume was increased stepwise from 70 to 1150 μl by winding measured lengths of tubing in the well of the NaI(Tl) crystal. Figure 7 shows the result of increasing the detector volume from 230 to 860 μl. The apparent resolution R'_{ji} decreases by 25%, whereas the peak area increases by a factor of 3.6 which corresponds with the relative increase in the detector volume. The experimental results are compiled in Table II.

It can be seen that the value of N_{ci} corresponding to the area of both peaks is proportional to the detector volume. The resolution, on the contrary, decreases as predicted by eqn. (22). Figure 8 shows the graphical representation of the apparent resolution R'_{ji}, normalized with respect to the true resolution $R_{ji}=3.1$, as a function of the reciprocal mean residence time t_d^{-1} in the detector. The simul-

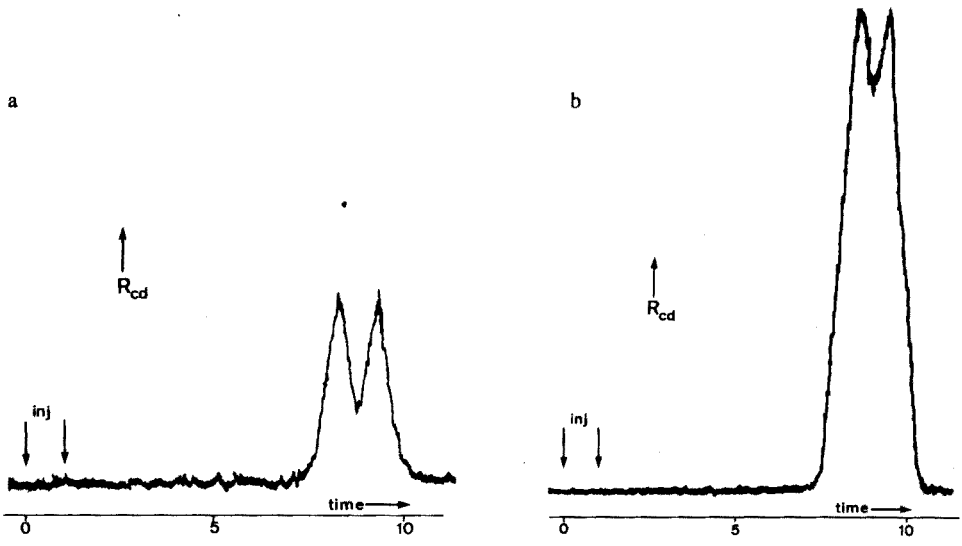

Fig. 7. Effect of the detector volume on the resolution and the peak area. Sample: ^{24}Na dissolved in eluant; double injection of 10 μl with 1 min time interval. Detection: NaI(Tl) flow detector; (a) detector volume 230 μl; (b) detector volume 860 μl. Further experimental conditions as in Table II.

TABLE II

DEPENDENCE ON THE DETECTOR VOLUME OF THE RATIO OF THE APPARENT AND TRUE RESOLUTION AND THE RELATIVE STANDARD DEVIATION σ/N_{ci}

Duplicate injections of 10 μl of ^{24}Na dissolved in eluant at a time interval of 1 min. Elution with 1.5 *M* HCl from cation exchanger. Flow rate 1.37 ml min^{-1}. Detection with NaI(Tl) crystal.)

V_d (μl)	t_d (min)	R'_{ji}	R'_{ji}/R_{ji}	N_{ci} (i.u.)	σ/N_{ci}
70	0.05	3.08	1.00	30	0.18
140	0.10	3.08	1.00	60	0.13
230	0.17	2.66	0.97	100	0.10
570	0.42	2.16	0.70	240	0.06
860	0.63	2.00	0.65	360	0.05
1150	0.84	1.91	0.62	490	0.05

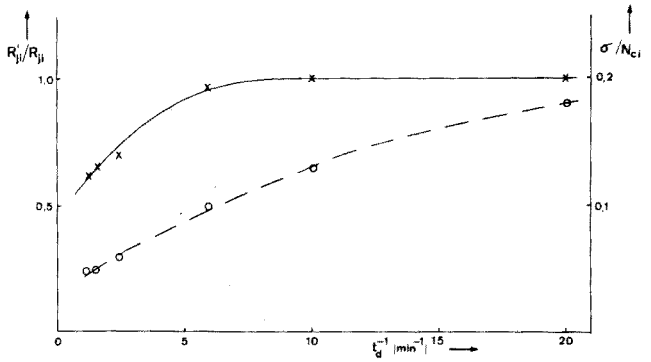

Fig. 8. Measured relative standard deviation (---) and ratio of apparent and true resolution (——) as a function of the residence time in the detector. Experimental conditions as in Table II.

taneous increase in the relative standard deviation σ/N_{ci} with smaller values of t_d is shown in Fig. 8.

Precision versus retention time

The relation between the retention time and the relative standard deviation is shown in Fig. 9. Equal amounts of radioactive ^{24}Na were injected at different flow rates. As predicted by eqn. (24), the retention time t_{Ri} decreases with the flow rate w according to a hyperbolic function, but Fig. 9 shows that the relative standard deviation σ/N_{ci} increases with increasing flow rate according to a parabolic relationship, as predicted by eqn. (25), if the background is neglected. The experimental results are summarized in Table III.

In addition to the increase of the number of counts at lower flow rates, a second favourable effect is shown by the data of Table III, *viz.* an increase in the theoretical plate number N_{pi}. According to eqn. (25), the contribution of the background to $\sigma_{N_{ci}}/N_{ci}$ is inversely proportional to the square root of N_{pi}. This means that the background contribution decreases by a factor of 1.7 by changing the flow rate from 1.79 to 0.21 ml min^{-1}.

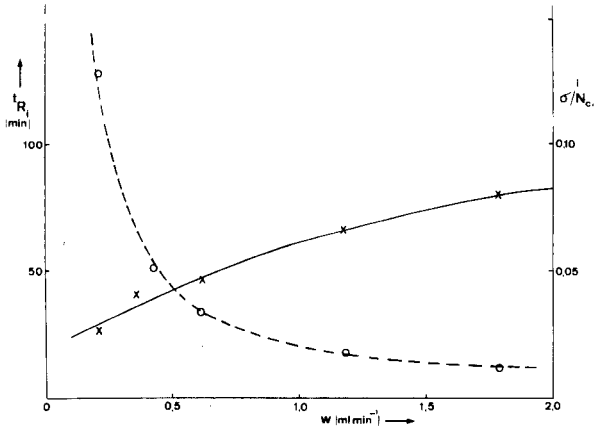

Fig. 9. Measured relative standard deviation (——) and retention time (---) as a function of the flow rate. Experimental conditions as in Table III.

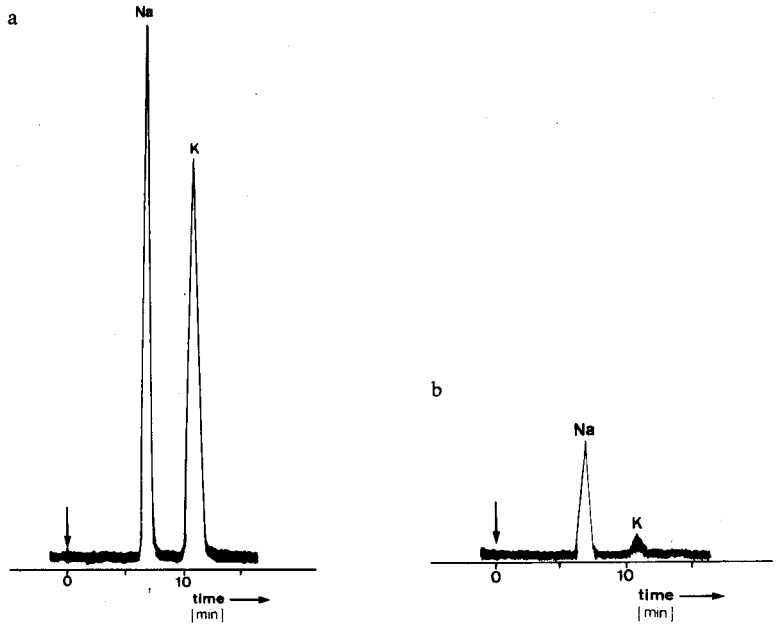

Fig. 10. Effect of energy discrimination. Sample: ^{24}Na and ^{42}K dissolved in eluant; injection volume: 40 μl. Eluant: 4 *M* HCl. Flow rate: 1.9 ml min^{-1}. Detection: NaI(Tl) flow detector; volume 150 μl. Further experimental conditions as in Fig. 5. (a) Without energy discrimination: Na–K peak area ratio = 0.9. (b) With energy discrimination: Na–K peak area ratio = 7.1.

Selectivity of the detector

The possibility of a selective detection is demonstrated by the use of a well-type NaI(Tl) crystal, which, in combination with a pulse-height analyser, allows radiation of different energies to be detected selectively; this can be used to discriminate between different types of radio nuclides.

TABLE III

DEPENDENCE OF THE RELATIVE STANDARD DEVIATION AND THE RETENTION TIME ON THE FLOW RATE

(Elution of ^{24}Na with 1.5 *M* HCl from cation exchanger. Detection with NaI(Tl) crystal. Detector volume 200 μl.)

w *ml min*$^{-1}$	t_{Ri} *(min)*	t_a *(min)*	N_{ci} *(i.u.)*	N_{pi}	σ/N_{ci}
1.79	12.0	0.11	157	850	0.08
1.18	17.7	0.17	222	1140	0.07
0.62	33.6	0.32	465	1660	0.05
0.43	51.4	0.46	583	2100	0.04
0.21	128.4	0.95	1325	2400	0.03

Figure 10 shows the chromatographic separation of sodium and potassium. The radionuclides to be detected are ^{24}Na (γ-ray energies 1.369 and 2.754 MeV) and ^{42}K (γ-ray energy 1.524 MeV). In Fig. 10(a) energy discrimination is not applied; the ratio of the sodium to potassium peak area is 0.9. The effect of energy discrimination is shown in Fig. 10(b), in which only the 2.754-MeV radiation of ^{24}Na was detected.

Energy discrimination results in a selective decrease in the counting efficiency as shown in Fig. 10. The area of the sodium peak has decreased by 20%, whereas the potassium peak is reduced to 2.5% of its original area; this is probably caused by sum-peaks of the 1.524-MeV radiation of ^{42}K.

SUMMARY

For column liquid chromatography the precision of flow counting of radioactivity is compared with that of batch counting. Theoretical derivations are presented to show the decrease of precision in flow counting as a function of the sample count rate, the background count rate and the residence time in the detector cell. A long residence time in the detector cell enhances the precision of the results, but this time can only be increased at the expense of either chromatographic resolution or retention time. The compromises which have to be made are treated quantitatively. Experimental results are shown which support the theoretical conclusions. The measurements were carried out with a GM counter, a NaI(Tl) crystal and an organic solid scintillator. It is demonstrated that the selectivity of radiometric detection can be used to improve the accuracy of the analytical results.

REFERENCES

1 H. Oster and E. Ecker, *Chromatographia*, 3 (1970) 220.
2 A. M. van Urk-Schoen and J. F. K. Huber, *Anal. Chim. Acta*, 52 (1970) 519.
3 G. B. Sieswerda and H. L. Polak, *J. Radioanal. Chem.*, 11 (1972) 49.
4 J. F. K. Huber and A. M. van Urk-Schoen, *Anal. Chim. Acta*, 58 (1972) 395.
5 J. F. K. Huber and J. A. R. J. Hulsman, *Anal. Chim. Acta*, 38 (1967) 305.

Analytica Chimica Acta, 78 (1975) 359–365

THE APPLICATION OF THERMAL AND MASS CHROMATOGRAPHY TO THERMAL OXIDATIVE DEGRADATION OF POLYMERS*

S. M. GABBAY and S. S. STIVALA

Department of Chemistry and Chemical Engineering, Stevens Institute of Technology, Hoboken, New Jersey 07030 (U.S.A.)

P. R. REED

Chromalytics Corporation, Route 82, Unionville, Pennsylvania 19375 (U.S.A.)

(Received 13th January 1975)

The detection and identification of the volatile products, resulting from the thermal oxidative degradation[1,2] of polymers, *e.g.*, polyolefins, are of interest and practical importance since they lead to an understanding of the kinetics and mechanisms. Many methods have been utilized to stabilize[3] and investigate[1,2] polyolefin oxidation both in the presence[4] and absence[5–8] of additives. The functional groups present in the non-volatile products can be examined by infrared spectroscopy (see refs. 1 and 2 for key references).

Some volatile products have been identified, mainly from polyethylene[9] and polypropylene[10] by the conventional technique of oxidizing the polymer in a separate reaction cell and condensing the volatiles subsequently in a trap cooled in a mixture of dry ice and acetone or in liquid nitrogen. The components of the condensate are then separated chromatographically and identified by chemical analysis, by mass and infrared spectroscopy, and/or by gas chromatography[9]. A major disadvantage is related to the initial step of trapping and separating the volatiles, since this generally yields non-reproducible results[10].

A standard pyrolyzer for oxidation cannot be mounted on any gas chromatograph since the oxygen atmosphere attacks the columns and the thermal conductivity detector. Recently, a relatively new technique (thermal and mass chromatography) was used to study the nature of the volatile products evolved during the thermal degradation of polyethylene[11] and polystyrene[12]. This paper describes a modification of that technique for the detection and identification of volatile products resulting from the thermal oxidation of polymers. This procedure simultaneously collects and analyzes the volatile oxidation products. The analytical data obtained provide a measure of the total gases evolved from the sample and also give gas chromatographic retention data, molecular weights, and weight ratios of the constituents evolved.

In essence, the technique used here is a combination of mass chromatography and thermal evolution analysis (t.e.a.), where the amount of volatiles evolved from the sample upon heating is monitored continuously.

* From the thesis to be submitted by S. M. Gabbay in partial fulfilment of the requirements for the degree of Doctor of Philosophy, Stevens Institute of Technology, 1975.

Mass chromatography[13], a relatively new chromatographic technique not to be confused with g.c.–m.s., utilizes two gas density balances as detectors to provide molecular weights of volatile products amenable to g.c. analysis.

EXPERIMENTAL

Material

The polyolefin used was a pure, unstabilized sample of poly(1-pentene) (IPP-1) obtained through the courtesy of Dr. Gianotti (Montedison Co., Italy).

Apparatus

Two instruments are connected in series: a thermal chromatograph (MP-3) and a mass chromatograph (MC-2) (Chromalytics Corporation, Division of Spex Industries). The flow system in the MP-3 and MC-2 (Fig. 1) consists of a sample chamber, flame ionization and thermal conductivity detectors, trap, splitter, splitter traps and two g.c. columns, each with a gas density balance detector. The solid sample chamber (Fig. 2) is a 1/4-in. o.d. (3/16-in. i.d.) quartz tube which is connected by a Swagelok fitting into a low mass firebrick oven. The sample is positioned in the tube between two heat-treated glass wool plugs.

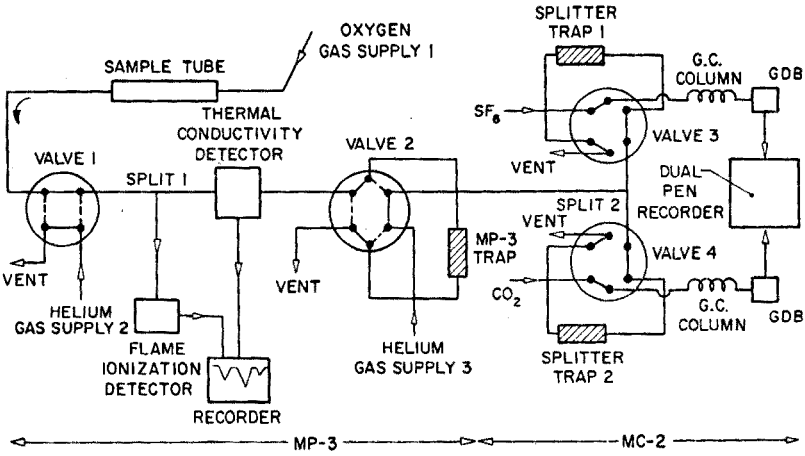

Fig. 1. Block diagram of the thermal and mass chromatograph.

The trap is a 12-in. × 1/8-in. stainless steel U-tube packed with a 6-in. layer of 8% Dexsil 300 GC on Chromosorb WHP, 80–100 mesh.

The g.c. columns are stainless steel, packed with a substrate of 10% Carbowax 20M (since polar vapors are involved) on 80–100 mesh Chrom WAW. For non-polar vapors, the columns can be packed with silicone gum SE-30 (10% w/w) on 60–80 mesh Chromosorb W.

Procedure

When the instrument is used for thermal degradation, all three gas supplies are helium. However, in this investigation, gas supply 1 was pure dry oxygen at a rate of 30 ml min^{-1}. Initially, an IPP-1 film sample was inserted between two glass wool

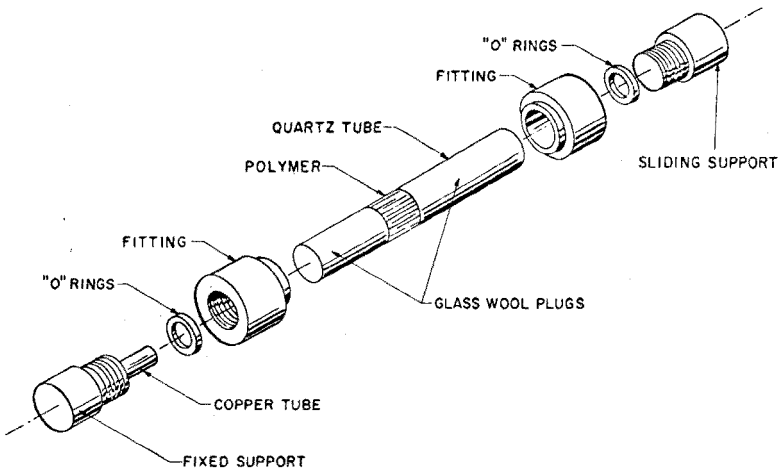

Fig. 2. Sample chamber.

plugs (previously heat treated) in order to position the sample in the quartz tube and prevent loss through gas-flow.

After assembly (with teflon O-rings and swagelok fittings) the sample was purged with helium and the furnace (preheated to 115°C) was moved into position over the sample. Gas supply 1 was then switched to pure dry oxygen (30 ml min^{-1}) for the reaction period of 75 min. At the outset of the oxidation, valve 1 was switched so as to direct the volatiles through the detection system to valve 2. At valve 2 the volatiles were trapped at room temperature (these products could also be vented or trapped at lower temperatures).

In following this path to valve 2, the volatile products are split: one half passes to the flame ionization detector (f.i.d.) and the other half passes through the thermal conductivity (t.c.) detector; when oxygen was purged for 75 min the t.c. detector was switched off. The f.i.d. response provides a measure of the total organic materials evolved. Alternatively, with an inert gas, the total evolved volatile product can be monitored with the t.c. detector. As indicated[14], the sample can either be heated isothermally (as in this work) or the temperature can be programmed, which permits the sample to be distilled and only the portions of interest are collected by switching valve 1. The same effect can be accomplished by switching valve 2; this has the added advantage of monitoring the volatile products as they are formed. The products which pass through the t.c. detector are trapped in preparation for subsequent g.c. and molecular weight analysis. Valve 2 is switched to reverse the flow through the trap in order to transfer the volatile products for mass chromatographic analysis. Rapid transfer is facilitated by ballistically heating the trap in less than 1 min. The volatile products introduced into the MC-2 are split by splitter 2, and then gas chromatographed simultaneously on two columns, each with a different carrier gas. Each volatile product from splitter 2 is collected in a trap identical to the one described above, then each of the traps is back-flushed and heated simultaneously, each with the desired carrier gas. Because each portion of the split

products is subjected simultaneously to g.c. analysis, one with SF_6 carrier and the other with CO_2, two responses are recorded for each product eluted. Fourteen volatile products from IPP-1 were detected and identified by retention times, peak enhancement, and molecular weights of the major products. Repeat runs indicated excellent reproducibility of results.

Calculations

Since the mass chromatographic segment consists of two gas chromatographs, each with a gas density balance detector, calculation of molecular weight is possible. The unique feature of this detector is a response related to the molecular difference between the carrier gas and the product eluted according to the following equation[14]:

$$d_x \approx w_x/A_x = k\, M_x/(M_x - M_g) \tag{1}$$

$$A_x = w_x \cdot k(M_x - M_g)/M_x \tag{2}$$

where d_x is the density of the volatile product VP_x, A_x the chromatograph peak area for VP_x from a given carrier gas, w_x the weight of eluted VP_x, k a constant depending on detector operating conditions, M_x the molecular weight of VP_x, and M_g the molecular weight of the carrier gas.

The value of k may be calculated from eqn. (1) for a known weighed internal standard, *e.g.*, any volatile liquid, from the measured values of A_x and the known values of w_x, M_x, and M_g. Once k is determined, eqn. (2) can be used to determine w_x for any known volatile product from its measured A_x. Alternatively, the molecular weight M_x of a volatile product may be calculated from its observed A_x if w_x is known.

In the thermal oxidative degradation of a polymer sample, the quantity w_x of a given volatile product is not known, and therefore eqn. (2) cannot be used to calculate its molecular weight M_x. To circumvent this problem, eqn. (2) is used for two carrier gases 1 and 2 of known molecular weights $(M_g)_1$ and $(M_g)_2$. As discussed above, each volatile product is split into two equal portions, (*i.e.*, w_x is equal in each carrier gas).

Rewriting eqn. (2) in the form

$$w_x = A_x M_x/k(M_x - M_g) \tag{2a}$$

we obtain for carrier gases 1 and 2, if w_x is equal in each carrier gas*,

$$w_x = \frac{(A_x)_1 M_x}{k_1[M_x - (M_g)_1]} = \frac{(A_x)_2 M_x}{k_2[M_x - (M_g)_2]} \tag{2b}$$

Rearranging, dividing both sides by k_2 and $(A_x)_1$, and letting k_1/k_2 equal K, we obtain:

$$M_x = \left\{K \cdot \frac{(A_x)_2}{(A_x)_1} \cdot (M_g)_1 - (M_g)_2\right\} \Big/ \left\{K \frac{(A_x)_2}{(A_x)_1} - 1\right\} \tag{3}$$

Hence, the molecular weight, M_x, of a volatile product x may be calculated from the observed A_x for two carrier gases, *i.e.*, $(A_x)_1$ and $(A_x)_2$, by means of eqn. (3) provided that the weight of VP_x, w_x in each carrier gas, is equal. For a given set of

* For the case where w_x is not equal in each carrier gas, the ratio between them must be kept constant and $K = \alpha k_1/\beta k_2$ where α and β are the corresponding weight fractions.

conditions (*e.g.*, rate of flow of the two carrier gases, temperature, column length, and packing materials) K is established from eqn. (1) with a known volatile compound as a standard so that M_x is known and A_x in each carrier gas is observed. Thus, if the subscript S is used in place of x in eqn. (3), K for the standard in two carrier gases 1 and 2 may be expressed as

$$K = \frac{M_S - (M_g)_1}{M_S - (M_g)_2} \cdot \frac{(A_S)_2}{(A_S)_1} \tag{4}$$

provided that the weight of the standard volatile compound w_S in each carrier gas is equal. Equation (4) not only provides the K needed to calculate the molecular weight of a volatile product, but also demonstrates that the instrument can be standardized with materials different from the unknown. Detailed discussions[13,15] of different aspects of mass chromatography have been published.

In determining the molecular weights of the volatile products of IPP-1 during the thermal oxidation, the MC-2 was standardized with three volatile standards, *i.e.*, acetone, isopropanol, isobutanol. The average value of K obtained from eqn. (4) was 0.340. To establish the accuracy of this value, the molecular weight of each alcohol was determined in a mixture of equal amounts of alcohols (C_1–C_5) when SF_6 and CO_2 were used as carrier gases. Table I shows the peak heights given by the alcohols in the corresponding carrier gases (peak heights were used instead of areas); the molecular weight of each alcohol determined from the MC-2 agrees well with the actual molecular weight.

TABLE I

MOLECULAR WEIGHTS OF A STANDARD MIXTURE OF ALCOHOLS (C_1–C_5) DETERMINED BY THE MC-2

Peak no.	*SF_6 Response (mm) × attenuation*	*CO_2 Response (mm) × attenuation*	M_x	*Actual*	*Material*
1	3.90 × 16	−2.4 × 1	32.24	32.04	Methanol
2	13.25 × 16	1.4 × 1	47.80	46.07	Ethanol
3	8.73 × 16	2.58 × 4	62.80	60.10	Propanol
4	7.97 × 16	4.70 × 4	75.25	74.12	Butanol
5	6.15 × 16	6.08 × 4	87.08	88.15	Pentanol

RESULTS AND DISCUSSION

Figure 3 shows a gas chromatogram of IPP-1 oxidized at 115°C for 75 min. The relative abundance, h_p/h_{CO_2}, of the volatile product was calculated from the ratios of the peak heights, h, of an oxidation product, p, to that of CO_2 (the first product appearing in the chromatogram, and the most abundant).

Values of h_p/h_{CO_2} ratios and their relative percentages are given in Table II in order of decreasing abundance of the volatile product relative to CO_2. The molecular weights for some of the volatile products, calculated from eqn. (3) with the value $K = 0.340$, are given in Table II. Other volatile products were determined by retention times since their peak heights were too small for accurate measurement.

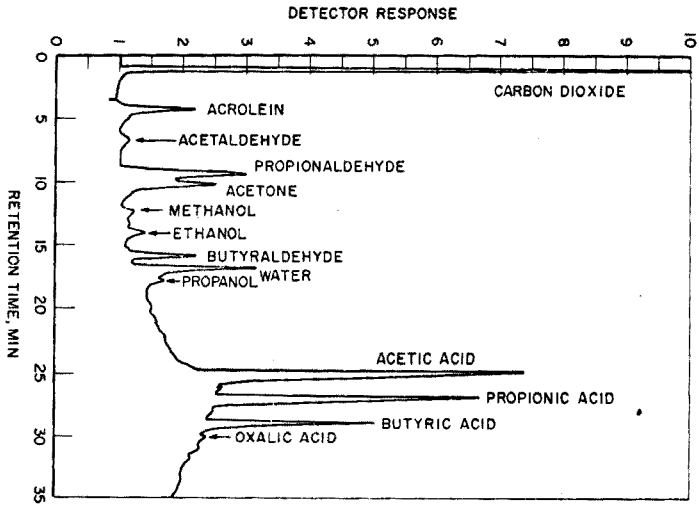

Fig. 3. Gas chromatogram of volatile products obtained from the thermal oxidative degradation of IPP-1 at 115°C.

TABLE II

RELATIVE ABUNDANCE, h_p/h_{CO_2}, OF VOLATILE OXIDATION PRODUCTS OF ISOTACTIC POLY(1-PENTENE) AT 115°C

Volatiles	h_p/h_{CO_2}	*Relative percentage*	*Calculated m.w.*	*Actual m.w.*
Carbon dioxide	1.00	65.3	—	—
Acetic acid	0.125	8.1	61.53	60
Propionic acid	0.116	7.6	74.50	74
Water	0.061	4.0	—	—
Propionaldehyde	0.055	3.6	58.58	58
Acetone	0.041	2.7	59.5	58
Butyric Acid	0.036	2.3	91.83	88
Butyraldehyde	0.033	2.2	—	—
Acrolein	0.033	2.2	—	—
Ethanol	0.011	0.7	—	—
Methanol	0.008	0.5	—	—
Propanol	0.005	0.3	—	—
Oxalic acid	0.003	0.2	—	—

As noted in Table II, the molecular weights of nine products could not be determined accurately because of their low concentrations. An assessment of the precision and accuracy of the MC-2 over a wide range of molecular weights has been given[16].

The identification of the products evolved during the thermal oxidative degradation of IPP-1 in this work was used[17] in conjunction with the non-volatile oxidation products identified by infrared spectroscopy to postulate a mechanism for the thermal oxidation of IPP-1.

The advantages of this technique are the efficient trapping of the volatile products, which minimizes secondary oxidation reactions, and the determination of

the molecular weight of virtually any material that can be chromatographed. A knowledge of the molecular weights of the products will simplify the choice of standards required in cases of peak-enhancement and/or in the determination of retention times of volatile products separated chromatographically. One of the problems encountered frequently in mass spectroscopy, *i.e.* the absence or the uncertainty of the parent ion peak which reveals the molecular weight of the unknown, is now alleviated since the MC-2 can complement these data.

SUMMARY

A modification of a relatively new technique (thermal and mass chromatography) is used to study the volatile products evolved in the thermal oxidative degradation of isotactic poly(1-pentene) at 115°C under 100% oxygen. This new technique allows certain data to be obtained much more easily and more reliably than before.

REFERENCES

1 L. Reich and S. S. Stivala, *Autoxidation of Hydrocarbons and Polyolefins*, Dekker, New York, 1969.
2 L. Reich and S. S. Stivala, *Elements of Polymer Degradation*, McGraw-Hill, New York, 1971.
3 W. L. Hawkins, *Polymer Stabilization*, Wiley-Interscience, New York, 1972.
4 S. S. Stivala, B. R. Jadrnicek and L. Reich, *J. Appl. Polym. Sci.*, 15 (1971) 2185, 2677; *Macromolecules*, 4 (1971) 61; 5 (1972) 20; *J. Polym. Sci.*, 9 (1971) 231.
5 S. S. Stivala, L. Reich and P. G. Kelleher, *Makromol. Chem.*, 59 (1963) 28.
6 B. R. Jadrnicek, S. S. Stivala and L. Reich, *J. Appl. Polym. Sci.*, 14 (1970) 2537; *Polym. Eng. Sci.*, 11 (1971) 265.
7 S. S. Stivala, G. Yo and L. Reich, *J. Appl. Polym. Sci.*, 13 (1969) 1289.
8 S. S. Stivala, E. B. Kaplan and L. Reich, *J. Appl. Polym. Sci.*, 9 (1965) 3557.
9 P. W. McKinney, *J. Gas Chromatogr.*, 2 (1964) 432.
10 R. G. Scholz, J. Bednarczyk and T. Yamanchi, *Anal. Chem.*, 38 (1966) 331.
11 E. Kiran and J. K. Güham, *J. Macromol. Sci., Chem.*, A8 (*1*) (1974) 211.
12 J. K. Gilham, private communication.
13 C. E. Bennett and D. G. Paul, *Advan. Chem. Ser.*, 125 (1973) 63.
14 C. E. Bennett, L. W. DiCave, D. G. Paul, J. A. Wegener and L. J. Levase, *Amer. Lab.*, May (1971) 67.
15 R. S. Swingle II, *J. Chromatogr. Sci.*, 12 (1974) 2.
16 A. C. Lanser, J. D. Ernst, W. F. Kwolek and H. J. Dutton, *Anal. Chem.*, 45 (1973) 14, 2344.
17 S. M. Gabbay and S. S. Stivala, paper presented at *IUPAC International Symposium on Macromolecules, Jerusalem, Israel, July 1975.*

Analytica Chimica Acta, 78 (1975) 367–373

FOAM CHROMATOGRAPHY: THE EXTRACTION AND SEPARATION OF A COPPER–CADMIUM SYSTEM BY BENZOYLACETONE-TREATED POLYURETHANE FOAM

G. N. LYPKA, H. D. GESSER and A. CHOW
Department of Chemistry, University of Manitoba, Winnipeg R3T 2N2 (Canada)
(Received 17th January 1975)

The use of open-pore polyurethane foam as a separation medium was first reported by Bowen[1], who used polyurethane foams as selective absorbants for a number of metal ions from aqueous solution. Schiller and Cook[2] used polyurethane foam to extract trace amounts of gold from natural waters. Polyurethane foams have also been used for the extraction and concentration of polychlorinate biphenyls[3] and other pesticides[4–6] from aqueous media.

Braun and Farag have made extensive studies on the use of open-pore polyurethane foam as a solid support for reversed-phase partition chromatography[7,8]. Specially treated foams have been used in the separation of a palladium, bismuth, and copper system[8]. Ion-exchange foams[9,10] and redox foams[11,12] have been prepared. Treated foams have been used for the separation of cobalt from nickel[13] as well as the recovery of gold from thiourea solutions[14]. Other papers deal with the separation of iron from copper, cobalt, and nickel[15], and the collection of trace amounts of silver[16] and mercury[17] on dithizone foams. Mercury has also been extracted from aqueous solution with sulfide-treated[18] and dithizone-treated[19] foams. In view of the wide applicability of solvent extraction systems, it was considered desirable to explore further the possibilities of using open-pore polyurethane foam systems as stationary second phases for modified solvent extraction processes. The use of benzoylacetone in the solvent extraction of metals has been extensively investigated by Starý and Hladky[20,21]. Extraction of cadmium by benzoylacetone has been described in detail[22].

This paper reports a study of the extraction of copper and cadmium by benzoylacetone-treated foam.

EXPERIMENTAL

Apparatus and reagents

A Perkin-Elmer 306 Atomic Absorption Spectrophotometer, Varian Techtron hollow-cathode lamps, and a Fisher Accumet Model 520 Digital pH Meter were used.

Open-pore polyurethane foams were cut from commercial sheets (density 1.20–1.35 lb/cu.ft.).

Benzoylacetone (1-phenyl-1,3-butanedione; J. T. Baker Chemical Co.) was used. All other chemicals were of reagent-grade unless otherwise specified. The water used was double-distilled and then deionized.

Preparation of standard and sample solutions

A 1169-p.p.m. stock solution of copper(II) was prepared by dissolving copper wire (99.90% A.C.S.; Matheson, Coleman, and Bell) in nitric acid, evaporating to dryness, and dissolving the residue in 0.1 *M* hydrochloric acid.

A 1000-p.p.m. stock solution of cadmium(II) was prepared by dissolving cadmium metal (99.9%; J. T. Baker) in a minimum amount of hydrochloric acid, and making the solution to volume with 0.1 *M* hydrochloric acid.

Sample solutions were adjusted to the desired pH with potassium hydroxide or hydrochloric acid solutions.

Procedures

Foam plugs (40 mm in diameter and 53 mm in length; average weight 1.4590 ± 0.0095 g) were cut from the foam sheets, soxhleted for 6 h with acetone, and then air-dried.

Pyrex columns (40-mm o.d.) were fitted with teflon stopcocks.

Experiments were done by placing the foams at the bottom of the column, adding the trial solution, then compressing the foam with a glass rod to "open" it. After air bubbles no longer emerged, the rod was removed, and the foams were allowed to expand to their normal size.

For static system experiments, 50.0 ml of metal solution was used, normally either 3.51 p.p.m. copper or 2.50 p.p.m. cadmium. The fluid capacity of a single foam plug was about 60 ml; this sufficed to ensure that all the sample solution was in contact with the foam. Contact time was 2 h, after which the foam was squeezed dry. The amount of metal extracted was determined by measuring the concentration of the metal solution before and after exposure to the foam.

All metal solutions were analyzed under standard conditions as listed in the Perkin-Elmer Handbook[23].

For flow-through systems, the foam was wetted with water at the desired pH, and 50.0 ml of test solution was passed through the foam, followed by a pH-adjusted water solution; 100.0-ml aliquots of effluent were collected and analyzed until no metal was detected in the solution.

Pretreatment of the foam with benzoylacetone was achieved by soaking the foams in a solution of benzoylacetone in acetone, draining them, and drying under vacuum. No change in the benzoylacetone concentration of the solution was detectable. When very dilute solutions of benzoylacetone were used, the concentration of benzoylacetone in acetone increased after contact with the foam, indicating that the benzoylacetone was not absorbed by the foam, but formed a surface coating. The amount of ligand remaining on the foam was calculated to be 0.0013 ± 0.0001 g.

Separation studies were done with solutions which contained 3.51 p.p.m. copper and 3.50 p.p.m. cadmium.

Where deviations are reported, the values refer to three or more trials.

RESULTS AND DISCUSSION

The pH-dependent extraction curves for untreated and treated foams, obtained under standard conditions for a static system, are shown in Fig. 1. The curves were very similar to those obtained in a solvent extraction process[21], the major

difference being a shift to a slightly higher $pH_{\frac{1}{2}}$ value. Both curves for cadmium extraction are similar, suggesting that the foam itself has an affinity for cadmium. Pretreatment in this case seems to lower the pH required for maximum extraction, though only to a small degree.

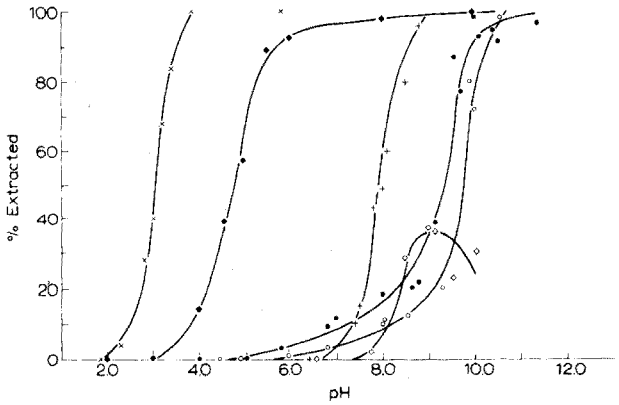

Fig. 1. The extraction of copper and cadmium by untreated and benzoylacetone treated polyurethane foam. (◆) Cu, benzoylacetone-treated foam. (◇) Cu, untreated foam. (×) Cu, solvent, extraction system[21]. (●) Cd, benzoylacetone-treated foam. (○) Cd, untreated foam. (+) Cd, solvent extraction system[21].

TABLE I

EXTRACTION OF COPPER AND CADMIUM BY BENZOYLACETONE-TREATED POLYURETHANE FOAM

Flow rate (ml min^{-1})	*Amt. Cu extracted (μg)*[a]	*% Cu extracted*[a]	*Amt. Cd extracted (μg)*[b]	*% Cd extracted*[b]
1.5	175.5	100	174.4	99.4
2.0	175.5	100		
3.0	175.5	100	174.1	99.2
6.0	170.5	97.2	174.1	99.2
12	158.5	90.4	174.1	99.2
18	152.5	87.0	174.1	99.2
250	123.5	70.4	160.1	91.2

[a] At pH 8.0.
[b] At pH 10.53.

Results for a study of flow rate effects on treated foams are shown in Table I.

Copper and cadmium were recovered from the treated foams by elution with 1.5 *M* hydrochloric acid, with corrections being made for residual volumes and concentrations. Of 171.6 ± 1.1 μg copper absorbed, 172.1 ± 1.4 μg were recovered, and of 100.5 ± 0.7 μg cadmium absorbed, 101.7 ± 5.0 μg were recovered, indicating quantitative recovery.

Recovery of trace amounts of metals by pretreated foams was also quantitative. After 300 ml of solution containing 17.5 μg of copper had been passed through the foam, 17.2 ± 0.5 μg was recovered in the acid wash. A similar run with 300 ml of

a solution containing 15.0 μg of cadmium gave a recovery of 14.7±0.3 μg. These results confirm that pretreated foams may serve as a useful preconcentration technique for trace analysis.

Separation studies on a static system are shown in Table II.

TABLE II

SEPARATION OF COPPER AND CADMIUM BY BENZOYLACETONE-TREATED POLYURETHANE FOAM IN A STATIC SYSTEM

pH	*Amt. Cd extracted (μg)*	*% Cd extracted*	*Amt. Cu extracted (μg)*	*% Cu extracted*
6.99	34.8±2.8	19.6±1.6	175.5	100
6.51	27.3±3.0	15.6±1.7	175.5	100
6.21	25.7±1.2	14.7±0.7	172.2±1.6	98.1±0.9
6.02	10.0±3.4	5.7±0.4	169.2±0.4	96.4±0.2

Extraction with consecutive foams in a static system proved to be effective for separating a copper–cadmium system by absorption. The system was run at pH 4.86, and after extraction of the solution with five foam plugs, 99.8±0.2% of the copper was extracted, together with less than 1.0 μg of cadmium.

Separation by elution techniques proved to be less effective (Table III). The foam was originally loaded with 175.1 μg of copper and 165.7 μg of cadmium, and eluted with water at various pH values. The recovery of cadmium from the foam was not what would be expected if the pH-dependent elution curve was the reverse of the pH-dependent extraction curve. Table IV gives data for flow-through extraction systems for copper–cadmium separations run at pH 4.84.

TABLE III

ELUTION OF COPPER AND CADMIUM FROM BENZOYLACETONE-TREATED FOAMS

(175.1 μg of copper and 165.7 μg of cadmium)

Elution pH	*Volume (ml)*	*Amt. Cd extracted (μg)*	*Amt. Cu extracted (μg)*
7.15	100	37.8±2.2	1.5±0.5
	100[a]	12.2±0.7	<0.5
6.05	100	11.2±1.2	<0.5
4.44	100	8.0±0.3	37.0±2.7

[a] Second 100-ml aliquot.

The fact that copper is washed off the foam suggests that the extraction process is actually an equilibrium process. At less than the optimal extraction pH, the copper involved in chelate formation is in equilibrium with the free copper ions in solution; once the copper has been bound to the column, copper is lost to the aqueous phase when copper-free water is passed.

The capacity of the benzoylacetone-treated foams was determined for both

TABLE IV

SEPARATION OF COPPER AND CADMIUM BY BENZOYLACETONE-TREATED POLYURETHANE FOAM IN A FLOW-THROUGH SYSTEM

(pH 4.84)

Portion of wash analyzed (ml)	*Amt. Cd recovered*[a] *(μg)*	*Amt. Cu recovered*[a] *(μg)*	*Amt. Cd*[b] *recovered (μg)*	*Amt. Cu*[b] *recovered (μg)*
0–100[c]	23.5±0.5	8.5±2.5	258±6.0	10.5±0.5
100–200	5.5±0.5	7.0±0.0	72.5±3.5	7.0±1.0
200–300	<0.5	3.0±0.0	8.5±2.5	3.0±1.0
Total	29.0±1.0	18.5±2.5	339±12	20.5±2.5
%	82.9±2.9	52.9±7.1	96.9±3.4	58.6±7.1

[a] Original solution: 0.35 p.p.m. Cu and 0.35 p.p.m. Cd.
[b] Original solution: 0.35 p.p.m. Cu and 3.50 p.p.m. Cd.
[c] Original solution volume.

static and flow-through systems, corrected against untreated foams. It was found that the molar absorption ratio was 1:5.6 copper–benzoylacetone. A ratio of 1:2 would be expected for simple chelate formation in a solvent extraction process. The variance may be caused by the physical nature of the system, in that the metal ion could only interact with ligand at the ligand–liquid interface. When foams having five times the regular amount of benzoylacetone were used, the molar absorption ratio at saturation was 1:23.1 copper–benzoylacetone. This reflects an increase in the amount of copper retained in the foam, from 117 μg to 143 μg copper. These results indicate that maximum extraction capacity is probably limited by the surface area of the foam, as absorption appears to be an interface reaction.

Extraction of copper by pretreated foams was shown to be slightly affected by the ionic strength of the solution (Table V), but at low concentrations of salt, which might occur during pH adjustment, the effect was negligible.

The extraction of copper was relatively unaffected by the amount of cadmium present (Table VI); this would be expected as the pH was too low for cadmium extraction. Cadmium extraction was affected by the amount of copper present,

TABLE V

EFFECT OF IONIC STRENGTH ON COPPER EXTRACTION BY BENZOYLACETONE-TREATED POLYURETHANE FOAM

pH	*KCl concn. (p.p.m.)*	*Amt. Cu extracted (μg)*	*% Cu extracted*
5.39	7	68.1±1.7	38.8±0.5
5.47	14	85.6±2.4	48.8±1.4
5.87	100	67.6	38.5
6.23	2096	66.0	37.6
6.33	10480	70.0	39.8

TABLE VI

EFFECT OF CADMIUM CONCENTRATION ON COPPER EXTRACTION AND COPPER CONCENTRATION ON CADMIUM EXTRACTION

(The volume of solution was 50 ml in all cases.)

pH	*Cu concn. (p.p.m.)*	*Cd concn. (p.p.m.)*	*% Cu extracted*	*% Cd extracted*
7.00	3.51	0.35	98.4±0.2	
7.00	3.51	3.50	98.5±0.2	
7.00	3.51	35.0	98.4±0.3	
7.00	3.51	175	98.8±0.2	
7.00	3.51	350	97.1±1.0	
10.00	0.25	2.50		88.8±0.4
10.00	2.50	2.50		70.7±0.5
10.00	25.0	2.50		53.9±1.6

probably because of competition for the ligand sites, as copper as well as cadmium would be extracted at the pH used.

Other extraction systems, similar to those utilized for the copper and cadmium system, but for other metals, are presently under study.

CONCLUSIONS

This work confirms earlier work that open-pore polyurethane foam may serve as a stationary support matrix for a modified solvent extraction process. Pretreatment of the foam with a relatively insoluble chelating agent, in this case benzoylacetone, and passage of an aqueous metal solution through the foam gives extraction curves resembling those obtained for solvent extraction systems.

Separation of metals is also feasible, at least on the microscale, by utilizing the pH-dependent nature of the extraction curves.

This work was supported by the Manitoba Research Council and the National Research Council of Canada.

SUMMARY

Open-pore polyurethane foam was shown to be a useful solid support for modified solvent extraction systems. Foams treated with benzoylacetone gave quantitative recovery of copper and cadmium from aqueous solution. Separation of a copper–cadmium system was achieved.

REFERENCES

1 H. J. M. Bowen, *J. Chem. Soc.*, (1970) 1082.
2 P. Schiller and E. B. Cook, *Anal. Chim. Acta*, 54 (1971) 364.
3 H. D. Gesser, A. Chow, F. C. Davis, J. F. Uthe and J. Reinke, *Anal. Lett.*, 4 (1971) 883.

4 J. F. Uthe, J. Reinke and H. D. Gesser, *Environ. Lett.*, 3 (1972) 117.
5 H. D. Gesser, A. B. Sparling, A. Chow and C. W. Turner, *J. Amer. Water Works Assoc.*, 65 (1973) 220.
6 J. Reinke, J. F. Uthe and H. O'Brodovich, *Environ. Lett.*, 4 (1973) 201; 6 (1974) 103.
7 T. Braun and H. B. Farag, *Talanta*, 19 (1972) 828.
8 T. Braun and H. B. Farag, *Anal. Chim. Acta*, 61 (1972) 265.
9 T. Braun, O. Békeffy, I. Haklits, K. Kádár and E. Majoros, *Anal. Chim. Acta*, 64 (1973) 45.
10 T. Braun and H. B. Farag, *Anal. Chim. Acta*, 68 (1974) 119.
11 T. Braun, H. B. Farag and A. Klimes-Szmik, *Anal. Chim. Acta*, 64 (1973) 71.
12 T. Braun and H. B. Farag, *Anal. Chim. Acta*, 65 (1973) 139.
13 T. Braun, L. Bakos and E. Huszár, *Anal. Chim. Acta*, 64 (1973) 77.
14 T. Braun and H. B. Farag, *Anal. Chim. Acta*, 65 (1973) 115; 66 (1973) 419.
15 T. Braun, L. Bakos and Zs. Szabó, *Anal. Chim. Acta*, 66 (1973) 57.
16 T. Braun and A. B. Farag, *Anal. Chim. Acta*, 69 (1974) 85.
17 T. Braun and A. B. Farag, *Anal. Chim. Acta*, 71 (1974) 133.
18 M. A. J. Mazurski, A Chow and H. D. Gesser, *Anal. Chim. Acta*, 65 (1973) 99.
19 D. Buksak and A. Chow, *Can. J. Chem.*, in press.
20 J. Starý, *Zh. Neorg. Khim.*, 4 (1959) 2412.
21 J. Starý and E. Hladky, *Anal. Chim. Acta*, 28 (1963) 227.
22 N. P. Rudenko and J. Starý, *Radiokhimiya*, 1 (1959) 52, 700.
23 *Analytical Methods for Atomic Absorption Spectrophotometry*, Perkin-Elmer, March 1971.

Analytica Chimica Acta, 78 (1975) 375–382

THE SEPARATION OF RHODIUM AND IRIDIUM BY ANION-EXCHANGE

G. A. KANERT and A. CHOW

Department of Chemistry University of Manitoba Winnipeg, Manitoba R3T 2N2 (Canada)

(Received 17th January 1975)

The separation of rhodium and iridium is one of the most difficult aspects of noble metal chemistry. Several methods involving precipitation, chromatography, ion-exhange or solvent extraction[1,2] exist, but these are often time-consuming or applicable to limited amounts of the metals. Ion-exchange methods are complicated by the difference in behavior of fresh and aged solutions of rhodium and iridium[3] caused by partial hydrolysis of the chloro complexes. Some cation-exchange procedures require the formation of noble metal–organic complexes before separation[4–6]. Most anion-exchange separations require either excesses of salts and acids[7] or Soxhlet extraction techniques to recover the iridium from the resin[3].

All of the stable chloro complexes of rhodium and iridium ($RhCl_6^{3-}$, $IrCl_6^{3-}$ and $IrCl_6^{2-}$) are completely adsorbed by a strongly basic anion-exchange resin. The chlororhodate and chloroiridate(III) species are not strongly retained by the resin[8] and can be eluted easily from the exchanger with dilute hydrochloric acid. However, the chloroiridate(IV) complex exhibits a strong affinity for the resin in 0.1–12 *M* hydrochloric acid.

The strong affinity of the chloroiridate(IV) species for a strongly basic anion-exchange resin provides a method for the separation of rhodium and iridium from dilute hydrochloric acid solutions: the rhodium species can be eluted from the resin with dilute hydrochloric acid while the quadrivalent iridium complex can be retained in the resin matrix. However, there is the problem of removing the iridium from the resin following the separation. In the separation by anion-exchange of iridium and platinum as their chloro complexes, Blasius and Rexin[9] eluted the iridium(IV) species with an iron(II) sulfate–7 *M* hydrochloric acid solution. The iron(II) sulfate reduced the iridium to the tervalent state, which was easier to remove from the resin, but no indication of the efficiency of the iridium recovery was given. This method is also complicated by the fact that iron must be removed from the iridium solution after elution.

The best anion-exchange method for separating and recovering rhodium and iridium in both the microgram and milligram range is that of Berman and McBryde[3]. A hydrochloric acid solution containing the chlororhodate(III) and the chloroiridate(IV) species was added to a resin column, in the chloride form, of Amberlite IRA-400. The resin bed had been treated previously with cerium(IV) solution to counteract the reducing effect of the resin on the iridium(IV) species. The rhodium was eluted with 0.8 *M* hydrochloric acid containing cerium(IV), and the iridium was recovered subsequently from the resin by Soxhlet extraction with 6 *M* hydrochloric acid. The quantitative elution of the iridium was attributed[3] to

the increase in temperature which enhanced the reducing properties of the resin, so that the iridium bound most intimately in the resin matrix was reduced and leached with the hot acid solution. Marks and Beamish[10] later modified this method slightly.

Although favorable separations were reported[3], the method has not found wide acceptance and it appeared that some simpler method for eluting the iridium would lead to a wider application for this technique. In the present work, heated columns and acid reservoirs were used for the elution of iridium from the resin since this method best simulated the Soxhlet extraction conditions and would simplify the iridium recovery by eliminating the need to remove the resin from the column for extraction.

EXPERIMENTAL

Apparatus and reagents

A Baird-Atomic Model 530 γ-spectrometer and Model 810C well-scintillation detector with a 4.4-cm diameter by 5.1-cm thick NaI(Tl) well-crystal, a Perkin-Elmer Model 306 atomic absorption spectrophotometer with a 10-cm single slot burner and Varian rhodium and iridium lamps, and a Unicam Model SP800B spectrophotometer were used. The jacketed ion-exchange columns were 0.5 cm in internal diameter and *ca.* 12 cm high; the acid reservoirs, holding *ca.* 125 ml, were attached by ground-glass joints to the columns. Haake Model FJ and Lauda Model K2R thermostated circulating baths were used.

A solution containing iridium (1 mg ml^{-1}) in 0.1 *M* hydrochloric acid was prepared from sodium chloroiridate ($Na_2IrCl_6 \cdot 6\ H_2O$) and a solution containing rhodium (1 mg ml^{-1}) in 1.2 *M* hydrochloric acid was prepared from sodium chlororhodate ($Na_3RhCl_6 \cdot 12\ H_2O$); both were obtained from Johnson Matthey and Mallory Limited (Toronto). Dilutions, with the same acid concentration, were made from these stock solutions. Iridium-192 (Amersham-Searle Limited, Don Mills, Ontario) was diluted before use. Reagent-grade chemicals were used, and water, purified by double-distillation followed by double-deionization, was used for dilutions and washings.

The ion-exchange resin used in all the experiments (except as indicated) was Amberlite IRA-400 (16–50 mesh; 8% crosslinking) conditioned with 3 *M* hydrochloric acid, then Soxhlet-extracted with 6 *M* hydrochloric acid for several hours and stored in 3 *M* hydrochloric acid. A resin bed 3 cm long and 0.5 cm in diameter was used in most cases.

RESULTS

Recovery of iridium

Initial studies were made to develop an improved method of recovering iridium from the resin. Radioactive iridium-192 was used as a tracer at a concentration sufficient to give *ca.* $7.8 \cdot 10^4$ counts min^{-1}. Each sample was counted five consecutive times for 100 s and corrected for background activity.

Samples of iridium were prepared by adding the tracer and stock iridium solutions to 6 mg of sodium chloride in a 30-ml beaker. To ensure the quadrivalent

state, a few ml of hydrochloric acid were added and the solutions evaporated. The residues were then treated with a few ml of aqua regia and evaporated to dryness, three times. The residues were treated with hydrochloric acid and evaporated to dryness three times. Immediately before use, each sample was treated with a few drops of hydrochloric acid, evaporated to dryness, and then dissolved in 2 ml of 0.8 *M* hydrochloric acid. The sample was then placed on a column; the flow rate was 0.5 ml min^{-1}.

The anion-exchange resin acted[3] as a mild reducing agent towards chloroiridate(IV), which necessitated the presence of an oxidizing agent to prevent the elution of the less strongly bound[8] tervalent species. Cerium(IV) has been used as the oxidizing agent[3] although this restricts the useful acid concentration range to 0.5–1 *M* hydrochloric acid. An evaluation was made of the iridium removed from the resin column by the passage of 0.002 *M* cerium(IV) sulfate in 0.8 *M* hydrochloric acid at a flow rate of *ca.* 0.8 ml min^{-1}. With a 500-μg iridium sample, the loss increased from 0.17% for the first 45 ml to a total of 0.29% for 100 ml and then more slowly, to a total of 0.45% for 250 ml of total eluant. Additional treatments of the sample with aqua regia, or final dissolution of the sample with the cerium solution, did not reduce this loss.

The efficiency of elution of iridium from the resin was poor at room temperature, as expected from the previous use[3] of Soxhlet extraction. The effect of elution temperature was studied with a sample of 500 μg of iridium on the resin, and a flow rate of 0.8 ml per min. Initially, 50 ml of cerium solution was passed through the column as before, to simulate rhodium elution, and this solution was removed by elution with 15 ml of 0.8 *M* hydrochloric acid. The flow through the column was stopped, and 105 ml of 6 *M* hydrochloric acid was added to the attached reservoir. Both the jacketed column and the reservoir were heated by circulating water from thermostatted temperature baths for 30 min. The column was then eluted with the hot acid and the recoveries were determined for several temperatures. The recovery of iridium increased from 60% at 25°C, 89% at 50°C, 93% at 65°C to 95% at 95°C. Thus recovery was maximal at the highest temperature but, even then, 5% was lost and there was some bubble formation in the columns. The colour of the intense brown chloroiridate(IV) complex band at the top of the resin bed disappeared slowly as expected. The eluted species were oxidized with chlorine, and then examined spectrophotometrically; mainly $IrCl_6^{3-}$, plus some other species, was found in the diluant. Elution with 12 *M* hydrochloric acid had only a minor effect on the recovery, and significantly increased the disruption of the column by gas formation.

The use of 1% and 4% hydroxyammonium or hydrazinium chloride to reduce the quadrivalent iridium complex on the column before elution at room temperature with dilute hydrochloric acid gave 88–96% recovery of iridium[3]. Recovery was independent of the concentration of reductant or of the acidic eluant; it appeared that the iridium was therefore not readily available for reduction. Reduction with 4% hydroxyammonium chloride in 9 *M* hydrochloric acid at 95°C gave an 82% recovery; a different iridium complex[11–13] may have been formed by reaction with the hydroxylamine.

Attempts were made to use the complexing ability[4] of thiourea with chloroiridate(IV) to obtain a more quantitative recovery. A 1% solution of thiourea in

9 *M* hydrochloric acid at 95°C gave 96% recovery of 500 μg of added iridium, *i.e.* 1% less than that obtained using the acid alone. Zinc chloride has been used[8] to recover the platinum(IV) chloro complex from IRA-400 resin, but 15% zinc chloride in 9 *M* hydrochloric acid at 95°C eluted only 95% of the iridium.

Various anion-exchange resins were tested for iridium retention under identical conditions; IRA-401 (4% crosslinking) gave 90%, and Dowex AGMP (macroporous) gave 91% recovery of the added iridium.

Studies with hot nitric acid as eluant were attempted; by attacking the polystyrene resin to some extent, it might be better able to leach out the iridium. The greater affinity of the nitrate ion compared with the chloride ion, for the resin[14] might also displace the iridium from the exchange sites in the resin matrix more readily. It was found that 8 *M* and 12 *M* nitric acid were equally efficient, and *ca.* 1% more effective at 95°C than an equal volume of 9 *M* hydrochloric acid. Spectrophotometric studies indicated that a small amount of the iridium was not eluted as the quadrivalent chloro complex.

The column bed was disrupted through bubble formation at the elevated temperature used, so the temperature of the eluting reagent was reduced to 74°C. The decreased temperature eliminated the bubbling and the percentage of iridium removed from the resin was 98.3%, *i.e.* more than was removed at 95°C with 12 *M* nitric acid. A comparison of the effect of temperature on the efficiency of 12 *M* nitric acid showed that, up to a volume of 60 ml of acid, a greater percentage of iridium was removed at 95°C, as would be expected. However, from 60 ml upwards, more iridium was removed at 74°C than at 95°C. This increased recovery at the lower temperature can be explained in the following manner: when the resin column is washed free of cerium(IV) and hydrochloric acid, the absorbed chloroiridate(IV) complex is no longer in the presence of an oxidizing agent and is then susceptible to reduction to the tervalent form by the resin. The elevated temperatures during the warm-up period of 30 min would have increased the rate of reduction of iridium by the resin. This quantity of chloroiridate(III) complex, more reactive kinetically than the quadrivalent species[12], could undergo an hydrolysis reaction in the essentially aqueous medium to form[12] a small amount of the first hydrolysis product $Ir(OH)_2Cl_5^{2-}$. (Although the presence of small amounts of the second and third hydrolysis products, $Ir(OH_2)_2Cl_4$ and $Ir(OH_2)_3Cl_3$ is possible, it is unlikely since their rates of formation are 15 and 66 times slower, respectively, than that for the first hydrolysis product[12,13].) The tervalent hydrolysed iridium species is then oxidized to the corresponding quadrivalent species on contact with the nitric acid. The spectrum obtained for the iridium eluted with 12 *M* nitric acid corresponded with the spectrum given for $Ir(OH_2)Cl_5$ by Chang and Garner[13], which suggests the presence of a small amount of this species. If the oxidized hydrolysed species is more difficult to remove from the resin than the original quadrivalent chloro complex, the increased iridium recovery at the lower temperature could be accounted for. The rate of reduction and hydrolysis would be faster at 95°C than at 74°C, and hence a larger portion of the absorbed iridium would be hydrolysed at the higher temperature, resulting in a larger amount of oxidized hydrolysed product on contact with the nitric acid.

The spectra obtained for the iridium solutions eluted with hydrochloric acid under various conditions and oxidized with chlorine were compared with the

spectrum given for $Ir(OH_2)Cl_5^-$. These also suggested the presence of a small amount of $Ir(OH_2)Cl_5^-$ present in the $IrCl_6^{2-}$ solutions. This indicates that a small amount of $Ir(OH_2)Cl_5^{2-}$ was formed by the reduction–hydrolysis reactions described above during the warm-up period. If the $Ir(OH_2)Cl_5^{2-}$ species is more difficult to remove from the resin than the tervalent chloro complex, the incomplete iridium recoveries on elution with hydrochloric acid could be accounted for.

It was considered that, by eliminating the hydrolysis conditions, better iridium recoveries from the resin could be expected on elution with either nitric or hydrochloric acid. A continuous flow through the column was required to prevent the formation of nitrogen dioxide. To prevent an appreciable hydrolysis reaction, the resin was washed free of cerium(IV) with a small amount of hydrochloric acid, and a small amount of 12 *M* nitric acid was added to the column at room temperature. The required volume of 12 *M* nitric acid eluant was then added to the reservoir and heated to 74°C while a flow of about 0.6 ml min^{-1} was maintained. This procedure recovered 99.1% of the iridium with 12 *M* nitric acid and 99.6% with 16 *M* nitric acid. At room temperature only 92.7% was eluted with the same amount of 16 *M* nitric acid. A spectrophotometric study of the eluted iridium showed that it was essentially identical to that obtained for $IrCl_6^{2-}$, indicating that the presence of more than one species during the previous elution studies was due to some slight hydrolysis of the chloro complex under the former conditions.

Similar results were obtained with hydrochloric acid although the recovery was slightly lower (98.6%). Spectrophotometric data again indicated that the formation of hydrolysis products was minimized.

Iridium samples of 100, 500 and 1000 μg were studied to determine the effect of sample size on iridium leakage from the resin during the sample loading and "rhodium elution". The efficiency of 150 ml of concentrated nitric acid in removing various quantities of iridium was also determined.

The samples were dissolved in 2 ml of 0.8 *M* hydrochloric acid and were fed with droppers onto the resin beds which had been previously washed, first with 20 ml of water, then by 20 ml of cerium(IV) solution. The columns were then eluted at a flow-rate of 0.8 ml min^{-1} with 250 ml of cerium solution to simulate the elution of rhodium from the resin. Following the "rhodium elution", the resin beds were washed free of cerium(IV) with 15 ml of 0.8 *M* hydrochloric acid.

The iridium was removed from the resin by passing 15 ml of concentrated nitric acid at room temperature through the columns, followed by an additional 135 ml of acid while water, at 75°C, was circulated through the jackets of both the resin columns and the acid reservoirs. The circulating water heated the acid to its equilibrium temperature (74°C) in about 20 min. The elution flow-rate was *ca.* 0.6 ml min^{-1}. The results of the study are shown in Table I. The results show essentially quantitative recovery of the iridium added. It was also found that 100–150 ml of nitric acid was sufficient to recover 99% of a sample of 100–1000 μg of iridium.

Separation of rhodium from iridium

The methods which gave maximal retention of iridium on the resin during rhodium elution and gave maximal iridium recovery were optimized as discussed.

The actual separation of rhodium and iridium was then evaluated by the combined procedures summarized below.

TABLE I

LEAKAGE AND RECOVERY OF IRIDIUM FROM RESIN

Sample (μg)	*Ir lost in "rhodium elution" and HCl wash*		*Ir on resin after 16 M HNO_3 elution (%)*	*Total Ir not recovered*	
	%	μg		%	μg
100	0.79	0.8	1.18	1.97	2.0
500	0.53	2.6	0.28	0.81	4.0
1000	0.44	4.4	0.69	1.13	11.3

Sample solutions containing rhodium and iridium, as their tervalent and quadrivalent chloro complexes respectively, were first treated with aqua regia and concentrated hydrochloric acid in the presence of 6 mg of sodium chloride to ensure that the iridium was in the form of the quadrivalent chloro complex. The dry sample residues were dissolved in 0.8 *M* hydrochloric acid and were fed onto jacketed ion-exchange resin columns of Amberlite IRA-400 resin. The resin beds had previously been treated with 0.8 *M* hydrochloric acid solution containing 0.002 *M* cerium(IV) sulfate to prevent reduction of the iridium. The rhodium was eluted with 150–250 ml of 0.8 *M* hydrochloric acid containing cerium(IV) sulfate as required by the rhodium content. Upon elution of the rhodium, the resin beds were washed free of cerium(IV) with 15 ml of 0.8 *M* hydrochloric acid. The iridium was removed from the resin by passing 15 ml of concentrated nitric acid at room temperature through the resin beds, followed by an additional 135 ml of acid as the resin columns and acid reservoirs were being heated to 74°C. A flow rate of 0.5–0.8 ml min^{-1} was used throughout. Spectrophotometric data indicated that the rhodium was eluted in the form of mixed complexes of the general form $RhCl_n(H_2O)_{6-n}^{3-n}$, where $n = 0$–6.

The rhodium and iridium were determined by atomic absorption as follows. The eluant containing rhodium was evaporated to dryness and the residue was dissolved in 1 *M* hydrochloric acid. The sample was diluted with 4 ml of 37.5% (w/v) sodium hydrogensulfate in 1 *M* hydrochloric acid and diluted to 50 ml with 1 *M* hydrochloric acid. The addition of sodium hydrogensulfate eliminated any effect of the sulfate ion from the cerium(IV) sulfate solution[15] and served to enhance the rhodium absorbance. Trials indicated a two-fold enhancement of the absorbance and showed no effect from the addition of 5 ml of 0.1 *M* cerium(IV) sulfate. The concentration of the sample solutions was determined by comparison with similarly prepared standards, at standard instrumental settings[16]. A two-fold scale expansion was used for the most dilute solutions. Iridium up to 25% (w/w) of the rhodium concentration had no effect on the analysis.

The iridium eluant was evaporated to dryness in the presence of 10 μg of sodium chloride. The residue was treated four times with 5 ml of hydrochloric acid and evaporated to dryness after each addition to reconvert the iridium to the easily dissolved chloro complex. The residue was then dissolved in 10 ml of

1 *M* hydrochloric acid containing 20,000 p.p.m. copper in the form of copper sulfate. Copper enhances[17] the iridium absorbance and eliminates any interference by up to 2000 p.p.m. sodium and up to 100 p.p.m. rhodium for a 20 p.p.m. iridium solution. The instrumental settings were standard[16] and, with five-fold scale expansion for only the most dilute solutions, the sample concentrations were determined by comparison with similarly prepared standards.

The results of the separation of various concentrations of rhodium and iridium are summarized in Table II. The recoveries for both rhodium and iridium were 98%, or greater, over the entire range studied. The percentage recovery of rhodium in general increased with increasing amounts of rhodium. The small amount of rhodium not recovered with the larger rhodium samples (500 and 1000 μg) suggested that when the Rh:Ir ratio was five, or greater, the iridium fraction would contain about 5% rhodium (w/w) with respect to the iridium content. When the Ir:Rh ratio was greater than five, the rhodium fraction would contain *ca.* 4% iridium (w/w) with respect to the rhodium content, through leakage of iridium from the resin as shown in the radioactive tracer studies.

TABLE II

THE SEPARATION OF VARIOUS AMOUNTS OF RHODIUM AND IRIDIUM

Ir added (μg)	*Rh added (μg)*	*Ir recovered (μg)*	*Rh recovered (μg)*
100	100	99[a] ± 2	99[a] ± 1
100	500	98 ± 1	495 ± 5
100	1000	98 ± 2	994 ± 2
500	100	498 ± 4	98 ± 0.5
500	500	497 ± 3	494 ± 2
500	1000	500 ± 3	996 ± 2
1000	100	992 ± 5	98 ± 0.5
1000	500	990 ± 4	494 ± 2
1000	1000	990 ± 4	995 ± 2

[a] Mean value of four samples ± mean deviation.

CONCLUSIONS

The quantitative elution of microgram and milligram quantities of iridium from a strongly basic anion-exchanger with hot concentrated nitric acid has been shown to be feasible, if reduction and hydrolysis reactions on the resin are minimized. The procedure involved is simpler than the Soxhlet extraction method previously employed, but requires slightly more time. However, the eluted iridium can be analyzed directly in the same vessel used to collect the effluent, thus minimizing the chance of sample loss on transferring the solution from one vessel to another as in the Soxhlet extraction methods. By eliminating the necessity of removing the resin from the column, the procedure described above may find wider application than the Soxhlet extraction method for the recovery of iridium from a strongly basic anion-exchanger.

Essentially quantitative separations and recoveries of rhodium and iridium were possible over the range 100–1000 μg. However, when the ratio of one metal

to the other was five or greater, the portion with the lesser amount of metal contained a small amount of the other metal.

The authors wish to express their thanks to the National Research Council of Canada, the Research Board of the University of Manitoba and Alcan for their financial support.

SUMMARY

The separation of rhodium and iridium in amounts of 100–1000 μg was achieved with a strongly basic anion-exchange resin. Rhodium was eluted with 0.8 *M* hydrochloric acid containing cerium(IV) sulfate. Iridium was recovered by eluting with concentrated nitric acid at 74°C, which minimized the formation of hydrolysis products. Recoveries of 98% or more were obtained for both metals.

REFERENCES

1 F. E. Beamish, *The Analytical Chemistry of the Noble Metals*, Pergamon, Toronto, 1966.
2 F. E. Beamish and J. C. Van Loon, *Recent Advances in the Analytical Chemistry of the Noble Metals*, Pergamon, Toronto, 1972.
3 S. S. Berman and W. A. E. McBryde, *Can. J. Chem.*, 36 (1958) 845.
4 E. W. Berg and W. L. Senn, Jr., *Anal. Chem.*, 27 (1955) 1255.
5 N. K. Pshenitsyn, K. A. Gladyshevskaya and L. M. Ryakhovo, *Analiz. Blagorod. Metal.*, (1959) 103; *Chem. Abstr.*, 54 (1960) 16280.
6 N. K. Pshenitsyn, K. A. Gladyshevskaya and L. M. Ryakhovo, *Vop. Anal. Blagorod. Metal. Tr. Vses. Soveshch.*, (1963) 72; *Chem. Abstr.*, 61 (1964) 6364.
7 M. L. Cluett, S. S. Berman and W. A. E. McBryde, *Analyst (London)*, 80 (1955) 204.
8 S. S. Berman and W. A. E. McBryde, *Can. J. Chem.*, 36 (1958) 835.
9 E. Blasius and D. Rexin, *Z. Anal. Chem.*, 179 (1961) 105.
10 A. G. Marks and F. E. Beamish, *Anal. Chem.*, 30 (1958) 1464.
11 F. A. Cotton and G. Wilkinson, *Advanced Inorganic Chemistry*, Interscience, 1st edn., 1962, p. 254.
12 I. A. Poulsen and C. S. Garner, *J. Amer. Chem. Soc.*, 84 (1962) 2032.
13 J. C. Chang and C. S. Garner, *Inorg. Chem.*, 4 (1965) 209.
14 S. Fisher and R. Kunin, *Anal. Chem.*, 27 (1955) 1191.
15 S. Kallman and E. W. Hobart, *Anal. Chim. Acta*, 51 (1970) 120.
16 *Analytical Methods for Atomic Absorption Spectrophotometry*, Perkin-Elmer Corp., Norwalk, Conn., 1971.
17 A. A. G. Houze, *J. S. Afr. Chem. Inst.*, 23 (1970) 115.

Analytica Chimica Acta, 78 (1975) 383–389

A RAPID METHOD FOR THE DETERMINATION OF SUB-PART PER BILLION AMOUNTS OF N-NITROSO COMPOUNDS IN FOODSTUFFS

D. H. FINE, D. P. ROUNBEHLER and P. E. OETTINGER
Thermo Electron Corporation, 85 First Avenue, Waltham, Massachusetts 02154 (U.S.A.)
(Received 1st February 1975)

Since Magee and Barnes[1] discovered that dimethylnitrosamine caused malignant tumors in the rat, there has been much concern about the possible widespread occurrence of N-nitroso compounds in the environment[2]. Many N-nitroso compounds are carcinogenic[3]; trace levels of dimethylnitrosamine and N-nitrosopyrrolidine have been found in cured foods such as fried bacon[4,5] and smoked fish[5,6].

Analytical methods, sensitive at the $\mu g\ kg^{-1}$ level in the original foodstuff, have been developed for the fourteen most volatile nitrosamines[4–7]. The procedures are complex and time-consuming, requiring digestion, extraction, and steam or vacuum distillation followed by extensive clean-up. To achieve sensitivity at the $\mu g\ kg^{-1}$ level in the original foodstuff, concentration of the extract by at least a factor of 1000 is essential. Even then, the nitrogen-specific Coulson electrolytic conductivity and/or the alkali flame ionization gas chromatograph (g.c.) detectors which are generally used[8] are not specific for N-nitroso compounds, and confirmation by gas chromatography–mass spectrometry (g.c.–m.s.) is mandatory. Redistilled and repurified solvents and reagents are needed, and elaborate precautions are required to obtain reliable results. The time required per analysis is long, and the cost per analysis is high.

To achieve $\mu g\ kg^{-1}$ sensitivity in the original material, the existing clean-up procedures have been designed to eliminate "interfering" compounds. Thus a negative result on a particular foodstuff indicates that none of the fourteen N-nitroso compounds tested are present; but does not imply the presence or absence of other N-nitroso compounds amenable to g.c. With the advent of the g.c.-thermal energy analyzer[9] (t.e.a.) interface[10], which is specified for N-nitroso compounds it is now possible to identify and quantify N-nitroso compounds amenable to g.c.

This paper reports a new analytical approach which requires only two or three simple steps; vacuum distillation from mineral oil (time required 50 min), extraction with dichloromethane (10 min) and, depending on the sensitivity required, concentration on a Kuderna Danish evaporator (20 min). An analysis therefore takes less than 90 min, with sensitivity routinely at the 0.05–0.01 $\mu g\ kg^{-1}$ concentration level. Moreover, because the clean-up has been kept to a minimum commensurate with g.c. column compatibility, the method facilitates quantitation of all N-nitroso compounds amenable to g.c. Since the gas chromatograph–thermal energy analyzer (g.c.–t.e.a.) is[11] unique in its selectivity to compounds containing extremely heat-labile nitroso groups, a rapid analysis procedure has been developed.

The foodstuff to be analyzed is ground up and mixed with alkali. Crude mineral oil is added; the contents are then heated gently under vacuum and the distillate is frozen out in a cold trap. The N-nitroso compounds dissolve in the mineral oil as it penetrates into the complex food matrices, so eliminating the need for digestion or fine grinding of the foodstuff. At the end of the extraction step the food matrix is still visible, even though the N-nitroso compounds have been removed. By keeping the oil under reduced pressure, all the compounds which are soluble in an oil–water emulsion and are more volatile than the oil are distilled as they are extracted.

In addition to N-nitroso compounds, organic and inorganic nitrates[11] give a response on g.c.–t.e.a. Combined extraction and vacuum distillation from warm mineral oil effectively overcomes this obstacle; inorganic nitrates and nitrites do not have sufficiently high vapor pressures to be distilled under these mild conditions, and organic nitrites decompose during heating. Although the crude distillate can be introduced directly into the g.c. without further clean-up, dichloromethane extraction is simple and extends the life of the g.c. column.

EXPERIMENTAL

Reagents

Because g.c.–t.e.a. is so selective, pure analytical reagents are not necessary; commercial grade sodium hydroxide, hydrochloric acid, and mineral oil are suitable. If the dichloromethane extract is to be concentrated on a Kuderna Danish evaporator, redistilled dichloromethane should be used.

Apparatus

A specially designed single column, temperature-programmable, gas chromatograph, equipped with a t.e.a. detector[11] was used. The t.e.a. trap was kept at −159°C. The gas chromatographic column was prepared from stainless steel tube (10 ft × $\frac{1}{8}$ in. o.d.) packed with 15% (w/w) FFAP (free fatty acid phase) on chromosorb W (acid washed, DMCS treated, 80–100 mesh). The column was temperature-programmed at 5°C min^{-1} from 140 to 210°C.

Procedure

About 20 g of the food sample, cut into thin slices or minced, was weighed into a 500-ml round-bottomed flask, to which was added 4 ml of 0.1 *M* sodium hydroxide and 20 ml of crude mineral oil. The contents were heated slowly under vacuum. The distillate was collected in a glass finger at −192°C. When the flask temperature reached 110°C (after *ca.* 40 min), the distillate was removed and the contents of the three cold fingers were combined. The inter-connecting tubing was rinsed with water, the washings plus distillate were transferred to a 125-ml separating funnel, 4 ml of 0.1 *M* hydrochloric acid was added, and the washings were extracted with dichloromethane (3 × 5 ml). The combined extracts can be analysed by g.c.–t.e.a. (sensitivity 5 $\mu g\ kg^{-1}$ of original foodstuff), but if increased sensitivity is required, the dichloromethane extract is concentrated on a 3-stage Kuderna Danish evaporator; concentration to 0.2 ml gives a sensitivity of 0.05 $\mu g\ kg^{-1}$. If greater sensitivity is required, more than 20 g of sample is taken.

N-Nitroso standards

Two standard nitrosamine calibration standards provided by the International Agency for Research in Cancer (IARC) of the World Health Organization, Lyon, France, and by the US Food and Drug Administration (FDA), Washington, D.C. were used. The IARC standard contained 23.9 μg of dimethylnitrosamine (DMN) per ml, 25.3 μg of diethylnitrosamine (DEN) per ml, 29.0 μg of dibutylnitrosamine (DBN) per ml and 30.0 μg of N-nitrosopyrrolidine (PYRN) per ml. The FDA standard contained 0.5 μg ml^{-1} of each of DMN, methylethylnitrosamine (DPrN), ethylbutylnitrosamine, propylbutylnitrosamine, methylamylnitrosamine, DBN, nitrosopiperidine, PYRN, nitrosomorpholine and diamylnitrosamine; a g.c.–t.e.a. chromatogram of this standard mixture is shown in Fig. 1.

RESULTS AND DISCUSSION

The IARC standard solution was added to canned tuna fish and canned corned beef at the 5 μg kg^{-1} concentration level. The chromatogram of the canned tuna fish, after recovery, is shown in Fig. 2(a) and that of the canned corned beef, in Fig. 3. Recoveries were 71–75% for DMN, 90% for DEN, 95–98% for DBN, and 100% for PYRN. The relatively low recovery of the most volatile compound, DMN, was attributed to losses during vacuum distillation.

Figure 2 (b) is the chromatogram from canned tuna fish, showing 0.20 μg kg^{-1} of DMN and 0.46 μg kg^{-1} of PYRN, identified from their retention times. Figure 4 is the chromatogram from a soya bean oil sample used to deep-fry codfish and french fries. The only g.c. peak observed was that of DPrN, which

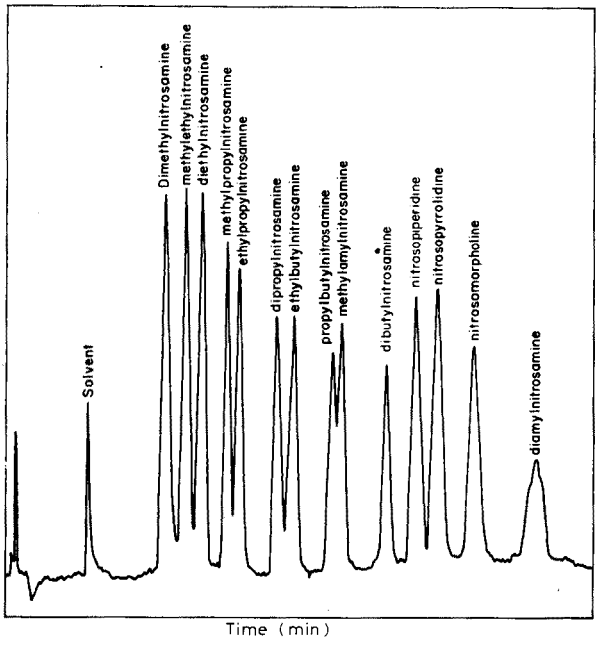

Fig. 1. Chromatogram (g.c.–t.e.a.) for a standard mixture of 14 volatile nitrosamines, each at a concentration of 0.5 μg ml^{-1}.

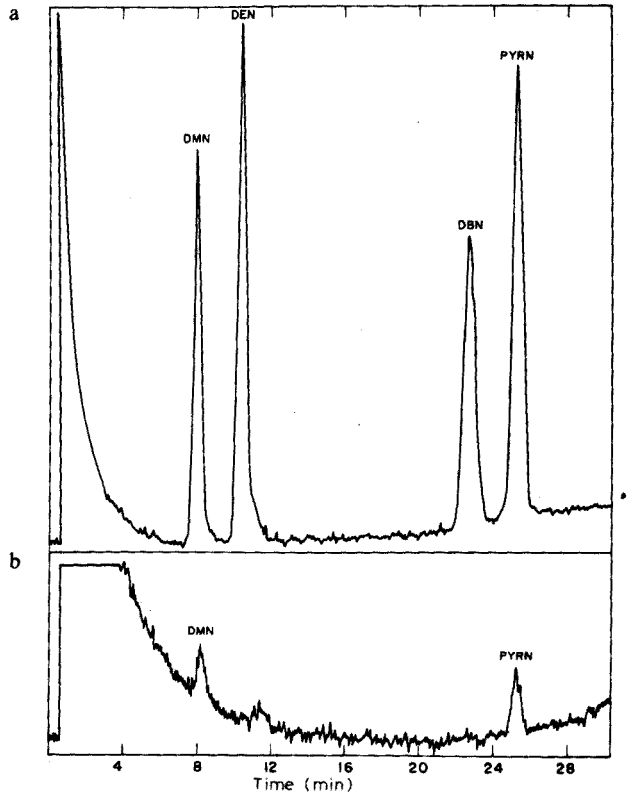

Fig. 2a. Chromatogram of canned tuna fish extract following recovery of a mixture of DMN, DEN, DBN, and PYRN, each at 5 μg kg^{-1}.

Fig. 2b. Chromatogram of a canned tuna fish extract, showing the presence of DMN (0.2 μg kg^{-1}) and PYRN (0.45 μg kg^{-1}).

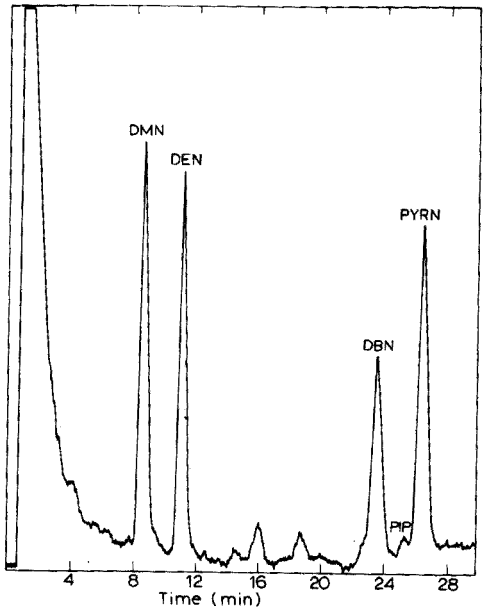

Fig. 3. Chromatogram from a canned beef extract following recovery of a mixture of DMN, DEN, DBN, and PYRN, each at 2 μg kg^{-1}.

was added as an internal standard at the 0.5 μg kg^{-1} level. Recovery of the DPrN was 100%. The soya bean oil was shown not to contain N-nitroso compounds amenable to our g.c. conditions, down to the 0.1 μg kg^{-1} level. Figure 3 shows that the corned beef extract gave several smaller peaks in addition to the DMN, DEN, DBN, and PYRN which were added intentionally. Nitrosopiperidine (0.2 μg kg^{-1}) was identified from its retention time but the other g.c. peaks did not match the retention times of the standard nitrosamines available. The concentration of the unknown peaks was *ca.* 0.1–0.6 μg kg^{-1} (estimated from the known mole response and assuming a molecular weight of 100).

Figure 5 shows the chromatogram of a fried bacon extract; DMN (5.9 μg kg^{-1}) and PYRN (52 μg kg^{-1}) were identified from their retention times. DPrN was added as an internal standard at the 0.5 μg kg^{-1} level. At a higher gain, t.e.a. showed the recovery of DPrN to be 100%. There are five unidentified g.c.

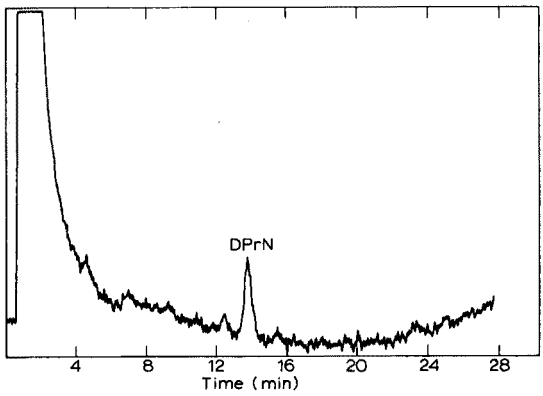

Fig. 4. Chromatogram from soya bean oil used to fry codfish and french fries. Dipropylnitrosamine (0.5 μg kg^{-1}) was added as an internal standard.

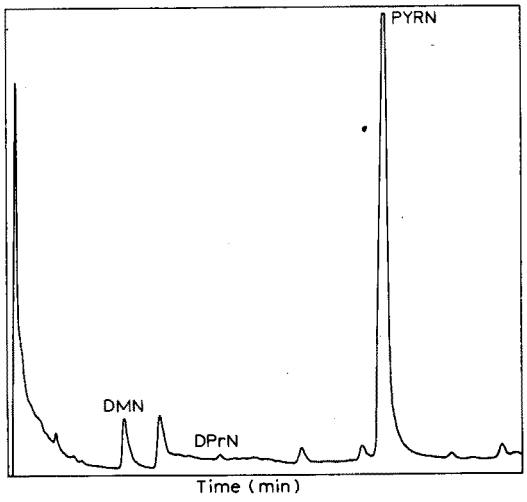

Fig. 5. Chromatogram of a fried bacon extract, showing DMN (5.9 μg kg^{-1}) and PYRN (52 μg kg^{-1}) Dipropylnitrosamine was added as an internal standard (0.5 μg kg^{-1}); the recovery was 95%.

peaks in Fig. 5; four of these are probably N-nitroso compounds at approximately 1 μg kg^{-1}. The g.c. peak immediately after that of DMN does not have the symmetrical peak shape characteristic of a N-nitroso compound; although it undoubtedly contains a labile nitroso group, it is probably not an N-nitroso compound.

The chromatograms presented do not show any evidence of compounds interfering with the analysis. In contrast to the procedures of existing techniques, clean-up has been kept to an absolute minimum. The only restraint is the necessity to obtain a representative extract which can be injected into a gas chromatograph.

Identification by g.c.–t.e.a. depends upon final identification of the nitrosyl radical, and can be compared directly with the use of g.c.–m.s. for NO^+ ion mass (29.997) identification. The selectivity of t.e.a. to nitrosyl radicals is at least as good as can be achieved by high-resolution m.s., for there is virtually no other organic compound which can pass through a trap at -159°C, and then react with ozone to give the characteristic emission in the near infra-red. Although the ion source of the mass spectrometer is non-selective, the t.e.a. catalytic pyrolyzer subjects the compounds to a very mild thermal shock, sufficient only to break the N–NO bond.

The selectivity of g.c.–t.e.a. to N-nitroso compounds is greater than any other analytical technique. This is explained by the fact that a compound giving a response on g.c.–t.e.a. must pass six successive screening steps as follows: (1) the compound must not decompose in the g.c. injection port (organic nitrites and N-nitroso amides decompose instantly, and the nitrosyl radical is eluted together with the solvent front); (2) the compound must have sufficient vapor pressure to elute from the g.c. column; (3) the compound must be eluted from the g.c. according to the column characteristics; (4) the compound must decompose under the mild catalytic pyrolysis conditions of the t.e.a. pyrolyzer; (5) the compounds must survive a cold trap at -159°C (virtually all organic compounds are trapped at this temperature); (6) the compound must react with ozone to give a characteristic emission in the near infrared.

Collaborative analyses with other laboratories are currently under way, and attempts to identify the "unknown" g.c.–t.e.a. peaks found in meat and fried bacon are in progress.

We thank Larry Keefer (National Cancer Institute, Bethesda, Maryland) and Fred Huffman, David Lieb and Firooz Rufeh (Thermo Electron Corporation) for many helpful discussions. We are indebted to Frank Campagna for technical assistance. Dr. E. Walker (IARC, Lyon, France) supplied the collaborative nitrosamine mixture; Tom Fazio (FDA, Washington) supplied the mixture of 14 nitrosamines. This work was supported by Contract NOICP45623 with the National Cancer Institute, U. S. Department of Health, Education and Welfare.

SUMMARY

A new analytical clean-up technique, designed specifically for the analysis of N-nitroso compounds with a thermal energy analyzer and a gas chromatograph, is described. Only two steps are required; vacuum distillation from mineral oil

followed by extraction with dichloromethane. The sensitivity for N-nitroso compounds in foodstuffs is at the 5 $\mu g\ kg^{-1}$ level, but if a dichloromethane extract is concentrated on a Kuderna Danish evaporator, a 100-fold increase is attainable. The method can be used for any foodstuff or biological material, and the quantitation of any N-nitroso compounds amenable to gas chromatography is possible.

REFERENCES

1 P. N. Magee and J. M. Barnes, *Brit. J. Cancer*, 10 (1956) 114.
2 W. Lijinsky and S. S. Epstein, *Nature (London)*, 225 (1970) 21.
3 P. N. Magee, *Food Cosmet. Toxicol.*, 9 (1971) 207.
4 N. P. Sen, B. Donaldson, J. R. Jyengar and T. Panalaks, *Nature (London)*, 241 (1973) 473.
5 N. T. Crosby, J. K. Foreman, J. F. Palframan, and R. Sawyer, *Nature (London)*, 238 (1972) 342.
6 T. Fazio, J. N. Damico, J. W. Howard, R. H. White and J. O. Watts, *J. Agr. Food Chem.*, 19 (1971) 251.
7 J. M. Essigmann and P. Issenberg, *J. Food Sci.*, 37 (1972) 684.
8 J. F. Palframan, J. Macnab and N. T. Crosby, *J. Chromatogr.*, 76 (1973) 307.
9 D. H. Fine, F. Rufeh and D. Lieb, *Nature (London)*, 247 (1974) 309.
10 D. H. Fine and D. P. Rounbehler, *J. Chromatogr.*, 109 (1975) 271.
11 D. H. Fine, D. Lieb and D. P. Rounbehler, *Anal. Chem.*, 47 (1975) 1188.

Analytica Chimica Acta, 78 (1975) 391–396

THE DETERMINATION OF ANIONIC DETERGENTS WITH THE BIS (ETHYLENEDIAMINE)COPPER(II) ION

P. T. CRISP, J. M. ECKERT and N. A. GIBSON

Department of Inorganic Chemistry, University of Sydney, Sydney, N.S.W. 2006 (Australia)

(Received 14th February 1975)

The method used in most countries for the determination of anionic detergents in waters and waste waters involves extraction of the detergent as an ion pair with the coloured methylene blue cation into chloroform, and spectrophotometry of the extract[1–3]. However, this method has several limitations and is tedious. The procedure set out in Standard Methods[3], for example, calls for a total of seven phase separations; these are necessary partly to remove impurities present in commercial methylene blue, and partly to reduce interference by other anions, such as cyanate, thiocyanate, nitrate and chloride, which also form ion pairs with the methylene blue cation. Blank absorbance values can still be quite high and corrections are always necessary. Further, despite the repeated extractions, interference by certain anions, notably chloride, remains a problem. The method is not applicable to brine samples[4].

Cationic metal complexes offer an attractive alternative to organic dyes. In the extraction of an anion from water into an organic solvent as an ion-association compound, the distribution ratio is sensitive to the charge, size and hydration energy of the extracting cation[5]. The considerable variation of these properties among complex metal cations might usefully be exploited in the search for a cation capable of extracting detergent anions more selectively than methylene blue is able to do.

Metal complexes are generally obtainable in a high state of purity and the choice is not limited to complexes which are intensely coloured. Because of the presence of the metal ion, there is the possibility of completing the determination by atomic absorption spectroscopy (a.a.s.), rather than colorimetrically. The merits of metal complexes in anionic detergent analysis were first explored by Taylor and Fryer[6] who, in 1969, published a colorimetric method in which tris(1,10-phenanthroline)iron(II) serves as the cation. The limit of detection of their method is 0.5 μg ml^{-1} (as sodium dodecyl sulphate), which is at least an order of magnitude worse than that of the methylene blue method.

Subsequently, Taylor and Waters[7] described a radiometric method with a detection limit of 0.005 μg ml^{-1} of detergent in potable and ground waters. The extracting cation is tris(1,10-phenanthroline)iron(II), labelled with iron-59. Although there are some interference problems (*e.g.* with iron and fluoride ions), which necessitate the use of an internal standard technique, the method appears to be much more selective than the methylene blue procedure.

The 1,10-phenanthroline complex of copper(II) has been examined as the

extracting cation by Le Bihan and Courtot-Coupez[8] for the determination of detergent in sea water. By using large sample volumes and a.a.s., these authors obtained a detection limit of 0.005 μg ml^{-1}; but to overcome interference by the other anions, a multiple extraction procedure was required.

In this paper, a new method is described for the determination of anionic detergents. The proposed method, in which the extracting cation is bis(ethylenediamine)copper(II), is simple, sensitive and highly selective, and can be completed colorimetrically or by atomic absorption spectrometry. It is particularly suited to saline waters.

EXPERIMENTAL

Instrumentation

A Beckman Acta V spectrophotometer and a Varian Techtron Model AA-6DA spectrophotometer were used.

Reagents

Standard reference anionic detergent solution. A solution containing 5.55% active linear alkyl sulphonic (LAS) acids, of mean molecular weight 318, was obtained from the U.S. Environmental Protection Agency. This solution was used to prepare a stock standard solution containing 1500 μg LAS ml^{-1}, which was stored at 0°C, and diluted further as required.

Ethylenediaminecopper(II) reagent. Dissolve 62.3 g of copper sulphate pentahydrate and 49.6 g of ammonium sulphate in water. Add 45.1 g (50 ml) of 1,2-diaminoethane (ethylenediamine) and dilute to 1 l with water. The reagent is stable for at least a month.

PHTTT reagent. Dissolve 0.42 g of 3-propyl-5-hydroxy-5-D-arabinotetrahydroxybutyl-3-thiozolidine-2-thione (PHTTT) in 1 l of 95% ethanol. If care is taken to prevent evaporation, the reagent is stable for several months.

PHTTT may be prepared by the following method which is based on that of Stiff[9]. Add 9 g of glucose to 3 g (4.2 ml) of 1-amino-propane (n-propylamine) and 5 ml of methanol in a beaker. Heat the mixture with stirring in a water bath at 60–65°C for 15 min. Add a solution of 9 g (7 ml) of carbon disulphide in 40 ml of ethanol and heat for a further 15 min. Allow the mixture to stand overnight at 0°C and filter off the pale yellow crystals. Recrystallise twice from methanol. The product is a white crystalline solid (m.p. 174–175°C).

Recommended procedure

Place a 150-ml water sample, containing not more than 15 μg of detergent per ml, in a 250-ml separating funnel and, if necessary, adjust the pH to 5–9. Add 10.0 ml of ethylenediamine-copper(II) reagent and 20.00 ml of chloroform. Shake for 1 min and allow to stand until the phases separate. Run the chloroform layer through a plug of cotton wool into a small conical flask and stopper the flask with a glass stopper. Take care to minimize evaporation of the chloroform. Complete the determination either colorimetrically or by a.a.s.

For colorimetry, pipette a 5.00-ml aliquot of the extract into a small glass-stoppered conical flask, containing 5.00 ml of PHTTT reagent. Measure the

absorbance of the solution in 1-cm cells at 435 nm against a 1:1 chloroform–PHTTT reagent reference solution. The colour developed by the PHTTT reagent is stable for at least 2 h.

For a.a.s., pipette a 10.00-ml aliquot of the extract into a 25-ml volumetric flask and adjust to volume with 0.1 *M* nitric acid. Shake vigorously for 30 s and allow to stand until the phases separate. Aspirate the aqueous layer directly from the flask; this can be done without removing the chloroform layer. An oxidizing air–acetylene flame is used; the lamp current is 3 mA, the wavelength 324.7 nm, and the spectral band pass 0.2 nm.

With either technique, carry out a blank determination with 150 ml of distilled water. The blank absorbance should be 0.000–0.001. Calculate the detergent concentration in the sample by reference to a previously prepared calibration graph.

RESULTS AND DISCUSSION

The concentration of copper in the ethylenediaminecopper(II) reagent is 0.25 *M* and the mole ratio of copper to ethylenediamine is 1:3. Under these conditions, the predominant species in solution is the aquated bis(ethylenediamine)copper-(II) ion, $[Cu(en)_2(H_2O)_2]^{2+}$. Formation of the tris(ethylenediamine) complex requires much higher concentrations of ethylenediamine[10]. The reagent therefore contains an excess of ethylenediamine and is buffered by this and by ammonium ion to a pH of 9–10.

The detergent anions are extracted into chloroform as the neutral species, $Cu(en)_2(\text{detergent})_2$. Evidence for this statement comes from a study of the compound formed by the reagent with sodium dodecyl sulphate. The compound was isolated in pure form (m.p. 205°C), and chemical analysis confirmed the 2:1 mole ratio of detergent anion to bis(ethylenediamine)copper(II).

The detergent analysis is completed colorimetrically after conversion of the weakly coloured bis(ethylenediamine)copper(II) ion ($\varepsilon_{max} = 38$ at 548 nm) to an intense yellow complex ($\varepsilon_{max} = 13{,}400$ at 435 nm, in 1:1 chloroform–ethanol) by addition of PHTTT to an aliquot of the chloroform extract. PHTTT is a sensitive colorimetric reagent which was developed for the determination of copper in water and waste water[9,11].

In the atomic absorption finish, the chloroform extract is shaken with dilute nitric acid which protonates the ethylenediamine; copper(II) passes into the aqueous phase, where it is determined directly.

Calibration

In the range 0–15 μg ml^{-1}, the concentration of detergent in a water sample (y μg ml^{-1}, as LAS) could be calculated from the measured absorbance (x) by means of the equation $y = 13.5\ x$.

A careful study of solutions containing low levels of LAS showed a slight but real curvature of the calibration graph between 0 and 1 μg ml^{-1}. For accurate determinations in this concentration range, the following relationship is recommended: $y = 17.3\ x - 41.5\ x^2$.

Beyond 20 μg ml^{-1}, the calibration graph showed significant curvature. Water samples containing more than 15 μg of detergent per ml should therefore

be appropriately diluted.

Because the working conditions of an atomic absorption spectrometer are optimized at the start of each run, standards must be measured with every batch of unknowns. Linear calibration graphs were obtained in the range 0–15 μg LAS ml^{-1}. For a typical graph, the line of best fit had a slope of 27.8 (μg LAS ml^{-1} per absorbance unit).

Precision, limit of detection and accuracy

The precision of the proposed method was assessed by carrying out repeated determinations of standard solutions containing 0.10, 1.00 and 10.00 μg LAS ml^{-1}. The results obtained by colorimetry are shown in Table I. Similar results were obtained by a.a.s.

With either technique, the standard deviation of a set of 12 absorbance readings at or near the blank level was found to be 0.001. The limit of detection (the concentration which gives an absorbance equal to twice this standard deviation) was 0.03 μg ml^{-1} (as LAS) for the colorimetric finish and 0.06 μg ml^{-1} for the a.a.s. finish.

The accuracy of the method was evaluated by determining the recovery of different concentrations of detergent added to sea water. Six duplicate determinations were carried out at each concentration; substantially the same recovery data were obtained with both techniques. The colorimetric results are presented in Table II.

TABLE I

PRECISION OF PROPOSED METHOD

LAS taken ($\mu g\ ml^{-1}$)	*Mean LAS found*[a] ($\mu g\ ml^{-1}$)	*s*	s_r (%)
0.10	0.07	0.01	14
1.00	0.99	0.03	3
10.00	10.02	0.07	1

[a] Mean of 6 determinations.

TABLE II

RECOVERY OF LAS FROM SEA WATER

LAS added ($\mu g\ ml^{-1}$)	*Mean LAS found*[a] ($\mu g\ ml^{-1}$)	*s*	*Mean recovery* (%)
0.10	0.08	0.01	80
1.00	0.98	0.04	98
10.00	9.74	0.13	97

[a] Mean of 6 determinations.

Interferences

The effects of various ions on the method were examined; the results are summarized in Table III. In no case was a recovery greater than 100% observed *i.e.*, there were no positive interferences. With the methylene blue method, positive interferences are much commoner than negative ones[3].

TABLE III

ALLOWABLE CONCENTRATIONS OF FOREIGN IONS[a]

Concentration	
0.5 *M*	Cl^-, F^-, NO_3^-, SO_4^{2-}
1000 μg ml^{-1}	SCN^-, ClO_4^-, NO_2^-, CH_3COO^-, Br^-, I^-, $P_3O_{10}^{5-}$, Mg^{2+}, Ca^{2+}
100 μg ml^{-1}	Cu^{2+}, Ni^{2+}
10 μg ml^{-1}	Al^{3+}, Cr^{3+}, Mn^{2+}, Zn^{2+}
1 μg ml^{-1}	Fe^{3+}, Co^{2+}, S^{2-}

[a] 97–100% recovery of 10.0 μg LAS ml^{-1} was obtained in the presence of the stated concentration.

The allowable concentrations in Table III are generally well above the concentrations of these ions in natural waters, with two exceptions. Highly polluted water can contain considerably more than 1 μg ml^{-1} of both iron(III) and sulphide ions. However, there is no interference from 100 μg S^{2-} ml^{-1} if the water sample is treated with 2 ml of 6% hydrogen peroxide for 5 min before addition of the ethylene–diaminecopper(II) reagent. Addition of 10 ml of 2% EDTA (disodium salt) solution suppresses interference by 100 μg Fe^{3+} ml^{-1}; the EDTA is unnecessary, however, if the iron is present mainly as hydrated iron(III) oxide.

Few natural waters would be expected to contain more than 1 μg Co^{2+} ml^{-1}, but it should be noted that up to 100 μg ml^{-1} do not interfere significantly if the pH of the reaction mixture is raised by omission of the ammonium sulphate.

The relative freedom of the proposed method from interference by inorganic anions is of special interest. Chloride ions, in particular, have very little effect. The recovery of 10.0 μg LAS ml^{-1} from 0.5 *M* NaCl is 98% and even in 5 *M* NaCl there is 86% recovery of detergent. The method is applicable to strong brine samples.

The proposed method should also be useful in marine and estuarine analyses, because it is not seriously affected by the ions present in sea water (see Tables II and III). The varying salinity of estuarine waters, from fresh water upstream to sea water at the river mouth, is therefore not a problem.

One of us (P.T.C.) received support during this work from an Australian Government Post-Graduate Research Award. We also acknowledge a debt to Dr. G. M. Eckert of Sydney Hospital for valuable advice.

SUMMARY

A method is described for the determination of anionic detergents. The detergent anions are extracted into chloroform as an ion-association compound with the bis(ethylenediamine)copper(II) cation. Determinations are completed by colorimetry or atomic absorption spectrometry. With a 150-ml water sample, the limit of detection is 0.03 μg ml^{-1} (as LAS) for colorimetry or 0.06 μg ml^{-1} for a.a.s. The method requires only one phase separation step and is highly selective. It is directly applicable to brine and sea-water samples.

REFERENCES

1 J. Longwell and W. D. Maniece, *Analyst (London)*, 80 (1955) 167.
2 D. C. Abbott, *Analyst (London)*, 87 (1962) 286.
3 *Standard Methods for the Examination of Water and Wastewater*, American Public Health Association, Washington, D.C., 13th edn., 1971, p. 339.
4 *Methods for Chemical Analysis of Water and Wastes*, U.S. Environmental Protection Agency, Water Quality Office, Manual 16020, Cincinnati, Ohio, 1971, p. 132.
5 N. A. Gibson and D. C. Weatherburn. *Anal. Chim. Acta*, 58 (1972) 159.
6 C. G. Taylor and B. Fryer, *Analyst (London)*, 94 (1969) 1106.
7 C. G. Taylor and J. Waters, *Analyst (London)*, 97 (1972) 533.
8 A. Le Bihan and J. Courtot-Coupez, *Bull. Soc. Chim. Fr.*, (1970) 406.
9 M. J. Stiff, *Analyst (London)*, 97 (1972) 146.
10 F. A. Cotton and G. Wilkinson, *Advanced Inorganic Chemistry*, Interscience, New York, 3rd edn., 1972, p. 917.
11 J. A. Corbett, *Talanta*, 13 (1966) 1089.

Analytica Chimica Acta, 78 (1975) 397–404

MUTUAL EFFECTS OF METALS IN EXTRACTIONS FROM FLUORIDE SOLUTIONS WITH OXYGEN-CONTAINING SOLVENTS

YU. A. ZOLOTOV, V. V. BAGREEV and I. M. KUTYREV

Vernadsky Institute of Geochemistry and Analytical Chemistry, Academy of Sciences, Moscow 117334 (U.S.S.R.)

(Received 17th March 1975)

Mutual influences of metals (co-extraction and extraction suppression) in the extraction of niobium, tantalum and zirconium from solutions of hydrofluoric acid oxygen-containing solvents have already been discussed[1–3], but such effects in fluoride systems have not been studied. In the present paper, the simultaneous extraction of niobium, tantalum and zirconium from solutions of hydrofluoric acid is described. Data on the individual extraction of niobium and tantalum from hydrofluoric acid solutions have been summarized[3], but there is practically no published data on the similar extraction of zirconium.

EXPERIMENTAL

Reagents and solutions

For the preparation of the initial 0.5 *M* metal solutions in hydrofluoric acid, a weighed sample of Ta_2O_5, Nb_2O_5 or ZrO_2 was dissolved in concentrated hydrofluoric acid by heating; for easier dissolution of the oxides, a few drops of concentrated nitric acid were also added. Each solution was evaporated to a small volume and diluted with water, and the metal hydroxide was precipitated by adding (1 + 1) ammonia solution. The freshly precipitated hydroxide was dissolved by addition of 20 *M* hydrofluoric acid from a polyethylene measuring cylinder, and each solution was then diluted to the required concentration of hydrofluoric acid.

The radioisotopes ^{182}Ta, ^{95}Nb and ^{95}Zr were employed for the determination of the distribution coefficient (D) of metals (^{95}Zr was first purified[4] from the daughter ^{95}Nb).

Procedures

All the experiments were carried out at 25 ± 1°C. Stoppered polyethylene 10-ml test tubes were used for contact of the two phases. The aqueous phase contained metals labelled with the radioactive isotopes, and hydrofluoric acid. The organic phase was tri-n-butyl phosphate, methyl isobutyl ketone, cyclohexanone, diethyl ether, diisopropyl ether or nitrobenzene. Equal volumes of organic and aqueous phase (3 ml) were shaken mechanically for about 15 min, and then separated by centrifugation. A 2-ml aliquot was pipetted from each phase and the γ-activity was measured with a scintillation counting system. The distribution coefficient (D) was obtained as the ratio of the γ-count rate of the two phases.

The conductivity measurements were carried out with a Messbrücke R-568 and a polyethylene conductivity cell, thermostated at $25 \pm 0.1°C$, with platinum electrodes at a frequency of $1 \cdot 10^4$ Hz. The cell constant was obtained from data on the conductivity of 0.1 and 0.01 *M* KCl solutions and was equal to $7.01 \cdot 10^{-2}$ cm^{-1}.

Extracts containing the required metal concentration were prepared by dilution of extracts containing 0.05 *M* tantalum or 0.01 *M* niobium by means of the organic phase obtained by shaking 2 *M* hydrofluoric acid solution with the organic solvents.

RESULTS

The effects of hydrofluoric acid concentration, tantalum concentration and the nature of the organic solvent on the extraction of micro quantities of niobium and zirconium (10^{-5} *M*) in the absence and in the presence of macro quantities of tantalum (0.1 *M*) were investigated. The tantalum extraction was studied in parallel.

The extraction of micro amounts of zirconium in the presence of macro amounts of niobium was also studied in some experiments.

Effect of hydrofluoric acid concentration

Figure 1 shows the results obtained for tributyl phosphate, methyl isobutyl ketone and cyclohexanone as plots of log *D vs.* the initial concentration of hydrofluoric acid in the 1–8 *M* range. Distribution coefficients of niobium and zirconium increase with increasing concentration of hydrofluoric acid. There is a significant decrease in the extraction of the micro component in the presence of tantalum in all the systems described. The degree of suppression (the ratio of the distribution coefficient of the micro component in the absence of the macro component to the corresponding value in the presence of macro component) decreases with increasing hydrofluoric acid concentration.

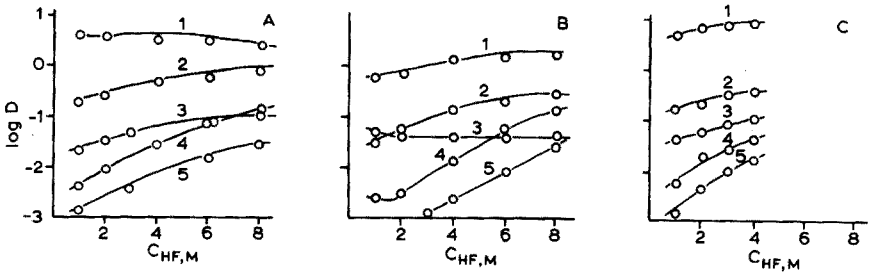

Fig. 1. Extraction of metals with tributyl phosphate (A), methyl isobutyl ketone (B) and cyclohexanone (C) depending on the HF concentration: 1, Ta (0.1 *M*); 2, Nb ($1 \cdot 10^{-5}$ *M*); 3, Zr ($1 \cdot 10^{-5}$ *M*); 4, Nb in the presence of Ta; 5, Zr in the presence of Ta.

The extraction of macro amounts of tantalum changes little in the acidity range studied; distribution coefficients decrease slightly in the case of tributyl phosphate and increase in the case of methyl isobutyl ketone, as the acid concentration increases.

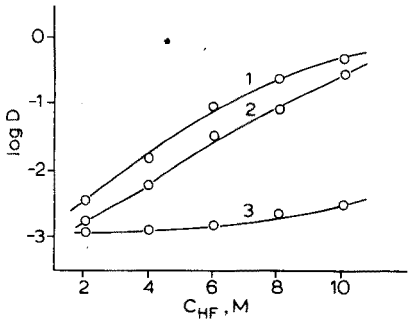

Fig. 2. Extraction of metals with diethyl ether depending on the HF concentration: 1, Nb (0.1 *M*); 2, Zr ($1 \cdot 10^{-4}$ *M*) in the presence of Nb; 3, Zr.

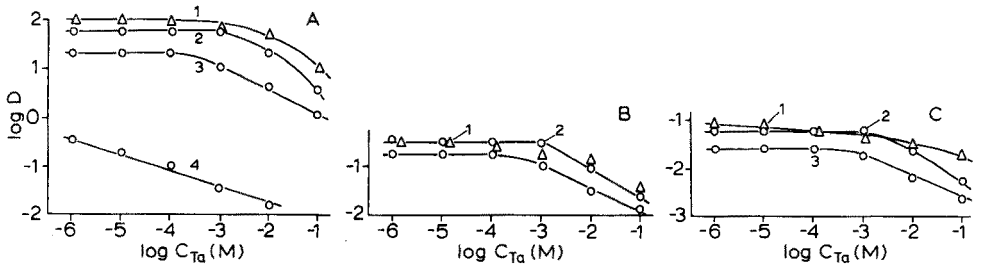

Fig. 3. Extraction of Ta (A), Nb (B) and Zr (C) depending on the Ta concentration: 1, cyclohexanone; 2, tributyl phosphate; 3, methyl isobutyl ketone; 4, nitrobenzene.

In the extraction of zirconium (10^{-4} *M*) with diethyl ether, a solvent of low polarity, the presence of large amounts of niobium leads to co-extraction of zirconium (Fig. 2). In the absence of niobium, D_{Zr} changes only slightly as the concentration of hydrofluoric acid increases; in the presence of niobium, the zirconium extraction increases with increase in the acid concentration.

Effect of concentration of the macro element

The influence of the tantalum concentration on the extraction of niobium and zirconium was investigated (Fig. 3). When tributyl phosphate is used D_{Nb} and D_{Zr} are constant in the 10^{-6}–10^{-3} *M* range of tantalum concentrations, and then decrease. These *D* values decrease more in the case of methyl isobutyl ketone and cyclohexanone than with the other solvents at 10^{-4} *M* concentrations of

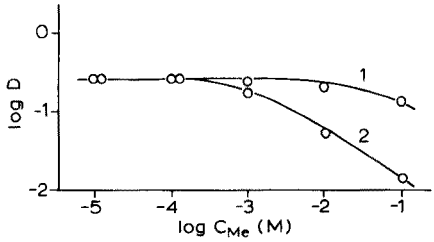

Fig. 4. Extraction of Nb with cyclohexanone from 2 *M* HF depending on its own concentration (1) and on the Ta concentration (2).

tantalum. The dependence of the D_{Ta} on the tantalum concentration is very similar for the first three solvents. For nitrobenzene, the tantalum extraction decreases monotonously in the concentration range studied.

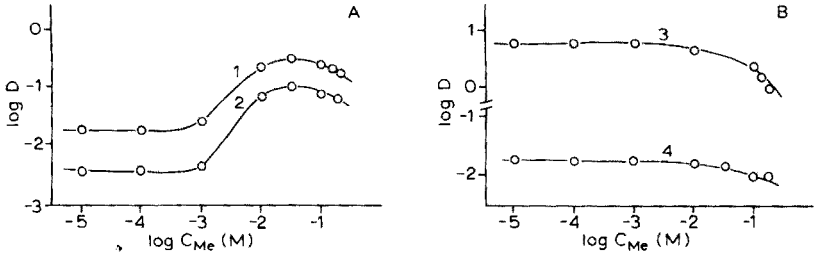

Fig. 5. Extraction of Nb and Zr with diethyl ether from M HF depending on the Nb concentration (A) and extraction of Nb and Ta depending on the Ta concentration (B): 1 and 4, Nb; 2, Zr; 3, Ta.

The extraction of niobium with cyclohexanone as a function of the niobium and tantalum concentration was also studied (Fig. 4). An increase in the niobium concentration leads to a slight decrease in the extent of its extraction. Tantalum, when it is present in concentrations above 10^{-3} M, substantially suppresses the extraction of niobium.

An investigation of the extraction of zirconium and niobium with diethyl ether depending on the niobium concentration showed that the curves $\log D_{Nb}$–$\log c_{Nb}$ and $\log D_{Zr}$–$\log c_{Nb}$ pass through a maximum (Fig. 5A). The distribution coefficients for the metals are constant within the 10^{-5}–10^{-3} M range of niobium concentrations. With 10^{-3}–0.02 M concentrations of niobium, the D_{Zr} value increases (co-extraction with niobium is observed), but at very high niobium concentrations, D_{Zr} begins to decrease. The dependence of $\log D_{Nb}$ on $\log c_{Nb}$ is analogous. Less co-extraction of zirconium with niobium took place when diisopropyl ether was used.

The influence of the tantalum concentration on the extraction of niobium, zirconium and tantalum itself with diethyl and diisopropyl ethers is of a different character (Figs. 5B and 6). The $\log D_{Ta}$–$\log c_{Ta}$ and $\log D_{Nb}$–$\log c_{Ta}$ plots remain essentially parallel to the abscissae up to tantalum concentrations of 10^{-3} M, but at higher concentrations of tantalum the extraction of the metals decreases, the drop being more obvious in the case of diethyl ether. There is no co-extraction,

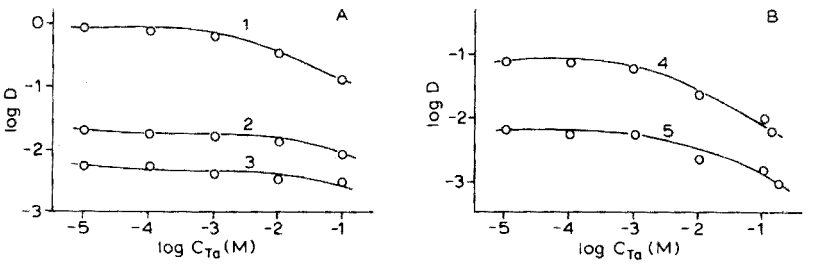

Fig. 6. Extraction of metals with diisopropyl ether from 8 M (A) and 4 M HF (B) depending on the Ta concentration: 1 and 4, Ta; 2 and 5, Nb; 3, Zr.

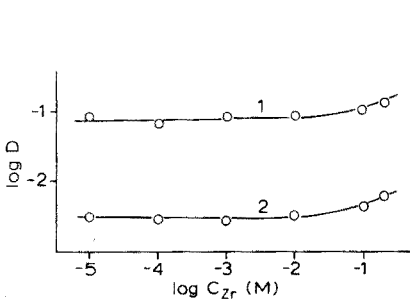

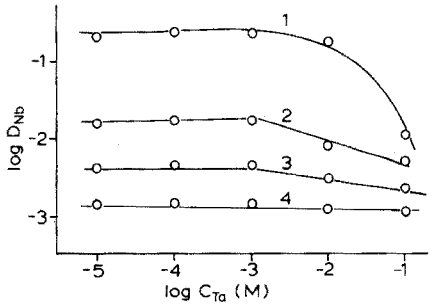

Fig. 7. Extraction of Zr with diethyl ether in the presence (1) and in the absence (2) of Nb depending on the Zr concentration C_{HF}, 8 *M*; C_{Nb}, 0.1 *M*.

Fig. 8. Extraction of Nb from 2 *M* HF with tributyl phosphate (TBP) and its solutions in benzene: C_{TBP}, 100% (1), 75% (2), 50% (3) and 25% (4).

and, in fact, the D_{Nb} values decrease at tantalum concentrations above 10^{-3}–10^{-2} *M*, *i.e.* suppression of niobium extraction is observed.

The relationship between $\log D_{Zr}$ and $\log c_{Zr}$ in the absence and in the presence of 0.1 *M* niobium is illustrated in Fig. 7. It can be seen that both the the plots obtained are of the same type. The degree of co-extraction of zirconium does not depend on its concentration.

The character of the dependence of D_{Nb} on changes in the tantalum concentration when the extractions are done with dilutions of tributyl phosphate in benzene is shown in Fig. 8. Extraction of niobium decreases with increase in the tantalum concentration when the 100, 75 and 50% solutions of tributyl phosphate are used. For the 25% solution, D_{Nb} remains practically constant within the range of tantalum concentrations studied.

DISCUSSION

Nature of the effects

The data obtained show that in the extraction of complex metal fluorides of Ta, Nb, and Zr with oxygen-containing solvents, extractable macro elements can have a considerable effect on the extraction of micro elements: both co-extraction and suppression of extraction can be observed. The simultaneous extraction of micro and macro elements in these systems is regulated by the same principles which have already been established for the HCl, HBr, HI and HSCN extraction systems[1–3]. The behaviour of micro components in the presence of macro components is governed in the same way by interactions of the extracted compounds in the organic phase.

The co-extraction observed for the solvents of relatively low polarity (Fig. 5A) may be explained by the formation of mixed ion associates of the micro and macro elements in the organic phase. An increase (up to a definite limit) in the concentration of the macro element favours the formation of complex mixed ion associates, which leads to co-extraction of the micro element. With further increase in the concentration, the mixed ion associates are destroyed owing to an increase in the dielectric constant of the organic phase and the co-extraction of the micro

elements is then lowered.

The suppression of extraction when solvents with relatively high dielectric constants and/or with substantial donor capacities are used, may be explained by dissociation of the complex metal halides in the organic phase. This dissociation gives rise to conditions that favour a display of the common ion effect (hydrogen ion). In the simplest form, the extraction of the micro element with such solvents can be represented by the equation:

$$H^+ + A^- \rightleftharpoons H^+_{(0)} + A^-_{(0)}$$

where A^- is the complex metal halide anion. The extraction constant is then:

$$K_{ex} = [H^+]_0[A^-]_0[H^+]^{-1}[A^-]^{-1}.$$

If $[A^-]_0/[A^-]$ is the distribution coefficient of the micro element, then:

$$D = K_{ex}[H^+][H^+]_0^{-1}$$

The $[H^+]$ value is high and practically constant. If the extraction and dissociation of the mineral acid are negligible in comparison with the extraction and dissociation of the complex acid of the macro element, $[H^+]_0$ will depend on the concentration of the macro element in the organic phase. Therefore the D value will be smaller in the presence of the macro element. The increasing suppression of the extraction of micro elements in the presence of tantalum as the hydrofluoric acid concentration increases (Fig. 1) is probably connected with the extraction of hydrofluoric acid and with its dissociation in the organic phase. It is known that the hydrofluoric acid is extracted to a considerable extent with tributyl phosphate and methyl isobutyl ketone[5,6] and so exercises a "buffering" action on the suppression of the extraction of niobium and zirconium by tantalum, decreasing the contribution of fluorotantalic acid to the $[H^+]_0$ value. The increase in the hydrofluoric acid concentration is accompanied by an increase in its "buffering" action and a decrease in the degree of suppression of the extraction of the micro element.

The difference in the decrease of the distribution coefficients with increasing tantalum concentrations for different solvents (Fig. 3) is connected also with their different capacities for extracting hydrofluoric acid. The extraction of hydrofluoric acid decreases in the order tributyl phosphate > methyl isobutyl ketone > nitrobenzene[5,6]; cyclohexanone is probably similar to methyl isobutyl ketone. The decrease in the extraction of the micro elements with increasing tantalum concentrations begins the earlier, the less readily the solvent extracts hydrofluoric acid.

The data in Fig. 8 suggest that the suppression of extraction is not connected with a decrease of the extractant concentration in the organic phase. If this factor were decisive, then the decrease in the concentration of tributyl phosphate in benzene would lead to an earlier and sharper drop in the niobium extraction with increasing tantalum concentrations. In fact, the opposite happens.

The suppressions of the niobium extraction by tantalum, when diethyl and diisopropyl ethers are used (Figs. 5 and 6), show no analogies; no reasonable explanation for this effect is as yet available.

Dissociation constants of $HTaF_6$ and $HNbF_6$ in cyclohexanone

The differences in the log D–log c curves for niobium and tantalum, in combination with other results described above, serve as a basis for the suggestion that fluorotantalic acid is considerably stronger than fluoroniobic acid. It has been shown earlier that tantalum and niobium are extracted from hydrofluoric acid solutions as $HTaF_6$ and $HNbF_6$[7]. From the data on conductivity of the extracts, the dissociation constants of these acids in cyclohexanone were calculated by the Fuoss–Kraus method. The results are presented in Table I. The following values of the dissociation constants were found: $3.6 \cdot 10^{-3}$ for $HTaF_6$ and $1.2 \cdot 10^{-3}$ for $HNbF_6$.

TABLE I

DISSOCIATION CONSTANTS OF FLUOROTANTALIC AND FLUORONIOBIC ACIDS IN CYCLOHEXANONE

Metal concentration in the organic phase (M)	*Equivalent conductivity, (Ohm^{1} cm^{2} $mole^{-1}$)*	*Activity coefficient in the organic phase ($f^2_{\pm(0)}$)*	*Acid dissociation constant*
$HTaF_6$			
$8.0 \cdot 10^{-4}$	90.9	0.561	$3.6 \cdot 10^{-3}$
$9.0 \cdot 10^{-4}$	83.1	0.556	
$1.0 \cdot 10^{-3}$	78.4	0.547	
$1.5 \cdot 10^{-3}$	67.3	0.511	
$2.0 \cdot 10^{-3}$	55.6	0.484	
$3.0 \cdot 10^{-3}$	45.2	0.454	
$4.0 \cdot 10^{-3}$	39.1	0.420	
$HNbF_6$			
$8.0 \cdot 10^{-4}$	88.6	0.560	$1.2 \cdot 10^{-3}$
$9.0 \cdot 10^{-4}$	77.6	0.560	
$1.0 \cdot 10^{-3}$	73.0	0.556	
$1.5 \cdot 10^{-3}$	59.5	0.521	
$2.0 \cdot 10^{-3}$	51.8	0.493	
$3.0 \cdot 10^{-3}$	41.7	0.458	
$4.0 \cdot 10^{-3}$	36.3	0.431	

TABLE II

PERCENTAGE METAL EXTRACTION OF OXYGEN-CONTAINING SOLVENTS

0.3 M HF and 0.5 M H_2SO_4; $c_{Ta} = 0.1$ M; $c_{Nb,Zr} = 1. \cdot 10^{-5}$ M)

Extractant	*Ta*	*Nb*		*Zr*	
		In absence of Ta	*In presence of Ta*	*In absence of Ta*	*In presence of Ta*
Methyl isobutyl ketone	89.1	15.2	0.65	2.6	0.2
Tributyl phosphate	99.7	22.5	5.7	7.4	2.4
Cyclohexanone	99.3	20.6	4.0	3.9	0.8

Possible applications of the extraction suppression

The suppression of the niobium and zirconium extraction in the presence of large amounts of tantalum may be of practical interest for improvement of the extraction separation of these metals. Some examples are given in Table II, where the results of the simultaneous extraction of niobium and tantalum, or zirconium and tantalum from 0.3 *M* HF–0.5 *M* H_2SO_4 solutions with MIBK, tributyl phosphate and cyclohexanone are presented. Data on the extraction of the micro elements in the absence of tantalum and on the extraction of tantalum itself are also shown. The extraction of niobium and zirconium in the presence of tantalum are decreased substantially, while 90–100% of tantalum itself is extracted.

SUMMARY

The simultaneous extraction of niobium, zirconium and tantalum from hydrofluoric acid solutions with oxygen-containing solvents has been studied. When solvents of relatively high dielectric constant—tributyl phosphate, methyl isobutyl ketone and cyclohexanone—are used, the extraction of micro amounts of niobium and zirconium is suppressed by the presence of macro amounts of tantalum. This suppression of extraction in the presence of tantalum is also evident with solvents of low polarity, such as diethyl and diisopropyl ethers, but with these solvents, zirconium is co-extracted with niobium. One of the principal causes of these mutual influences of metals is dissociation and association of the compounds extracted in the organic phase. The formation of mixed ion associated in the extract allows co-extraction of one metal with another. Conversely, the dissociation of complex acids in the organic phase causes suppression of extraction of micro elements by the common ion effect.

REFERENCES

1 Yu. A. Zolotov and V. I. Golovanov, *Dokl. Akad. Nauk SSSR*, 191 (1970) 92; 193 (1970) 626.
2 Yu. A. Zolotov and V. I. Golovanov, *Proc. of International Solvent Extraction Conference ISEC 71, The Hague, 19–23 April. Vol. I*, Soc. Chem. Ind., London, 1971, p. 625.
3 Yu. A. Zolotov, B. Z. Iofa and L. K. Chuchalin, *Extrakciya Galogenidnych Komplexov Metallov (Extraction of Halide Complexes of Metals)*, *Nauka*, Moscow, 1973.
4 V. Pfeifer and H. Bildstein, *Solvent Extraction Chemistry, Proc. Internat. Conf., Gothenburg, Sweden*, North-Holland, Amsterdam, 1967, p. 142.
5 G. P. Giganov and V. D. Ponomarev, *Tr. Inst. Met. Obogashch., Akad. Nauk Kaz. SSR*, 5 (1962) 108.
6 R. Bock and M. Herrmann, *Z. Anorg. Allg. Chem.*, 284 (1956) 288.
7 A. I. Nikolaev, E. G. Il'in, B. Ya. Spivakov, A. G. Babkin, Yu. A. Buslaev and Yu. A. Zolotov, *Zh. Neorg. Khim.*, 20 (1975) 194.

Analytica Chimica Acta, 78 (1975) 405–409

THE COEXTRACTION OF RHENIUM WITH PYRIDYLAZONAPHTHOLATES OF INDIUM, IRON(III) AND THALLIUM(III)

YU. A. ZOLOTOV, N. V. SHAKHOVA and O. A. KISELEVA

Vernadsky Institute of Geochemistry and Analytical Chemistry, Academy of Sciences, Moscow (U.S.S.R.)

(Received 3rd March 1975)

1-(2-Pyridylazo)-2-naphthol (PAN) forms "cationic" complexes with metal ions such as In, Fe(III), Tl(III), Co(III), and Cu(II)[1–5]. This is connected with the polydentate character of the reagent: the coordination capacity of the metal ion may not be sufficient for the formation of a neutral complex. As the central atom in such compounds usually has free coordination places, the "cations" mentioned (in relation to PAN) exist, in several cases, in the form of neutral complexes with a mixed coordination sphere. In the absence of suitable ligands, the cations exist as such. Their extraction is possible only in the presence of sufficiently hydrophobic anions as has been shown, for example, for indium pyridylazonaphtholate[1].

It seemed probable that some metal-containing anions also act as the co-ions in the formation of these extractable complexes. In this case, the coextraction of two metals would be possible. From this point of view, it was worthwhile to study the influence of perrhenate ions on the extraction of cationic pyridylazonaphtholates and to estimate the possibility of rhenium coextraction. Among the known cationic complexes of PAN, the singly charged cations seemed of greatest interest. Extraction systems with indium, iron(III), and thallium(III) pyridylazonaphtholates have already been studied. According to published data, indium and thallium(III) form 1:1 and 1:2 complexes with PAN whereas iron(III) forms a 1:2 compound[4–6].

EXPERIMENTAL

Reagents and solutions

Iron(III) solution was obtained by dissolution of freshly precipitated iron(III) hydroxide in 6 *M* hydrochloric acid[7]; iron(III) concentration was established by titration with standard EDTA solution. The radioactive isotope ^{59}Fe was purified by extraction with diethyl ether from 6 *M* hydrochloric acid. Standard solutions of thallium sulphate and indium nitrate and solutions of the radioisotopes ^{144}In and ^{204}Tl were used. Solutions of the other elements were prepared by dissolving precisely weighed amounts commercial reagents. Solutions of 1-(2-pyridylazo)-2-naphthol in organic solvents were prepared by accurate weighing. The solvents were purified by established methods[8].

Procedures

A solution of the appropriate radioisotope (^{59}Fe, ^{114}In, or ^{204}Tl) was added to an aliquot of indium, iron(III) or thallium(III) solution. Then 1 ml of a 0.02 *M* solution of PAN in an organic solvent and 1 ml of isoamyl alcohol (the system with indium), or 2 ml of a 0.01 *M* PAN solution (for other systems), were added, followed by a solution of ammonium perrhenate, and some solution appropriate for the necessary pH adjustment. Finally, water was added to bring the total volume of the aqueous phase to 2 ml.

The extractions were carried out in 10-ml test-tubes fitted with ground-glass stoppers during 30 min in an air thermostat at 25±1°C. After the phase separation, the γ-activity of aliquots of each phase was measured by a scintillation counter with a NaI(Tl) crystal (indium and iron extraction). When thallium was extracted, after evaporation of the solutions in glass plates under an infra-red lamp, the β-activity of ^{204}Tl was measured by an analogous method.

RESULTS AND DISCUSSION

Extraction of indium

In the presence of PAN, indium is extracted with chloroform, 1,2-dichloroethane and other solvents without the introduction of special anionic additives[1–5]. However, such extractions have usually been carried out from acetate, hydrogen phthalate, and other buffer solutions, where the corresponding anions are probably suitable partners. The data obtained here showed that in the absence of suitable co-ions, the extraction of indium is low.

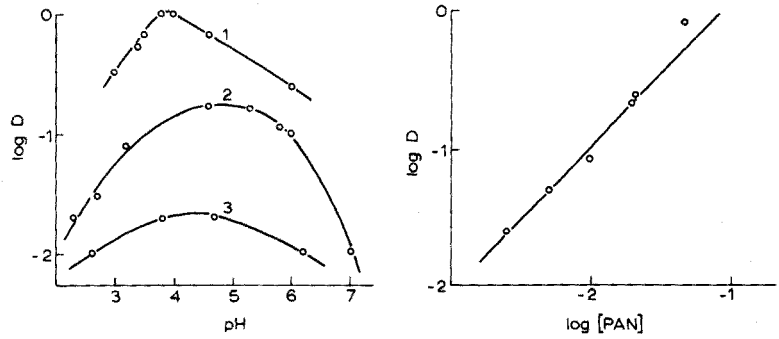

Fig. 1. Extraction of indium in the presence of 0.3 *M* NH_4ReO_4 by 0.01 *M* solutions of PAN in various solvents: 1, Mixture (1:1) of dichloroethane and isoamyl alcohol; 2, Dichloroethane; 3, Dichloroethane, in the absence of NH_4ReO_4.

Fig. 2. Extraction of indium in the presence of 0.3 *M* NH_4ReO_4 depending on the concentration of PAN in dichloroethane.

The introduction of perrhenate ions favours an increase in the extent of extraction of indium by dichloroethane (Fig. 1). The extraction of indium does not depend on its concentration over the range 10^{-6}–10^{-4} *M*; this indicates that under the extraction conditions used (0.3 *M* NH_4ReO_4, pH 4.2), indium does not form polynuclear compounds and, consequently, can hardly be extracted in the form

of $In_2(PAN)_3$ as some authors have suggested[9].

The influence of the concentration of PAN on the extraction of indium in the presence of perrhenate was investigated. It was shown by the bilogarithmic method that the ratio of indium to PAN in the compounds which are extracted is 1:1 (Fig. 2). The chelate "cation" formed is unsaturated with respect to the reagent and seems to contain coordinated water. This is confirmed by the fact that the addition of isoamyl alcohol enhances the extraction (Fig. 1). In the extraction of indium by a solution of PAN in a mixture (1:1) of dichloroethane and isoamyl alcohol, the extraction equilibrium at pH 3.25 is attained during a 30-min phase contact. The degree of indium extraction in the presence of perrhenate ions increases with the dielectric constant of the solvent in the order: chloroform < dichloroethane < nitrobenzene (Fig. 3). Such a dependence of the extraction on the dielectric constant of the solvent usually indicates extraction of an ion associate. It seems reasonable to suggest that the cationic indium pyridylazonaphtholate is extracted in the form of an ion associate with the perrhenate ion. The extraction of indium increases with the perrhenate concentration, which suggests that rhenium

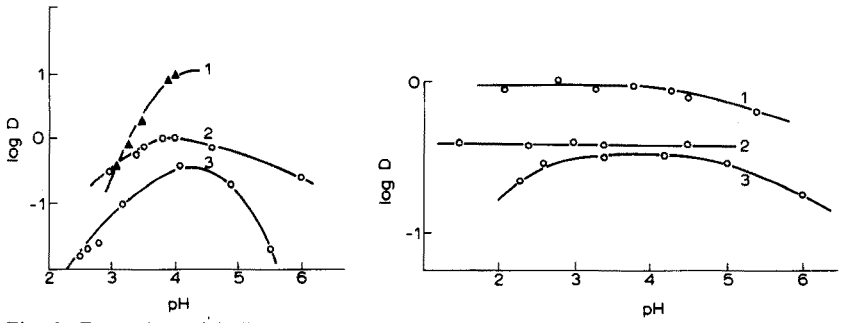

Fig. 3. Extraction of indium in the presence of 0.3 *M* NH_4ReO_4 by 0.01 *M* solutions of PAN in mixtures (1:1) of isoamyl alcohol with nitrobenzene (1), dichloroethane (2) and chloroform (3).

Fig. 4. Extraction of iron(III) in the presence of 0.3 *M* NH_4ReO_4 by 0.01 *M* solutions of PAN in nitrobenzene (1), dichloroethane (2) and chloroform (3).

TABLE I

RESULTS OF DETERMINATION OF INDIUM, IRON(III) AND RHENIUM IN EXTRACTS

(All results are given as 10^{-5} mol l^{-1}. The initial concentration of Re(VII) was 0.3 mol l^{-1}.)

Indium extraction		*Iron extraction*	
In extracted	*Re extracted*[a]	*Fe extracted*	*Re extracted*[a]
2.5	3.0	1.0	0.9
2.3	3.6	0.8	1.2
2.4	3.2	0.9	1.4
5.2	6.0	1.2	1.5
4.8	6.0	1.3	1.0
5.0	5.8	1.3	1.3

[a] Rhenium content after deduction of the blank assay results.

enters the ion associate being extracted. Analysis of the organic phase confirmed the extraction of rhenium (Table I). As this element forms no extractable compounds with PAN, its extraction is possible only as perrhenate in an ion-association complex.

Extraction of iron(III)

According to published data[5], iron(III) forms a $Fe(PAN)_2^+$ chelate with PAN. The extraction of the iron(III) complex with PAN by various solvents in the presence of 0.3 *M* ammonium perrhenate was therefore investigated. The addition of perrhenate enhances the extraction of iron(III) by dichloroethane, analogously to the extraction of indium. The extraction of iron in the presence of the perrhenate ion increases in the series of solvents: chloroform < dichloroethane < nitrobenzene (Fig. 4). Apparently, in this case the cationic iron pyridylazonaphtholate is again extracted in the form of an associate with the perrhenate ion. Introduction of isoamyl alcohol does not enhance the extraction of iron(III); unlike indium pyridylazonaphtholate, the iron(III) chelate with PAN probably does not contain coordinated water. The extraction of iron increases with the perrhenate concentration. Analysis of the organic phase confirmed the participation of rhenium in the formation of the extracted compound (Table I). The time necessary for attainment of the extraction equilibrium for iron(III) with 0.01 *M* PAN solution in dichloroethane is 30 min. During longer mixing times, no decomposition of the pyridylazonaphtholate was observed.

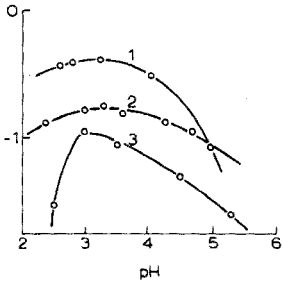

Fig. 5. Extraction of thallium(III) in the presence of 0.5 *M* NH_4ReO_4 by 0.01 *M* solutions of PAN in nitrobenzene (1), dichloroethane (2) and chloroform (3).

Extraction of thallium(III)

As for the first two systems, the addition of the perrhenate ion enhanced the extraction of thallium. The extraction again increases with the dielectric constant of the solvent in the order chloroform < dichloroethane < nitrobenzene (Fig. 5), which again suggests the extraction of an ion associate. The extraction of thallium pyridylazonaphtholate also depends on the concentration of ammonium perrhenate. During extraction of thallium with a 0.01 *M* solution of PAN in dichloroethane (pH 2.3), the time necessary for attainment of equilibrium is 30 min.

SUMMARY

The extraction of indium, iron(III), and thallium(III) complexes with 1-(2-pyridylazo)-2-naphthol is enhanced by the presence of perrhenate ion. Rhenium

is coextracted with these metals in the form of ion associates of the $InA_2^+ReO_4^-$ type, where A is the anion 1-(2-pyridylazo)-2-naphthol.

REFERENCES

1 Yu. A. Zolotov, I. V. Seryakova and G. A. Vorobyeva, *Talanta*, 14 (1967) 737.
2 S. I. Gusev and G. A. Kurepa, *Tr. Perm. Med. Inst. (Trans. Perm. Medic. Inst.)*, 108 (1972) 21.
3 G. Goldstein, D. L. Manning and O. Menis, *Anal. Chem.*, 31 (1959) 192.
4 S. Shibata, *Anal. Chim. Acta*, 25 (1961) 348.
5 R. P. Pantaler in *Prom. Khim. Reaktivov Osobo Chist. Veshchestv*, Inst. of Chem. Reagents, Moscow, 1964, p. 99.
6 B. F. Pease and M. B. Williams, *Anal. Chem.*, 31 (1959) 1044.
7 Yu. V. Karyakin and I. I. Angelov, *Chist. Khim. Reaktivy*, Goskhimisdat, Moscow, 1955, p. 140.
8 A. Weissberger, E. S. Proskauer, J. A. Riddick and E. E. Tups, *Organic Solvents Physical Properties and Methods of Purification*, Interscience, New York, 1955.
9 K. L. Cheng and B. L. Goydish, *Anal. Chim. Acta*, 34 (1966) 154.

Analytica Chimica Acta, 78 (1975) 411–422

A FLUORESCENCE METHOD FOR STUDIES OF SPENT SULFITE LIQUOR AND HUMIC SUBSTANCES IN SEA WATER

TOM ALMGREN, BJÖRN JOSEFSSON and GUNNAR NYQUIST

Department of Analytical Chemistry, University of Gothenburg, Fack, S-402 20 Göteborg 5 (Sweden)

(Received 26th February 1975)

Spent liquors from sulfite pulp mills are discharged into the Baltic Sea at different locations. This addition of considerable amounts of organic material is of special interest for two main reasons: (i) tracing the water flow pattern using the concentration distribution of the organic materials; and (ii) pollution, which may cause damage to fish resources.

Common methods for the determination of sulfite pulp wastes are u.v. spectrophotometry[1,2], the Pearl–Benson colorimetric nitroso procedure[3,4] and spectrofluorimetry[5–8]. Serious shortcomings of the u.v. absorption methods and the nitroso method are that they are not specific for spent sulfite liquor because humic substances and other materials interfere.

The present investigation was carried out in order to establish a procedure by which the concentration of spent sulfite liquor in different waters might be determined with reproducibility, specificity and rapidity. The main constituents in spent sulfite liquors are water-soluble lignin sulfonates (60–65%) and sugars (25%). Since the lignin sulfonates are the more conservative material, different methods have been proposed to form specific compounds from them such as vanillin. Nitrobenzene oxidation of lignin sulfonates, however, is not a specific test for lignin sulfonates, since lignin and humic substances also give vanillin according to Hornke and Heinisch[9] and Morrison[10]. Treatment of lignin sulfonates with hot alkali to form vanillin is a better method, since unsulfonated lignins form vanillin only in poor yield. The extracted vanillin can then be identified by paper or gas chromatography[11]. This method is, however, very time-consuming and difficult to carry out on board ship.

Lignin sulfonate solutions are highly fluorescent and can be detected at very low concentrations. Fluorescence spectrometry also offers the advantages of sensitivity, specificity and speed of analysis. The detection limit in natural waters is complicated by the presence of humic substances, which also belong to the group of polyphenols, and possess similar fluorescence characteristics, as has been shown by Thruston[6] and Almgren and Josefsson[8]. In earlier work, a standard addition method was proposed where the intensity of the background humic substances was first determined in river water samples collected above the discharge site of the spent sulfite liquors. In the sea it is difficult to establish the background of humic substances. In the Scandinavian area, the concentration is mostly dependent on the outflow from rivers which are rich in humic substances. Because of dispersion effects, the concentration of humic substances is to some extent inversely propor-

tional to the salinity[12–14].

The present research was directed to establishing a suitable standard for water-soluble humic substances representative of the waters studied. An attempt was made to differentiate between the amount of spent sulfite liquor as lignin sulfonates and the concentration of humic substances.

EXPERIMENTAL

Apparatus

All fluorescence excitation and emission spectra were measured on an Aminco–Bowman SPF spectrofluorimeter. The excitation source was either a high-intensity xenon lamp producing a continuous spectrum with peaks at 400 nm and at 900 nm (beyond the range of the instrument), or a high-intensity xenon–mercury lamp producing high intensity at the various mercury lines by superimposition of the xenon continuum. The instrument was supplied with a photomultiplier tube (Aminco–Bowman R106) with an optimal working range of 300–500 nm. By using a ratio system, where the beam is split into reference and sample beams, variations in lamp intensity are automatically nullified. The sensitivity is decreased by approximately 10% when this item is used, but the increase in stability was considered more important for quantitative measurements. The instrument was also used for phosphorescence analysis. A rotating shutter (Aminco–Bowman) was attached to the cell holder, and permitted separation of different emission lifetimes by varying the speed of rotation. For all fluorescence measurements, 1-cm quartz cells were used. Phosphorescence measurements were carried out at 77°K in a quartz capillary tube and a Dewar bottle with the bottom tip constructed of quartz.

Ultraviolet absorption data at discrete wavelengths were obtained on an Unicam SP500 spectrophotometer; u.v. absorption spectra of lignin sulfonates and humic substances were recorded on a Beckman Acta III spectrophotometer. Quartz cells with 1- and 10-cm path lengths were used for the absorption measurements.

Sampling procedure

All samples of natural water were taken with a 1-l Ruttner plastic sampler. The samples were generally stored in 0.5-l dark glass bottles, but for comparison some duplicate samples were stored in clear glass bottles. The analyses were carried out as soon as possible within 3 days; in the meantime, the bottles were stored at about 4°C. The samples were filtered through a 0.45-μm Millipore filter to reduce particle scattering.

Sampling areas

The method was tested during the period from October 1972 to January 1974. These tests were made in two different types of water. The first area suitable for this purpose was Hanö Bay (Fig. 1), which is a shallow bay with moderate water exchange in the south-west part of the Baltic Sea. There is a high natural content of humic substances together with lignin sulfonates from the waste water of a paper mill. The mouth of the outlet pipe is at station 15. The output of lignin sulfonates is $15 \cdot 10^6$ kg year^{-1}, which is nearly 2000 kg h^{-1}. The second test area was the inner part of the archipelago of the Swedish west coast. Havstensfjord and Byfjord

are situated inside the islands Orust and Tjörn. A small river (4 m^3 s^{-1}) runs into the Byfjord. The water exchange between the fjords and the sea (Skagerrak) is restricted. The salinity of the water above the pycnocline (at about 12 m) is about 24 ‰ mainly because of dilution of the North Sea water with Baltic Sea water. There are no paper mills in the vicinity and the concentration of lignin sulfonates should therefore be low.

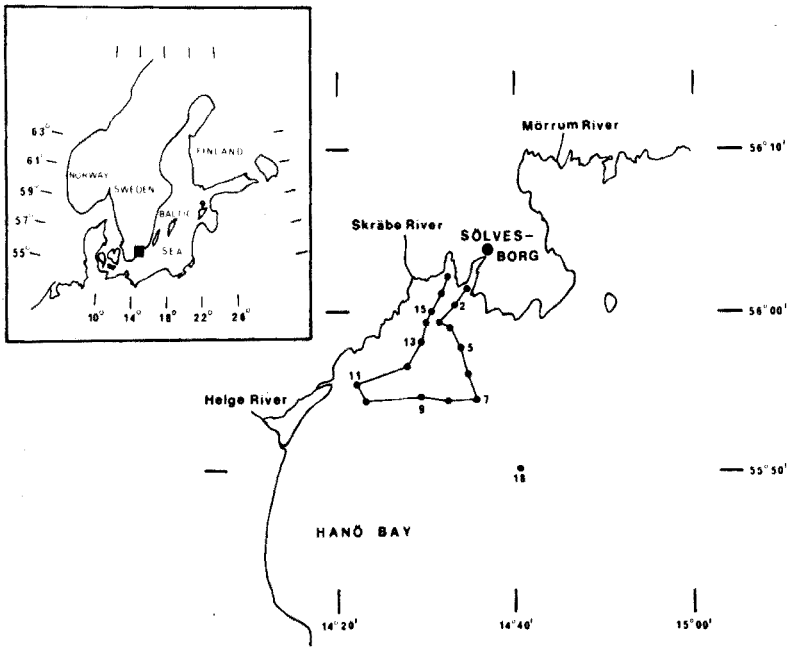

Fig. 1. The location of the stations in the Hanö Bay. Inserted: The location of Hanö Bay (square) on the map of Scandinavia.

Chemicals

All chemicals were of analytical grade. Triply distilled water was used and great care taken to avoid contamination from polyethylene tubing.

Prepared standards

Sodium lignin sulfonate was prepared by the Finnish Paper and Pulp Research Institute and is commercially available. It was extracted from a technical acidic calcium hydrogensulfite cook by ion-pair amine extraction. The absorptivity at 280 nm was 13.7 l g^{-1} cm^{-1} (Fig. 2). The lignin sulfonate was dissolved in triply distilled water. The humic substances were isolated from brownish river water late in the autumn. The water was first pumped through a sand filter packed with gravel at the top and fine sea sand at the bottom; the dissolved humic substances (or fulvic acids) were then enriched on a chelating resin as described below. The technique is similar to that described by Siegel and Degens[15] for amino acids, but the resin was loaded with iron(III) instead of copper. Iron appears to be a very efficient ligand metal for fulvic acids[16].

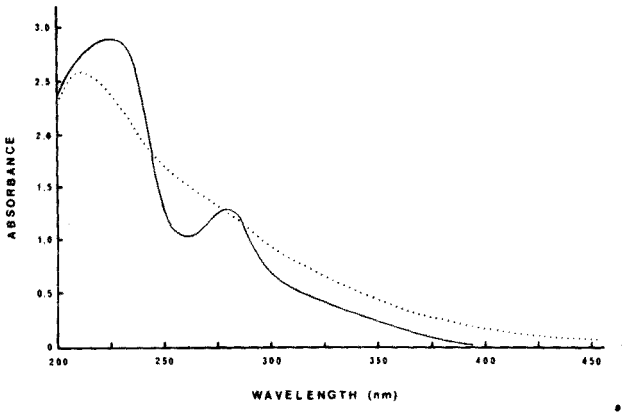

Fig. 2. Absorption spectra for 100 p.p.m. humic substances (· · · · ·) and 100 p.p.m. lignin sulfonates (——) with a cell path length of 1 cm.

A column (50 × 200 mm) was loaded with 50–100 mesh Chelex 100 in the iron(III) form and attached behind the sand filter. The river water was pumped at a rate of 5 l h^{-1}. After 100 l of water had passed through, the column was washed with distilled water and brought back to the laboratory. A 5 × 20 mm Chelex 100 column in the NH_4^+ form was attached in series after the iron column; this column takes up iron and free metal ions from the eluant. The retained humic acids were eluted with 500 ml of 3 *M* ammonia solution. The ammonia was evaporated in a rotary evaporator leaving the humic substances in a dry form. By this method, 200–300 mg of humic material was isolated from the river water. The material was easily redissolved in distilled water and had the same fluorescence characteristics as the river water itself.

Standard addition technique

This method is an extension of the procedure described by Almgren and Josefsson[8]. The water samples were excited at 315 nm and emission spectra were recorded from 350 to 500 nm. The optimal conditions were selected by varying the slits, the amplification and the excitation wavelength. When the only fluorescent substances present were humic substances, a straight line with a negative slope was obtained on plotting the emission intensity *versus* salinity owing to the dilution effect; the concentration of humic substances is low in the North Sea water. When, however, an effluent of non-saline water containing large amounts of lignin sulfonates was introduced a positive deviation from the line occurred (Fig. 3). Furthermore, on close inspection of the spectrum, a shift of the intensity maximum to shorter wavelengths, caused by lignin sulfonate emission, was observed (Fig. 4). Since the salinity range is narrow in Hanö Bay, a sample of average salinity (station 18), indicating no lignin sulfonate contribution, was chosen as a standard. Different amounts of lignin sulfonates were added to this standard. A plot of the increase in intensity *versus* the amount of lignin sulfonates added, produced a calibration curve which could be used for evaluating the concentration of lignin sulfonates in the samples.

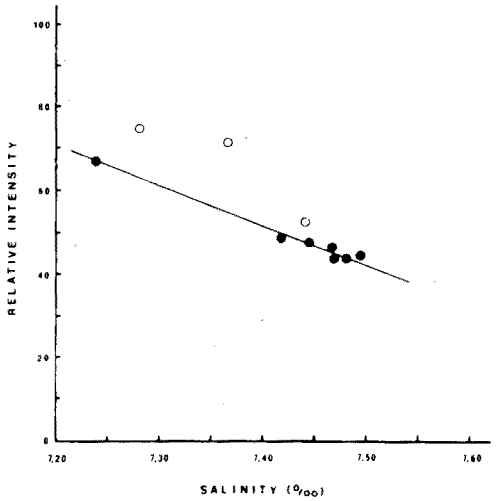

Fig. 3. Relative fluorescence emission intensity versus salinity for samples from Hanö Bay. Open circles represent samples with a marked decrease in wavelength of maximum emission. The excitation wavelength was 315 nm.

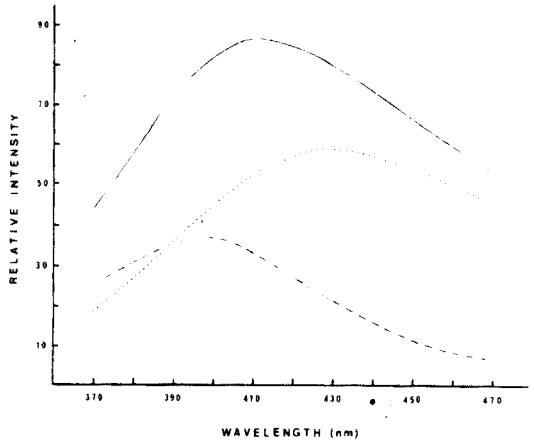

Fig. 4. Fluorescence emission spectra for 2.5 p.p.m. humic substances (· · · · · ·), 0.5 p.p.m. lignin sulfonate (– – –) and a mixture of 2.5 p.p.m. humic substances and 0.5 p.p.m. lignin sulfonate (——). The excitation wavelength was 315 nm. The apparatus settings were the same in all three cases.

Dual wavelength technique

The fluorescence peaks of humic substances and lignin sulfonates have intensity maxima at different wavelengths (Fig. 4). The maximum for humic substances appeared at 420–430 nm depending to some extent on the excitation wavelength. Lignin sulfonates showed an intensity maximum at 390–400 nm. A mixture of humic substances and lignin sulfonates gave an intensity maximum somewhere between 390–400 nm and 420–430 nm depending on the concentration of the different components (Figs. 4 and 5). The fluorescence intensity of lignin sulfonates was about 3 times stronger than the intensity of humic substances in the range

0.01–10 mg l^{-1}. Thus a low concentration of lignin sulfonates could be detected in the presence of a relatively high background of humic substances.

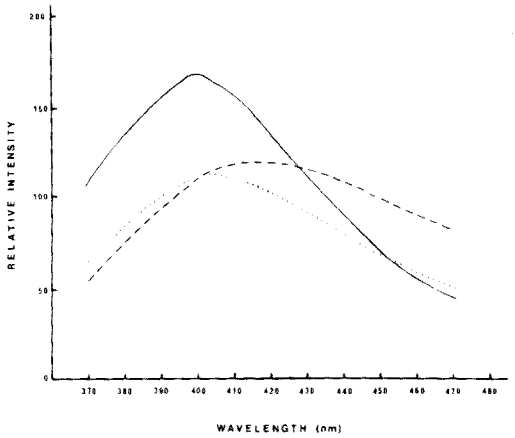

Fig. 5. Fluorescence emission spectra for different mixtures of lignin sulfonates and humic substances. 2.0 and 1.0 (——), 1.0 and 2.0 (· · · · · ·) and 0.5 and 4.0 (– – – – –) p.p.m. lignin sulfonate and humic substances respectively, were used. The excitation wavelength was 315 nm.

If the absorption in the sample is low ($A < 0.02$), the fluorescence intensity is directly proportional to the concentration of the substances giving rise to the fluorescence. The equation for the fluorescence intensity is then given by:

$$I_F = k_1 C_A + k_2 C_B \tag{1}$$

where I_F is the fluorescence intensity, C_A and C_B are the concentrations of the two substances A and B, and k_1 and k_2 are constants which include the quantum efficiency, the intensity of the excitation radiation, the molar absorptivity coefficient and the apparatus constants.

The concentrations of lignin sulfonates and humic substances were determined by a dual wavelength procedure from the emissions at 390 and 430 nm.

$$\text{At 390 nm eqn. (1) will give:} \quad X = A_L c_L + A_H c_H \tag{2}$$

$$\text{At 430 nm eqn. (1) will give:} \quad Y = B_L c_L + B_H c_H \tag{3}$$

where X and Y are the relative fluorescence intensitites at the two wavelengths; c_L and c_H are the concentrations of lignin sulfonates and humic substances, respectively; A_L and B_L are the lignin sulfonate constants at 390 and 430 nm; and A_H and B_H are the constants for the humic substances at the two wavelengths. The constants were determined from standard solutions of known concentration of lignin sulfonates and humic substances in distilled water. The exciting wavelength was 315 nm, and the emission spectra were recorded over the range 350–430 nm. The relative intensities of the standard solutions were registered at 390 and 430 nm and plotted against the concentrations. The apparatus settings were not changed during the measurements, thereby avoiding changes in the apparatus constants. The plot of relative intensities *versus* the concentrations showed a linear relationship from at least 0.05 p.p.m. up to 7–8 p.p.m. (Inner filter effects occurred at higher concentra-

tions.) This straight line relationship was valid for all four standard curves. The constants A_L, B_L, A_H and B_H are the slopes of the straight lines.

From eqns. (2) and (3) it is possible to derive the following expressions for the concentrations of lignin sulfonates and humic substances:

$$c_L = \frac{XB_H - YA_H}{A_L B_H - B_L A_H} \tag{4}$$

$$c_H = \frac{YA_L - XB_L}{A_L B_H - B_L A_H} \tag{5}$$

The relative intensities X (390 nm) and Y (430 nm) were obtained from the emission spectrum of the unknown sample.

Methods of improving peak separations

In order to increase the difference between the emission peaks of the humic substances and lignin sulfonates different chemical and physical approaches were tried. The effect of pH was examined by comparing spectra taken at pH 3, 8 and 10. The ability of humic substances to form complexes with metals is well known, and the effect of different amounts (10–100 p.p.m.) of copper(II) was examined. Phosphorescence provides, apart from the excitation and the emission wavelengths, a third possibility for differentiation, namely determination of emission life-time. The phosphorescence properties of humic substances and lignin sulfonates were examined at 77°K. In order to obtain a suitable glass from the sample at this temperature, the sample, methanol and ethanol were mixed in the proportions 10:45:45 (v/v) and frozen rapidly by inserting the capillary tube containing the mixture into liquid nitrogen. The emission spectra were recorded at different shutter speeds for both substances.

RESULTS

Absorption measurements

The absorption curves of lignin sulfonates and humic substances are shown in Fig. 2. The humic substances show no maximum or minimum above 210 nm. The lignin sulfonates give a maximum at 280 nm and a minimum at 260 nm. The diminishing absorbance around 200 nm in both cases may be due to luminescence, so that these are probably not true maxima. The humic substances have a higher absorbance in the visible region than the lignin sulfonates, because humic substances are colored (yellow to brown, depending on the concentration). Lignin sulfonates are colorless and absorb only in the ultraviolet region.

The absorbances of natural waters from Hanö Bay and Byfjord are shown in Tables I and II, column 5. From Fig. 2, it is easy to obtain the absorptivity coefficients for lignin sulfonates and humic substances at 350 nm. These coefficients (2.58 and 4.52 $l\ g^{-1}\ cm^{-1}$) were used to calculate the theoretical absorbances of the water samples, from the concentrations of lignin sulfonates and humic substances obtained from the fluorimetric measurements (Tables I and II, column 6). The ratios between the calculated absorbance and the measured absorbance are given in column 7 of the Tables. The poor correlation shown by the sample from station 15

(Table I) is probably due to inner-filter effects in the sample or to other substances in the water from the outlet, which absorb in this region. The samples from station 1 and 2. just outside Sölvesborg harbour, were probably also polluted with other u.v.-absorbing substances.

TABLE I

RESULTS OF MEASUREMENTS FOR HANÖ BAY

(January 31, 1974)

Station	*Salinity* (‰)	*Humic substances (p.p.m.)*	*Lignin sulfonate (p.p.m.)*	$A_{meas.}$[a]	$A_{calc.}$[a]	$\frac{A_{calc.}}{A_{meas.}}$ (%)
1	7.18	2.32	0.74	0.159	0.124	78.0
2	7.23	2.46	0.91	0.215	0.135	62.8
3	7.61	1.70	0.54	0.096	0.091	94.8
4	7.59	1.87	0.62	0.113	0.101	89.4
5	7.59	1.89	0.65	0.136	0.102	75.0
6	7.65	1.61	0.52		0.086	93.5
7	7.52	1.81	0.55	0.096	0.096	100.0
8	7.47	1.84	0.56	0.097	0.098	101.0
9	7.47	1.79	0.55	0.094	0.095	101.1
10	7.52	1.77	0.54	0.090	0.094	104.4
11	7.59	1.59	0.50	0.084	0.085	101.2
12	7.52	2.08	0.57	0.113	0.109	96.5
13	7.63	1.66	0.53	0.088	0.089	101.1
14	7.63	1.66	0.53	0.090	0.089	98.9
15	7.27	2.90	3.20	0.705	0.214	30.3
16	6.06	2.36	0.71	0.151	0.125	82.8
17	6.20	2.31	0.71	0.147	0.123	83.7

[a] 350 nm and with cell pathlength, 10 cm.

TABLE II

RESULTS OF MEASUREMENTS FOR HAVSTENSFJORD AND BYFJORD

(January 23, 1974. H = Havstensfjord, B = Byfjord. The numbers at each station indicate the depth.)

Station	*Salinity* (‰)	*Humic substances (p.p.m.)*	*Lignin sulfonate (p.p.m.)*	$A_{meas.}$[a]	$A_{calc.}$[a]	$\frac{A_{calc.}}{A_{meas.}}$ (%)
HO	22.5	1.86	0.01	0.106	0.086	81.1
BO	9.0	8.26	0	0.435	0.369	84.8
B10	25.9	1.93	0.02	0.092	0.089	96.7
B16	28.8	1.18	0.02	0.058	0.055	94.8
B20	29.0	1.40	0.02	0.064	0.063	98.4

[a] At 350 nm.

Standard addition technique

On two occasions, November 1972 and December 1972, the standard addition technique was studied on samples from Hanö Bay. On the first occasion

a promising plot of relative fluorescence intensity *versus* salinity was obtained (Fig. 3). The three deviating points, representing stations 15, 16A (close to 16) and 17, also showed a definite shift in wavelength maxima to 410 nm. The concentrations of the three samples are given in Table III; the estimated error was ±0.02 p.p.m. On the second occasion, however, a different pattern appeared. The fluorescence intensity was independent of salinity and from the mean of 29 samples, 6 samples showed a considerable deviation, namely stations 15 (surface and bottom), 15A (surface, close to 15), 16 (surface and bottom), 16B (surface, close to 16) and 17 (surface). However, no significant wavelength shifts of peak maxima could be observed. The error in the determined concentration (Table III) was estimated to be ±0.03 p.p.m.

TABLE III

CONCENTRATION OF LIGNIN SULFONATES IN HANÖ BAY DETERMINED BY THE STANDARD ADDITION TECHNIQUE

(s = Surface sample, b = bottom sample)

Station	*November 1972 (p.p.m.)*	*December 1972 (p.p.m.)*
15 (s)	0.10	0.43
15 (b)		0.24
15A (s)		> 1.78
16 (s)		0.29
16 (b)		0.12
16A (s)	0.20	
16B (s)		1.12
17 (s)	0.27	0.17

Dual wavelength technique

The results of the dual wavelength technique for Hanö Bay and Byfjord are shown in Tables I and II, columns 3 and 4. It should be noted that all stations in Hanö Bay contained lignin sulfonates. The highest concentration was again found at station 15, the outlet point of the paper mill, but in the inner part of the bay the content of lignin sulfonates was also higher (station 1, 2, 16, 17 and to some extent 4,5) than at the outer stations. Except for those stations with increased concentrations, the mean concentration of lignin sulfonates was about 0.55 p.p.m. with small variations between the stations.

The concentration of humic substances in Hanö Bay showed some variations, with the highest concentrations near the river mouths and at the stations with the lowest salinities. The content of humic substances was about 3–4 times higher than the concentration of lignin sulfonates. At station 15 the concentration of humic substances was relatively high, probably because of the humic substances contributed by the paper mill, which uses river water. In Byfjord the concentration of humic substances was relatively high. At the time of sampling, the surface water contained high concentrations of humic substances because the fresh water from Bäve river was not mixed with the sea water but formed a thin layer on the surface.

Photodecay

The irradiation time for the sample in the cell was as short as possible. Several successive spectra were run on the same sample as a check, and a slight decay was observed.

Effect of pH and copper(II) complex formation

No significant changes in fluorescence properties were observed when solutions of humic substances and lignin sulfonates were acidified to pH 3 with hydrochloric acid. When the solutions were treated with sodium hydroxide to pH 10, however, the emission intensity of both standards, excited at 315 nm, was lowered by *ca.* 15%; the lignin sulfonate emission peak was shifted from 390 to 420 nm, whilst the peak of humic substances remained unaltered at 420 nm. A remarkable decrease in emission intensity was also observed when 200 p.p.m. of copper(II) chloride was added to 10 p.p.m. of lignin sulfonates or humic substances. With the same excitation wavelength (315 nm), a 25% decrease in intensity was observed for the emission of lignin sulfonates compared with a 50% decrease for the humic standard, but no shifts in the wavelength maxima were noted.

Phosphorescence properties

Within the limits of detection of the equipment used, the lignin sulfonates and humic substances showed no differences with respect to phosphorescence lifetime, peak wavelength and intensity. The phosphorescence lifetimes (seconds) of both substances were too long to be measured by the rotating shutter at the lowest speed, and both had a peak maximum at 430 nm when excited at 315 nm; a possible detection limit of about 100 p.p.b. was obtained at this wavelength.

DISCUSSION

It has been shown that u.v. measurements cannot be used to determine the presence of lignin sulfonates in sea water containing humic substances and unknown pollutants from river water and other effluents. In mildly polluted water, the u.v. absorbance is mainly due to the presence of humic substances, which can therefore be determined. Bladh[17], for instance, measured the concentration of yellow substances in the Baltic at 380 nm, where the absorptivity coefficient is 2.75 $l\ g^{-1}\ cm^{-1}$. In order to determine the concentration of both lignin sulfonates and humic substances, it is convenient to use the fluorimetric method with measurements at two wavelengths described above. The apparatus must, however, be standardized with aqueous solutions of lignin sulfonates and humic substances. The standard addition method is restricted to areas where representative samples containing only humic substances are available, which limits the application of the method mainly to river environments.

Humic substances may be isolated from different waters as described in the Experimental section, and lignin sulfonates are commercially available in an isolated form. Since manufacturing processes differ, there are no standard lignin sulfonates; but for intercalibration purposes, it is possible to use a standard material which can be compared directly with the effluent from a paper mill. The variation in the characteristics of the lignin sulfonates and the ratio of the lignin sulfonates to total solids

must be investigated when an absolute value for the spent sulfite liquor concentration from a specific paper mill is needed.

The characteristics of humic substances may vary from water to water. The problem has been to determine them in absolute units. Kalle[18] defined the emission intensity of humic substances in an arbitrary unit related to quinine sulfate. However, it seems better to relate the fluorescence to standards of lignin sulfonates and humic substances than to quinine sulfate. The apparatus constants of the fluorimeter are dependent on the excitation and emission properties of the standards.

The standard deviation was ± 0.025 p.p.m. at a lignin sulfonate concentration of 0.5 p.p.m., and the detection limit was 0.010 p.p.m. of lignin sulfonates, when the concentration of humic substances was 3 p.p.m.

The concentrations of lignin sulfonates determined in the Hanö Bay agree well with a preliminary box model calculation made by Svansson[19], who predicted a lignin sulfonate concentration of *ca.* 0.45 p.p.m. in the bay, using a value for the output of $15 \cdot 10^6$ kg of lignin sulfonates per year. Dissolved forms of lignin sulfonates are relatively conservative materials and decompose in about 170 days, according to Kalninsh *et al.*[20]. Lignin sulfonates can therefore be used as a tracer in studying water flow patterns. Humic substances determined simultaneously will give additional information.

The authors express their thanks to Professor David Dyrssen for valuable discussions. The valuable help of the Swedish Coast Guard and the Fishery Board of Sweden is gratefully acknowledged. This work was supported by the National Swedish Environment Protection Board and the Swedish Natural Science Research Council. The English has been revised by Mrs Enrica Ratti-Moberg, and Dr. Rodger Dawson.

SUMMARY

A fluorimetric method is described for the determination of lignin sulfonates and humic substances simultaneously in sea water. To express the concentrations in absolute values, dissolved humic substances were isolated from river water and used as a standard along with a lignin sulfonate standard. In the two-component system, measurements at two wavelengths were used to determine the concentrations of lignin sulfonates and humic substances in mixtures, since their fluorescence intensities were found to be additive. The method can be used to detect lignin sulfonates in sea water at concentration levels down to 0.01 p.p.m. when the content of humic substance is 3 p.p.m.

REFERENCES

1 I. Hedlund and K. Wilson, *Sv. Papperstidn.*, 60 (1957) 582.
2 A. Lindberg, *Vattenhygien*, 19 (1963) 106.
3 V. F. Felicetta and J. L. McCarty, *Tappi*, 46 (1963) 337.
4 C. A. Barnes, E. E. Collias, V. F. Felicetta, O. Goldschmid, B. F. Hrutfjord, A. Livingston, J. L. McCarty, G. L. Toombs, M. Waldichuk and R. Estley, *Tappi*, 46 (1963) 347.
5 R. F. Christman and R. A. Minear, *The Trend in Engineering, University of Washington*, 19 (1967) 3.

6 A. D. Thurston, *J. Water Pollut. Contr. Fed.*, 42 (1970) 1551.
7 D. J. Baumgartner, M. H. Feldman and C. L. Gibbons, *Water Res.*, 5 (1971) 533.
8 T. Almgren and B. Josefsson, *Sv. Pappenstidn.*, 76 (1973) 19.
9 R. Hornke and L. Heinisch, *Papier*, 15 (1961) 186.
10 R. J. Morrison, *J. Soil Sci.*, 9 (1958) 130.
11 V. F. Felicetta and J. E. McCarty, *Tappi*, 46 (1963) 351.
12 E. K. Duursma, *Neth. J. Sea Res.*, 1 (1961) 1.
13 K. Kalle, *Oceanogr. Mar. Biol. Ann. Rev.*, 4 (1966) 91.
14 N. K. Höjerslev, *Report no. 16*. University of Copenhagen. Department of Physical Oceanography, 1971.
15 A. Siegel and E. T. Degens, *Science*, 151 (1964) 1098.
16 J. Shapiro, *J. Amer. Water Works Ass.*, 56 (1964) 1062.
17 J. O. Bladh, *Report No. 138*, Institute of Marine Research, Lyjsekil, Sweden, 1972.
18 K. Kalle, *Deut. Hydrogr. Z.*, 16 (1963) 153.
19 A. Svansson, *Fishery Research Board*, Gothenburg, private communication, 1973.
20 A. J. Kalninsh, E. A. Auninsh and R. F. Reizinsh, *Ambio Special Report*, 1 (1972) 23.

Analytica Chimica Acta, 78 (1975) 423–429

SPECTROPHOTOMETRIC DETERMINATION OF RUTHENIUM WITH 3-(2-PYRIDYL)-5,6-DIPHENYL-1,2,4-TRIAZINE

LAL C. KAMRA and GILBERT H. AYRES

Department of Chemistry, The University of Texas at Austin, Austin, Texas 78712 (U.S.A.)

(Received 31st January 1975)

Numerous reagents have been proposed for the spectrophotometric determination of the platinum elements. A recent reference work[1] lists more than thirty spectrophotometric reagents for ruthenium; the various methods differ considerably in sensitivity, selectivity, solution conditions, etc. Work in this laboratory has continued in a search for additional reagents in the hope of finding methods that are more sensitive and/or more selective than existing methods. A report that 3-(2-pyridyl)-5,6-diphenyl-1,2,4-triazine (PDT) could be used as a sensitive reagent for iron and for copper[2,3], and the similarity of this reagent to 2,4,6-tri(2′-pyridyl)-s-triazine (TPTZ) which has been used for the determination of ruthenium[4], suggested the possibility of use of PDT as a chromogenic reagent for some of the platinum elements. Because of the apparent color intensity and stability observed in preliminary tests with ruthenium solutions, this system was studied in detail.

EXPERIMENTAL

Apparatus

Absorbance scanning was done with a Cary Model 14 spectrophotometer. Absorbance measurements at fixed wavelength were made with a Beckman Model DU quartz spectrophotometer, in matched silica cells of 1.00-cm optical path. A Mettler Type M-5 microbalance was used for small-quantity weighing requiring a high degree of accuracy. A Beckman Century SS pH meter, with combination calomel and glass electrode, was used for pH measurements. Volumetric ware used for critical transfers and dilutions was of Class A tolerance.

Reagents

Standard ruthenium solution. Ruthenium(III) chloride hexahydrate (A. D. Mackay, Inc.) was dissolved in 1:20 hydrochloric acid; the filtered solution was diluted to known volume with distilled water. Aliquots of the solution were assayed by evaporation, reduction with hydrogen, and weighing as metal. Concordant results from six aliquots showed the stock solution to contain 794 p.p.m. of ruthenium. To a measured volume of this solution, excess of hydroxyammonium chloride was added and the solution was heated at 50–60°C for several hours, during which time the pH of the solution was progressively increased by addition of small increments of dilute sodium hydroxide until the solution was neutral.

In this way the ruthenium was reduced to the +2 state[5]. The solution was diluted to known volume; solutions of lower concentration were prepared as needed, by dilution with 0.10 *M* hydrochloric acid.

PDT reagent. This chemical (Aldrich Chemical Co., Inc.) was used as received. Reagent solutions in 95% ethanol were prepared at appropriate concentrations, for studying the variables in order to define the recommended procedure, 0.10% (w/v) solution was used.

Buffer. Acetic acid and sodium acetate were used to prepare buffers of total acetate concentration 1 *M*, in the pH range 3.5–6.

Other reagents. Common laboratory reagents were ACS reagent grade. Because PDT is a very sensitive color reagent for iron, very low iron impurity in other reagents is required. (Practical grade hydroxyammonium chloride is unsuitable because of its iron content.) For interference tests, cations were used in the form of nitrates or chlorides, and anions were used in the form of sodium or potassium salts. The other platinum elements were from standard solutions prepared in previous investigations in this laboratory.

Recommended procedure

Into a 10-ml volumetric flask transfer 2.0 ml of ruthenium solution to give a final concentration in the range of about 0.5–3.5 p.p.m. ruthenium (*i.e.*, 5–35 μg). Add 2.0 ml of 0.10% PDT reagent and 1.0 ml of pH 5 buffer; dilute to the mark with distilled water. Support the flask in a water bath at 85°C for 30 min. Cool to room temperature, add water to replace any solvent lost by evaporation, and measure the absorbance at 485 nm against a reagent blank prepared simultaneously with the sample. (For routine measurements a water blank is satisfactory.) The spectral absorption of the system is shown in Fig. 1, curve A. Make analytical measurements at 485 nm.

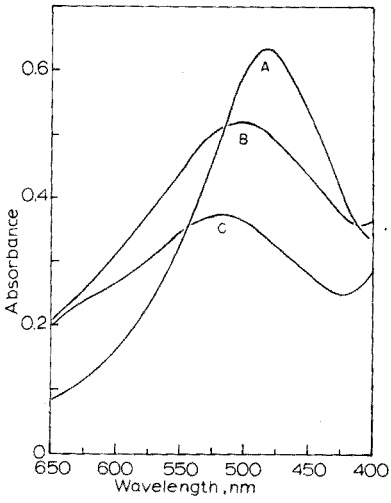

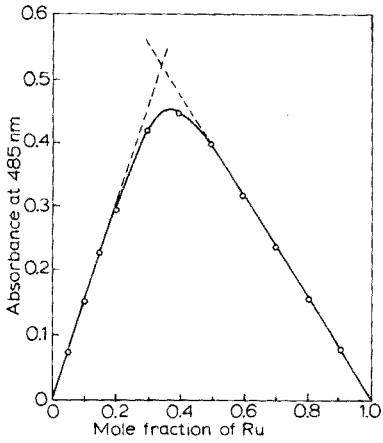

Fig. 1. Spectral curves of Ru–PDT complex; 3.0 p.p.m. of ruthenium. (A) By recommended procedure, 20% ethanol. (B) 40% ethanol. (C) 60% ethanol.

Fig. 2. Continuous variations plot; total concentration of reactants, $1.0 \cdot 10^{-4}$ *M*.

RESULTS

Calibration, range, sensitivity

The ruthenium–PDT system conforms to Beer's law over the range investigated (0.4–3.6 p.p.m., absorbance about 0.08–0.76); the plot of absorbance *versus* concentration is a straight line which passes through the origin. The optimal working range for measurement at 1.00-cm optical path is 0.50–3.4 p.p.m. The specific absorptivity is 0.21 p.p.m.$^{-1}$ cm^{-1}; the molar absorptivity is $2.1 \cdot 10^4$ l mole^{-1} cm^{-1}; the Sandell sensitivity is 0.0048 μg cm^{-2}. Therefore, the method is much more sensitive for ruthenium than many existing methods[1] and is somewhat more sensitive than by the use of TPTZ reagent[4].

Effect of experimental variables

Samples containing a fixed amount (2.0 p.p.m.) of ruthenium were developed and measured by the recommended procedure, except that the amount of reagent was varied. Full color development required 1.0 ml of 0.10% reagent, which is about a 15-fold molar ratio of ligand to metal; larger amounts of reagent had no additional effect on the absorbance. In order to ensure full development of somewhat larger amounts of ruthenium, 2.0 ml of reagent was used in the recommended procedure.

When the pH was varied by addition of sodium hydroxide or hydrochloric acid, maximal absorbance for 2.0 p.p.m. ruthenium occurred with solutions of pH between 4.4 and 5.7; the absorbance decreased rapidly on either side of these limits.

The influence of ethanol (solvent for the reagent) was tested by following the recommended procedure except for the addition of varying amounts of 95% ethanol to the sample solution. Maximal absorbance was produced in solutions containing up to 20% ethanol by volume; this amount of ethanol is contained in the 2.0 ml of reagent solution used. Larger amounts of ethanol caused progressively lower absorbances and a shift of absorption peak toward longer wavelengths (Fig. 1, curves B and C).

Effect of temperature and time; reproducibility

At optimal conditions of other variables, full development of the magenta color was produced by boiling the reaction mixture for 10 min, or by heating at 85°C for 25 min. A standard development time of 30 min at 85°C was adopted. Eleven samples, each containing 2.0 p.p.m. of ruthenium, were prepared by the recommended procedure; the absorbance was measured as soon as the solution had cooled to room temperature. All absorbances were within the range 0.417–0.425 (average, 0.421; standard deviation, 0.002). Measured at intervals of several hours over a period of 5 days, absorbances were constant within experimental error; therefore, no special precautions regarding time stability need to be taken.

Effect of foreign ions

Varying amounts of the foreign ions were taken with 2.0 p.p.m. of ruthenium, and the color was developed in the usual way. The tolerance for a foreign ion was taken as the largest amount that gave an absorbance differing by no more than

TABLE I

EFFECT OF FOREIGN IONS

(Ruthenium concentration, 2.0 p.p.m.)

Foreign ion	*Tolerance (p.p.m.)*	*Tolerance (p.p.m.) with masking agent*		*Foreign ion*	*Tolerance (p.p.m.)*
		Phosphate	*EDTA*		
Rh(III)	18	[a]	[a]	Sodium, potassium,	
Pd(II)	6	[a]	[a]	bromide, iodide,	>2800
Os(IV)	3.5	14	21	nitrate, perchlorate	
Ir(IV)	6	[a]	15	Fluoride	>700
Pt(IV)	6	20	[a]	Sulfate	2000
Cu(II)	0	[a]	4	Phosphate	1200
Ni(II)	2	[a]	8	EDTA	40
Co(II)	14	[a]	[a]	Citrate	4
Fe(II)	0	[a]	1	Tartrate	25
Fe(III)	0	[a]	1		
Au(III)	1	2	4		
Zn(II)	80	150	100		

[a] No increase in tolerance.

0.01 from that produced by ruthenium alone. For some of the interfering ions, increased tolerance was achieved by addition of a masking agent, such as phosphate (1000 p.p.m.) or EDTA (40 p.p.m.). Results of tolerance tests are given in Table I. Because the tolerance for some of the ions is quite small, separation of ruthenium is required when those ions are present.

Separation of ruthenium

Ruthenium may be separated quantitatively from other metal ions in solution by distillation of its tetroxide; although osmium tetroxide is also volatile, osmium is removed by selective oxidation before the distillation. The apparatus and procedure were essentially as given by Embry and Ayres[4]. The sample solution, to which nitric acid had been added, was boiled gently (hood!) to volatilize osmium tetroxide, and then was evaporated to a small volume. The material was transferred to the distillation apparatus, along with 5 ml of sulfuric acid and 2 ml of 70% perchloric acid. The receivers each contained about 10 ml of 6 *M* hydrochloric acid and about 100 mg of hydroxyammonium chloride (to reduce the higher oxidation states of ruthenium). Distillation was carried out over about 20 min, while dry nitrogen was passed through the apparatus until it cooled to room temperature. The combined receiving solutions were evaporated to half the

TABLE II

SEPARATION OF RUTHENIUM BY DISTILLATION

Ru taken (mg)	0.50	1.00	1.50	5.00[a]	5.00[a]
Ru found (mg)	0.48	0.98	1.43	4.90	4.88

[a] Contained also 25 mg of each of the other platinum elements.

original volume, brought to pH 5 by addition of sodium hydroxide, and finally diluted to exactly 50 ml. Aliquots of this solution were measured by the recommended procedure, and the ruthenium concentration was read from a calibration plot. Results of several distillation separation are shown in Table II.

STUDY OF REACTION AND PRODUCT

Method of continuous variations

This method[6,7] was applied with a series of solutions in which the total concentration of reactants (ruthenium + PDT) was kept constant at $2.0 \cdot 10^{-4}$ *M*, but the mole fraction of components was varied. In a plot of absorbance *versus* mole fraction of ruthenium (Fig. 2), extrapolation of the initial and final portions of the curve gave an intersection at 0.33 mole fraction of ruthenium, corresponding to the ratio Ru:PDT = 1:2.

Mole ratio method

This method[8] was applied with a series of solutions containing ruthenium at a fixed concentration of $3.0 \cdot 10^{-5}$ *M*, the concentration of PDT being varied. A plot of absorbance *versus* moles of PDT per mole of ruthenium (Fig. 3) showed a break at a 2:1 ratio of ligand to metal. In another series of solutions the PDT concentration was constant, and the ruthenium concentration was varied. The absorbance *versus* mole ratio plot showed a break at 0.50 mole of ruthenium per mole of PDT, again confirming the reaction stoichiometry Ru:PDT = 1:2.

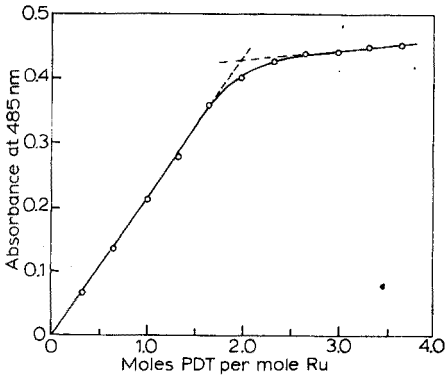

Fig. 3. Mole ratio plot; ruthenium concentration, $3.0 \cdot 10^{-5}$ *M*.

Ion-exchange tests

The complex is positively charged, as shown by its retention on a cation-exchange resin (Bio-Rad AG50W-X12) but not on an anion-exchange resin (Amberlite IRA-400).

Isolation and analysis of the complex

Ruthenium(III) chloride hexahydrate, 0.40 g (about 1.2 mmole), was dissolved in about 75 ml of 0.1 *M* hydrochloric acid, and 7 g of hydroxyammonium chloride was added. The solution was heated and slowly neutralized, as

described in the preparation of the standard solution. PDT (0.80 g; about 2.5 mmole), dissolved in 50 ml of 95% ethanol, was added, and the mixture was heated to boiling for 15 min, forming the colored complex. The solution was evaporated to about half the original volume; addition of an excess of the alkali salt of an appropriate anion caused formation of a brown-black precipitate. After 1 h at room temperature, the precipitate was filtered off, and washed several times with water and then with benzene (in which PDT is soluble but the complex is not), and finally with ether; the solid was air-dried below 60°C. In this way, the perchlorate, iodide, and acetate salts were prepared. The dry solids were purple-black, and soluble in water (containing about 20% ethanol) to give magenta-colored solutions having absorption spectra identical with that represented in Fig. 1, curve A.

Elemental analysis (C, H, N, and Cl by Galbraith Laboratories, Inc.; Ru by the present method) of the perchlorate salt, presumed to be $Ru(C_{20}H_{14}N_4)_2(ClO_4)_2$, were as follows:

	% Ru	% C	% H	% N	% Cl
Calculated	10.98	52.18	3.06	12.17	7.70
Found	9.24	55.04	3.42	14.37	6.76

Although the percentages of C, H, and N found are higher (and therefore of Cl and Ru are lower) than the calculated values, they are closer to the presumed composition than to any hydrate of that salt, or to any other reasonable stoichiometry of Ru:PDT:ClO_4. High values of C, H, and N could be caused by contamination of the compound with other solution components during its isolation, such as by redox products of ruthenium(III) and hydroxyammonium chloride. In the analysis of the iodide salt, the value found for carbon was low, and for iodine the value was high, compared with values calculated for $Ru(C_{20}H_{14}N_4)_2I_2$. Complex salts of this kind are known to be difficult to purify.

From the 6-coordinate property of ruthenium and its 1:2 reaction ratio with PDT, it is apparent that PDT is a tridentate ligand; it is reasonable to assume that coordination occurs by bonding from the pyridyl nitrogen and the two adjacent nitrogen atoms of the triazine.

From spectrophotometric data (Figs. 2 and 3), the provisional formation constant of the $Ru(PDT)_2$ complex is estimated[9] to be of the order of 10^{11}.

It should be noted that solutions of ruthenium(III) treated directly with PDT reagent at pH 5 gave solutions of the same color and same absorption spectrum as ruthenium solutions that had been reduced with hydroxyammonium chloride or with hypophosphite[5]. Apparently the PDT is acting also as a reducing agent toward ruthenium(III) under these experimental conditions.

The authors gratefully acknowledge financial support provided by National Science Foundation grant GP-27347.

SUMMARY

Ruthenium(II) reacts with 3-(2-pyridyl)-5,6-diphenyl-1,2,4-triazine (PDT) in

water–alcohol solution at pH 5 to give a magenta-colored cationic complex having an absorption peak at 485 nm. The color is fully developed by heating at 85°C for 30 min. The system conforms to Beer's law; the optimal concentration range for measurement at 1.00-cm optical path is about 0.5–3.4 p.p.m. of ruthenium. The molar absorptivity is $2.1 \cdot 10^4$ l mole^{-1} cm^{-1}. The effects of reagent concentration, heating temperature and time, pH, and alcohol concentration have been studied. Common anions do not interfere. Separation from interfering cations is effected by distillation and recovery of ruthenium tetroxide. Spectrophotometric methods of continuous variations and of mole ratios, and elemental analysis of solid salts isolated from solution, indicate a ruthenium-to-PDT stoichiometry of 1:2, the PDT acting as a tridentate ligand.

REFERENCES

1 F. E. Beamish and J. C. Van Loon, *Recent Advances in the Analytical Chemistry of the Noble Metals*, Pergamon, Oxford, 1972.
2 A. A. Schilt and P. J. Taylor, *Anal. Chem.*, 42 (1970) 220.
3 C. D. Chriswell and A. A. Schilt, *Anal. Chem.*, 46 (1974) 992.
4 W. A. Embry and G. H. Ayres, *Anal. Chem.*, 40 (1968) 499.
5 G. Ciantelli, P. Legittimo and F. Pantani, *Anal. Chim. Acta*, 53 (1971) 303.
6 P. Job, *Ann. Chim. (Paris)*, 9 (*10*) (1928) 113.
7 W. C. Vosburgh and G. R. Cooper, *J. Amer. Chem. Soc.*, 63 (1941) 437.
8 J. H. Yoe and A. L. Jones, *Ind. Eng. Chem., Anal. Ed.*, 16 (1944) 111.
9 L. Meites and H. C. Thomas, *Advanced Analytical Chemistry*, McGraw–Hill, New York, 1958, p. 294.

Analytica Chimica Acta, 78 (1975) 431–438

THE COLORIMETRIC DETERMINATION OF PHOSPHATES IN WATER AT LOW P.P.M. LEVELS BY AUTOMATIC DISCRETE-SAMPLE ANALYSIS

J. RAMÍREZ-MUÑOZ
Beckman Instruments, Inc., Irvine, California 92664 (U.S.A.)
(Received 26th February 1975)

Colorimetric methods are commonly recommended for the determination of phosphates in water[1,2]. The possibility of converting different forms of phosphorus to orthophosphates allows these methods to be utilized for the determination of all forms of phosphorus in water and wastes. The AMA 40 system (Beckman Automated Materials Analyzer)[3] provides a means of determining phosphorus concentrations in series of 30–36 samples of water or wastes samples in each run with simultaneous measurement of comparison standards and blanks under identical operating conditions.

The present paper describes the use and capabilities of automatic discrete-sample analysis for the colorimetric determination of phosphorus. Two different methods have been tested and adapted; both of these are based on the reduction of the reaction product formed by phosphates (as orthophosphate) and molybdate. Recommended operating conditions are given and series of results are summarized to illustrate the analytical capabilities of the automatic methods.

Selection of method

Most of the recommended colorimetric procedures for the determination of phosphorus are based on the conversion of the original forms of phosphorus to orthophosphate. Polyphosphate ion and some phosphorus-containing organic compounds may be converted to orthophosphates by hydrolysis with sulfuric acid; organic compounds containing phosphorus may be converted by digestion with ammonium persulfate.

Colorimetric methods for orthophosphate are considered as classical methods and can be grouped into three categories: (a) direct complex formation, without reduction, for which probably the best example is the formation of the yellow molybdovanadophosphate complex with maximum absorption at 315 nm in the presence of vanadium(V) and molybdenum(VI)[4,5]; (b) complex formation and reduction to molybdenum blue[6–8], which can be achieved by treatment with reducing ions such as iron(II) or tin(II), with hydrazine[9,10], with hydroquinone[11–13], or with ascorbic acid[14,15], and (c) by extraction of the molybdophosphate complex, *e.g.* with a 20% mixture of 1-butanol in chloroform, and measurement at 310 nm[16]; the extract can also be treated with tin(II), the blue color remaining in the organic phase[17,18].

Very many modifications of these experimental methods have been reported; the reduction of phosphomolybdate complex by tin(II) or ascorbic acid was chosen

for the present work, because these methods are frequently recommended for manual analysis of waters and wastes for phosphorus[1,2].

EXPERIMENTAL

Instrumentation

An AMA 40 System was used. The disruption module was not utilized because only homogeneous liquid samples were examined. A Beckman Model 25 spectrophotometer was used as readout module; the spectrophotometer was used with the standard 1P28 multiplier phototube without the need for installing a red-sensitive multiplier phototube (R-446). Readings were recorded with a Low-Profile Ten-Inch recorder and a teletype (via intercoupler).

Standard, diluents and blanks

A stock solution of 100 p.p.m. phosphorus was prepared by dissolving 0.4393 g of reagent-grade potassium dihydrogenphosphate in deionized–distilled water and diluting to 1 l. The salt was previously dried to constant weight in an oven at 105°C. Working standard solutions were prepared from this stock solution by dilution with deionized–distilled water. A series of 20, 10, 5, 2, 1, 0.5, 0.2, and 0.1 p.p.m. was prepared.

Deionized–distilled water was used as diluent and as blank in all experiments.

Filtering

Samples can be filtered, if necessary, by filter tubes from original samples placed in the T-cups. Filtering should be done before transfer of aliquots by pipetter–diluters. A filter probe should be installed in pedestal position No. 4 and filter tubes should be inserted in the T-cups.

Tin(II) method

Reagents for reagent pumps. A 1.25% (w/v) solution of ammonium molybdate is prepared as follows: add 77.5 ml of reagent-grade concentrated sulfuric acid slowly to 500 ml of water with constant stirring. Allow the solution to cool completely. Dissolve 12.500 g of reagent-grade $(NH_4)_6\ Mo_7O_{24}.4\ H_2O$ in 200 ml of water, and add slowly to the sulfuric acid solution.

For the 0.625% (w/v) solution of tin(II) chloride, dissolve 1.2500 g of reagent-grade $SnCl_2.2\ H_2O$ in 10 ml of reagent-grade concentrated hydrochloric acid by gentle warming and stirring; dilute the solution to 200 ml with water. Do not keep this solution for more than seven days, unless refrigerated.

Operating conditions. These are summarized in Table I. If high-reading blanks are expected, the reference cell can be prepared with a blank solution processed in the same way as the standards and samples. (This solution decays and should be used for only a small number of standards and samples.) The zero suppression control of the spectrophotometer can also be used to bring the blank readings to 0.000 A.U. when water is used in the reference cell.

Analytical setup. The procedure followed is summarized in the analytical setup represented in Fig. 1, which shows the preparation needed for simultaneous analysis in different concentration ranges. For analyses in the range 0–2 p.p.m. P

TABLE I

OPERATING CONDITIONS

Instrumental setup	*Tin(II) method*	*Ascorbic acid method*
Disruption timer[a]	15 s	15 s
Filter probe[b]	Position No. 4	Position No. 4
Pipetter–diluter	Position No. 5 Diluting solution: water Volumes: 2.5 ml + 2.5 ml TC to TT1	Position No. 5 Diluting solution: water Volumes: 2.5 ml + 2.5 ml TC to TT5
Reagent pumps	Position No. 6 Reagent: ammonium molybdate Volume: 1.25 ml. TT1 Position No. 7 Reagent: Tin(II) chloride Volume: 0.5 ml. TT1	Position No. 6 Reagent: special reagent Volume: 0.8 ml. TT5
Mixer	Position No. 8. TT1	Position No. 7. TT5
Sampling probe	Position No. 13. TT1	Position No. 21[c]. TT5
The following conditions are common to both methods: Wavelength, 700 nm. Reference cell, water. Sampling timer, position 4 (5 ml). Slit program, normal. Recorder chart speed, 5 in. min^{-1}. Recorder span setting, 100 mV. Solvent pump, not used. Sample vacuum, 15 in. Model 25 spectrophotometer operation, double beam. Lamp, W. Setting, 1 A.		

[a] Disruptor is not used. Disruption time is set at 15 s to perform each working cycle in 60 s (40 working positions in 48 min).
[b] Not used if samples are not to be filtered.
[c] After incubation at 50°C.

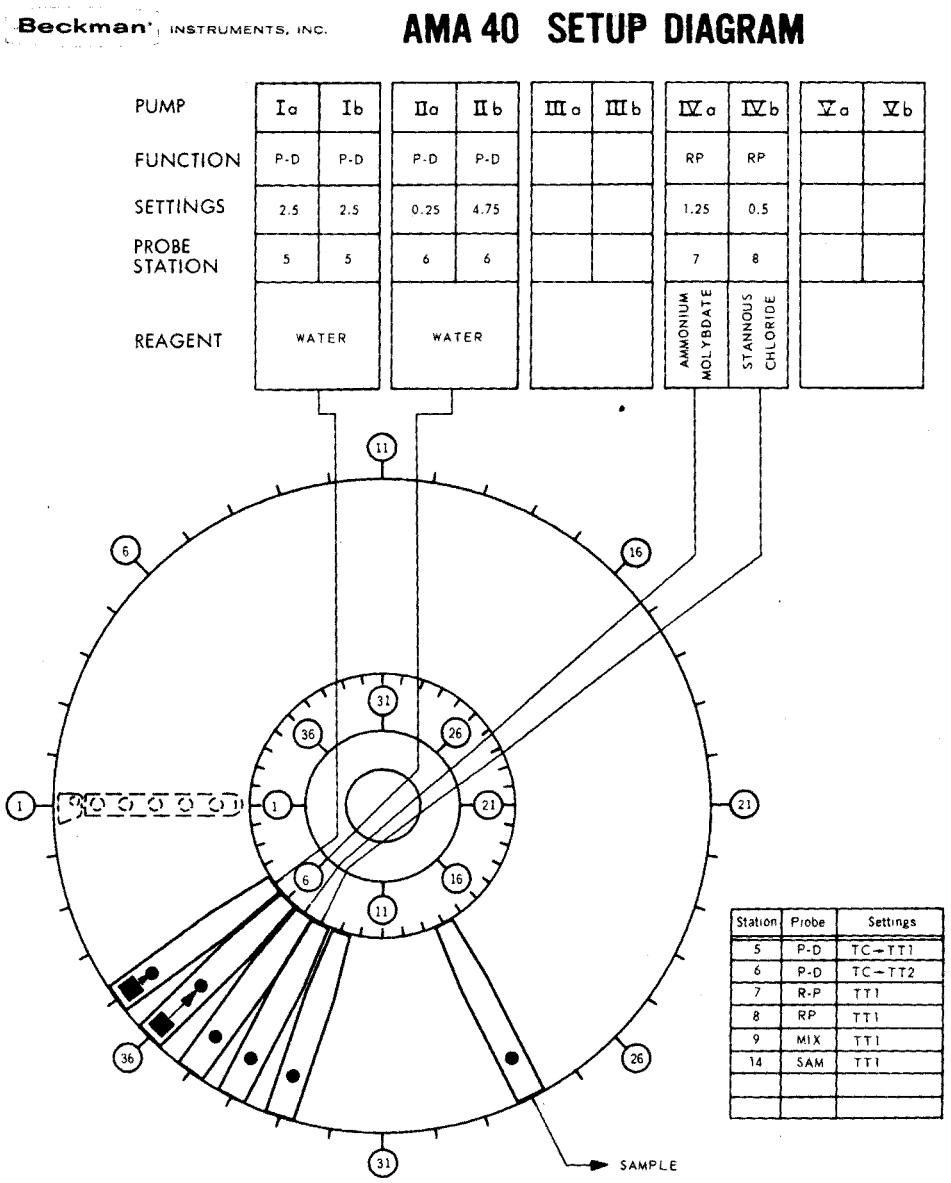

Fig. 1. Instrumental setup for phosphorus by the tin(II) method. Simultaneous automatic preparation for ranges 0–2 p.p.m. and 0–20 p.p.m. P. P-D, pipetter–diluter. RP, reagent pump. Mix, mixer. SAM, sample probe. TC, T-cup. TT, T-tube.

only, pumps IIa and IIb are not used; pump IVa leads to station 6 and pump IVb to station 7; the mixer and sample probe are then used at stations 8 and 13. The standards contain 2, 1, 0.5, 0.2 and 0.1 p.p.m. P. The same setup is used for the range 0–20 p.p.m. P, but with standards of 20, 10, 5, 2, and 1 p.p.m. P; the pipetter–diluter setting is then changed from 2.5+2.5 ml (dilution ratio 1:2) to 0.25+4.75 ml (dilution ratio 1:20).

If the phosphorus concentration of the original sample is less than 0.05 p.p.m. P, the automatic dilution step at station 5 should be eliminated, and for each blank, standard (1.0, 0.5, 0.2, and 0.1 p.p.m. P), and sample, 5.0 ml of solution should be pipetted manually directly into position TT1 of the corresponding T-tube. Then the procedure can be continued automatically.

Alternatively, the pipetter–diluter at station 5 can be used to transfer and dilute the blanks and standards (2.0, 1.0, 0.5, 0.2, and 0.1 p.p.m. P) and then switched off, before the samples are pipetted as above.

The use of undiluted samples increases the relative sensitivity by a factor of two.

The instrument can be used to determine phosphorus in both ranges if two pipetter–diluters are used (Fig. 1). The second pipetter-diluter is used to dilute by transfer (dilution ratio 1:20). Highly diluted samples are thus kept for a second run just in case they show concentrations of phosphorus higher than 2 p.p.m.

Ascorbic acid method

Special reagent. Prepare this reagent freshly by mixing 400 ml of cold 2.5 *M* sulfuric acid, 40 ml of potassium antimonyl tartrate solution, 120 ml of molybdate solution and 240 ml of 0.1 *M* ascorbic acid (USP grade).

For the potassium antimonyl tartrate solution, dissolve 1.3715 g of reagent-grade $K(SbO)C_4H_4O_6.1/2\ H_2O$ in water and dilute to 500 ml; store in a dark flask.

For the ammonium molybdate solution, dissolve 20.000 g of reagent-grade $(NH_4)_6\ Mo_7O_{24},\ H_2O$ in water and dilute to 500 ml; store in a plastic flask.

All the separate components of the mixture are stable if refrigerated.

Operating conditions. These are summarized in Table I. If high-reading blanks are expected, the reference cell can be prepared with a blank solution processed in the same way as the standards and samples.

Analytical setup. Only one reagent is used, so that the procedure is simpler than that shown in Fig. 1. Pumps Ia and Ib lead to station 5 in the same way (the setting being TC→TT5). The only other pump used is IVa, from which the special reagent is added at station 6. The mixer and sampling probe are used as indicated in Table I; incubation at 50°C is done between stations 7 and 21.

This setup is used for samples containing 0–2 p.p.m. P with standards containing 2, 1, 0.5, 0.2 and 0.1 p.p.m. P. The same setup can be used for 0–20 p.p.m. P, with the standards and pipetter–diluter setting described for the tin(II) method.

Low phosphorus concentrations can be treated as described for the tin(II) method.

RESULTS

Repeatability and linearity

The methods were tested for repeatability by readings of the same standard (Table II). The repeatability for water samples with low phosphorus contents is shown in Table III.

Linear and quadratic fits were calculated from standard readings. For the

TABLE II

REPEATABILITY OF ABSORBANCE READINGS OF STANDARDS

Standard (p.p.m.)	*Number of readings*	*Average reading*	*s*	s_r (%)	*Spread*
Tin(II) method					
1	5	0.357	0.0048	1.34	0.011
1	6	0.354	0.0088	2.48	0.023
Ascorbic acid method					
2	5	0.444	0.0040	0.90	0.010
2	6	0.444	0.0037	0.83	0.010

TABLE III

PHOSPHORUS IN WATER SAMPLES BY THE TIN(II) METHOD

Samples	*Average absorbance*[a]	*s*	s_r (%)	*Spread*	*P found (p.p.m.)*
A	0.017_3	0.0015	8.81	0.003	0.05_1
B	0.016_7	0.0006	3.46	0.001	0.04_9
C	0.017_3	0.0006	3.33	0.001	0.05_1

[a] Average of 3 results.

tin(II) method, the slope fit coefficient was 0.033986, and the quadratic fit coefficients were 0.036341 and −0.00014. For the ascorbic acid method, the respective coefficients were 0.02209, 0.02206 and 0.000002.

Measurement of phosphorus in water samples

Three water samples with low phosphorus contents were analyzed in triplicate by the tin(II) method; the results are given in Table III.

Other samples were measured by interpolation with standards processed under the same conditions by both the tin(II) method and the ascorbic acid method. A comparison of some results is presented in Table IV.

DISCUSSION

Final volumes were selected so that more than 5 ml of prepared solution could be removed by suction at the sampling station.

The deionized–distilled water used as diluent and as blanks should be phosphorus-free or contain an extremely low concentration of phosphate; the water used must be carefully tested. Since blanks are treated in the same way as standards and samples, zero correction by means of the suppression control of the instrument is recommended. The tin(II) method normally produces higher blank readings than the ascorbic acid method, but they can easily be zeroed.

The precision observed (Table II) justifies reporting the final results with three significant figures down to 0.100 p.p.m. However, only two significant figures

TABLE IV

COMPARISON OF RESULTS FOR PHOSPHORUS IN WATER SAMPLES

Samples	*Tin(II) method*			*Ascorbic acid method*		
	Average absorbance[a]	s_r (%)	*P found (p.p.m.)*	*Average absorbance*[a]	s_r (%)	*P found (p.p.m.)*
AA	0.141_3	2.86	0.41_7	0.088_0	1.97	0.39_8
BB	0.136_3	2.58	0.40_3	0.088_7	1.30	0.40_2
CC	0.139_3	1.10	0.41_2	0.094_7	2.20	0.42_9

[a] Average of 3 results.

should be used for values from 0.100 p.p.m. to 0.010 p.p.m. The precision observed justifies the use of a single reading for each sample in routine work. One or two blanks and the standards are read at the beginning of each run; 30–36 samples can be examined in each single automatic run.

Linear responses are obtained over the concentration ranges described for measurements at 700 nm. Slightly higher sensitivity can be achieved by operating at 865 nm, but noise conditions make readings at 700 nm preferable; there is then no need to change the normal multiplier phototubes to others of the red-sensitive type.

The ascorbic acid method has some advantages: (a) lower blank readings; (b) a single reagent instead of two, which reduces the time needed to prime and clean reagent pumps; (c) hydrochloric acid solutions are avoided; and (d) better precision is obtained. However, in some respects the tin(II) method is better: (a) no incubation is needed; (b) greater analytical sensitivity is obtained; and (c) the reagents need not be freshly prepared.

The automated system described is suitable for the routine analysis of water samples for phosphates. Low concentration levels may be measured with sufficient accuracy even in the range 0.100–0.010 p.p.m. P. The repeatability found is very good; the relative standard deviation is less than 3%, which is better than the repeatability to be expected in manual analysis of pipetted aliquots and reagent addition under the usual repetitive operating conditions. The reproducibility is also good between different working sessions.

Calibration graphs are linear in the ranges 0–2 and 0–20 p.p.m. P. Experimental setups are very simple to prepare for either of the methods recommended. Finally, readings in multiple sample analysis can be obtained at the rate of 60 per hour.

SUMMARY

Two colorimetric methods based on the formation of molybdenum blue (the tin(II) and ascorbic acid methods) have been adapted for the routine automatic determination of phosphate in water samples. Repeatability and linearity of both methods in discrete-sample automatic analysis are satisfactory. Some water samples

were analyzed by both methods to compare final analytical results. An analytical rate of 60 readings per hour can be obtained.

REFERENCES

1 Environmental Protection Agency, *Methods for Chemical Analysis of Water and Wastes*, Cincinnati, Ohio, 1971, p. 235.
2 American Society for Testing and Materials, *1971 Annual Book of ASTM Standards, Part 23*, Philadelphia, Pa., p. 41.
3 D. G. Rohrbaugh and J. Ramírez-Muñoz, *Anal. Chim. Acta*, 71 (1974) 311.
4 R. E. Kitson and M. G. Mellon, *Ind. Eng. Chem., Anal. Ed.*, 16 (1944) 379.
5 K. P. Quinlan and M. A. Desesa, *Anal. Chem.*, 27 (1955) 1626.
6 M. Rockstein and P. W. Herron, *Anal. Chem.*, 23 (1951) 1500.
7 M. Zimmermann, *Angew. Chem.*, 62 (1950) 291.
8 M. Jean, *Anal. Chim. Acta*, 14 (1956) 172.
9 D. F. Boltz and M. G. Mellon, *Anal. Chem.*, 19 (1947) 873.
10 M. Macheboeuf and J. Delsal, *Bull. Soc. Chim. Biol.*, 25 (1943) 116.
11 R. E. Kitson and M. G. Mellon, *Ind. Eng. Chem., Anal. Ed.*, 16 (1944) 466.
12 N. S. Ging and J. M. Sturtevant, *J. Amer. Chem. Soc.*, 76 (1954) 2087.
13 N. S. Ging, *Anal. Chem.*, 28 (1956) 1330.
14 P. S. Chen, Jr., T. Y. Toribara and H. Warner, *Anal. Chem.*, 28 (1956) 1756.
15 D. N. Fogg and N. T. Wilkinson, *Analyst (London)*, 83 (1958) 406.
16 C. Wadelin and M. G. Mellon, *Anal. Chem.*, 25 (1953) 1668.
17 W. A. Pons, Jr. and J. D. Guthrie, *Ind. Eng. Chem., Anal. Ed.*, 18 (1946) 184.
18 F. L. Schaffer, J. Fong and P. Kirk, *Anal. Chem.*, 25 (1953) 343.

Analytica Chimica Acta, 78 (1975) 439–450

THE NON-AQUEOUS REACTIONS OF SOME 1,4-BENZODIAZEPINES

ROBERT B. HAGEL and EILEEN M. DEBESIS

Quality Control Department, Hoffmann-La Roche Inc., Nutley, New Jersey 07110 (U.S.A.)

(Received 20th January 1975)

The literature describes adequately the syntheses and pharmacological properties of numerous 1,4-benzodiazepines. However, the amount of data available regarding the analytical chemistry of these compounds, especially their behavior during non-aqueous titrations, is limited. In order to discuss effectively the reactions of these compounds as acids or bases, some knowledge of the structures of the various species present in solution during a titration is required.

The question of the reactions of 3-hydroxy-1,4-benzodiazepin-2-ones during the course of non-aqueous titrations arose while this laboratory was seeking to develop a suitable assay for lorazepam*. An acceptable procedure for most 1,4-benzodiazepines is titration with 0.1 *M* perchloric acid in glacial acetic acid; however, attempts to titrate lorazepam using this system resulted in broad, poorly defined potential breaks at the equivalence point. The addition of acetic anhydride to the system sharpened the potential breaks, but led to consistently low assay results when compared with other analytical data. Because lorazepam is similar structurally to oxazepam, the standard method of analysis for oxazepam *i.e.* titration as an acid with tetrabutylammonium hydroxide (TBAH)[1], was applied to lorazepam. The object of this investigation was to determine the exact nature of the reaction of lorazepam with TBAH.

Several authors have described possible reactions for 1,4-benzodiazepin-2-ones in solution. Bogat-Skii and Andronati[2] proposed the pH-dependent structures shown in eqn. (1),

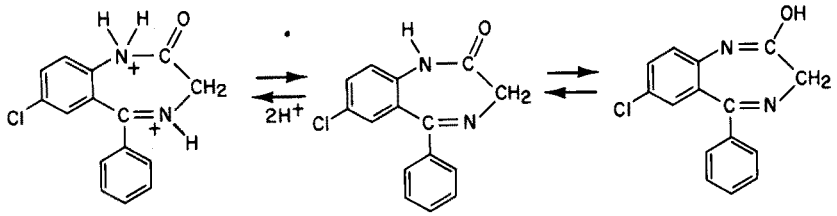

(1)

and suggested on the basis of spectral evidence that the enol form predominates in basic solution.

Andronati *et al.*[3] later proposed the different enolic form shown in eqn. (2) and two possible conversions of the lactam in an alkaline medium; these involve a lactam–enol tautomerism and a lactam–lactim tautomerism. A combination of

* For the chemical names and structures of all the compounds referred to in this report, see Table I.

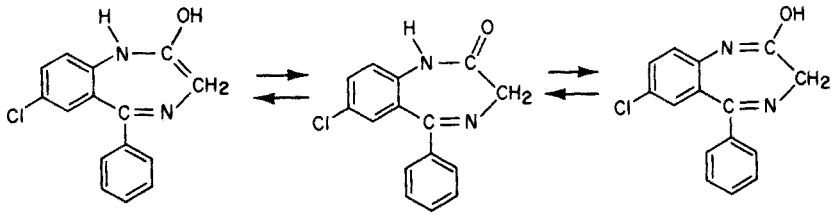

(2)

structural and spectral data leads the present authors to suggest that, of these, only the lactam–lactim tautomerism occurs.

Davidson and Smyth studied[4] the behavior of several benzodiazepines at various pH values and concluded, from u.v. spectral measurements, that diazepam, nitrazepam, medazepam, oxazepam, lorazepam, and chlordiazepoxide all exhibited protonation reactions in an acidic medium, but only nitrazepam, oxazepam, and lorazepam exhibited deprotonation under basic conditions. The common structural feature of nitrazepam, oxazepam, and lorazepam is a proton at the N_1 position.

More recently, Barrett *et al.* have studied[5] 3-hydroxy-1,4-benzodiazepin-2-ones. On the basis of u.v. spectrophotometric measurements of the characteristic red shift of the $\pi^* \leftarrow \pi$ band of the phenyl ring resulting from deprotonation at some adjacent site, they concluded that the pH-dependent solution species can be described by eqn. (3), where R = H, Cl, etc.

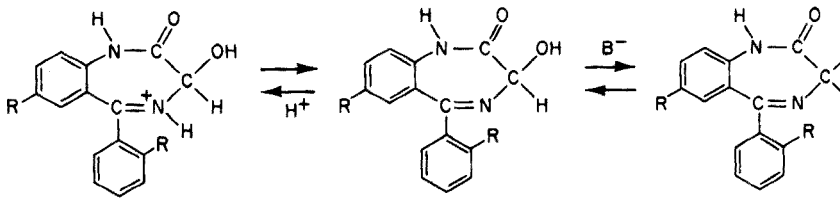

(3)

In eqn. (3) two equilibrium reactions are described for benzodiazepines with

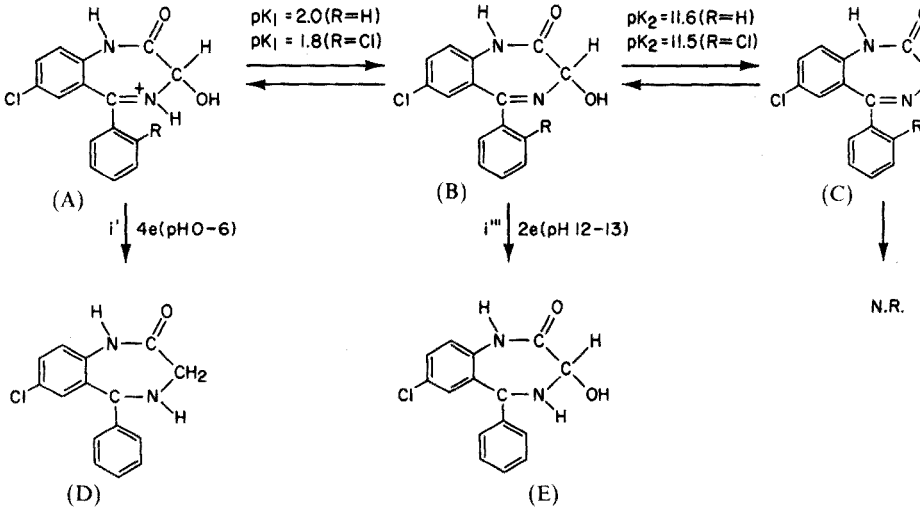

(4)

the oxazepam structure. The first is well known, and involves protonation at the N_4 position with a pK_a value of 1–2 depending on adjacent substitution. The second reaction is described by Barrett *et al.*[5] as the deprotonation ($pK_a \sim 11$–12) of the 3-hydroxy group.

In support of this theory, Goldsmith *et al.*[6] have studied the polarographic behavior of both oxazepam and lorazepam over a very wide pH range (0–14) and propose several polarographic reactions (scheme 4)
in order to explain their experimental observation of two different reductions. Furthermore, they were unable to observe a reduction for species (C).

Because of the weakly acidic nature of alcohols, a careful consideration of the structures involved led to the suspicion that deprotonation might not occur at the 3-hydroxy oxygen but rather at the N_1 nitrogen, leading to compounds F or G (eqn. (5)) rather than C, as proposed by Barrett *et al.*[5].

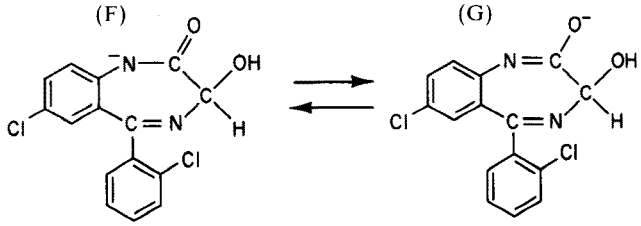

(5)

Since it is not conclusive enough to determine the exact nature of the reaction, the spectroscopic evidence has been combined with titrimetric analyses of a series of substituted 1,4-benzodiazepines. By proper choice of substitution at the 1, 2, and 3 positions, it should be possible to determine both the site of deprotonation and, to a limited extent, the effect of a substitution at the 3 position on the titration of 1,4-benzodiazepines as both acids and bases.

EXPERIMENTAL

Chemicals and reagents

The benzodiazepines were prepared by standard synthetic methods by the Organic Chemical Research Division, Roche Labs., Inc. Purity criteria and structural determinations for these compounds include acceptable u.v. and visible spectra, mass spectrometry, n.m.r., t.l.c. and titrimetric assay procedures. All other chemicals were ACS reagent grade or the equivalent. Spectral quality solvents were used to prepare all solutions.

Non-aqueous titrimetry

Samples (*ca.* 300 mg) of each benzodiazepine dissolved in glacial acetid acid, dimethyl formamide, or acetonitrile, were titrated with 0.1 *M* perchloric acid in glacial acetic acid or with 0.1 *M* TBAH in 10% methanol in benzene.

The titrations were performed with an automatic recording Metrohm Potentiograph Model E436 equipped with a combination glass electrode with an internal calomel reference.

Ultraviolet absorbance measurements

Solutions (*ca.* 5 mg l^{-1}) of lorazepam and Ro 5-3027 were prepared in 0.1 *M* HCl, 0.1 *M* NaOH, distilled water (pH 5.6), and acetonitrile, and the u.v. absorbance was measured with a Cary Model 14 recording spectrophotometer.

Lorazepam (30 mg) was weighed into a 100-ml volumetric flask and diluted to volume with acetonitrile. Portions (10 ml) of this solution were transferred to each of five 100-ml volumetric flasks; 10 ml of acetonitrile was pipetted into each of five additional 100-ml flasks to serve as references. To each of the sample and reference flasks was added 0.1, 0.3, 0.5, 0.7 and 0.9 ml, respectively, of 0.11 *M* TBAH. Each sample then was diluted to volume with methanol, and the u.v. spectra were measured in the 400–280 nm range *versus* the corresponding reference. Samples and references were diluted 20-fold with methanol; the spectra were then measured from 280–220 nm.

pK_a Determinations

A number of pK_a values, not available in the literature, were determined spectrophotometrically by the techniques described by Albert and Serjeant[7].

RESULTS AND DISCUSSION

In order to determine the site of deprotonation of lorazepam, a series of 1,4-benzodiazepines, described in Table I, were analyzed as both acids and bases by two non-aqueous titrimetric methods. The titrants of choice were perchloric acid and tetrabutylammonium hydroxide. The criteria for acceptability of the resulting titration curves were a measurable potential break, and assay results which were quantitative for standard samples.

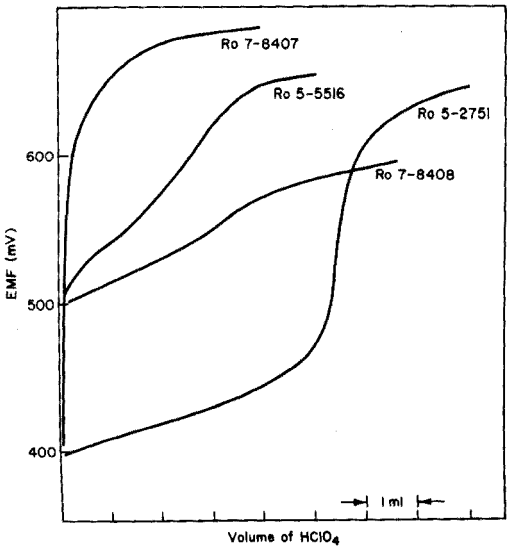

Fig. 1. The equivalence points of the potentiometric titrations of several 1,4-benzodiazepines with 0.1 *M* perchloric acid in glacial acetic acid. For a description of the compounds see Table 1.

TABLE I

STRUCTURES AND PROPERTIES OF 1,4-BENZODIAZEPINES

Sample identification/name	*Structure*	pK_1	pK_2	*Titration with*	
				$HClO_4$	*TBAH*
Ro 7-8408 Lorazepam 7-chloro-5-(2-chlorophenyl)-1,3-diphydro-2H-1,4-benzodiazepin-2-one	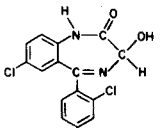	1.3	11.5	No	Yes
Ro 5-6789 Oxazepam 7-chloro-5-phenyl-1,3-dihydro-2H-1,4-benzodiazepin-2-one	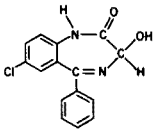	1.7	11.3	No	Yes
Ro 5-5516 7-chloro-5-(2-chlorophenyl)-3-hydroxy-1,3-dihydro-1-methyl-2H-1,4-benzodiazepin-2-one	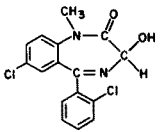	0.5	—	No	No
Ro 5-3027 7-chloro-5-(2-chlorophenyl)-1,3-dihydro-2H-1,4-benzodiazepin-2-one	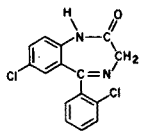	2.15	11.7	Yes	Yes
Ro 20-3715 7-chloro-2-hydroxy-1-methyl 5-phenyl-2,3-dihydro-1H-1,4-benzodiazepine	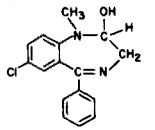	5.69	—	Yes	No
Ro 5-2751 7-chloro-5-(2-chlorophenyl)-1,3-dihydro-3-methyl-2H-1,4-benzodiazepin-2-one	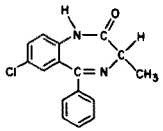	2.97	11.7	Yes	Yes
Ro 5-3367 7-chloro-5-(2-fluorophenyl)-1,3-dihydro-2H-1,4-benzodiazepin-2-one	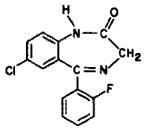	2.57	11.8	Yes	Yes
Ro 7-8407 7-chloro-5-(2-chlorophenyl)-1,3-dihydro-3-acetoxy-2H-1,4-benzodiazpin-2-one	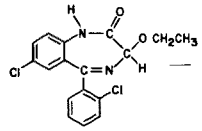	—	10.1	No	Yes

TABLE I

STRUCTURES AND PROPERTIES OF 1,4-BENZODIAZEPINES

Sample identification/name	*Structure*	pK_1	pK_2	*Titration with*		*Sample identification/name*	*Structure*	pK_1	pK_2	*Titration with*	
				$HClO_4$	*TBAH*					$HClO_4$	*TBAH*
Ro 5-5345						Ro 5-2807					
Tenazepan	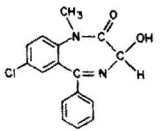	1.60	—	—	No	Diazepam	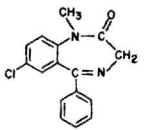				
7-chloro-1,3-dihydro-3-hydroxy-1-methyl-5-phenyl-2H-1,4-benzodiazepin-2-one						7-chloro-1,3-dihydro-1-methyl-5-phenyl-2H-1,4-benzodiazepin-2-one		3.7	—	Yes	No
Ro 97-1274	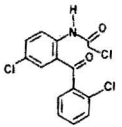										
2-(2-chloroacetamido)-2′,5-dichlorbenzophenone		—	11.2	—	Yes						

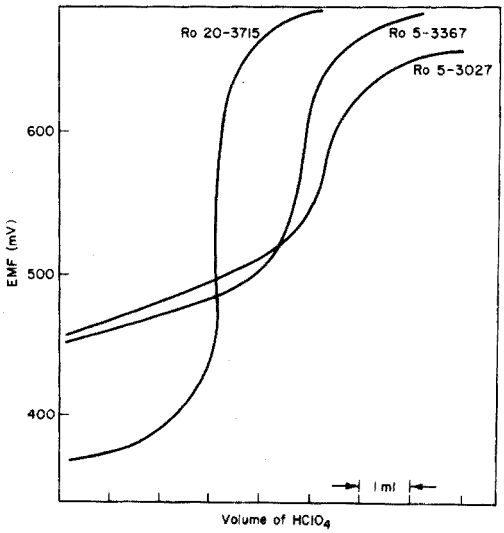

Fig. 2. The equivalence points of the potentiometric titrations of several 1,4-benzodiazepines with 0.1 *M* perchloric acid in glacial acetic acid. For a description of the compounds see Table I.

Titration with perchloric acid in glacial acetic acid

Figures 1 and 2 contain a series of curves derived from the potentiometric titration of several 1,4-benzodiazepines with 0.1 *M* perchloric acid in glacial acetic acid. The structures of the compounds titrated and p*K* values (where available) for some of the compounds are given in Table I, which also indicates whether they could be titrated as acids or bases with the systems selected for investigation.

The 3-hydroxy compounds, lorazepam, oxazepam (not shown), and Ro 5-5516, and the 3-acetoxy derivative, Ro 7-8407, all behave similarly when titrated as bases. The reaction is the protonation of the N_4 nitrogen, with an approximate pK_a value of 1–2 depending on adjacent substitution. The potentiometric and visual end-points are poorly defined for these compounds and are characteristic of extremely weak bases. These curves would not be suitable for the purpose of equivalence point definition. In contrast, compounds which do not have a 3-hydroxy substituent, *viz.* Ro 5-3027, Ro 20-3715, Ro 5-2751 and Ro 5-3367, exhibit useful breaks at their equivalence points.

There are several factors which might influence protonation at the 4-position. These are: (a) the possible leveling effect of an alcohol (via the 3-hydroxy group) in solution; (b) the inductive effect of an alcohol substituted at various positions of the diazepine ring; (c) the steric effect of a substituent at the 3-position.

To determine the effect of an alcoholic group in solution, several experiments were carried out. Benzyl or amyl alcohol was added separately, in equivalent quantities, to different samples of Ro 5-3367. The perchloric acid titrations of these samples, presented in Fig. 3 along with an untreated sample, are normal and, allowing for differences in sample weights, show a similar potential break. The addition of alcohol at low concentrations does not seem to exert any leveling effect

toward perchloric acid in the system under study. Furthermore, the 2-hydroxy compound (Ro 20-3715) also exhibits a sharp equivalence point, indicating little electronic influence by a hydroxyl group removed by more than one ring position.

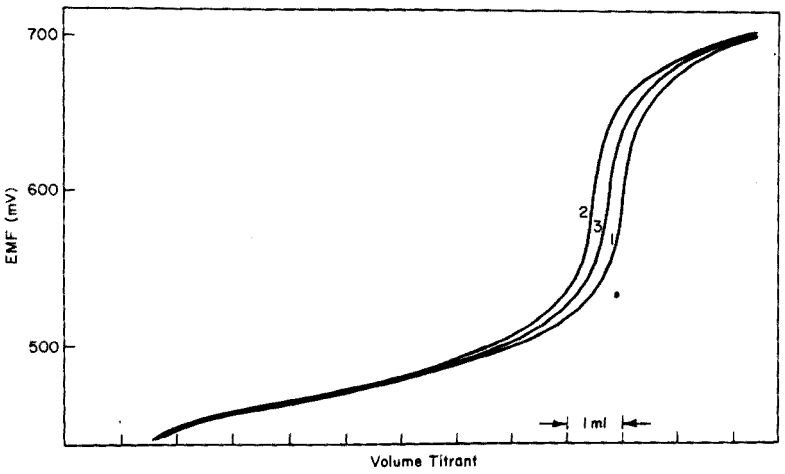

Fig. 3. The non-aqueous titration of Ro 5-3367 with 0.1 *M* perchloric acid in glacial acetic acid. (1) Without additive. (2) Plus 0.1 ml of amyl alcohol. (3) +0.1 ml of benzyl alcohol.

Minor steric hindrance was also ruled out by the successful titration of the 3-methyl derivative, Ro 5-2751; the curve, shown in Fig. 1, breaks sharply at the equivalence point.

Apparently hydroxy or acetoxy substitution at the 3-position exerts a strong electronic effect on the protonation of the N_4 nitrogen, possibly by decreasing the electron density at the position inductively thus decreasing the basicity at that position.

Titration with tetrabutylammonium hydroxide

The primary interest of this work was to study the reaction of lorazepam with TBAH. In order to determine the nature of the reaction of 3-hydroxy-1,4-benzodiazepines with TBAH, and hence locate the site of deprotonation in basic solution, a series of compounds with preferentially blocked positions was selected for analysis. (If the reactions described in eqns. (2) and (3), are considered, the compound of primary interest, lorazepam, is seen to contain hydrogens at both the N_1 and the 3-hydroxy positions.)

Figures 4 and 5 contain a series of typical curves illustrating the potentiometric titration of several 1,4-benzodiazepines with 0.11 *M* TBAH. (Curves for oxazepam and Ro 20-3715 are not included but reference to Table I indicates the nature of their behavior.) The first compounds to be considered are Ro 5-5516, Ro 20-3715, diazepam, and Ro 5-5345. In these molecules a methyl group replaces the proton at the N_1 position; none of them exhibits a useful potential break although they may or may not be 3-hydroxy substituted.

Ro 20-3715 also eliminates the possibility of the direct titration of a ring alcohol, since the 2-hydroxy group did not react with TBAH.

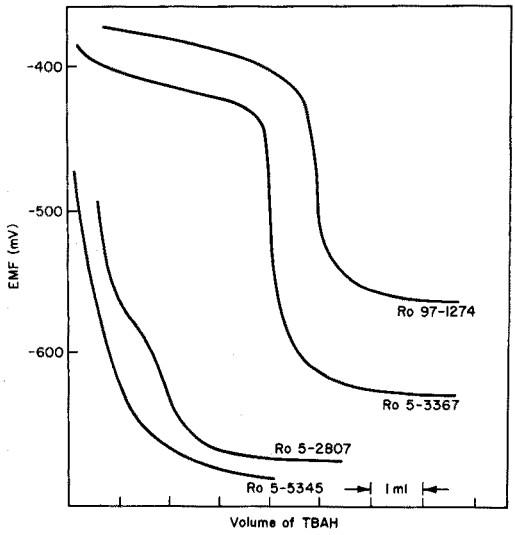

Fig. 4. The equivalence points of the potentiometric titrations of several 1,4-benzodiazepines with 0.11 *M* tetrabutylammonium hydroxide in methanol–benzene. For a description of the compounds see Table I.

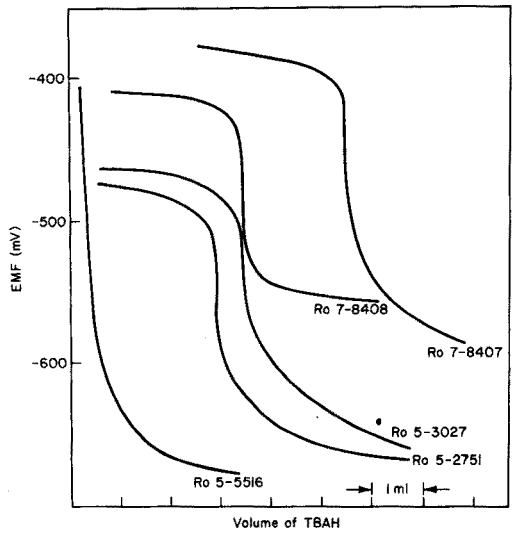

Fig. 5. The equivalence points of the potentiometric titrations of several 1,4-benzodiazepines with 0.11 *M* tetrabutylammonium hydroxide in methanol–benzene. For a description of the compounds see Table I.

The second group of compounds to be considered in Table I are lorazepam, oxazepam, Ro 5-3027, Ro 5-2751, Ro 5-3367, and Ro 7-8407, which are characterized by a proton at the N_1 position and may or may not be 3-substituted. Figures 4 and 5 show that these compounds exhibit useful potential breaks at their equivalence points. From the structures of this series it is concluded that the presence (lorazepam, oxazepam) or absence (Ro 5-3027, Ro 5-2751, Ro 5-3367), or blockage of the 3-hydroxy group (Ro 7-8407) does not affect seriously the acidity of the compound. Furthermore, comparison of the pK_a values for lorazepam and Ro

5-3027 (11.5 *vs.* 11.7) indicates minor effects on the acidity arising from 3-hydroxy substitution. In addition to the benzodiazepines described above a substituted benzophenone, Ro 97-1274; was also titrated with TBAH; its curve, which appears in Fig. 4, shows a sharp break that should be useful analytically. Here, again, the absence of a hydroxyl group adjacent to the carbonyl does not hinder the titration of the amido-nitrogen. (The pK_a of this compound was determined spectrophotometrically to be 11.2, a value similar to that for benzodiazepines of similar structure.)

U.v. spectrometry

Further evidence for deprotonation at the nitrogen in the 1-position is suggested by a comparison of the u.v. spectra of lorazepam and Ro 5-3027, which differ structurally in terms of the 3-hydroxy substituent. The spectra are almost identical in neutral and basic media but differ in acid (see Table II). This would be expected from the strong similarity in structures of lorazepam and Ro 5-3027 assuming that similar mechanisms for deprotonation act for both compounds. The pK_2 values of these compounds are also very close (11.5 *vs.* 11.7) indicating that the same reaction is taking place during deprotonation.

TABLE II

SPECTRAL CHARACTERISTICS OF Ro 7-8408 AND Ro 5-3027

Compound	*Solvent*	λ_{max} *(nm)*
Ro 7-8408	0.1 *M* HCl	370, 320, 285 (sh), 230
($pK_1 = 1.3$,	0.1 *M* NaOH	340, 275 (sh), 232
$pK_2 = 11.5$)	Water	316, 254 (sh), 230
	Phosphate buffer pH 6.0	315, 254 (sh), 229,
	Acetonitrile	316, 254 (sh), 226
Ro 5-3027	0.1 *M* HCl	370, 286 (sh), 240
($pK_1 = 2.15$	0.1 *M* NaOH	342, 276 (sh), 228
$pK_2 = 11.7$)	Water	315, 255 (sh), 230
	Acetonitrile	316, 254 (sh), 224

Differences observed in the values of pK_1 for lorazepam and Ro 5-3027 (1.3 *vs.* 2.15) and the u.v. spectra in acidic media (maxima at 232, 310 (shoulder) and 368 nm *vs.* 240, 286, and 368 nm) can be ascribed to the strong influence of the hydroxyl group at position-3 on the protonation of the nitrogen in the 4-position in lorazepam and its ultimate influence on the $\pi^* \leftarrow \pi$ phenyl ring transition.

Closer scrutiny of the u.v. spectra in acid, base, neutral and acetonitrile solutions, and of the u.v. spectra of partially titrated samples of lorazepam, also leads to some observations regarding its behavior during titration.

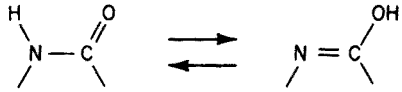

(6)

In basic solution, the tautomerism represented in eqn. (6) has been postulated[3] by Andronati *et al.* on the basis of u.v. measurements.

TABLE III

ABSORPTIVITY VALUES DURING TITRATION OF LORAZEPAM WITH TBAH AT SEVERAL U.V. MAXIMA

Sample number	*% Titrated*	*(Shoulder) 365 nm*	*(Peak) 317 nm*	*(Shoulder) 255 nm*	*(Peak) 230 nm*
1	1	0	3.14	18.1	57.4
2	34	0.02	3.13	18.1	57.4
3	57	0.10	3.08	18.8	57.8
4	80	0.17	3.02	18.8	57.8
5	103	0.25	2.99	18.8	57.8

Table II presents similar measurements for the u.v. spectra of lorazepam; the spectra of neutral (pH 6) and non-aqueous (acetonitrile) solutions are identical. It appears that the same molecular form is present in the non-aqueous solvent as in an essentially neutral medium. To determine the nature of the species of lorazepam present in solution during the course of a non-aqueous titration, a series of partially titrated samples was prepared. Table III contains a set of absorptivity values measured for lorazepam *versus* the percent of titration, at several u.v. maxima. During the titration the intensities of the maxima did not change significantly with pH, except for the appearance of a weak band at about 365 nm associated with the formation of some ionic species in solution. Because of the relative insensitivity of the u.v. spectrum toward the reaction of lorazepam with a base, the postulated tautomerism may not occur to any great extent.

SUMMARY

The data presented for the behavior of 3-hydroxy-1,4-benzodiazepines during non-aqueous titrations indicate that: (a) the first stage protonation during titration as a base with perchloric acid occurs at the N−4 position and is relatively unaffected by substitution at the 3-position, except when the substituent is electron-withdrawing; (b) deprotonation during titration as an acid with tetrabutylammonium hydroxide occurs at the N-1 position rather than at the 3-OH substituent; (c) the similarity of the u.v. spectra of neutral and basic solutions of lorazepam indicate that a tautomerism in basic solution postulated previously does not occur to any great extent; and (d) titration with tetrabutylammonium hydroxide should be acceptable as an assay method for lorazepam.

REFERENCES

1 *National Formulary XIII*, 1970, p. 501.
2 A. V. Bogat-Skii and S. V. Andronati, *J. Gen. Chem. USSR*, 39 (1969) 416.

3 S. A. Andronati *et al.*, *J. Gen. Chem. U.S.S.R.*, 40 (1970) 1862.
4 I. E. Davidson and W. F. Smyth, *Proc. Soc. Anal. Chem.*, 9 (1972) 209.
5 J. Barrett, W. F. Smyth and I. E. Davidson, *J. Pharm. Pharmacol.*, 25 (1973) 387.
6 J. A. Goldsmith, H. A. Jenkins, J. Grant and W. F. Smyth, *Anal. Chim. Acta*, 66 (1973) 427.
7 A. Albert and E. P. Serjeant, *The Determination of Ionization Constants*, Chapman and Hall, London, 1971.

Analytica Chimica Acta, 78 (1975) 451–457

BINDING STUDIES ON SUBSTITUTED BENZOIC ACIDS

PART I. 3,5-DINITROSALICYLIC ACID—ACID DISSOCIATION AND COMPLEXATION WITH NICKEL(II) AND COBALT(II)

PHALGUNI CHAUDHURI

Institut für Anorganische Chemie der Universität Basel (Switzerland)

ROGER S. TAYLOR

Department of Inorganic and Structural Chemistry, The University, Leeds (England)

(Received 20th February 1975)

Although the binding of 3,5-dinitrosalicylic acid (DNSA) to several metal ions including Fe(III)[1], U(VI)[2,3], V(IV)[4], Mg(II)[5], Co(II)[6], Ni(II)[6], Al(III)[7], Ga(III)[7] and In(III)[7], has been investigated, the potential of DNSA as a colorimetric indicator does not seem to have been exploited. Acid dissociation constants have in some cases been determined spectrophotometrically but such techniques have only been applied to metal ion binding for the Group IIIa metals[7] and for magnesium[5]; it has been suggested that DNSA could find application as an indicator of magnesium-ion concentration in interactions with biochemically important molecules such as nucleic acids. The kinetics of binding of the related ligand 5-nitrosalicylic acid (NSA) to a series of complexes of magnesium[8] and nickel[9] has been studied by the spectrophotometric T-jump technique to elucidate the mechanism of ternary complex formation with these metals.

The present study, undertaken to find if DNSA functions as an indicator for nickel(II) and cobalt(II), is part of an investigation into aromatic substituent effects on metal-ion coordination.

EXPERIMENTAL

Reagents

The chemicals used were of the highest purity available; DNSA, recrystallized twice from water, was standardized against 0.1 *M* sodium hydroxide. Solutions of pH 5–7 contained 10^{-2} *M* dimethylarsinate buffer.

Apparatus

A Polymetron 42 D pH-meter, fitted with a Metrohm EA 152 combined electrode, and calibrated with Merck standard buffer solutions was used. U.v.-visible absorption measurements were made with Beckman DK2a and Acta III, and Carey 118 spectrophotometers.

Techniques.

All measurements were made at 25.0°C and 0.1 *M* ionic strength made up

with sodium perchlorate, except where otherwise stated. Measurements of pH were made on solutions flushed with nitrogen to remove dissolved carbon dioxide and pH was adjusted to the required value by dropwise addition of 0.1 *M* sodium hydroxide or 0.1 *M* perchloric acid.

RESULTS AND DISCUSSION

Acid dissociation constants

The protolytic equilibria for DNSA (H_2L) can be expressed as:

$$H_2L \rightleftharpoons HL^- + H^+; K_1 \quad (1)$$

$$HL^- \rightleftharpoons L^- + H^+; K_2 \quad (2)$$

Spectrophotometric measurements in the range 300–400 nm showed that formation of H_2L was not extensive in 0.1 *M* perchloric acid; this is not consistent with some reported values of pK_1. To estimate pK_1 at 0.1 *M* ionic strength, the molar absorptivity for H_2L was determined. Spectrophotometric data for the formation of H_2L at various wavelengths in the range 300–380 nm at 1.0 *M* ($NaClO_4$), were analysed by a Benesi–Hildebrand[10] treatment according to eqn. (3):

$$\frac{1}{\varepsilon_{HL} - \varepsilon_{obs}} = \frac{1}{\varepsilon_{HL} - \varepsilon_{H_2L}} + \frac{1}{\varepsilon_{HL} - \varepsilon_{H_2L}} \cdot \frac{K_1}{[H^+]} \quad (3)$$

where ε_{obs} represents the absorptivity at a particular analytical hydrogen ion concentration, $[H^+]$, and ε_{HL} is the absorptivity for the species HL^-. A linear least-squares fit of data[11], as in eqn. (3), weighted $(\varepsilon_{HL} - \varepsilon_{obs})^2$, yielded $pK_1 = 0.27 \pm 0.02$ and a value for ε_{H_2L}. Applying this value to measurements at 0.1 *M* ionic strength gives:

$$K_1 = \frac{\varepsilon_{obs} - \varepsilon_{H_2L}}{\varepsilon_{HL} - \varepsilon_{obs}} \cdot [H^+] \quad (4)$$

The value $pK_1 = 0.25 \pm 0.02$ was found. The determination of pK_2 was carried out by spectrophotometric titration of DNSA with 0.1 *M* sodium hydroxide between pH 4 and 9 (Fig. 1). A least-squares fit of the absorbance data was made according to:

$$\log_{10}\left(\frac{\varepsilon_{obs} - \varepsilon_{HL}}{\varepsilon_L - \varepsilon_{obs}}\right) = n(pH) - pK_2 \quad (5)$$

where ε_L is the molar absorptivity for L^{2-}, and pH was read directly from the meter. This gave $pK_2 = 7.20$ and $n = 0.99 \pm 0.02$, in good agreement with the expected value of $n = 1$. Spectra for L^{2-}, HL^- and H_2L species are shown in Fig. 2, and maxima and minima in the range 250–500 nm are given in Table I.

Metal-binding constants

The equilibria which may be important (charges omitted) are:

$$M + L \rightleftharpoons ML; K_{ML} \quad (6)$$

$$M + HL \rightleftharpoons MHL; K_{MHL} \quad (7)$$

At any pH in the range 3–7, the apparent binding constant, *K*, can be defined as

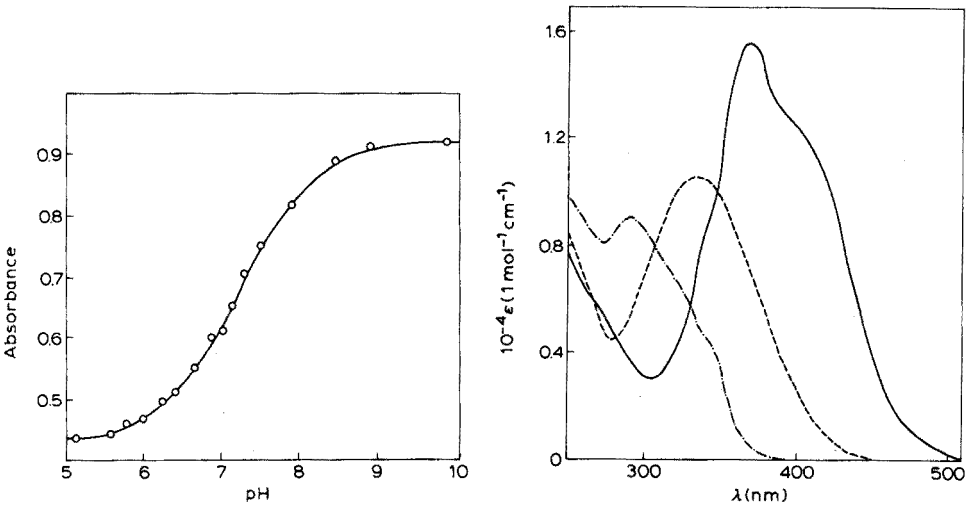

Fig. 1. The dependence of absorbance at 370 nm on pH for the titration of HL^- with 0.1 *M* sodium hydroxide, $T = 25°C$, $I = 0.1$ *M* sodium perchlorate, $[DNSA] = 6.0 \times 10^{-5}$ *M*.

Fig. 2. Spectra of different protonated forms of DNSA; H_2L (·—·—·), HL^- (– – – –), L^{2-} (——).

TABLE 1

SPECTRAL DETAILS OF DNSA SPECIES AND THE NICKEL AND COBALT COMPLEXES

Species	λ_{max} (ε) nm (l mol^{-1} cm^{-1})	λ_{min} (ε) nm (l mol^{-1} cm^{-1})
L^{2-}	369 (15500)	304 (3000)
HL^-	334 (10500)	278 (4400)
H_2L	290 (9000)	274 (8100)
NiL	359 (15000)	290 (2800)
CoL	360 (14300)	289 (2800)

$$K = \frac{[ML]+[MHL]}{[M]([HL]+[L])} \doteq \frac{K_{ML}+K_{MHL}\{H^+\}/K_1}{(1+K_{MHL}\{H^+\}/K_1)} \tag{8}$$

where $\{H^+\}$ is obtained directly from the measured pH and is not the thermodynamic quantity a_{H^+}. An iterative least-squares fit of the absorbance data was made according to:

$$\frac{1}{(\varepsilon_{obs}-\varepsilon'_L)} = \frac{1}{(\varepsilon_C-\varepsilon'_L)} + \frac{1}{(\varepsilon_C-\varepsilon'_L)} \cdot \frac{1}{K[M]_f} \tag{9}$$

where ε_C and ε'_L are the molar absorptivities of metal complex and ligand at a particular pH, and $[M]_f$ is the free metal concentration. This was used to evaluate K at pH 4.0, 5.0, 6.0 and 7.0 for cobalt and nickel at several wavelengths in the range 300–400 nm. At every pH except 7.0, $[M]_f \approx [M]_{total}$. At pH 4.0, the binding was so weak that a value of ε_C obtained at other pH values was required to analyse the data. This does not introduce an error unless the species MHL makes a significant

contribution to the absorbance. Experiments at pH 2.0 showed no spectral changes, even in the presence of 0.03 *M* metal, under which conditions the species MHL should be observable if it is significant. Typical plots of eqn. (9) are shown in Fig. 3

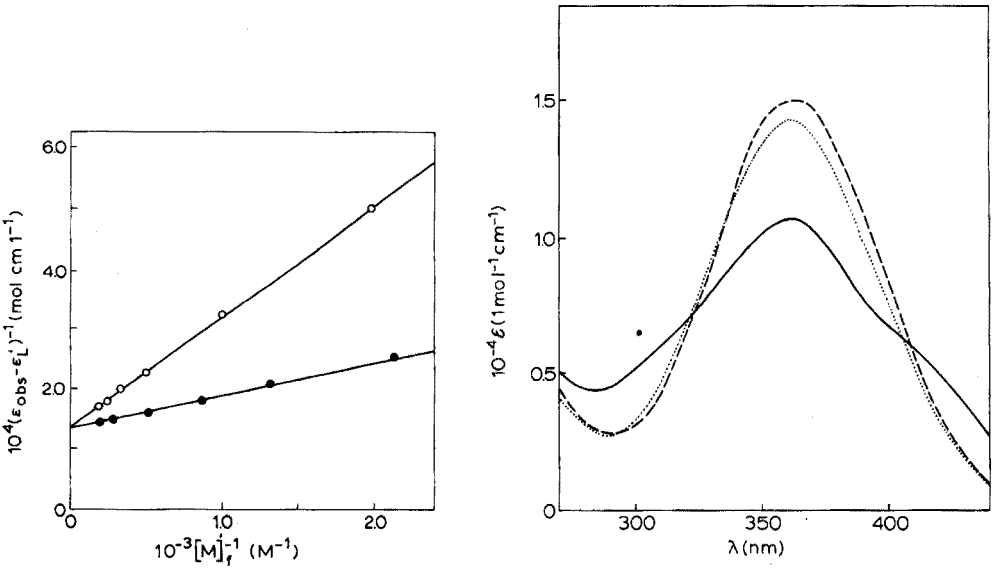

Fig. 3. Plots for determination of *K* at pH 7.00 for Co(II), $\lambda = 370$ nm (○), and Ni(II), $\lambda = 368$ nm (●) with DNSA at 25°C and $I = 0.1$ *M* sodium perchlorate.

Fig. 4. Spectra of NiL (– – – –) and CoL (· · · · · ·) compared with the spectrum of DNSA alone at pH 7.00 (——).

TABLE II

VALUES OF APPARENT BINDING CONSTANTS, *K*, FOR THE REACTIONS OF Ni(II) AND Co(II) WITH DNSA

(At 25°C and 0.1 *M* ionic strength (sodium perchlorate), as a function of pH.)

pH	*Nickel(II)*			*Cobalt(II)*		
	λ (nm)	*K (l mol⁻¹)*	*K (calc)*[a] *(l mol⁻¹)*	*λ (nm)*	*K (l mol⁻¹)*	*K (calc)*[a] *(l mol⁻¹)*
4.00	368	8.9	8.9	370	4.9	5.0
5.00	368	74±14	72	370	45±2	42
	358	70±7		350	42±3	
	303	70±8		310	41±4	
6.00	368	705±40	670	370	395±25	390
	358	712±45		350	370±20	
	303	690±75				
7.00	368	4150±250	4340	370	2680±150	2540
	358	4110±220		350	2460±120	
	303	4430±210				

[a] *K* (calc) from computed values of K_{ML} and K_{MHL}.

and values of K are collected in Table II. From these, it is possible to obtain K_{ML} and K_{MHL} from eqn. (8). At 0.1 M sodium perchlorate and 25°C, $K_{NiL} = 4.12 \pm 0.02 \cdot 10^4$ l mol^{-1}, $K_{NiHL} = 1.78 \pm 0.42$ l mol^{-1}, $K_{CoL} = 0.66 \pm 0.01 \cdot 10^4$ l mol^{-1}, and $K_{CoHL} = 0.83 \pm 0.22$ l mol^{-1}. Spectra of CoL and NiL are shown in Fig. 4.

DISCUSSION

This study provides evidence for the complexes NiL and CoL. The very small values of K_{NiHL} and K_{CoHL} imply that these complexes are of the outer-sphere or ion-pair type; the ion-pairing constants, K_0, for the interaction of a 2+ metal-ion with a 1− ligand can be estimated by the Eigen–Fuoss treatment[12,13] with activity coefficient corrections as suggested by Davies[14]. For a medium of 0.1 M ionic strength, K_0 should be 2 l mol^{-1}. The values obtained for K_{MHL} are somewhat lower, and this reflects the decrease in the negative charge on the carboxylate resulting from the electron-withdrawing action of the nitro groups. This inductive effect also increases the acid strength of the carboxylate[15] and this, together with the hydrogen bond stabilisation of HL[16], reduces the tendency for inner-sphere complexes to form. The values of pK_1, pK_2, K_{NiL} and K_{CoL} are lower than those for salicylic acid itself[17]; this is another consequence of the electron-withdrawing power of the nitro groups. The values obtained for K_{NiL} and K_{CoL} can be compared with those of Dube and Dhindsa[6] (Table III); the difference between their values for the stability of the cobalt and nickel complexes, $\log K_{NiL} - \log K_{CoL} = 0.92$, is much larger than our value of 0.23. Moreover for the salicylic acid and 5-sulphosalicylic acid systems (at 20°C) the corresponding values[17] are 0.23 and 0.30. Another major difference between the two studies is the great difference in values for pK_1 shown in Table III. The value obtained by Bartusek[2] is also much too high.

TABLE III

ACID DISSOCIATION CONSTANT AND NICKEL(II) AND COBALT(II) BINDING CONSTANTS FOR DNSA

T (°C)	I (M)	(Medium)	pK_1	pK_2	Log K_{CoL}	Log K_{NiL}	Ref.
25	0.1	($NaClO_4$)[a]	0.27	7.20	3.82	4.05	This work
35	0.1	(KNO_3)[b]	2.96	7.61	3.88	4.80	6, 18
20	0.1	(KNO_3)[b]	2.25	7.40	—	—	2
25	0	[c]	0.70	—	—	—	15

[a] Spectrophotometric study.
[b] Potentiometric study.
[c] Conductimetric study.

Such inconsistencies will always be encountered when pK_a values are determined by potentiometric titration under conditions where $K_a \geq c_L$, since the group in question is extensively ionised even in the absence of added base. The spectrophotometric (and conductimetric) techniques avoid such problems. In general it seems reasonable to question pK_a values obtained potentiometrically where the quoted

value is $\leqslant 1+\log_{10} c_L$, unless allowance has been made for partial dissociation of the acid in the absence of added base. Although DNSA will find little application in trace metal analysis since binding constants are too low, it may be possible to use it as a colorimetric indicator of cobalt(II) and nickel(II) concentrations between 10^{-5} *M* and 10^{-2} *M*, depending on the pH, in the pH range 4–8. An advantage is that solutions of DNSA are much more stable than those of murexide[19]. 3,5-Dinitrosalicylic acid could be used to determine binding constants of Ni(II) and Co(II) with species such as nucleic acids which exhibit no, or only small, spectral changes on complexation. Such studies with magnesium have involved eriochrome black T[20,21] or calmagite[22] as indicator, but with cobalt(II) the stability constant[23] of the ETB–metal complex is far too high for such indicators to be useful. Some difficulty, however, may be encountered if interaction between the nucleotide bases and the aromatic benzene ring occurs; such an effect has been observed with caffeine and salicylic acid[24].

Part of this work was carried out at the Max-Planck-Institut für Biophysikalische Chemie, Göttingen. We thank the Max Planck Gesellschaft (P.C.) and the Royal Society, London (R.S.T.), for the award of post-doctoral Fellowships, and Prof. Eigen and Dr. H. Diebler for granting research facilities.

SUMMARY

The values of pK_1 and pK_2 for 3,5-dinitrosalicylic acid (DNSA, H_2L) have been determined at 25.0°C and 0.1 *M* ionic strength (sodium perchlorate) as 0.25 and 7.20, respectively. The binding of nickel(II) and cobalt(II) has been investigated over the pH range 1.0–7.0 at the same temperature and ionic strength. Values of log K_{ML} for the formation of the unprotonated complexes are 4.05 ± 01 and 3.82 ± 01 for nickel(II) and cobalt(II) respectively. Values for log K_{MHL} are close to 1 l mol^{-1} for both metals; it seems probable that these species are not inner-sphere complexes, and possible reasons for this are suggested. The stability constants obtained are compared with others in the literature, and the possibility of using DNSA as a metal-ion indicator is discussed briefly.

REFERENCES

1 C. Vassilliadis, G. Manoussatis and G. Colovas, *Chim. Chronika*, 29 (1964) 322.
2 N. Bartusek, *Collect. Czech. Chem. Commun.*, 32 (1967) 116.
3 S. S. Dube and S. S. Dhindsa, *J. Inorg. Nucl. Chem.*, 32 (1970) 1041.
4 S. S. Dube and S. S. Dhindsa, *J. Inorg. Nucl. Chem.*, 32 (1970) 543.
5 R. S. Taylor, *Talanta*, 21 (1974) 1210.
6 S. S. Dube and S. S. Dhindsa, *Indian J. Chem.*, 7 (1969) 823.
7 V. I. Kuznetsov and N. N. Basargin, *Zh. Neorg. Khim.*, 7 (1962) 814.
8 G. R. Cayley and D. N. Hague, *J. Chem. Soc. Faraday I*, 68 (1972) 2259.
9 D. N. Hague and K. Kinley, *J. Chem. Soc. Dalton*, (1974) 249.
10 H. A. Benesi and J. H. Hildebrand, *J. Amer. Chem. Soc.*, 71 (1949) 2703.
11 R. H. Moore and R. K. Ziegler, *Los Alamos Report LA 2367*, (1959), and Addenda.
12 M. Eigen, *Z. Phys. Chem. (Frankfurt am Main)*, 1 (1954) 176.
13 R. M. Fuoss, *J. Amer. Chem. Soc.*, 80 (1958) 5059.
14 C. W. Davies, *Ion Association*, Butterworths, London, 1962, p. 39.

15 L. G. Bray, J. F. J. Dippy, S. R. C. Hughes and L. W. Laxton, *J. Chem. Soc., London*, (1957) 2405.
16 G. E. K. Branch and D. L. Yabroff, *J. Amer. Chem. Soc.*, 56 (1935) 2568.
17 D. D. Perrin, *Nature (London)*, 182 (1958) 741.
18 S. S. Dube and S. S. Dhindsa, *Curr. Sci.*, (1968) 642.
19 G. Schwarzenbach and H. Gysling, *Helv. Chem. Acta*, 32 (1949) 1314.
20 J. Shack and B. S. Bynum, *Nature (London)*, 184 (1959) 635.
21 H. Krakauer, *Biopolymers*, 10 (1971) 2459.
22 A. M. Willemsen and G. A. J. van Os, *Biopolymers*, 10 (1971) 945.
23 M. Kodama, *Bull. Chem. Soc. Jap.*, 40 (1967) 2575.
24 J. H. Stern, J. A. Devore, S. L. Hansen and D. Yavuz, *J. Phys. Chem.*, 78 (1974) 1922.

Analytica Chimica Acta, 78 (1975) 459–462

SHORT COMMUNICATION

A graphical method for evaluating the dynamic measuring range of potentiometric gas-sensing electrodes

ELO HARALD HANSEN and NIELS RHOD LARSEN
Chemistry Department A, The Technical University of Denmark, Building 207, DK-2800 Lyngby (Denmark)
(Received 10th February 1975)

For the analytical chemist contemplating the use of ion-selective electrodes, one of the most important parameters for which prior knowledge is required is the dynamic measuring range within which a particular electrode exhibits a linear, preferably Nernstian response. This may be implemented simply if the electrode is available by calibrating under circumstances similar to those in which the electrode is to be used; or it may be calculated theoretically if all the pertinent data are procurable, *e.g.*, selectivity coefficients. With potentiometric gas electrodes, however, the calculation of the dynamic measuring range is very simple because of the electrolyte layer is given by the Henderson Hasselbalch equation which, for the gas sensors[1–5], the choice of the most favourable parameters in individual assays in order to obtain optimal measuring conditions has been discussed. Although it is therefore an extension of these previous discussions, this communication seeks rather to present a simple and generally applicable graphical method which, through logarithmic representation, depicts the dynamic measuring range for potentiometric gas-sensing electrodes.

These electrodes generally utilize a glass electrode and a reference electrode joined by an aqueous electrolyte, the pH of which changes whenever an alkaline (or acidic) gas diffuses into it. The electrolyte layer—which normally consists of the acid or base corresponding to the gas to be measured—is separated from the sample solution either by a porous membrane or by an air gap[1–5]. The pH in the electrolyte layer is given by the Henderson–Hasselbalch equation which, for the NH_3–NH_4^+ system (chosen to illustrate the present method) becomes:

$$pH_e = pk_a - \log[NH_4^+]_e + \log[NH_3]_e \quad (1)$$

where the suffix e denotes the electrolyte solution. The term $[NH_3]_e$ will, however, be a function of the ammonia concentration in the sample solution, $[NH_3]_s$, *i.e.*:

$$[NH_3]_e = p[NH_3]_s \quad (2)$$

where p is the partition coefficient. By substitution, eqn. (1) gives:

$$pH_e = pk_a + \log p - \log[NH_4^+]_e + \log[NH_3]_s \quad (3)$$

The range within which a linear relationship between pH_e and $\log[NH_3]_s$

exists (the dynamic measuring range) is therefore restricted to that region in which the first three terms of eqn. (3) remain constant. Since pk_a and $\log p$ can be fixed readily at a constant level experimentally[1], the dynamic measuring range is in consequence limited to the range within which the term $\log[NH_4^+]_e$ does not change either at very low $[NH_3]_s$ values, through depletion of the ammonium content of the electrolyte layer, or at relatively high $[NH_3]_s$ values, as a result of ammonia hydrolysis in the electrolyte solution.

Figure 1A shows a logarithmic diagram (Hägg diagram[6]) in which eqn. (3) has been depicted for two different concentrations of ammonium in the electrolyte solution. The abscissa is pH_e and the ordinate is $\log c$, where c is the molar concentration. Lines a_1 and a_2 thus represent $[NH_4^+]_e = 10^{-1}$ M and 10^{-3} M, respectively, while b_1 and b_2 are the corresponding base lines reflecting the ammonia concentrations in the sample solutions, $[NH_3]_s$, of the two systems (the curvature of the a-lines around the points of intersection with the OH^--line will be explained later). The point of intersection between the a- and b-lines of the two systems involved is set here at $pH_e = 9.3$, which is the approximate pk_a value for NH_4^+; *i.e.* the partition coefficient, p, is assumed to equal unity. According to eqn. (2), p reflects the partition of ammonia between the electrolyte solution and the sample solution; this assumption is therefore valid only if the ionic strength of the two solutions is nearly identical. Another value of p will, however, merely imply that the b-lines would be shifted along the abscissa axis to a parallel position such that the point of intersection with the a-lines would be $pH_e = pk_a + \log p$.

In the analysis of ammonium-containing samples with ammonia gas-sensing electrodes, the ammonium ions can, depending on the choice of pH_s, be converted to ammonia either quantitatively or partially. To relate the pH_e signal to the total ammonium/ammonia nitrogen content of the sample, eqn. (2) may be rearranged:

$$[NH_3]_e = p'([NH_3]_s + [NH_4^+]_s) \tag{4}$$

where p' may be considered a conditional partition coefficient, the value of which will be a function of pH_s: for total conversion $p' = p \simeq 1$ ($\mu_s \simeq \mu_e$); for partial conversion $p' < p$, *e.g.* at $pH_s = pk_a - 1$, $p' = 0.1$, $\mu_s \simeq \mu_e$ (F).

Each electrolyte solution will naturally contain a certain amount of ammonia originating from the hydrolysis of ammonium ions, the value of which is given by the intersection of the b-lines with the H_3O^+-line, *i.e.* for $[NH_4^+]_e = 10^{-1}$ M, $[NH_3]_e = [H_3O^+] = \text{antilog}(-5.2) = 6 \cdot 10^{-6}$ M (point 1); and for $[NH_4^+]_e = 10^{-3}$ M, $[NH_3]_e = \text{antilog}\ (-6.2) = 6 \cdot 10^{-7}$ M (point 2). Hence, if electrodes embodying these electrolytes are exposed to samples containing smaller amounts of ammonia, ammonia diffuses from electrolyte to sample in order to establish equilibrium, resulting in a decrease in $[NH_4^+]_e$. Thus, the $[NH_3]_e$ values given by these points of intersection constitute the theoretical lower sensitivity limits for the respective electrolyte concentrations (a).

For $[NH_3]_s$ increasing above the value given by point 1 (or 2), the electrode signal pH_e will be related linearly to $\log[NH_3]_s$. This will hold until the amount of NH_4^+ formed by hydrolysis of ammonia in the electrolyte layer increases to the point where it becomes significant compared with the $[NH_4^+]$ already present in the electrolyte solution. The increase in $[NH_4^+]_e$, $\Delta[NH_4^+]_e$, is equal to $[OH^-]$, which indirectly is given by pH_e since the hydrolysis of ammonia represents the only

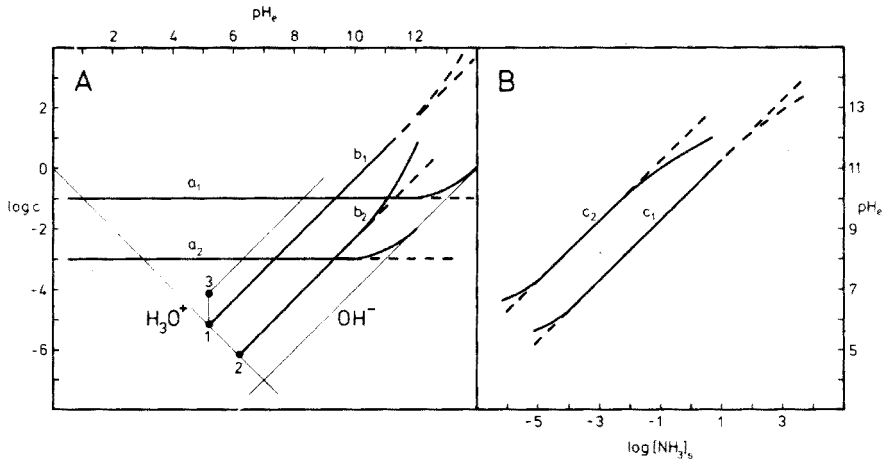

Fig. 1. (A) Logarithmic diagram (Hägg diagram) for the NH_4^+/NH_3 system. The a-curves indicate electrolyte concentrations of $[NH_4^+]_e = 10^{-1}$ *M* and 10^{-3} *M*, respectively; b_1 and b_2 are the corresponding $[NH_3]_s$-curves. (B) For ammonia gas electrodes employing the above electrolyte concentrations, calibration curves (c) depict the dynamic measuring range attainable in practice.

way in which the hydroxide ions can be generated. The $\Delta[NH_4^+]_e$ value can, therefore, for any value of pH_e, be read readily from the OH^--line in the logarithmic diagram. By adding $\Delta[NH_4^+]_e$ to the original $[NH_4^+]_e$ value, the "actual" $[NH_4^+]_e$ *i.e.* the value used in eqn. (3) and graphically depicted (a_1 and a_2) in Fig. 1A is found. As the "actual" and the original ammonium concentration in the electrolyte will be identical except in the vicinity of the intersection point of the *a*- and OH^--lines, the *a*-curves will, however, only deviate from straight lines in this region. The ammonia curves (b_1 and b_2) are subject to similar deviations from the straight-line relationship, since $\log[NH_4^+]_e$ and $\log[NH_3]_s$ are of opposite sign in eqn. (3).

The solubility of ammonia in aqueous systems corresponds to *ca.* 15 *M* at room temperature. However, since it is implied in eqn. (3) that $\log p$ remains constant (p is here set equal to unity), the upper limit of sensitivity is therefore restricted by this condition. In consequence, the b_1-curve has been dotted above $\log[NH_3]_s \simeq 1$.

Discussion

The dynamic measuring range can be established in this way. If a deviation from linearity amounting to 1% is allowed, the upper sensitivity limit is determined by $\log[OH^-] = \log \Delta[NH_4^+]_e \leqslant \log[NH_4^+]_e - 2$: for $[NH_4^+]_e = 10^{-1}$ *M* (a_1), this corresponds to $\log[NH_3]_s = 0.7$, or $[NH_3]_s = 5$ *M* (b_1); and for $[NH_4^+]_e = 10^{-3}$ *M* (a_2), $\log[NH_3]_s = -3.3$, or $[NH_3]_s = 5 \cdot 10^{-4}$ *M* (b_2). The theoretical lower sensitivity limit, determined by the ammonia concentration in the electrolyte solution itself, is the same for the two electrolyte concentrations, hence $[NH_3]_s = 6 \cdot 10^{-6}$ *M* (point 1) and $6 \cdot 10^{-7}$ *M* (point 2), respectively. In practice, however, it is not possible to reach these theoretical limits, and it is not advisable to use observations too close to the sensitivity limit for precise evaluations. With the air-gap electrode, the practical lower limit of sensitivity was approximately 1 decade above the theoretical limit[4].

As mentioned previously, Fig. 1A is constructed with the provision that $p = 1$.

If $p \neq 1$ (eqn. (2), *e.g.*, $\mu_s \neq \mu_c$) or $p' \neq 1$ (eqn. (4), *e.g.*, partial conversion), and the ammonia lines (b_1 and b_2) have therefore been shifted to parallel positions along the abscissa axis, the theoretical lower limits of sensitivity will then be determined for each electrolyte concentration by the point of intersection between the respective b-line and the vertical line drawn through the point corresponding to the conditions in the electrolyte solution itself, *i.e.*, by point 1 or 2; *e.g.* for $[NH_4^+]_e = 10^{-1}$ M and $p' = 0.1$ and $pk_a = 9.3$, the lower sensitivity limit will be determined by point 3. This is, of course, because it is not possible to measure a pH_e value which is smaller than the pH value in the electrolyte itself. Thus for a given electrolyte concentration, by using partial conversion ($p' < 1$, *e.g.*, enzymatic analysis by a monitoring procedure), the theoretical lower limit of sensitivity might easily be substantially reduced by an amount which may be evaluated directly from the logarithmic diagram, which therefore may prove very valuable in predetermining the experimental conditions to be used[7]. In contrast, the measurement of more concentrated samples is preferably done by the partial conversion technique (*i.e.*, $p' < 1$) if they are not diluted.

In Fig. 1B the calibration curves, as derived from the logarithmic diagram, are shown in the conventional manner, where curve c_1 represents $[NH_4^+]_e = 10^{-1}$ M and curve c_2 corresponds to $[NH_4^+]_e = 10^{-3}$ M, and the practical lower limit of sensitivity has been chosen to be 1 decade above the theoretical value[4]. The extent of the dynamic measuring range is seen to depend strongly on the choice of $[NH_4^+]_e$. Thus, an ammonia gas sensor applying a 10^{-1} M ammonium electrolyte solution will yield a Nernstian response within the range *ca.* 10^{-4}–5 M, *i.e.*, over close to 5 decades, while an electrolyte solution of 10^{-3} M will result in a Nernstian response in the range *ca.* 10^{-5}–$5 \cdot 10^{-4}$ M NH_3, *i.e.* over less than two decades. Although the lower limit of sensitivity is decreased with the latter of these two electrolytes, namely 1 decade, only the potential applications of the electrode can say whether this is necessary or warranted.

The discussion in this communication of an ammonia gas-sensing electrode is valid for other gas electrodes which operate essentially in the same manner. When the gas reacts as an acid, *e.g.*, SO_2, H_2S or CO_2, equations analogous to eqn. (3) may be derived and depicted in a logarithmic diagram, which will allow the dynamic measuring range to be deduced for any electrolyte concentration used, the extent again being confined to the pH_e range within which the concentration of electrolyte base, corresponding to the acid gas being measured, remains constant. It should be noted, however, that additional restrictions might be imposed, *e.g.*, the carbon dioxide content of the air may limit the applicable range of a carbon dioxide gas-sensor, but such limitations may be incorporated easily in the logarithmic diagram by appropriate lines or curves[5].

REFERENCES

1 J. Růžička and E. H. Hansen, *Anal. Chim. Acta*, 69 (1974) 129.
2 E. H. Hansen, H. Bergamin Filho and J. Růžička, *Anal. Chim. Acta*, 71 (1974) 225.
3 J. Růžička, E. H. Hansen, P. Bisgaard and E. Reymann, *Anal. Chim. Acta*, 72 (1974) 215.
4 E. H. Hansen and J. Růžička, *Anal. Chim. Acta*, 72 (1974) 353.
5 U. Fiedler, E. H. Hansen and J. Růžička, *Anal. Chim. Acta*, 74 (1975) 423.
6 G. Hägg, *Kemisk Reaktionslära*, Almqvist and Wiksell AB, Stockholm, 1969, pp. 70–72.
7 N. R. Larsen, E. H. Hansen and G. G. Guilbault, *Anal. Chim. Acta*, in press.

Analytica Chimica Acta, 78 (1975) 463–465

SHORT COMMUNICATION

Determination of iron(III) in minaral samples by titration with EDTA and a coated-wire ion-selective indicator electrode

R. W. CATTRALL and CHIN-POH PUI

Department of Inorganic and Analytical Chemistry, La Trobe University, Bundoora, 3083, Victoria (Australia)

(Received 21st January 1975)

The development of a coated-wire ion-selective electrode which is selective for the tetrachloroferrate(III) ion was recently reported[1]. This electrode based on the tetrachloroferrate(III) salt of Aliquat 336S as the electroactive compound was used for the analysis of some rocks and minerals by direct potentiometry of solutions which contained stringently controlled amounts of chloride.

In this communication, the use of the electrode for the potentiometric titration of iron(III) with EDTA in solutions obtained by the dissolution of certain mineral samples is described.

Experimental

Construction of the electrode. The preparation of the tetrachloroferrate(III) salt of Aliquat 336S (General Mills Chemicals, Inc.) and the construction of the coated platinum wire electrode have been described elsewhere[1]. Potential measurements were made with an Orion Model 801 digital pH meter.

Dissolution of mineral samples. The following procedures for decomposing the ore samples were similar to those reported previously[1].

Wet-ash weighed samples of iron pyrites (to give a final solution containing a total iron(III) concentration of about 10^{-2} *M*) with a concentrated sulfuric–nitric acid mixture. Evaporate to dryness and fume twice with concentrated nitric acid. Again evaporate to dryness and dissolve the residue overnight, with magnetic stirring, in a solution containing 5 *M* lithium chloride (May and Baker reagent grade) and 1 *M* hydrochloric acid (Analar). Adjust the pH of the solution to about 1 by addition of solid lithium hydroxide (glass–calomel combination electrode), and rinse the electrode with 6 *M* lithium chloride solution. Titrate the iron solution with a 0.025 *M* EDTA solution which contains 6 *M* lithium chloride, the tetrachloroferrate(III)-selective electrode being used to indicate the end-point; stir magnetically.

For silicate rock samples containing 10–15% iron, mix the weighed powdered samples (to give a final solution containing a total iron(III) concentration of about 10^{-2} *M*) with approximately six times as much lithium metaborate (BDH reagent grade), and fuse in a high-purity graphite crucible at 900°C in a muffle furnace for 10–15 min. Pour the melt into dilute nitric acid and stir with a teflon-coated

magnetic bar until dissolved. Evaporate the solution to near dryness on a hot plate and fume twice with concentrated nitric acid to oxidize all the iron. Evaporate to dryness, and dissolve the residue in a solution containing 5 *M* lithium chloride and 1 *M* hydrochloric acid overnight. Adjust the solution containing the silica residue to pH 1 by addition of solid lithium hydroxide and titrate as described above.

Standard EDTA solution. Dissolve the disodium salt (Analar) in a solution containing 6 *M* lithium chloride, and standardize against a zinc solution to an eriochrome black T end-point[2].

Results and discussion

In the determination of iron(III) by direct potentiometry with the coated wire tetrachloroferrate(III)-selective electrode a very careful control of the total chloride ion concentration in the solutions is necessary[1], because the electrode responds to the chloride ion itself, and because the formation of tetrachloroferrate(III) is highly dependent on the total chloride ion concentration. This stringent control of the chloride ion concentration can be largely avoided if the analysis is carried out by potentiometric titration rather than by direct potentiometry since a very accurate determination of the electrode potential is not then required.

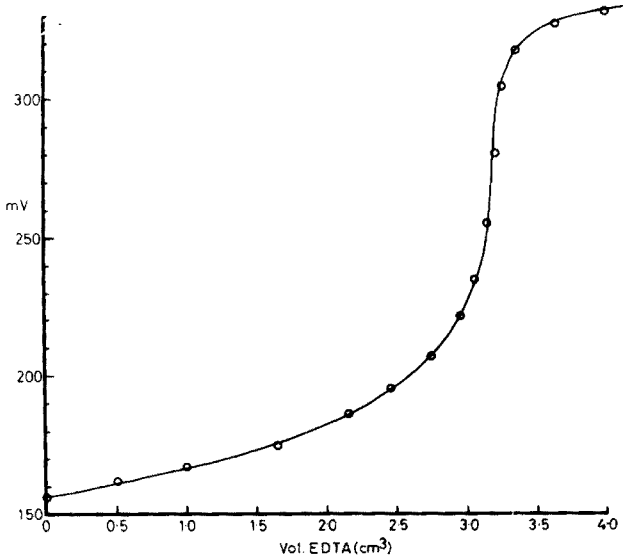

Fig. 1. Titration of 10 cm^3 of a 0.016 *M*. Solution of iron(III) containing 0.050 *M* aluminium and 6 *M* total chloride at pH 1 with a 0.050 *M* EDTA solution.

The method relies on the relatively large change in potential associated with the decrease in concentration of the tetrachloroferrate(III) species on complexation of iron(III) by EDTA. In addition, the high stability of the iron(III) complex with EDTA ($\log K_{FeY} = 25.1$) makes it possible to titrate in quite strongly acid solutions (pH 1), so that the method becomes highly selective. The high selectivity of the method is adequately demonstrated by the titration of iron(III) in the presence of aluminium; Fig. 1 shows that the presence of quite large amounts of aluminium has no effect on the position of the end-point.

TABLE I

ANALYSIS OF MINERAL SAMPLES

Ore	*Titration method* % *Fe*	*Direct potentiometry*[1] % *Fe*	*Conventional method* % *Fe*
Pyrites	42.88 ± 1.48[a]	42.85 ± 0.49	43.14 ± 1.46[b]
Silicate rock	11.16 ± 1.04	11.89 ± 0.74	11.81[c]

[a] Uncertainties are expressed as $\pm 2\sigma$.
[b] Titrimetric method[2].
[c] X-ray fluorescence spectroscopy.

Analysis of mineral samples. The results by potentiometric titration for samples of iron pyrites and silicate rock are reported in Table I, which also shows comparative results. Reasonable agreement was obtained for the analyses by potentiometric titration, by direct potentiometry and by conventional techniques. Potentiometric titration with the tetrachloroferrate(III)-selective electrode thus provides a rapid method for the determination of iron in solution without stringent control of the total chloride ion concentration of the solution. Moreover, the analysis of solutions of rocks and minerals can be carried out without filtering the solutions to remove the silica residue.

We are grateful to the Australian Research Grants Committee for financial support.

REFERENCES

1 R. W. Cattrall and Pui Chin-Poh, *Anal. Chem.*, 47 (1975) 93.
2 A. I. Vogel, *A Text-book of Quantitative Inorganic Analysis*, Longmans, London, 3rd edn., 1961, (a) p. 433; (b) p. 287.

Analytica Chimica Acta, 78 (1975) 466–469

SHORT COMMUNICATION

An atomic absorption spectrometric study of the distribution ratio of molybdenum 1-pyrrolidinecarbodithioate for the methyl isobutyl ketone–water system

ALBERT P. LEE and D. F. BOLTZ

Department of Chemistry, Wayne State University, Detroit, Michigan 48202 (U.S.A.)

(Received 20th January 1975)

Ammonium 1-pyrrolidinecarbodithioate (APCDT)[1] is an effective chelating agent in the organic solvent extraction of the heavy metals[2–11]. The metal–chelate complex is extracted into a solvent such as chloroform or methyl isobutyl ketone (MIBK), and the resultant solution is utilized in spectrophotometric or atomic absorption determination of metals and non-metals[12]. In the atomic absorption spectrometric determination of copper, Allan[13] extracted the copper–APCDT complex with a number of miscible and immiscible solvents including MIBK[13]. Kalt and Boltz[4] used chloroform to extract the molybdenum–APCDT complex in the spectrophotometric determination of molybdenum. The extraction of the metal–chelate complex is usually pH-dependent[14,15] and the optimized extraction condition can be obtained from the relationship between the pH and the distribution ratio of the complex in the water–organic solvent system.

In this investigation, the distribution of the reagent, APCDT, in the water–MIBK system as a function of the pH of the aqueous phase was studied spectrophotometrically. In a similar manner the distribution of the molybdenum–PCDT complex was studied by atomic absorption spectrometry. Thus, by evaluating the distribution ratios, the optimal pH for the extraction of the molybdenum pyrrolidinecarbodithioate complex has been determined.

Experimental

Standard molybdenum(VI) solution ($1.0 \cdot 10^{-3}$ M). Dissolve 2.420 g of sodium molybdate dihydrate, $Na_2MoO_4 \cdot 2\,H_2O$, in water and dilute to 1 l. Dilute 10.0 ml of this solution to 100 ml with water.

Ammonium 1-pyrrolidinecarbodithioate (APCDT) solutions. For solution I (3.0 % w/v), dissolve 1.5 g of the purified ammonium 1-pyrrolidinecarbodithioate in water and dilute to the mark in a 50-ml volumetric flask; prepare the solution daily. For solution II ($5.0 \cdot 10^{-2}$ M), dissolve 0.823 g of the purified compound in water and dilute to the mark in a 100-ml volumetric flask. Prepare fresh solution daily.

All reagents were reagent grade. Ammonium 1-pyrrolidinecarbodithioate (Fisher A-182) was recrystallized from absolute ethanol. The water used was double-distilled. The MIBK was used without further purification.

Solutions of hydrochloric acid, potassium chloride, ammonium acetate, acetic acid, potassium dihydrogen phosphate, sodium hydroxide, triethylamine, ammonium hydroxide, and ammonium chloride were prepared and used as buffers to adjust the pH of the aqueous solution in the study of the distribution ratio.

Apparatus. The atomic absorption spectrometric measurements were made with a Beckman Model 1301 atomic absorption accessory unit, a Beckman Model DB-G spectrophotometer equipped with a Beckman potentiometer recorder, a Beckman laminar flame burner, and a Beckman neon-filled molybdenum hollow-cathode tube. Spectrophotometric absorbance measurements were made in 1.000-cm matched silica cells with a Cary 14 spectrophotometer. All pH measurements were made with a Corning Model 110 pH meter equipped with glass and calomel electrodes.

Atomic absorption spectrometer instrument parameters were: air pressure, 21 lb; acetylene pressure, 4.5 lb; wavelength, 313.3 nm; slit width, 0.20 nm; lamp current, 21 mA.

Determination of the distribution ratio of 1-pyrrolidinecarbodithioate in the MIBK–water system. Transfer 5 ml of the APCDT solution II and 15 ml of buffer solution to a 125-ml separatory funnel. Mix well. Add 20 ml of MIBK to the aqueous solution and extract for 3 min. Measure the pH of the aqueous phase. Measure the absorbance of the aqueous phase at 335 nm against the corresponding blank solution.

Determination of the distribution ratio of molybdenum(VI)–1-pyrrolidinecarbodithioate complex in the MIBK–water system. Transfer 2.0 ml of the $1.0 \cdot 10^{-3}$ *M* standard molybdenum(VI) solution to a 125-ml separatory funnel containing 15.0 ml of buffer solution. Add 3.0 ml of the 3.0% (w/v) APCDT solution I and mix well. Allow the mixture to stand for about 30 min. Add 20.0 ml of MIBK and extract for 3 min. Let the funnel stand until the separation of the immiscible layers is complete. Aspirate the aqueous phase into the burner of the atomic absorption spectrophotometer and measure the per cent transmittance at 313.3 nm. Repeat the procedure with different pH buffers.

Atomic absorption determination of molybdenum in the aqueous phase. Aspirate $0.50 \cdot 10^{-4}$ *M*–$2.0 \cdot 10^{-4}$ *M* molybdenum(VI) solutions in the specified pH buffer into the burner of the atomic absorption spectrophotometer and measure the per cent transmittance at 313.3 nm. Plot the absorbance *vs.* the molybdenum(VI) concentration.

Results

Distribution ratio of 1-pyrrolidinecarbodithioic acid. The distribution ratio of the chelating agent, APCDT, in the MIBK–water depends on the pH. The pertinent data and calculations of the distribution ratio, *D*, are summarized in Table I. At pH 8 the efficiency of extraction of 1-pyrrolidinecarbodithioic acid for equal volumes of aqueous and organic phases is 98%. The $pH_{\frac{1}{2}}$ value obtained from the linear plot of log *D vs.* pH for the values given in Table I is 5.9.

Distribution ratio of molybdenum–pyrrolidinecarbodithioate. The atomic absorption spectrometric determinations showed that the molybdenum(VI)–PCDT complex has similar distribution ratios in the MIBK–water system. The complex is almost completely extracted below pH 5.6, but it is not appreciably when the

TABLE I

DISTRIBUTION RATIO AND $pH_{\frac{1}{2}}$ VALUES FOR 1-PYRROLIDINECARBODITHIOIC ACID IN THE MIBK–WATER SYSTEM

pH	*Absorbance*[a]	$([MR]+[R^-])\cdot 10^5$ *(M)*[b]	$[HR]_0\cdot 10^5$ *(M)*[c]	*D*	*log D*
4.9	0.035	65	1185	18.2	1.26
5.6	0.210	392	858	2.19	0.34
6.0	0.375	698	552	0.790	−0.10
6.2	0.500	932	318	0.342	−0.47
6.4	0.555	1033	217	0.210	−0.68
6.6	0.570	1061	189	0.178	−0.75
6.8	0.620	1155	95	0.082	−1.09

[a] $\varepsilon = 53.6$ l mole^{-1} cm^{-1}.
[b] $[R^-]$ = [1-pyrrolidinecarbodithioate ion].
[c] [HR] = [1-pyrrolidinecarbodithioic acid].

pH exceeds 6.6. The calculation of the distribution ratio, *D*, is summarized in Table II. The Beer's law calibration plot obtained from the a.a.s. determination of molybdenum in aqueous solutions of pH 5.5–8, which was used to calculate the molar concentration of molybdenum(VI) left in the aqueous layer after extraction, extended to a molybdenum concentration of $1.5\cdot 10^{-4}$ *M*. The $pH_{\frac{1}{2}}$ evaluated from the linear plot of log *D* *vs.* pH for the values shown in Table II, is 6.1.

TABLE II

DISTRIBUTION RATIO FOR THE MOLYBDENUM(VI)–1-PYRROLIDINECARBODITHIOATE COMPLEX IN THE MIBK–WATER SYSTEM

pH	*Absorbance*	$[C_{Mo}]_{aq}\cdot 10^4$ *(M)*	$[C_{Mo}]_{org}\cdot 10^4$ *(M)*	*D*	*log D*
5.80	0.0177	0.13	0.87	6.7	0.83 (0.76)[a]
6.05	0.0580	0.52	0.48	0.92	0.035 (0.00)
6.20	0.0757	0.69	0.31	0.45	−0.35 (−0.35)
6.40	0.0942	0.88	0.12	0.14	−0.87 (−0.91)
6.60	0.105	0.95	0.02	0.021	−1.69 (−1.29)

[a] Results in brackets were obtained from a duplicate set of measurements.

REFERENCES

1 H. Malissa and E. Schoffmann, *Mikrochim. Acta*, (1955) 187.
2 A. S. Berger, W. Likussar and D. F. Boltz, *Microchem. J.*, 16 (1971) 286.
3 I. M. Gibalo, I. P. Alimarin and P. Davaadorzh, *Vestn. Mosk. Univ., Ser. II, Khim.*, 20 (1965) 73.
4 M. B. Kalt and D. F. Boltz, *Anal. Chem.*, 40 (1968) 1086.
5 H. K. Y. Lau, H. A. Droll and P. F. Lott, *Anal. Chim. Acta*, 56 (1971) 7.
6 W. Likussar and D. F. Boltz, *Anal. Chem.*, 43 (1971) 1273.
7 W. Likussar, C. Sagan and D. F. Boltz, *Mikrochim. Acta*, (1970) 683.
8 W. Likussar, G. E. Sparks and D. F. Boltz, *Anal. Chim. Acta*, 52 (1970) 349.
9 R. W. Looyenga and D. F. Boltz, *Anal. Lett.*, 2 (1969) 491; *Mikrochim. Acta*, (1971) 507; *Talanta*, 19 (1972) 82.
10 L. Rocks and H. Malissa, *Anal. Chim. Acta*, 30 (1964) 106.

11 A. Traub and D. F. Boltz, *Mikrochim. Acta*, (1969) 749.
12 G. D. Christian and F. J. Feldman, *Anal. Chim. Acta*, 40 (1968) 173.
13 J. E. Allan, *Spectrochimica Acta*, 17 (1961) 459, 467.
14 J. Ramirez-Munoz, *Flame Notes, Beckman*, 1 (1966) 8.
15 W. Slavin, *At. Absorption Newslett.*, 3 (1964) 141.

Analytica Chimica Acta, 78 (1975) 470–473

SHORT COMMUNICATION

The estimation by n.m.r. of iodine value and average molecular weight of marine oils containing wax esters

P. J. KE and R. G. ACKMAN

Environment Canada, Fisheries and Marine Service, Halifax Laboratory, P.O. Box 429, Halifax, Nova Scotia B3J 2R3 (Canada)

D. L. HOOPER

Department of Chemistry, Dalhousie University, Halifax, Nova Scotia (Canada)

(Received 27th January 1975)

In recent publications[1–4], n.m.r. has been shown to complement other analytical procedures such as gas chromatography and mass spectrometry in lipid research. This recent interest results mainly from the introduction of less expensive n.m.r. spectrometers[5], and this has initiated the wide-spread application of n.m.r. to direct quality control[3,4] and non-destructive analysis[1]. A rapid n.m.r. procedure for determining the content of wax esters in marine lipids has been developed[4]. A further study has demonstrated the calculation, from n.m.r. data, of the average molecular weight and iodine value of marine oils containing a mixture of wax esters and triglycerides.

Experimental

Spermaceti (BDH Ltd.) and lard (Bio-Research Lab., Montreal) were used as model samples of wax esters and triglycerides, respectively. Oils of the sperm whale (*Physeter cacodon*) and baracudina (*Paralepis rissoi kryøyeri*) were prepared as before[4]. The average molecular weight was determined by depression of the freezing point in benzene; the iodine value was measured by Wijs' method. A T-60 spectrometer (Varian Associates) was used to record the 60-MHz spectra (Fig. 1) at room temperature for 10% (w/w) solutions of oil samples in deuterochloroform containing 1% (v/v) tetramethylsilane (Stohler Isotope Chemicals). Assignments of each group of signals (Fig. 1) and evaluations of the integrals were made as described previously[4] Group A signals are those of olefinic protons superimposed on the signal of the methine proton of the glyceryl moiety of the triglycerides. Group B contains the signals of methylene protons, respectively, in the glyceryl moiety of triglycerides and in the $-COOCH_2-$ group of wax esters. Groups C, E and F are indicated by their chemical shifts to be the signals of CH_2 groups bonded respectively to two sp^2 carbons, one sp^2 carbon and one sp^3 carbon, and two sp^3 carbons. Group D (a triplet overlapped with group E) is the signal of CH_2 groups in the α-position to the carboxyl group in the fatty acid moieties of

wax esters and triglycerides. Group G contains the signals for the protons of terminal methyl groups in both triglycerides and was esters.

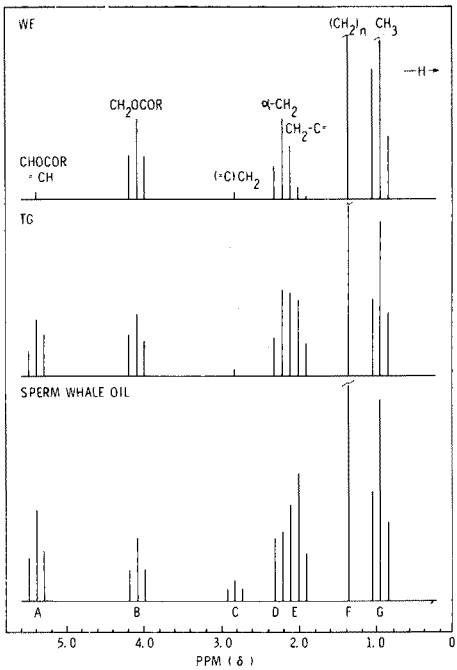

Fig. 1. N.m.r. spectra of model wax ester and triglycerides, and of sperm whale oil.

Calculation

If the integrals for groups A, B, G and for total integration are I_a, I_b, I_g and I_t, respectively, the mole fraction (m_1) of triglycerides in the marine oil, and the integration area per proton (P), are given[4] by:

$$m_1 = \frac{2I_g}{2I_g - 3I_b} - 2 \qquad (1)$$

$$P = \frac{2I_g - 3I_b}{6} \qquad (2)$$

The total number of protons (T) and the number of olefinic protons (U) in marine oil can also be calculated by:

$$T = \frac{I_t}{P} = \frac{6I_t}{2I_g - 3I_b} \qquad (3)$$

and

$$U = \frac{I_a}{P} - m_1 = \frac{6I_a - 6I_b + 2I_g}{2I_g - 3I_b} \qquad (4)$$

A general molecular structural formula for a marine oil containing wax esters may be written as:

Triglycerides (m_1): $CH_2OCO(CH_2)_a(CH{=}CH)_xCH_3$
$CHOCO(CH_2)_b(CH{=}CH)_yCH_3$
$CH_2OCO(CH_2)_c(CH{=}CH)_zCH_3$

Wax ester ($1-m_1$): $CH_3(CH{=}CH)_v(CH_2)_eOCO(CH_2)_d(CH{=}CH)_wCH_3$

The average molecular weight (MW) of these marine oils can therefore be expressed by:

$$MW = m_1[173.1+45.1+14.03(a+b+c)+26.04(x+y+z)] + (1-m_1)[30.07+44.0+14.03(d+e)+26.04(v+w)] \quad (5)$$

Equations (3) and (4) can be rewritten as:

$$T = m_1[14+2(a+b+c)+2(x+y+z)]+(1-m_1)[6+2(d+e)+2(v+w)] \quad (6)$$

$$U = 2[(x+y+z)m_1+(v+w)(1-m_1)] \quad (7)$$

By substituting eqns. (6) and (7) into eqn. (5), a simplified equation can be derived:

$$MW = 88.03m_1+6.01U+7.01T+31.99 \quad (8)$$

Since m_1, U and T can be calculated from eqns. (1), (3) and (4), the average molecular weight of a marine oil containing wax esters can be found simply from eqn. (8).

The iodine value, used as an index of the unsaturation of oils, can be calculated[6] from:

$$\text{Iodine value} = \frac{12691U}{MW} \quad (9)$$

Results and discussion

Table I shows the results for six samples with various degrees of unsaturation and contents of wax esters. The standard deviations shown for the n.m.r. method were derived from at least 6 determinations on each oil. The agreement between the f.p. and n.m.r. methods of determining the average molecular weight is good for all samples.

TABLE I

COMPARISON OF THE VALUES FOR THE AVERAGE MOLECULAR WEIGHT AND IODI VALUE OF MARINE WAX ESTER OILS GIVEN BY THE N.M.R. AND CONVENTIONAL METHO

Sample	*Wax ester %, mole*	*Av. mol. weight (±s)*		*Iodine value (±s)*	
		F.p.	*N.m.r.*	*Wijs'*	*N.m.r.*
Model wax ester	99.6	443	438±18	4.2	1.6±1.4
Model triglyceride	0.0	869	860±24	31.0	34.0±1.2
Mixture A[a]	97.1	419	429±10	6.0	7.4±2.4
Mixture B[a]	83.0	480	481±12	10.2	14.2±2.1
Barracudina oil	84.6	502	492±26	120.3	115.6±4.4
Sperm whale oil	76.2	531	536±17	76.2	78.5±3.8

[a] Mixtures A and B were prepared by mixing the model wax ester and triglyceride.

In early work[6], iodine values determined by n.m.r. for nine triglyceride oils showed an error of about 10% for coconut oil, which has a low iodine value of 8.5. The accurate measurement of the integral for the signals of group A is difficult, particularly for the less unsaturated wax ester oil (Fig. 1); this gives the largest errors in the calculation of the number of olefinic protons and hence in the iodine values from eqns. (4) and (9). Although iodine values in the range 4.2–14.2 could not be determined accurately (Table I), the n.m.r. method can be used successfully for marine wax ester oils with higher iodine values.

The total time spent in obtaining the n.m.r. data is about 15 min per sample. Calculations from eqns. (8) and (9) can be carried out very rapidly. This non-destructive n.m.r. method can be applied to the analysis of 50-mg samples of marine oils containing as little as 3 mg of wax esters, and is considerably more convenient than thin-layer chromatographic techniques[7].

REFERENCES

1 J. Schaefer and E. O. Stejskal, *J. Amer. Oil Chem. Soc.*, 51 (1974) 210.
2 J. C. Casey and C. A. Miles, *J. Sci. Food Agr.*, 25 (1974) 1151.
3 K. Van Putte and J. Van Den Enden, *J. Amer. Oil Chem. Soc.*, 51 (1974) 316.
4 P. J. Ke, R. G. Ackman and D. L. Hooper, *Anal. Chim. Acta*, 69 (1974) 253.
5 F. W. Karasek, *Res./Develop.*, November (1971) 51.
6 L. F. Johnson and J. N. Shoolery, *Anal. Chem.*, 34 (1962) 1136.
7 R. G. Ackman, S. N. Hooper, S. Epstein and M. Kelleher, *J. Amer. Oil Chem. Soc.*, 49 (1972) 378.

Analytica Chimica Acta, 78 (1975) 474–478

SHORT COMMUNICATION

The determination and identification of molecular lead pollutants in the atmosphere

J. W. ROBINSON, LARRY RHODES and D. K. WOLCOTT

Department of Chemistry, Louisiana State University at Baton Rouge, Baton Rouge, Louisiana 70803 (U.S.A.)

(Received 20th November 1974)

It has recently been reported that lead in the atmosphere has been detected both as particulate lead and as lead in the "free molecular" form (or "non-filterable" lead). The terms "particulate lead" and "molecular lead" refer only to the physical form of the lead and not to the chemical form. For example, it is possible to have lead bromide existing as particulate lead (fine particles) or molecular lead (free vapor); the same is true of lead oxide, lead chloride, *etc.*

The conventional method of determining the total lead concentration in the atmosphere is to collect the particulate material from a known volume of air and to determine the lead concentration of the particulates; thus no account is taken of uncollected lead pollutants. Any lead compounds in the vapor form (*i.e.* "free molecular" lead) escape detection and erroneous data for total lead concentrations are achieved. These errors may be gross or negligible, depending on local conditions, but only limited information on the extent of this error is available. In order to clarify the situation it is essential to accumulate more data on "molecular" lead concentrations.

Over the past several years, several analytical approaches to this problem have been investigated with poor results. A common concentration of lead in the air is 1 μg m^{-3}. When liquid scrubbing solutions are used there is a severe blank problem; after 1 m^3 of air has been scrubbed, a total of 1 μg of lead may be trapped (assuming 100% trapping efficiency) in as much as 100 ml of scrubbing solution and frequently the blank arising from the scrubber is greater than the sample lead content. The same problem arises when solid scrubbers such as activated charcoal are used; often the lead concentration in the carbon is orders of magnitude greater than the concentration of lead to be measured.

In an effort to overcome these problems the following technique was developed. The system is highly sensitive and the trapped "molecular" lead can be distinguished from the lead blank of the carbon.

Analytical procedure

A diagram of the equipment used is shown in Fig. 1. The particulates were filtered out on a graphite disc (Item Poco Spectra 109-3; 6-mm diameter and

0.5-mm thick). The filtered air was then drawn through a carbon bed, made of pure graphite activated *in situ*, which was maintained at room temperature and effectively adsorbed the non-filterable lead.

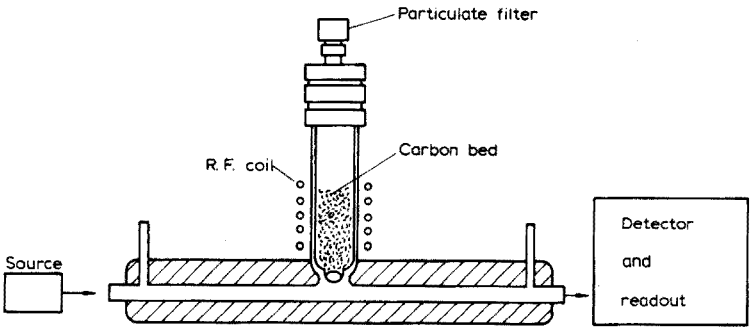

Fig. 1. Diagram of equipment. The carbon bed is 3 in. high and the light path is 18 in. long.

A 500-cm^3 sample of air was drawn through the system at a flow rate of 200 cm^3 min^{-1}. The air flow was then stopped, the r.f. coils were energized, and the carbon bed was heated to 1500°C. Non-particulate lead compounds and very small particulates adsorbed on the carbon bed were thus atomized into the vapor phase and swept with a stream of cleaned air into the cross-piece of the atomizer where they were determined by atomic absorption spectrometry. From this, the "molecular" lead in the air was calculated.

The filter, containing particulate lead, was then dropped onto the hot carbon bed. The filter coupled with the r.f. and rapidly became heated, liberating free lead atoms which were then swept into the cross-piece and measured by a.a.s.

After each determination, the instrument was checked and standardized by the addition of 10^{-10} g of lead in the form of 1 μl of standard lead solution. This precaution ensured that no unsuspected error had intruded.

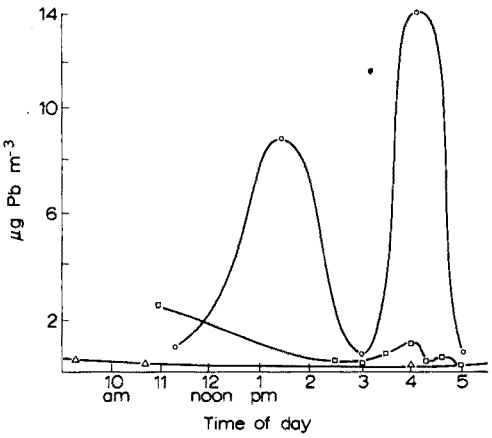

Fig. 2. Diurnal variation in concentration of "molecular" lead in the air: (●) July 1; (▲) July 3; (■) July 15.

Previous results of diurnal variations have already been reported[1]. Typical results are illustrated in Fig. 2; it can be seen that the lead concentration varied significantly throughout the day and that maxima occurred during peak traffic periods, but that other factors appear to have a greater effect on the total lead content. The weather conditions had a profound effect on the concentration of "molecular" lead in the atmosphere. For instance, on July 26, 1974, the temperature had reached 95°F; a summer thunderstorm took place in the early afternoon, followed by warming and very high humidity. An air sample taken during this period flooded the instrument with lead, so that accurate data could not be obtained, but it appeared that the "molecular" lead had reached concentrations as high as 100 or 200 $\mu g\ m^{-3}$. In contrast, during the period from September 25 to October 25, the weather was very dry and considerably cooler, with a constant influx of northern wind; the "molecular" lead content of the atmosphere during these days was extremely low, frequently at levels less than 0.1 $\mu g\ m^{-3}$.

Source of molecular lead

The source of molecular lead was a puzzle. Previous studies by other workers had indicated that the amount of tetraethyl lead in the atmosphere was always very low[2], *i.e.* less than 0.1 $\mu g\ m^{-3}$. However, these data were taken in latitudes considerably north of Baton Rouge and may well be in keeping with the above-mentioned data found during September and October, 1974. Preliminary work in this laboratory with a gas chromatography–mass spectrometry combination indicated that the tetraethyl lead content was indeed less than 0.1 μg

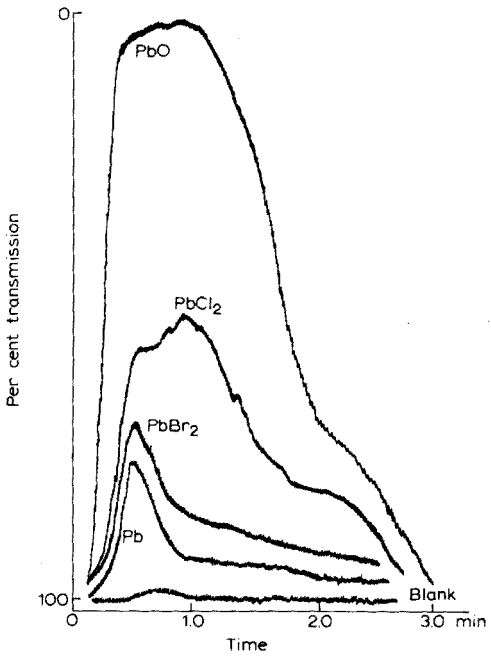

Fig. 3. Atomic absorption traces of lead arising from vapors of lead salts generated by salt crystals in a polyethylene bag maintained at room temperature.

m^{-3}, although no accurate measurements were made at this time. Tetraethyl lead could come from the simple evaporation of gasoline or from incompletely burned gasoline. Tetraethyl lead is not stable for long periods (1 h) in the atmosphere, but products of decomposition have not been completely identified.

In an effort to identify other sources of "molecular" lead, attention was directed to inorganic lead compounds. Lead halides issue from auto exhausts as airborne particulates and as aggregates which fall upon the highway. Possibly some lead could issue from the auto exhaust in the "molecular" form, but lead in this form would not be expected to remain in this form in the air for very long. However, if the vapor pressure of lead salts is significant, then appreciable amounts may arise by simple evaporation. In addition to auto exhausts, lead from natural sources would generate "molecular" lead. It was calculated that lead bromide at a pressure of 10^{-10} atm. would be sufficient to provide 1 μg Pb m^{-3} of air. Conceivably other salts also could be a source of "molecular" lead in the atmosphere. To check out this hypothesis, various lead salts were placed in porcelain crucibles and put in 1-l polyethylene bags fitted with 0.01 μm filters on closure. The vapors of lead salts were allowed to come to equilibrium with the atmosphere inside the bag; after several hours, 500 cm^3 of the air was drawn from the bag through the filter into the a.a.s. system for measurement of the "molecular" lead concentrations. The data shown in Fig. 3 show that the "molecular" lead absorption signals registered from different lead compounds were quite easily measurable.

An apparent difficulty with this reasoning is that the vapor pressure of lead salts (*e.g.* lead bromide) would not be expected to generate enough "molecular" lead to be detected at room temperature. But it must be pointed out that in the past vapor pressures of lead compounds have not been measured at room temperature but calculated from vapor pressures measured at significantly higher temperatures, and at a state of equilibrium between the gas and the normal crystal lattice; extrapolations to room temperature indicate that the vapor pressure arising from a normal lattice will be very low. However, unless special care is taken, the crystal surfaces will contain minute cracks and other faults, and the energy required for a molecule to escape is reduced near such faults. These are non-equilibrium conditions and usually such vapor must be eliminated before reproducible measurements of the true vapor pressure can be made. In practice, this source of vapor may be significant; lead bromide crystals formed rapidly in an auto exhaust, thrown onto the highway and constantly exposed to traffic, would contain an abundance of faults and could possibly be a source of vapors of lead compounds—or "molecular" lead.

Based on these data and hypotheses, it seems possible that "molecular" lead may reach the atmosphere by the following mechanism. First, the lead is burned in the automobile and leaves the exhaust as inorganic lead in the particulate form, which falls on the highway where it is exposed to traffic, sunlight and humidity. The elevated temperatures may cause slight but significant evaporation of the lead salts, generating "molecular" lead pollutants.

To check the effect of sunlight on the system, further plastic bags containing lead halide salts were exposed to sunlight for about 1 h, then 500 cm^3 of air were taken through the filter and "molecular" lead was measured as before. There was a significant increase in the "molecular" lead content, often two or three times

greater than that measured from the unexposed lead salts. These results seemed to confirm the effect of sunlight on the system. Less positive proof was found for the effect of humidity which also appears to increase the "molecular" lead content in the air.

The chemical form of lead in the air has not been determined, nor has the mechanism of lead generation, photochemical reactivity, or the ultimate fate of the lead. This problem will be studied by ESCA.

Health effects

The health effects of particulate lead in the atmosphere have been a source of controversy for several years; the subclinical effects appear to be serious. Pollutants in the particulate form are fairly easily removed by the nose from the air train, and so must go through the digestive system before they can reach the blood stream. However, if lead is in the "molecular" form, it can go to the lungs, and may then directly enter the blood stream. "Molecular" lead might then pose a more serious health hazard than particulate lead.

Studies must be made to find out the effects of lead pollutants under conditions of high temperature and humidity. Health effects can be estimated only when the compounds present, their source, their concentrations and their final chemical and physical fates are known.

Preliminary studies have also shown the presence of "molecular" cadmium. It is quite conceivable that this is a general phenomenon and that numerous metal compounds exist in the air in the vapor state. This is an addition to molecular arsenic, selenium and mercury. Detection and determination of these metals will be reported on at a later date.

The authors wish to thank the Environmental Protection Agency for financial support under Grant Number R. 800771.

REFERENCES

1 J. W. Robinson and D. K. Wolcott, *Environ Lett.*, 6 (1974) 321.
2 A. Loveskog, *Int. Clean Air Congr. Proc.*, 2nd, Washington, 1970.

Analytica Chimica Acta, 78 (1975) 479–482

SHORT COMMUNICATION

The incremental evolution, collection and determination of mercury in soils at the p.p.b. level as a function of temperature

A. B. CAREL
Continental Oil Company, Ponca City, Oklahoma 74601 (U.S.A.)
(Received 11th February 1975)

Various approaches to analyses for mercury in soils are presented in the literature. These include flameless atomic absorption[1], combustion–atomic absorption[2], x-ray fluorescence[2], silver amalgamation and atomic absorption[3], and evolution and amalgamation on preweighed gold or silver foil[4]. Thermal curves, obtained by atomic absorption of mercury released during controlled continuous heating, were used by Watling[5] to identify the release temperature of various known inorganic mercury compounds synthetically mixed in rock samples.

Wimberley[6] recently used an induction furnace at *ca.* 1,000°C to liberate the total mercury from soil and other samples, amalgamating and desorbing the mercury from gold and sweeping the released mercury through a long cell while measuring the absorption of the mercury vapor at 253.7 nm. This method can be used routinely to assay a variety of samples for total mercury, but it is difficult to determine the temperature at which the various portions of the total mercury are being released. In this communication, the DuPont Model 950 TGA instrumentation was used to volatilize the mercury from soil samples in preselected temperature ranges. The mercury was amalgamated on gold screens contained in train assemblies attached to the TGA furnace. The amalgamated mercury was then liberated and determined as described by Wimberley[6].

Construction and description of equipment

The glass train containing the gold screen and associated gas scrubbers which was attached to the DuPont TGA balance assembly is shown in Fig. 1. The nitrogen sweep gas at 100 ml min^{-1} enters the TGA balance assembly through a tube of silver gauze, which scrubs the nitrogen of interfering materials, and then passes through the furnace tube containing the soil sample. The soil sample (*ca.* 1 g) is contained in a Coors porcelain boat No. 2 resting inside the furnace tube and centered midway in the furnace. The evolved gas is passed through a K_2CO_3–$Mg(ClO_4)_2$ scrubber[6], through a three-way valve used to divert the flow as the various mercury increments are evolved, then through the gold screen where the mercury is amalgamated, and finally exits through another silver gauze scrubber to prevent back-diffusion of interferents. Ball and joint sockets are used for rapid removal of the glass train containing the gold screen. The gold screens

were formed from 1-in. circles of 100-mesh screen so as to fit snugly into the recess of the glass holder. When the released mercury had been collected from the desired temperature range of interest, the gold screen was removed, and the amount of mercury collected was determined by the method of Wimberley[6].

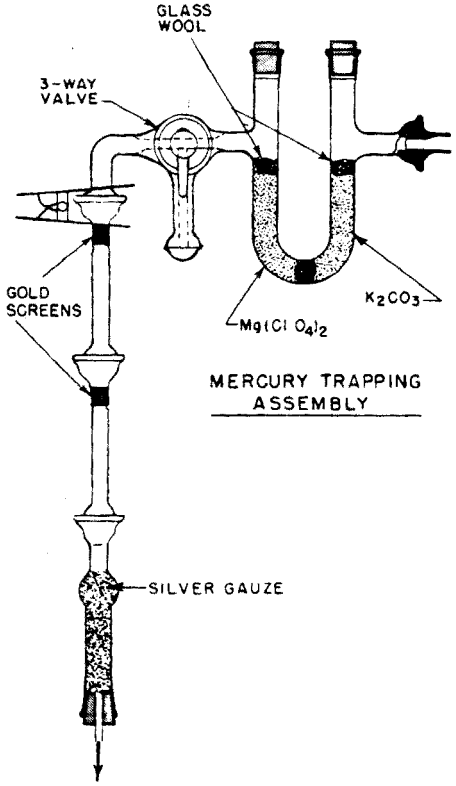

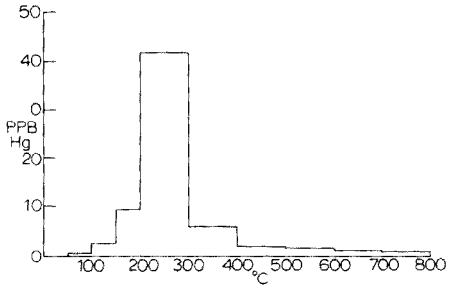

Fig. 1. Mercury trapping assembly.

Fig. 2. Mercury evolved *vs.* temperature for soil sample 1.

Results and discussion

Experiments were made with as many as three gold traps connected in series (Fig. 1). Mercury vapor was injected into the Tygon tubing upstream of the TGA but below the silver gauze trap, with nitrogen flows of 100 and 1,000 ml min^{-1}; the amalgamated mercury on the individual gold screens was then determined by the Leco method[6]. Negligible mercury concentrations were found on the second and third traps at nitrogen flow rates of 100 ml min^{-1}; however, three successive gold traps would not completely collect the mercury at flow rates of 1,000 ml min^{-1}. It was necessary to scrub the TGA furnace tube thoroughly after each soil analysis to obtain reproducible results.

The temperature programming of the TGA instrument and the ability to hold a specific temperature, provide a wide variety of operating conditions for evolving the mercury from a soil sample. An example of the TGA conditions and the mercury data obtained on duplicate 1.0-g soil samples is shown in Table I.

TABLE I

SUMMARY OF MERCURY DATA OBTAINED FROM SOIL SAMPLES BY TGA AND LECO METHODS

TGA conditions[a]	*Hg found (p.p.b.)*	
	Sample 1	*Sample 2*
Ambient–50°C	0.1	0.2
50–100°C	0.4	0.3
100–150°C	2.4	2.3
150–200°C	9.5	9.5
200–300°C	41.7	41.5
300–400°C	6.0	4.1
400–500°C	1.7	0.9
500–600°C	1.3	0.5
600–700°C	0.9	0.5
700–800°C	0.6	0.4
Total	64.6	60.2
Leco standard Hg analysis of TGA 800°C residue	< 1.0	< 1.0
Leco standard Hg analysis of total sample	72–72	73–75
TGA from 20°C to 800°C and hold 15 min.		
Collect total sample on a single gold trap	59	59

[a] The temperature programming was 5°C min^{-1} for the first 4 ranges and 20°C min^{-1} for subsequent ranges. In all cases, the temperature at the top of each range was held for 15 min.

The released mercury was collected in 50°C-increments from ambient to 200°C and in 100°C-increments from 200°C to 800°C. (Fig. 2). Also included are the analyses of the total samples by collecting the total TGA mercury evolved from ambient to 800°C on a single gold screen and the analyses of the total samples by the Leco[6] method.

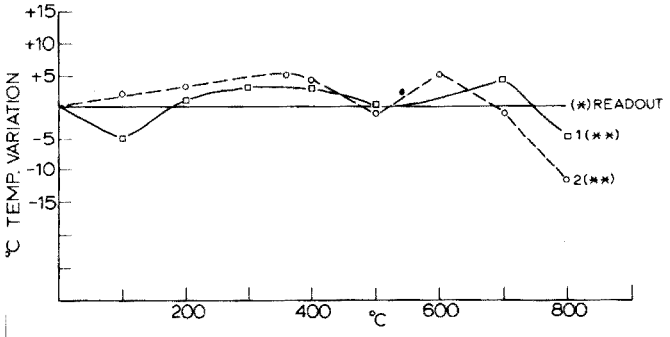

Fig. 3. Soil temperature by pyrometer (1) when programming at 5 C. Min^{-1} *vs.* TGA readout, (2) after holding 5 min at TGA readout temperature. (*) Thermocouple in center of quartz tube above sample. (**) Thermocouple in soil sample in ceramic boat sitting in quartz tube.

Figure 3 shows the temperature variations obtained by measuring the temperature of the soil sample (with a Leeds and Northrup potentiometer) as it was being heated in the TGA furnace assembly under conditions similar to those

used in the standard analysis. The temperature variation (thermocouple in the soil sample) *versus* TGA readout (where the TGA thermocouple is located in the center of the quartz tube above the soil sample) is $\pm 5°C$ in the range of ambient to 700°C and $\pm 12°C$ from 700°C to 800°C.

The method described provides a means of determining the temperature at which mercury is released from soil samples. Standard inorganic mercury compounds can be added to soil samples as described by Watling[5] for identification of the types of mercury compounds released from specific samples.

REFERENCES

1 R. Hatch and W. T. Ott, *Anal. Chem.*, 4 (1968) 2085.
2 H. G. Henry, K. R. Stever, W. L. Barry and H. H. Heady, *Allied Spectrosc.*, 26 (1972) 288.
3 W. W. Vaughn, *U.S. Geol. Surv. Circ. 540*, 1967.
4 W. W. Whitton, *Calif. J. Technol.*, 4 (1904) 35.
5 B. J. Watling, *Trans. Inst. Min. Metall., Sect. B*, 81 (1972) 47.
6 J. W. Wimberley, *Anal. Chim. Acta*, 76 (1975) 337.

Analytica Chimica Acta, 78 (1975) 483–486

SHORT COMMUNICATION

Fluorescence of gentisic acid

MERIAN S. STALLINGS and STEPHEN G. SCHULMAN
College of Pharmacy, University of Florida, Gainesville, Florida 32610 (U.S.A.)
(Received 17th January 1975)

Gentisic acid (2,5-dihydroxybenzoic acid or 5-hydroxysalicylic acid) is a minor metabolite of salicylic acid and aspirin and has been employed in the palliative treatment of rheumatoid arthritis[1]. Little information about the electronic absorption or fluorescence of gentisic acid appears to be available. As a result of our interest in the electronic structure, analytical toxicology and chemistry of this compound, the present study of the solvent and acidity dependences of its electronic spectra was undertaken.

Experimental

Apparatus. Absorption spectra were taken on a Beckman DB-GT spectrophotometer. Fluorescence spectra were taken on a Perkin-Elmer MPF-2A fluorescence spectrophotometer whose monochromators were calibrated against the xenon line emission spectrum and whose output was corrected for instrumental response by means of a rhodamine-B quantum counter. An Orion Model 801 pH meter, with a Beckman silver–silver chloride-glass combination electrode, was used.

Reagents. Gentisic acid (Eastman Organic Chemicals, Inc.) was recrystallized from chloroform.

Chloroform (Matheson, Coleman and Bell, Inc., spectroquality) and sulfuric acid (Mallinckrodt Chemical Works) were used without further purification. Distilled–deionized water was used to make dilutions of the sulfuric acid and to prepare acetate, phosphate, and borate buffers as well as sodium hydroxide solutions for absorption and fluorescence titrimetric studies. The sodium acetate, sodium borate, and mono- and dibasic sodium phosphate buffer solutions were $\leqslant 1 \cdot 10^{-3}$ M in each buffer ion to avoid reactions with the excited gentisic acid species.

Results

The long-wavelength absorption maxima and fluorescence maxima of gentisic acid in representative regions of the Hammett acidity and pH scales are presented in Table I.

The ground-state dissociation constants (pK_a) for the equilibria between the various prototropic species derived from gentisic acid were estimated from the midpoints of the variations of the absorption spectra with pH and Hammett acidity (absorptiometric titrations) and are presented in scheme 1, below.

TABLE I

LONG-WAVELENGTH ABSORPTION (λ_a) AND FLUORESCENCE (λ_f) MAXIMA OF GENTISIC ACID IN AQUEOUS MEDIA

	λ_a (nm)	λ_f (nm)
18 *M* H_2SO_4 (cation)	340	[a]
1 *M* H_2SO_4 (uncharged species)	328	[a]
pH 7 phosphate buffer (monoanion)	318	442
0.01 *M* NaOH (dianion)	330	437

[a] Fluorescence was not observed from gentisic acid in the Hammett acidity and pH regions where the cation and neutral molecules were excited.

Discussion

The long-wavelength absorption maxima of the various species derived from gentisic acid lie[2] at longer wavelengths than their counterparts in unsubstituted salicylic acid. This shows that the lone-pairs of the oxygen atom in the 5-position are substantially involved in the transition to the lowest excited singlet state (the ^1L_b state). The successive shifts to shorter wavelengths upon dissociation of the cation and the neutral molecule are analogous to those in salicylic acid, and correspond[2] to dissociation of the protonated carboxyl group of the cation and neutral carboxyl group of the neutral molecule, respectively. The shift of the absorption spectrum of the singly charged anion to longer wavelengths, near pH 10, corresponds[3] to dissociation of the 5-hydroxy group and has no counterpart in salicylic acid[2]. The shift to longer wavelengths indicates the greater degree of interaction of the lone-pairs on the charged hydroxy group, relative to those on the undissociated 2-hydroxy group, with the carboxylate function in the lowest excited singlet state. The potentiometric pK_a values[4] of 2.97 and 10.50 previously reported are in agreement with the values obtained spectrophotometrically in these experiments. Above pH 12, the 2-hydroxy group is ionized. However, as the pH is raised above 12, the titration medium becomes pink to red in color and a complex indeterminate array of spectral bands appears. Although it is possible to estimate a pK_a value of 13.9 from the disappearance of the dianion absorption, the spectral properties of the trianion are uncertain; the trianion is probably oxidized rapidly to a *p*-benzoquinone. The proposed sequence of ground state protolytic equilibria of gentisic acid is shown below:

Scheme 1

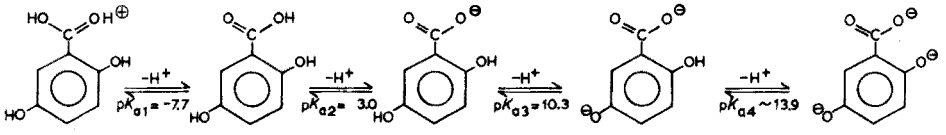

(1)

In concentrated sulfuric acid and aqueous sulfuric acid solutions, gentisic acid is non-fluorescent. However, a blue-green fluorescence at 442 nm appears above

pH 1.5 and rises to maximum intensity at about pH 4.5. The midpoint of this fluorometric titration occurs at pH 3.0 and therefore coincides with the ground state pK_a. Consequently, it may be assumed that the cation and neutral molecule, derived from gentisic acid, do not fluoresce and that the fluorescence above pH 2 must arise from direct excitation of the singly charged anion. However, the wavelength of fluorescence is much too long to originate from the monoanion depicted in scheme 1 and is in the general region where the monoanion of salicylic acid fluoresces[2]. Consequently, it is presumed that the phototautomerism which accounts for the unusually long wavelength of fluorescence in salicylate also explains the anomalous fluorescence wavelength of the gentisate monoanion. The phototautomerism of the gentisate monoanion is represented in scheme 2; G represents the ground-state (absorbing) monoanion and E represents the excited-state (fluorescing) anion.

Scheme 2

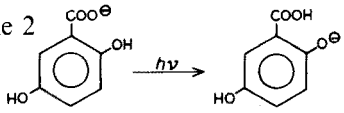

G E (2)

The fluorescence of the gentisate monoanion remains constant in intensity from pH 4.5 to *ca.* pH 9. Above pH 9 the fluorescence of the monoanion is quenched and there is a slight blue shift to 437 nm. This process is complete at about pH 12 and is centered at pH 10.3 or $pH = pK_{a3}$. Apparently, this spectroscopic transformation corresponds to the ionization of the 5-hydroxy group, in the ground-state, to form the dianion. Since the ionization of the 5-hydroxy group is accompanied by a red shift of the long-wavelength absorption maximum and might also be expected to produce a red shift of the fluorescence spectrum of the phototautomer, it is concluded that in the dianion, phototautomerization does not occur subsequent to excitation. Thus, the dianion represented in scheme 1 is the species responsible for fluorescence at 437 nm. The fluorescence of only the dianion can be observed from pH 12–H_- 16.9. However, in this interval its intensity rises with increasing NaOH concentration. At $H_- \geqslant 16.9$ there is a fluorescence red shift to 460 nm, probably as a result of dissociation of the 2-hydroxy group to form the trianion. However, because of the erratic behavior of the fluorimetric titration in concentrated NaOH solutions, attributed to the same oxidation process which interfered with the absorptiometry in basic solution, definite conclusions cannot be drawn regarding this aspect of the fluorimetric titration.

From the analytical point of view, it is relatively unimportant that the emission in concentrated basic media cannot be quantified because the intensity of fluorescence of the dianion and the trianion are about five hundred times less than that of the monoanion. The fluorescence of the monoanion is detectable down to about $3 \cdot 10^{-9}$ *M* (comparable to the limit of detection of salicylate by fluorimetry), in the pH interval 5.0–9.0, where its intensity is constant and maximal. Consequently, these pH conditions are optimal for the fluorimetric analysis of gentisic acid in aqueous media. It is possible to determine gentisic acid in the presence of salicylic acid if the latter is not in great excess. By adjusting to pH 5–9, where the intense fluorescences of the monoanions of both molecules occur, and monitoring the total fluorescence intensity at, say 440 nm, and then changing to pH 12–14 or to pH < 1,

where only salicylic acid fluoresces intensely. The concentration of gentisic acid can be determined by difference.

Although gentisic acid does not fluoresce in water at pH values where the uncharged molecule exists, it fluoresces moderately at 408 nm in chloroform. This suggests that the failure of the neutral molecule to fluoresce is caused by solvent quenching of the excited neutral molecule or zwitterion. It is not known at present if this is a general phenomenon for 5-substituted salicylic acids.

REFERENCES

1 C. O. Wilson and O. Gisvold, *Textbook of Organic, Medicinal and Pharmaceutical Chemistry*, Lippincott, Philadelphia, 4th edn., 1962, pp. 65, 594.
2 P. J. Kovi, C. L. Miller and S. G. Schulman, *Anal. Chim. Acta*, 61 (1972) 7.
3 W. L. Paul and S. G. Schulman, *Anal. Chim. Acta*, 69 (1974) 195.
4 J. Tsin-jao, L. Sommer and A. O. Rae, *Collect. Czech. Chem. Commun.*, 27 (1962) 1171.

Analytica Chimica Acta, 487–491

SHORT COMMUNICATION

Dual-wavelength spectrophotometry

Part V. Increased sensitivity in inorganic spectrophotometry

SHOZO SHIBATA, MASAMICHI FURUKAWA and TADASHI HONKAWA
Government Industrial Research Institute, Kita-ku, Nagoya (Japan)
(Received 24th February 1975)

Although the dual-wavelength technique is used primarily for the rapid measurement of small absorbance changes at fixed pairs of wavelengths in turbid materials[1], it is also useful for the measurement of transparent solutions. Previous papers in this series[2–5] dealt with the general technique and analytical advantages of dual-wavelength spectrophotometry. Related papers have subsequently appeared[6–12], and the analytical potentialities of dual-wavelength spectrophotometry have been reviewed[13,14]. In this paper, the application of the dual-wavelength technique to inorganic spectrophotometry with highly sensitive chromogenic reagents is reported.

Principle of the method

Since the dual-wavelength technique is not yet very familiar in analytical chemistry, the principle involved and important problems related to this communication are briefly described. In dual-wavelength measurement, light from a highly stabilized tungsten–iodide or deuterium lamp is divided into two beams in two grating monochromators. The light beams of different wavelength from the two gratings are time-shared through a single cell by means of a rotating sector, and the difference in absorbance ΔA between the absorbances at wavelengths λ_1 and λ_2 is measured. Even a very slight change in the absorbance of a sample can be determined accurately with the maximum scale expansion range of absorbance because the various sample and cell errors which may occur in classical spectrophotometry are eliminated; only one cell is used and the radiation at λ_1 and λ_2 is incident on the same position of the cell. A schematic reprentation of the principle of the method is shown in Fig. 1.

The photosignals are converted to electrical signals by means of a head-on

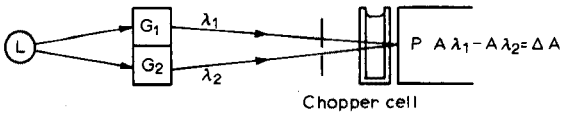

Fig. 1. Principle of dual-wavelength spectrophotometry. (L) lamp; (G_1, G_2) grating; (P) photomultiplier.

type photomultiplier and are led into the gate circuit through the pre-amplifier. The gate circuit, operated by reference signals synchronized with the chopper, transmits alternate signals in the sequence λ_1 signal, zero signal, λ_2 signal, zero signal and so on, to the respective hold circuits provided for the λ_1, λ_2 and zero signals. Undesirable influences such as light source fluctuation are removed automatically by controlling the voltage applied to the photomultiplier by means of the reference signal (λ_1 signal), to hold the difference between the applied voltage and the reference voltage constant at zero. The signal-hold circuit feeds back this output to give a correction which makes the pre-amplifier output zero when no photosignal is received. This prevents any spurious signals that may be caused by the dark current of the photomultiplier or stray light. The λ_2 signal is used as the sample signal, and linear recording is made either of transmittance or, through a log converter, of absorbance. By these electrical techniques the peak noise is reduced to 0.0002 of the absorbance. The absorbance scale is therefore expanded one hundred-fold in comparison with conventional spectrophotometers, and this technique is useful for measuring very small amounts of samples and for observing the behaviour of substances in very low absorbance ranges.

Highly sensitive inorganic spectrophotometry

Many highly sensitive chromogenic reagents for metals with molar absorptivities of the order of 10^5 are now known. In this paper, analogs of 4-(2-pyridylazo)-1,3-diaminobenzene (PADAB) are used for the determination[15,16] of micro- amounts of cobalt. The principle of the method is simple. Figure 2 shows the absorption spectra of the cobalt-3,5-diCl-PADAB (4-[(3,5-dichloro-2-pyridyl)azo]-1,3-diaminobenzene) chelate against a water blank, and Fig. 3 shows the differential absorption spectra against a reagent blank.

In the conventional method the net absorbance at maximum wavelength against water or reagent is measured. In dual-wavelength measurements, λ_1 is set to the wavelength for the absorption peak of the chelate and λ_2 to the wavelength for the absorption peak of the reagent. The decrease in the reagent absorption

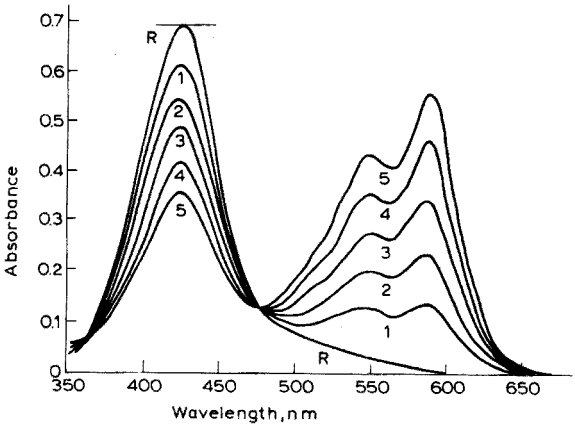

Fig. 2. Absorbance curves of 3,5-diCl-PADAB(R) and its cobalt complex in 3 *M* hydrochloric acid solution. Reagent, $1.9 \cdot 10^{-5}$ *M*; Cobalt, $\times 10^{-6}$ *M* 1) 1, 2) 2, 3) 3, 4) 4, and 5) 5.

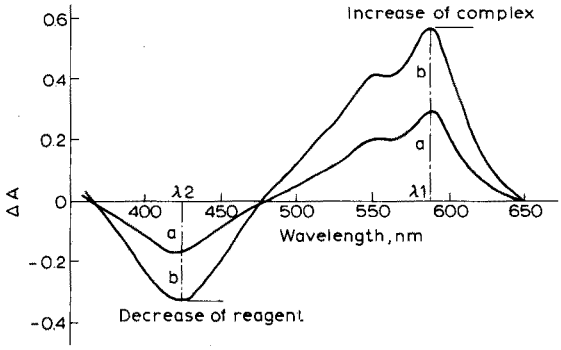

Fig. 3. Differential absorption spectra of cobalt complexes. $\Delta A = A_{\lambda_1} - (-A_{\lambda_2}) = A_{\lambda_1} + A_{\lambda_2}$.

caused by the chelate reaction is directly additive to the change in absorbance caused by the chelate formation in the reaction, so that the apparent molar absorptivity of the cobalt chelate is increased appreciably.

Experimental

Standard cobalt solution. High-purity metal wire (99.99%) was dissolved in nitric acid (1 + 1) and 10 ml of perchloric acid was added. The mixture was evaporated until fumes of perchloric acid appeared. After cooling, the solution was diluted to 1 l with redistilled water.

5-Cl-PADAB (4-[(5-chloro-2-pyridyl)azo]-1,3-diaminobenzene) and 3,5-diCl-PADAB solution. Ethanolic 10^{-3} *M* solutions were prepared from the pure reagents synthesized in this laboratory: 5-Cl-PADAB is available from Merck.

Apparatus. A Hitachi 356 two-wavelength spectrophotometer was used with 1-cm cells. This apparatus can be used as a dual-wavelength and as a conventional double-beam spectrophotometer.

Procedure. To a 25-ml volumetric flask, transfer a suitable aliquot of sample solution containing up to 0.1 p.p.m. of cobalt, and add 0.1–0.2 ml of ethanolic 0.05%

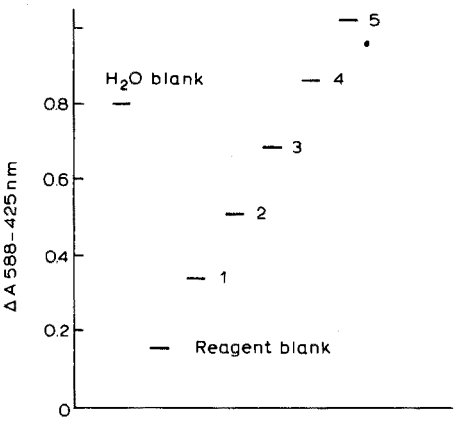

Fig. 4. Calibration data for the determination of cobalt with 3,5-diCl-PADAB. Concentrations of 3,5-diCl-PADAB and cobalt as in Fig. 2.

reagent solution. Adjust to pH 5.0 with 0.2 *M* sodium acetate–0.2 *M* acetic acid buffer solution, and mix. Then add 10 ml of (1+1) hydrochloric acid, dilute to volume, and mix. Measure the absorbance for λ_1 588 nm and λ_2 425 nm.

Results and discussion

Figure 4 shows the results of dual-wavelength measurements in which λ_1 and λ_2 were set at 588 and 425 nm, respectively, to determine the peak-to-peak distance $\Delta A_{588-425\ nm}$. Since Beer's law holds good at each wavelength, it is evident that ΔA is proportional to the concentration. This was verified by the conventional

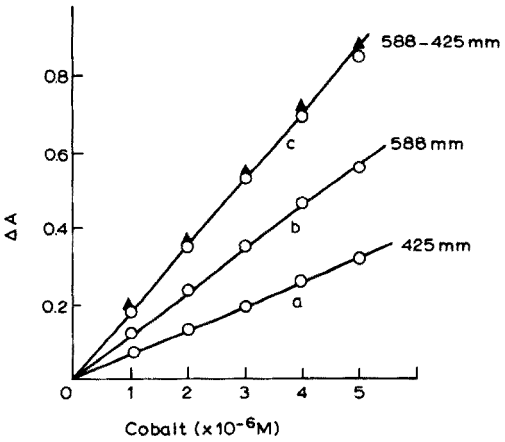

Fig. 5. Confirmation of the dual-wavelength method by the conventional technique. a) Decrease of reagent (Initial concentration, $1.9 \cdot 10^{-5}$ *M*; in reality these values are negative), b) Increase of cobalt complex, c) Dual-wavelength measurements, ▲ calculated value.

method and calculation; the results obtained are shown in Fig. 5, where curve *a* corresponds to the decrease of the reagent absorbance, curve *b* to the increased absorbance of the cobalt chelate, and curve *c* shows the agreement between the dual-wavelength measurement and the calculated value. The small differences between the experimental and calculated values are probably caused by the small absorption of the reagent at 588 nm. The preferable conditions for this method are therefore that the coloured complex formed should be stable, and the absorption of the reagent should be as small as possible at the maximum wavelength of the coloured complex, although this is not a necessary condition.

TABLE I

DETERMINATION OF P.P.B. AMOUNTS OF COBALT WITH 5-Cl-PADAB

Cobalt taken (p.p.b.)	*Absorbance*[a]	*Cobalt found (p.p.b.)*
2.0	0.0056±0.0003	1.9
4.0	0.0115±0.0005	3.9
8.0	0.023±0.002	7.8

[a] Average of 3 results.

The calibration curve for 1–4 p.p.b. of cobalt with 5-Cl-PADAB was linear through the origin, with a slope corresponding to a value for $\Delta A_{570-424\ nm}$ of 0.0028 per p.p.b. of cobalt. Consequently, up to 5 p.p.b. amounts of cobalt can be determined with reasonable accuracy; the results for synthetic cobalt samples are shown in Table I. The dual-wavelength method increases the apparent molar absorptivity of the cobalt–5-Cl-PADAB complex from $1.13 \cdot 10^5$ l mole^{-1} cm^{-1} to $1.75 \cdot 10^5$ l mole^{-1} cm^{-1}.

REFERENCES

1 B. Chance, *Science*, 120 (1954) 767.
2 S. Shibata, M. Furukawa and K. Goto, *Anal. Chim. Acta*, 46 (1969) 271.
3 S. Shibata, M. Furukawa and K. Goto, *Anal. Chim. Acta*, 53 (1971) 369.
4 S. Shibata, K. Goto and Y. Ishiguro, *Anal. Chim. Acta*, 62 (1972) 365.
5 S. Shibata, M. Furukawa and K. Goto, *Anal. Chim. Acta*, 65 (1973) 49.
6 Y. Morita and T. Yoneda, *Bunseki Kagaku*, 22 (1973) 1028.
7 Y. Morita, K. Ogure and A. Nomura, *Bunseki Kagaku*, 22 (1973) 1147.
8 S. Maeda, H. Kobayashi and K. Ueno, *Bunseki Kagaku*, 22 (1973) 1365.
9 T. Inoue, M. Tatsuzawa, Mei-shen Lo and Y. Tanaka, *Bunseki Kagaku*, 23 (1974) 1289.
10 T. Honkawa, *Anal. Lett.*, 7 (1974) 575.
11 M. Sangal, V. Sitakara Rao and K. B. De, *Z. Anal. Chem.*, 271 (1974) 208.
12 T. Kato, H. Kuzuya and T. Nagatsu, *Biochem. Med.*, 10 (1974) 320.
13 T. J. Porro, *Anal. Chem.*, 44 (1972) 93A.
14 S. Shibata and M. Furukawa, *Bunseki Kagaku*, 23 (1974) 1545.
15 S. Shibata, M. Furukawa, Y. Ishiguro and S. Sasaki, *Anal. Chim. Acta*, 55 (1971) 231.
16 S. Shibata, M. Furukawa and K. Goto, *Anal. Chim. Acta*, 71 (1974) 85.

Analytica Chimica Acta, 78 (1975) 492–494

SHORT COMMUNICATION

Periodate oxidation analysis of carbohydrates

Part V. Spectrophotometric determination of periodate with phenolphthalin

SUSUMU HONDA, KIMIKO ADACHI, KAZUAKI KAKEHI, HIDETAKA YUKI and KIYOSHI TAKIURA

Faculty of Pharmaceutical Sciences, Osaka University, Toneyama, Toyonaka, Osaka-fu (Japan)

(Received 14th January 1975)

Determination of the amount of periodate reduced in the Malaprade reactions of α-glycols and α-hydroxycarbonyls provides useful structural information for carbohydrates. The usual titrimetric determinations of periodate[1–3] require more than 10 μmole of sample. An ultraviolet spectrophotometric method[4] and electrometric methods[5,6] have been suggested to provide greater sensitivity. In the present communication, a simple spectrophotometric method, based on the oxidation of phenolphthalin is described.

Experimental

Materials. Reagent-grade phenolphthalin (Tokyo Kasei Kogyo Co., Ltd.) was used without further purification. Samples of carbohydrates were of the highest grade commercially available. Other chemicals and solvents were of reagent grade.

Apparatus. A Shimazu UV-200 spectrophotometer was used with 1-cm cells.

Standard procedure for the determination of periodate. To a sample solution (1.00 ml) containing *ca.* 1 μmole of periodate, add an ethanolic $6 \cdot 10^{-3}$ *M* phenolphthalin solution (5.00 ml), and $5 \cdot 10^{-2}$ *M* phosphate buffer (pH 11.6, 10.0 ml). After 8 min, add $2 \cdot 10^{-1}$ *M* sodium sulfite (1.00 ml), and read the absorbance at 555 nm. Prepare a calibration curve in the same way with 1-ml aliquots of standard periodate solutions in the range $3 \cdot 10^{-4}$–$4 \cdot 10^{-3}$ *M* periodate.

Oxidation of carbohydrates with periodate. To a 10^{-2} *M* solution (5.00 ml) of a carbohydrate sample add 10^{-1} *M* sodium metaperiodate (5.00 ml), and maintain the solution at 25°C, shielding from the light. Dilute aliquots (1.00 ml) to 25.0 ml at specific reaction times, and determine the amounts of periodate in these solutions as described above.

Analysis of alditols. Mix equal volumes of a $4 \cdot 10^{-4}$ *M* sample solution and $4 \cdot 10^{-3}$ *M* sodium metaperiodate, and maintain the solution at 25°C, shielding from light. Determine the concentration of periodate after 1 h as described above.

Results and discussion

The reaction between phenolphthalin and periodate. Phenolphthalin is oxidized

by periodate in alkaline solutions to produce a red color, which shows an absorption maximum at 555 nm. When the hydrogen ion concentration of the added phosphate buffers is varied, the absorbance shows a plateau in the pH range 11.3–11.7. At pH 11.6, the reaction between phenolphthalin and periodate is quite rapid, and the absorbance reaches a plateau value after 8 min. The absorbance is, however, only half of that given by an equimolar amount of phenolphthalein.

After the periodate reaction, the gradual increase in absorbance caused by atmospheric oxidation of phenolphthalin can be prevented by the addition of sodium sulfite; absorbances then remain constant for at least 24 h.

The reagent solution. Ethanol was used to dissolve the phenolphthalin; precipitation occurred in solutions above $6 \cdot 10^{-3}$ *M*. The use of other solvents, *e.g.* methanol and 2-methoxyethanol, gave results which did not differ significantly from those obtained with ethanol. The reagent solution was stable for at least a week.

Calibration. Under the recommended conditions, the calibration graph for periodate was linear over the range $3 \cdot 10^{-4}$–$4 \cdot 10^{-3}$ *M* periodate. The relative standard deviation over this range was about 3.3%.

Interferences. The effects of iodate and some typical aldehydic fragments formed from carbohydrate samples by oxidation were examined. In the determination of 1 μmole of periodate, there was no interference from 1 μmole of formaldehyde, formic acid or a dialdehyde prepared by periodate oxidation of methyl-α,D-glucopyranoside; 1 μmole of iodate did not interfere, while 10 μmoles caused a positive error of only 2%.

Periodate consumption of carbohydrates. The amounts of periodate reduced by various carbohydrates were determined by the proposed method, and the results were compared with those obtained by the standard titrimetric method[3]. Table I shows that good agreement was found.

TABLE I

PERIODATE CONSUMPTION OF SELECTED CARBOHYDRATES[a]

Carbohydrate	*Phenolphthalin method*		*Titrimetric method*[b]	
	3 h	*24 h*	*3 h*	*24 h*
D-Glucose	4.80	4.97	4.94	4.94
D-Fructose	4.00	4.21	4.02	4.25
L-Rhamnose	3.58	3.62	3.56	3.64
D-Sorbitol	5.02	5.00	5.02	5.01
D-Glucuronic acid	4.90	4.93	5.02	5.07
D-Glucono-δ-lactone	5.33	5.50	5.43	5.47
Cellobiose	4.22	4.88	4.33	4.94
Sucrose	2.80	3.11	2.89	3.08
Raffinose	4.72	5.45	4.78	5.34

[a] Oxidation in an unbuffered medium at 25°C; concentration of carbohydrate, $5 \cdot 10^{-3}$ *M*; initial concentration of sodium metaperiodate, $5 \cdot 10^{-2}$ *M*. Consumption of periodate in mole/mole of carbohydrate.

[b] Method of Fleury and Lange[3].

The method was also used for the determination of alditols. The amounts of periodate reduced after 1 h by $2 \cdot 10^{-4}$ *M* solutions of erythritol, D-xylitol and

D-sorbitol were 101%, 98.8% and 99.8%, respectively, of the theoretical amounts. the relative standard deviations (10 determinations) being 2–3%.

REFERENCES

1 E. Müller and O. Friedberger, *Ber. Bunsenges. Phys. Chem.*, 35 (1902) 2652.
2 L. Malaprade, *C. R. Acad. Sci.*, 186 (1928) 382; *Bull. Soc. Chim. Fr.*, 43 (1928) 683.
3 P. F. Fleury and J. Lange, *J. Pharm. Clin.*, 17 (1933) 107; 17 (1933) 196.
4 J. S. Dixon and D. Lipkin, *Anal. Chem.*, 26 (1954) 1092.
5 K. Takiura and K. Koizumi, *Yakugaku Zasshi*, 78 (1958) 961.
6 S. Honda, K. Sudo, K. Kakehi and K. Takiura, *Anal. Chim. Acta*, 77 (1975) 274.

Analytica Chimica Acta, 78 (1975) 495–497

SHORT COMMUNICATION

Reaction of thioureas with the Folin–Ciocalteu reagent

EMMANUEL T. RAKITZIS

Department of Biological Chemistry, University of Athens Medical School, Athens 620 (Greece)

(Received 21st February 1975)

The Folin–Ciocalteu reagent[1] yields a blue colour with phenolic compounds, cysteine[2], and some buffers and monosaccharides when present in high concentration[3,4]. The present communication reports that thioureas also react with the Folin–Ciocalteu reagent to give a blue colour which may form the basis for a photometric determination of these compounds.

Experimental

Apparatus. Absorbances (1-cm light path) were read with a Gilford spectrophotometer.

Reagents. All reagents were of analytical grade. Thiourea, diphenylthiourea (Fluka), phenylthiourea (Macalaster Bicknell Co.), S-methylisothiourea (Kahl) and Folin–Ciocalteu reagent (Fisher Scientific Co.) were used.

Procedure. The standard procedure for the determination of phenolic amino acids in trichloroacetic acid filtrates of biological materials was used[5]. Dissolve the sample in 0.5 *M* sodium hydroxide; to 4 ml of the solution add 2 ml of 5% (w/v) trichloroacetic acid, followed by 1 ml of freshly diluted (1+2, v/v) Folin–Ciocalteu reagent. After a few minutes measure the absorbance at 700 nm.

Results and discussion

The visible absorption spectra given by the four compounds tested were identical to that of tyrosine. Figure 1 shows that a straight-line relationship exists between concentration and absorbance for phenylthiourea, diphenylthiourea, and S-methylisothiourea. The molar absorptivity calculated from the data of Fig. 1 is 11,100 l mole^{-1} cm^{-1} for phenylthiourea, 17,800 l mole^{-1} cm^{-1} for diphenylthiourea, and 5,800 l mole^{-1} cm^{-1} for S-methylisothiourea. These values were reproducible and are higher, for two of the compounds tested, than that of tyrosine[1,6]. For thiourea the graph curves upwards, suggesting that association phenomena are taking place.

The pH of the reaction of phenolic compounds with the Folin–Ciocalteu reagent is critical[1,7]. When the trichloroacetic acid was replaced with water, the absorbances were about 70% of those shown in Fig. 1.

The principal component of the Folin–Ciocalteu reagent is phosphomolybdic acid, which reacts with thiourea to give a blue colour[8,9]. It has also been

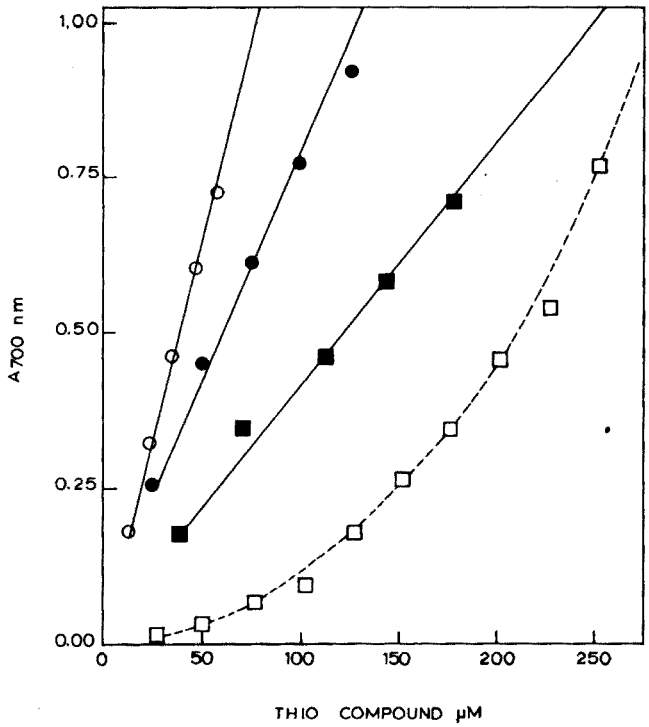

Fig. 1. Dependence of colour formation on the concentration of the thio compound used. Phenylthiourea (●), diphenylthiourea (○), S-methylisothiourea (■), and thiourea (□). For thiourea the actual concentrations are 40 times higher than shown. Concentrations refer to values in the final trichloroacetic acid–alkali–phenol reagent mixture.

observed that amidinothiourea gives a precipitate with phosphomolybdic acid[10]. Reaction of the Folin–Ciocalteu reagent with thioureas may occur because these compounds exist in a thio–thiol equilibrium mixture[11].

Analytical methods for thioureas, which have been summarized[11,12], appear to be far from adequate, and frequently require the use of nonaqueous media. The present findings offer an alternative in this respect. The Folin–Ciocalteu reagent may also be useful for the determination of isothiocyanates, after conversion to the corresponding thioureas[13,14].

REFERENCES

1 O. Folin and V. Ciocalteu, *J. Biol. Chem.*, 73 (1927) 627.
2 S. Chou and A. Goldstein, *Biochem. J.*, 75 (1960) 109.
3 M. A. Peters and J. R. ,Fouts, *Anal. Biochem.*, 30 (1969) 299.
4 J. O'Sullivan and G. E. Mathison, *Anal. Biochem.*, 35 (1970) 540.
5 M. L. Anson, *J. Gen. Physiol.*, 22 (1938) 79.
6 E. T. Rakitzis, *Biochem. J.*, 141 (1974) 601.
7 O. H. Lowry, N. J. Rosebrough, A. L. Farr and R. J. Randall, *J. Biol. Chem.*, 193 (1951) 265.
8 B. E. Reznik and L. P. Tsyganok, *Zh. Anal. Khim.*, 19 (1964) 584.
9 F. Feigl, *Spot tests in organic analysis*, Elsevier, Amsterdam, 7th edn., 1966, p. 131.

10 F. C. Garcia and S. C. Selva, *Anales Real. Soc Espan. Fis. Quim., Ser. B.*, 61 (1965) 875.
11 M. B. Devani, C. J. Shishoo and M. G. Shah, *Analyst (London)*, 98 (1973) 759.
12 E. E. Reid, *Organic chemistry of bivalent sulfur, Vol. 5*, Chemical Publishing Co., New York, (1963), pp. 23–24.
13 B. C. Verma and S. Kumar, *Analyst (London)*, 98 (1973) 900.
14 J. A. Vinson, *Anal. Chem.*, 41 (1969) 1661.

Analytica Chimica Acta, 78 (1975) 498–500

SHORT COMMUNICATION

The determination of iodide by its inhibitory effect on the reduction of phenosafranine by EDTA

F. SIERRA, C. SANCHEZ-PEDREÑO, T. PEREZ, C. MARTINEZ and M. HERNANDEZ
Department of Analytical Chemistry, Faculty of Science, University of Murcia, Murcia (Spain)
(Received 24th January 1974)

A kinetic study of the photochemical reaction between phenosafranine (3,7-diamino-5-phenylphenazinium chloride) and EDTA has already been described[1]. It was found that the reaction is strongly inhibited by the presence of iodide, even in very small amounts. In this communication, a new method is described for the determination of iodide traces based on this inhibitory effect. Iodide retards the rate of photochemical bleaching of the dye by EDTA, and the kinetic procedure is easily carried out by measuring the time necessary for the sample to reach a predetermined absorbance value. The method permits the determination of iodide in ranges extending from 0.2 p.p.m. to 15 p.p.m.

As indicated previously[1], the photochemical oxidation of EDTA by phenosafranine is the result of a complicated mechanism similar to that suggested by earlier workers for the photooxidation of polyaminopolycarboxylic acids by thiazine dyes. The iodide ion deactivates the excited dye molecules which are involved in the photochemical reaction.

Experimental

Reagents and apparatus. These were the same as described previously[1].

Procedure. To the reaction cell of the photometric titration unit, add 1 ml of $2 \cdot 10^{-4}$ *M* phenosafranine, 2 ml of 0.1 *M* EDTA, 2 ml of acetate pH 5.5 buffer (for samples with a very low amount of iodide, use pH 4.6 buffer) and different volumes of standard potassium iodide solution (10^{-3} or 10^{-4} *M*); the final concentration of iodide should be between 0.2 and 15 p.p.m. Dilute with distilled water to 25 ml. Remove oxygen from the solution by bubbling pure nitrogen (99.997%) through it for 20 min. Then, switch on the halogen lamp of the illumination device[1] and measure the time needed for the absorbance to be reduced to 1/10th of its initial value.

Calibration graphs are constructed by plotting the iodide concentration (in the ranges 1.5–15 and 0.2–1.5 p.p.m.) against t_x/t_0, where t_x is the time required for the photoreduction of the samples, and t_0 the time required by an iodide-free sample. Appropiate illumination must be chosen in order to obtain a value of t_0 in the 150–200-s range. A typical calibration graph is shown in Fig. 1. The slope of the calibration graph for 0–15 p.p.m. of iodide at pH 5.5 for illumination of 18000 lux is similar.

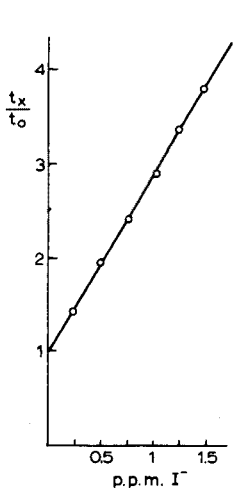

Fig. 1. Calibration graph for iodide in a medium buffered at pH 4.6. Illumination 11000 lux.

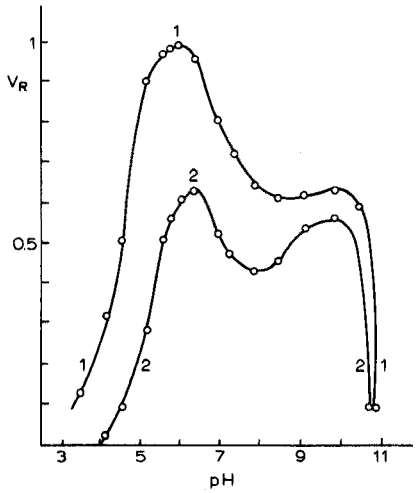

Fig. 2. Rate of photoreduction as a function of pH. 1, Without iodide. 2, In the presence of 5 p.p.m. of iodide. (Expressed in relation to the maximum value.)

Iodide in unknown samples, is determined in the same way. In order to obtain exact and reproducible results, the reagent concentrations and the light intensity must be kept constant throughout the series of measurements, and calibration graphs should be established frequently.

Results and discussion

For a fixed concentration of iodide, the time necessary for the photoreduction of phenosafranine depends on the light intensity, the pH and the concentrations of dye and polyaminopolycarboxylic acid present.

Influence of pH. The photoreduction reaction rates of phenosafranine with EDTA, both in the presence and absence of iodide, are strongly dependent on the pH of the medium. The relative rates of the two processes at different pH values from 3.5 to 11 are shown in Fig. 2; curve 1 corresponds to a series of samples which contained 10^{-5} *M* phenosafranine and $4 \cdot 10^{-3}$ *M* EDTA without iodide whereas curve 2 refers to similar samples which also contained $4 \cdot 10^{-5}$ *M* iodide. On the basis of these results, a pH value between 4.5 and 6 was chosen for this work; in this range the effect of iodide on the photochemical reaction rate is considerable, but the times for bleaching are still not very long.

Influence of EDTA concentration. The time required for bleaching decreases with increasing EDTA concentrations. For samples containing $3 \cdot 10^{-5}$ *M* phenosafranine and $4 \cdot 10^{-6}$ *M* iodide at pH 5.5, the time for bleaching decreased rapidly when $3 \cdot 10^{-4}$–$5 \cdot 10^{-3}$ *M* EDTA was added, but then remained constant for the range $7.5 \cdot 10^{-3}$–$3 \cdot 10^{-2}$ *M* EDTA; increased concentrations of EDTA above 10^{-2} *M* had virtually no effect on the time. In the proposed method $8 \cdot 10^{-3}$ *M* solutions of EDTA are recommended.

Interferences. Chloride and bromide do not interfere up to concentrations

of 1000 p.p.m. For metal ions that form stable complexes with EDTA, a suitable excess of EDTA must be added to form the chelates. Obviously substances which may be reduced by the leuco form of phenosafranine also interfere.

Sensitivity and reproducibility. In the absence of interfering ions, the reproducibility of the recommended procedure is very good. For 5 determinations of 0.175 mg of iodide, the average deviation from the mean was 1.5% and the maximum deviation was 3%.

The limit of determination of the method is 0.2 μg ml^{-1}. For smaller amounts of iodide, the differences in the bleaching times between the blank and sample solutions becomes so small that errors become excessive. For more than 20 p.p.m. of iodide, reaction times are prolonged, and dilution is recommended.

REFERENCE

1 F. Sierra, C. Sánchez-Pedreño, T. Pérez, C. Martínez and M. Hernandez, *Anal. Chim. Acta*, 78 (1975) 277.

Analytica Chimica Acta, 78 (1975) 501–506

SHORT COMMUNICATION

N-Nitrosodiphenylamine as a reversible high-potential redox indicator in titrations with cerium(IV)

G. GOPALA RAO, MURALIKRISHNA GANDIKOTA and S. G. VISWANATH
Department of Chemistry, Andhra University, Waltair (India)
(Received 22nd December 1974)

During a survey of the diphenylamine derivatives available as indicators of high redox potential, Gandikota and Rao[1] found that 2-nitrodiphenylamine is useful for the titration of iron(II) with cerium(IV) sulphate, potassium dichromate, and sodium vanadate, having a formal transition potential of 1.09 V in 0.5–2 *M* sulphuric acid, and properties superior to ferroin in some respects. Further work has shown that N-nitrosodiphenylamine is another useful indicator of high redox potential. N-nitrosodiphenylamine is easily prepared in 95% yield by the action of nitrous acid on diphenylamine in mineral acid solution; it is manufactured in large tonnages for industrial use, and is therefore available at an economic price.

Investigations into the use of N-nitrosodiphenylamine as a reversible redox indicator for titrations of iron(II), hydroquinone, arsenic(III) and antimony(III) with cerium(IV) solution are described below. Iron(II) can be titrated in 0.5–1.5 *N* sulphuric, hydrochloric, and perchloric acids without the addition of phosphoric acid. N-nitrosodiphenylamine is a much better indicator than ferroin in the titration of arsenic(III) and antimony(III); at the concentration employed, it has a pale yellow colour, and the product of oxidation with cerium(IV) sulphate is a vivid violet, which is stable for longer than 2 h in sulphuric acid media. An advantage over diphenylamine is that arsenic(III) and antimony(III) can be titrated in hydrochloric acid media.

Experimental

Indicator solution. A solution (0.01 *M*) of N-nitrosodiphenylamine (Fluka, Pract.) in glacial acetic acid is stable for 10 weeks when stored in a cupboard; 0.2 ml is adequate for 50 ml of titration mixture. The absorption spectra of the indicator and its oxidized form obtained with a Spekol single-beam spectrophotometer fitted with a grating monochromator are shown in Fig. 1. The disproportionation of the violet oxidation product of N-nitrosodiphenylamine proceeds at a slower rate than oxidized diphenylamine. In 2.5 *M* sulphuric acid, it is sufficiently stable for the absorption spectrum to be measured. The molar absorptivity is 35000 l mol^{-1} cm^{-1}, and this shows a decrease of *ca.* 6% in 1 h.

Reagents. Prepare a solution (0.05 *M*) of cerium(IV) sulphate in 0.5 *M* sulphuric acid from cerium(IV) oxide obtained by heating cerium(III) carbonate

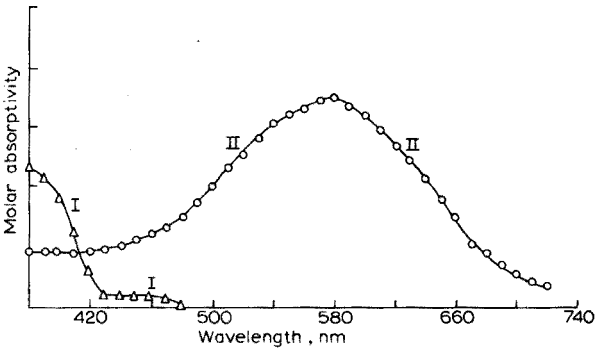

Fig. 1. Absorption spectra of N-nitrosodiphenylamine(I) and its oxidized form (II). Each division on the vertical axis represents 50 l mole^{-1} cm^{-1} for I, and 5000 l mole^{-1} cm^{-1} for II.

and standardize against A.R. grade sodium oxalate[2,3] with ferroin as indicator, or with A.R. grade arsenic trioxide with diphenylamine as indicator[4]. Prepare solutions (0.05 *M*) of arsenic(III), hydroquinone, and iron(II) from A.R. grade products and check against the standard cerium(IV) sulphate. Keep the iron(II) and hydroquinone solutions at an overall acidity of 0.5 *M* sulphuric acid, and the arsenic(III) solution at 0.15 *M* in sulphuric acid. Prepare a solution (0.05 *M*) of antimony(III), in 2.5 *M* hydrochloric acid, from pure antimony trichloride and standardize against potassium bromate. Prepare a catalyst solution by adding 20.8 ml of 0.1 *M* potassium iodide and 4.16 ml of 0.1 *M* potassium iodate to a 250-ml volumetric flask and dilute to the mark; 1 ml is sufficient for arsenic(III) titrations, but 2 ml is required for antimony(III) solutions.

Results and discussion

Titration of iron(II) with cerium(IV) sulphate. N-Nitrosodiphenylamine is recommended for the titration of iron(II) in 0.25-0.8 *M* sulphuric acid. The slightest excess of cerium(IV) sulphate over that corresponding to the equivalence point gives an easily discernible colour; the addition of 0.01 ml of the oxidant in excess

TABLE I

TITRATION OF IRON(II) WITH CERIUM(IV) SULPHATE

Iron(II) taken (meq)	*Iron(II) found (meq)*		
	0.5 M H_2SO_4	*1 M HCl*	*1 M $HClO_4$*
0.1826	0.1823	—	0.1824
0.2283	0.2280	—	—
0.2654	—	0.2650	0.2653
0.2740	0.2736	—	0.2741
0.3096	—	0.3095	—
0.3538	—	0.3535	—
0.3566	0.3562	—	0.3567
0.3877	0.3875	0.3879	—
0.4104	0.4108	0.4100	0.4106

gives an intense violet colour. In titrations of iron(II) in hydrochloric acid media, the colour of iron(III) chloride does not interfere with the end-point; during the titration, the violet colour of the oxidized indicator appears and disappears intermittently, and after the end-point, the colour transition can be reversed many times. With ferroin, an orange red colour persists almost to the end-point, and warning of its approach is not so clear as with the new indicator. Moreover, the violet colour of oxidized N-nitrosodiphenylamine is stable for *ca.* 2 h; the pale blue colour of ferriin reverts in 20 min to the orange red colour of ferroin. The results in Table I show that satisfactory recoveries were obtained in sulphuric, hydrochloric and perchloric acid media.

Acetic acid (5.0 *M*), phosphoric acid (0.6 *M*), nitric acid (1.0 *M*), vanadium(IV) (0.06 *M*), manganese(II) (0.06 *M*), copper(II) (0.002 *M*), and arsenic(III) (0.0025 *M*) did not interfere. Tungstic acid (0.0005 *M*) did not interfere, but the oxidized indicator changed colour with increasing tungstic acid concentrations until at 0.0001–0.0002 *M* the colour was greenish-blue instead of violet although the solution remained clear. Titrations in 2 *M* acid media gave premature end-points.

According to Rao *et al.*[5], oxalic acid interferes in the titration of iron(II) with cerium(IV) sulphate, when N-phenylanthranilic acid is used as indicator. With N-nitrosodiphenylamine the interference is much less. The results obtained with various indicators are shown in Table II.

TABLE II

COMPARISONS OF DIFFERENT INDICATORS

(Solutions contained 5 ml of 0.05 *M* iron(II), 5 ml of 5 *M* sulphuric acid, *x* ml of 0.05 *N* oxalic acid and 0.2 ml of 0.01 *M* indicator solution in a final volume of 50 ml.)

Vol. of oxalic acid (ml)	*Excess cerium(IV) sulphate, consumed (ml)*			
	Ferroin	*NPA*[a]	*DAS*[b]	*NDA*[c]
1.0	0.02	0.02	Nil	Nil
2.0	0.06	—	0.03	Nil
3.0	0.10	0.10	0.08	0.05

[a]N-Phenylanthranilic acid.
[b]Diphenylamine sulphonic acid
[c] N-Nitrosodiphenylamine.

In the presence of oxalic acid, the oxidized indicator colour changes to that of the reduced form after a period of 1 h; this behaviour is more marked with ferroin, N-phenylanthranilic acid and diphenylamine sulphonic acid. Apart from direct reaction between oxalic acid and cerium(IV), as assumed by Csanyi and Szoke[6], it appears that its interference is associated with reduction of the oxidized indicator.

Titration of hydroquinone with cerium(IV) sulphate. Furman and Wallace[7] showed that the reaction of hydroquinone with cerium(IV) is stoichiometric; they used potentiometric end-points and diphenylamine as a reversible indicator.

Kolthoff and Lee[8] proposed the use of ferroin. N-Nitrosodiphenylamine is an excellent indicator for this titration in 1–2 *N* sulphuric or hydrochloric acid (Table III). In 3–4 *N* acid media, premature end-points were obtained, the apparent titre being 0.03 ml low in 3 *N* acid and 0.12 ml low in 4 *N* acid. A similar effect was noticed with diphenylamine. This undoubtedly arises from the slow rate of reduction of the oxidized indicator by hydroquinone at high acidities; the redox potential of Q/H_2Q increases with increasing hydrogen ion concentration. The indicator correction with N-nitrosodiphenylamine is negligible, as with ferroin, in titrations with 0.05 *M* cerium(IV). With diphenylamine, a correction of 0.05 ml was proposed[7]. N-Nitrosodiphenylamine has two advantages over ferroin; the alternate appearance and disappearance of the violet colour during the titration gives warning of the approach of the end-point, and the colour of the oxidized N-nitrosodiphenylamine is stable for 8 min (stability of ferriin *ca.* 1 min). When N-phenylanthranilic acid was used, accurate titrations were possible in 1 *N* sulphuric acid, but the red colour of the oxidized indicator faded considerably within 1 min and entirely disappeared after 3 min; in 2 *N* sulphuric acid medium, the titration was unsatisfactory, the red colour being completely discharged in 20 s.

TABLE III

TITRATION OF HYDROQUINONE WITH CERIUM(IV) SULPHATE AND WITH N-NITROSODIPHENYLAMINE AS INDICATOR

Hydroquinone taken (meq)	*Hydroquinone found (meq)*	
	1 N H_2SO_4	*1 N HCl*
0.2489	0.2486	—
0.2987	0.2982	—
0.3485	0.3482	0.3483
0.3958	—	0.3954
0.4453	—	0.4448
0.4480	0.4473	0.4476

Barium diphenylamine sulphonate has been used as a reversible indicator for titrations of hydroquinone with cerium(IV) sulphate in sulphuric acid media[9], but requires an indicator correction of 0.02 ml of 0.1 *M* cerium(IV) sulphate; a green colour appears 1 ml before the true end-point and this changes through greenish-yellow to red-brown, which finally leads to a turbid greenish-yellow within 3 min. Under the conditions used, pure quinone has a light yellow colour.

Titration of antimony(III) with cerium(IV) sulphate. Although Willard and Young[10] proposed the titration of antimony(III) in hydrochloric acid solution at 50°C, using ferroin as indicator, Pribil[11] reported difficulties, and titration to an iodine monochloride end-point was also unsatisfactory[12]. In contrast, titrations with N-nitrosodiphenylamine as indicator in 1–2 *N* sulphuric acid containing 1 ml of the iodine catalyst are simple and accurate to within 0.2%. The colour change at the end-point is from light yellow to violet. If the indicator is added at the beginning of titrations of antimony(III) in 1 *N* hydrochloric acid, the colour change at the end-point is from pale yellow to light orange-red, and an indicator correction

of 0.02 ml of 0.05 *M* cerium(IV) solution is required. However, if the indicator is added *ca.* 1 ml before the end-point results are accurate, and the colour change is from pale yellow to violet. In 2 *N* hydrochloric acid, 2 ml of iodine catalyst solution are required. Results are shown in Table IV.

TABLE IV

TITRATION OF ARSENIC(III) AND ANTIMONY(III) WITH CERIUM(IV) SULPHATE WITH N-NITROSODIPHENYLAMINE AS INDICATOR

Arsenic(III) (meq)		*Antimony(III) (meq)*		*Arsenic(III) (meq)*		*Antimony(III) (meq)*	
Taken	*Found*	*Taken*	*Found*	*Taken*	*Found*	*Taken*	*Found*
In 1 NH_2SO_4				*In 1 N HCl*			
0.2500	0.2499	0.2380	0.2380	0.2500	0.2499	0.2380	0.2383
0.3000	0.2990	0.2856	0.2844	0.3000	0.3000	0.2856	0.2854
0.3500	0.3495	0.3332	0.3328	0.3500	0.3493	0.3332	0.3328
0.4000	0.3994	0.3808	0.3798	0.4000	0.3994	0.3808	0.3802
0.4500	0.4487			0.4500	0.4490		

TABLE V

DIFFERENTIAL TITRATION OF IRON(II) AND ARSENIC(III)

Amount of iron(II) (meq)		*Amount of arsenic(III) (meq)*	
Taken	*Found*	*Taken*	*Found*
0.2341	0.2336	0.2000	0.1996
0.2809	0.2809	0.2500	0.2494
0.3745	0.3738	0.4000	0.4000
0.4194	0.4192	0.4500	0.4598

TABLE VI

TRANSITION POTENTIALS OF N-NITROSODIPHENYLAMINE

H_2SO_4	*Titrand*	*Transition potentials (E) (V vs. NHE)*	H_2SO_4	*Titrand*	*Transition potentials (E) (V vs. NHE)*
0.5	Iron(II)	0.93	1.0	Antimony(III)	0.83
1.0	Iron(II)	0.94	2.0	Antimony(III)	0.84
2.0	Iron(II)	0.93	1.0	Arsenic(III)	0.85
1.0	Hydroquinone	0.87	2.0	Arsenic(III)	0.85
2.0	Hydroquinone	0.86			

Titrations of arsenic(III) with cerium(IV) sulphate. In 1–2 *N* sulphuric or hydrochloric acid media, using N-nitrosodiphenylamine as indicator, titrations of arsenic(III) (Table IV) provided the same observations as those of antimony(III).

Differential titration of iron(II) and arsenic(III) with cerium(IV) sulphate.

Iron(II) and arsenic(III) can be titrated consecutively in 1 *N* sulphuric acid. After the iron(II) end-point, 1 ml of the catalyst mixture is added and the titration completed. The volume of cerium(IV) added between the first and the second end-points corresponds to arsenic(III). Table V gives typical results.

Transition potentials of N-nitrosodiphenylamine. Transition potentials in the various redox systems, determined by the method of Knop[13], are recorded in Table VI. Cerium(IV) sulphate was used as titrant. These transition potentials, which are subject to an error of ± 0.01 V, change with change of titrand. The transition potential of diphenylamine (Fe(III)/Fe(II) system) therefore changes from 0.76 V to 0.93 V upon introduction of the N-nitroso group, and the colour of the oxidized indicator changes from blue-violet (diphenylamine) to a more stable violet colour (N-nitrosodiphenylamine).

REFERENCES

1 Muralikrishna Gandikota and G. Gopala Rao, *Anal. Chim. Acta*, 72 (1974) 163.
2 H. H. Willard and P. Young, *J. Amer. Chem. Soc.*, 50 (1928) 1322.
3 V. Panduranga Rao and G. Gopala Rao, *Talanta*, 2 (1959) 370.
4 Muralikrishna Gandikota and G. Gopala Rao, *Anal. Chim. Acta*, 65 (1973) 231.
5 G. Gopala Rao, P. Jagan Mohan and M. N. Sastri, *Z. Anal. Chem.*, 156 (1957) 336.
6 L. J. Csanyi and F. Szoke, *Z. Anal. Chem.*, 175 (1960) 187.
7 N. H. Furman and J. H. Wallace, *J. Amer. Chem. Soc.*, 52 (1930) 1443.
8 I. M. Kolthoff and T. S. Lee, *Ind. Eng. Chem., Anal. Ed.*, 18 (1946) 452.
9 I. M. Kolthoff and R. Belcher, *Volumetric Analysis, Vol. III*, Interscience, New York, 1957, p. 165.
10 H. H. Willard and P. Young, *J. Amer. Chem. Soc.*, 55 (1933) 3268.
11 R. Pribil, *Chem. Listy*, 39 (1945) 19.
12 E. W. Hamock, R. A. Brown and E. H. Swift, *Anal. Chem.*, 20 (1948) 1048.
13 J. Knop, *Z. Anal. Chem.*, 85 (1931) 253.

Analytica Chimica Acta, 78 (1975) 507–512

SHORT COMMUNICATION

A simplified automated curcumin method for the determination of boron in sea water

GÖRAN ÖSTLING

Department of Analytical Chemistry, University of Gothenburg, Fack, S-402 20 Göteborg 5 (Sweden)

(Received 27th February 1975)

Automated procedures for the determination of boron in aqueous solutions based on different chromophoric reagents have been developed by several authors (Table I). The modified curcumin method described by Uppström[1,2] has been shown to give reliable results and was later automated with Autolab equipment[11]. Since there is a demand for still shorter response times, a study of the method was undertaken to increase the reaction rate and reduce the sample processing. A less complex apparatus was desired since it would probably give a smaller standard deviation and be more reliable. These objectives were achieved by combining some of the reagents and further optimizing the procedure for automatic analysis.

LE I

OMATED PROCEDURES FOR THE DETERMINATION OF BORON IN AQUEOUS JTIONS

le	*Reagent*	*Range*	*Standard deviation*	*Sampling rate per h*	*Ref.*
r (nuclear reactor liquid)	Carminic acid	0.1–16 p.p.m.	0.2 p.p.m.	—	1
r (heavy water reactor)	Chromotropic acid	0.1–10 p.p.m.	0.1 p.p.m.	—	2
ous solution	Phthalein violet	—	—		3
tissue	Azomethine H	~10 p.p.m.		40	4, 5
lved steel samples	Carminic acid	0.001–0.010% B in steel	0.00025% B in steel	20	6
lved steel samples	Carminic acid	~20 p.p.m. B in steel	0.00014% at 0.0003% B in solution	30	7
ous solution	Chromotropic acid	~5 p.p.m.	—		8
ge and river water	Carminic acid	0.05–3 p.p.m.	1% at 3 p.p.m.	10	9
al and sewage water	CHMB (fluorescence)	5–100 $\mu g\ l^{-1}$		10	10
ater	Curcumin	0.1–6 p.p.m.	0.045 p.p.m. at 3 p.p.m.	240	11
ater	Curcumin	0.1–6 p.p.m.	0.025 p.p.m.	240	Present method

Main reaction steps

Quantitative ester formation between curcumin and boric acid requires a

strongly acidic and nearly water-free solution. In the previously automated procedure[11], this was achieved by first removing the excess of water with propionic acid anhydride and then adding a mixture of sulphuric and acetic acids. The water-eliminating step involving propionic anhydride is very slow, but can be catalyzed by hydrochloric acid, which is generated, with carbon monoxide and dioxide, by the reaction of oxalyl chloride with water. Finally, a buffer is added to destroy the interfering proton complex of curcumin and the absorbances of the samples are measured at 540 nm. A flow scheme for this method is shown in Fig. 1.

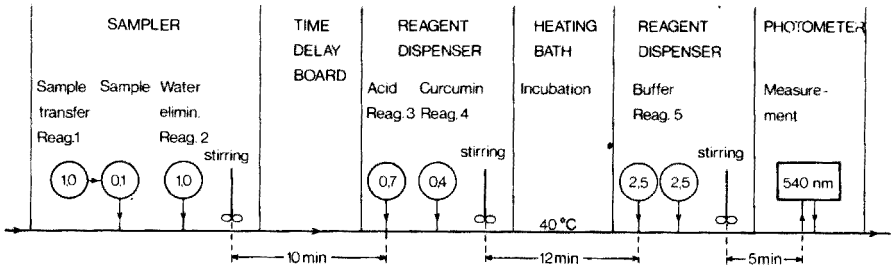

Fig. 1. Autolab flow scheme for the determination of boron according to Hulthe *et al.*[11].

Crawley[13], who introduced the chemical water-elimination step in the curcumin method, used acetic acid anhydride and hydrochloric acid as catalyst; he observed that the heat formed in the reaction decomposed the boron–curcumin complex and therefore performed the analysis in three steps: first the water elimination, second the complex formation and third the pH adjustment. This procedure was also followed by Uppström[12], who used propionic acid anhydride and oxalyl chloride in order to obtain a more easily controlled reaction.

When the Uppström reagents are used, there is, however, no marked breakdown of the boron–curcumin complex during elimination of water. It is thus possible to dissolve the curcumin in the propionic acid anhydride and the oxalyl chloride in the sulphuric–acetic acid mixture.

Experimental

Apparatus. The automatic equipment used here is an Autolab System (Linson Instrument AB, Stockholm, Sweden). The system is a single-channel, discrete type

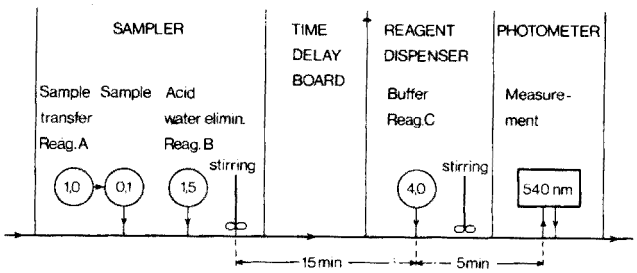

Fig. 2. Autolab flow scheme for the reported technique.

and has previously been described by several workers[14–17]. The precision of the various components and the carry-over and cross-contamination effects in the system have been studied[18]. Briefly, the apparatus processes the samples in open sample tubes, the different reagents are added by syringes, mixing is achieved by rotating teflon rods and the analysing module is a filter photometer with digital read-out and printer. A photograph of the system together with a brief description has been given previously[11]. Figure 2 shows the apparatus setup in the new version.

Reagent A. To 500 ml of propionic acid anhydride (97%, BDH Chemicals) add 10 g of carefully dried ammonium acetate (in a vacuum desiccator) and 250 ml of anhydrous acetic acid. When all the ammonium acetate has dissolved, add 750 mg of curcumin (BDH Chemicals). This reagent is stable for approximately three weeks.

Reagent B. To 750 ml of anhydrous acetic acid add 250 ml of concentrated sulphuric acid portionwise while cooling, in an open flask. Add 10 ml of oxalyl chloride (zur Synthese, Merck–Schuchardt) in 0.5-ml aliquots; between additions allow the reaction to pass its maximum. Then stopper the flask lightly so that the gases formed may escape. Allow the reagent to stand in a hood overnight. Gently swirl the bottle until no more bubbles are formed.

Reagent C (buffer solution). Mix 90 ml of ethanol (96%), 180 g of ammonium acetate and 135 ml of anhydrous acetic acid, and make up to 1 l with water.

Unless stated otherwise all chemicals were of analytical grade from Merck, Darmstadt.

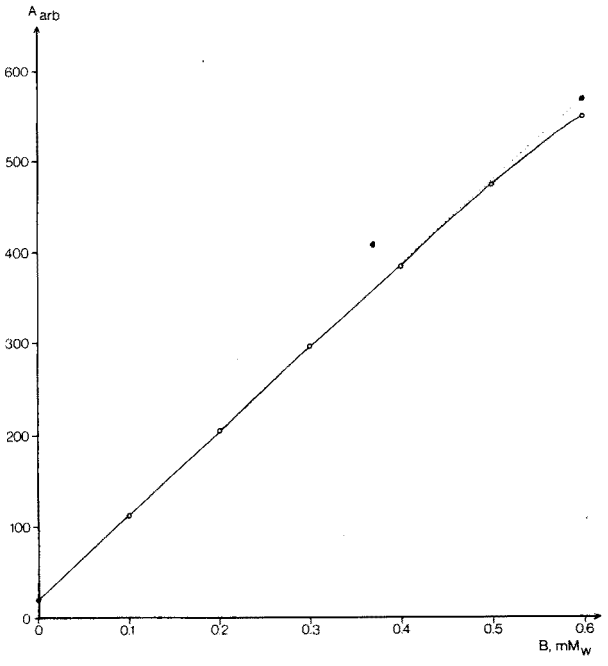

Fig. 3. Calibration curve: (—○—) original curve; (---○---) after transformation.

Results

Calibration and precision. Figure 3 shows a calibration curve for the expected concentration range in sea water and brackish water. Table II shows the run from which this curve was obtained. The response was linear up to about 0.4 mM_w boron and for higher concentrations somewhat repressed. Analysis by straight-line regression calculation showed a standard deviation of 1.8% (0.005 mM_w B) for a solution containing 0.3 mmole boron per kg of water (mM_w). When the various solutions were treated as seven separate groups, the standard deviation for the same solution became 0.5% (0.0015 mM_w B). Thirty replicate determinations on the 0.3 mM_w boron solution gave a standard deviation of 0.4%. A BASIC program, transforming the measured absorbances of the calibration curve to a best straight-line fit gave the equation $A = 916.3[B] + 20.5$, where $A = A_{arb} + 10^{-16} A_{arb}{}^{6.3}$; the standard deviation was 0.6% for the 0.3 mM_w boron solution.

The carry-over was evaluated from this and other calibration curves to be 4. (1)%.

Interferences. Of the reported interfering substances fluoride and nitrate are of interest when natural waters are analysed.

TABLE II

PRINTED RESULTS OF A CALIBRATION RUN WITH THE MODIFIED AUTOLAB SETUP

(Values corrected for carry-over are asterisked. Computed values are written parenthesis to the right of the original analysis. Samples 37 and 38 were not used in the calculations.)

[B] mM_w	Sample no.	A_{arb}	Mean A_{arb}	[B] mM_w	Sample no.	A_{arb}	Mean A_{arb}
0	1	20		0.4	22	*379 (383)	
0	2	20		0.4	23	382	
0	3	19		0.4	24	385	384
0	4	20	20	0.4	25	387	
0	5	19		0.4	26	384	
0	6	19					
0.1	7	*109 (113)		0.5	27	*469 (473)	
0.1	8	111		0.5	28	474	
0.1	9	112	112	0.5	29	473	473
0.1	10	113		0.5	30	472	
0.1	11	113		0.5	31	471	
0.2	12	*202 (206)		0.6	32	*549 (552)	
0.2	13	203		0.6	33	551	
0.2	14	204	205	0.6	34	550	551
0.2	15	205		0.6	35	550	
0.2	16	206		0.6	36	551	
0.3	17	*292 (296)		0	37	(42)	
0.3	18	294		0	38	(23)	
0.3	19	294	296	0	39	21	
0.3	20	297		0	40	19	
0.3	21	298		0	41	19	

A 0.3 mM boron solution gave an absorption of 0.15 when measured against a solution with the same boron concentration which was 0.5 mM in fluoride. For a normal fluoride concentration in sea water of $7 \cdot 10^{-5}$ M, the negative error in a boron determination would be negligible.

Nitrate gave a positive error: a potassium nitrate solution (140 mg N l^{-1}) gave an absorption of 0.19. A NO_3–N concentration of 500 μg l^{-1} would correspond to an error slightly lower than the standard deviation for the boron analysis.

Analysis of boron samples in 0,10, 20, 30 and 40% synthetic sea water, prepared as reported by Hansson[19], gave identical results, hence there is no salt error.

Discussion

The apparatus setup requires only one reagent dispenser and four syringes in this new version. The original heating bath could be replaced by a time-delay board and the system as a whole became more compact, cheaper and more easily inspected and manoeuvred.

The heat released from the water-eliminating reaction in this version seems to favour the complex formation (Fig. 4). The reaction between boron and curcumin is essentially complete within 5 min and stops at a molar absorptivity of $1.6\,(1) \cdot 10^5$, a value about 10% lower than that reported by Spicer and Strickland[20].

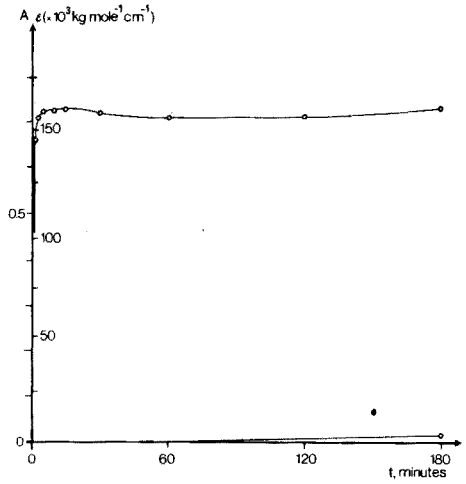

Fig. 4. The absorbance of a 0.3 mM boron sample as a function of time to the buffer addition.

A slow coloration of boron-free samples can be noticed during the time that the samples are in the strongly acidic solution. However, this coloration also affects the similarly treated calibration solutions and is therefore compensated for, provided that the buffer (reagent C) is added after the same time interval to all solutions.

The processed sample solution has, after the buffer addition, the same properties as these reported by Uppström[12], who described an extraction procedure for enrichment of the coloured complex which also could be applied here.

Manual procedure

A manual method can be directly derived from the described automated

procedure: a 0.5-ml sample is mixed thoroughly with 5 ml of reagent A, 7.5 ml of reagent B is added and the solution mixed again. After 20 min, 20 ml of reagent C is added, and the absorbance can then be measured within 24 h. For high precision work, reagent B should be added along the tube wall, and reagent C added after the same time interval to all samples.

When the boron concentration range is considerably lower, say less than 0.1 m*M*, a scaling up of the sample and reagents and an extraction as described by Uppström[12] are recommended. Thereby an increase in sensitivity by a factor of about 300 may be obtained.

REFERENCES

1 T. F. Demmit, *Automation in Analytical Chemistry, Technicon Symp., 1965*, Mediad, New York, 1966, p. 204.
2 H. James and G. H. King, *Automation in Analytical Chemistry, Technicon Symp., 1966*, Mediad, New York, 1967, p. 123.
3 W. D. Fletcher, *Nucl. Sci. Abs.*, 22 (*10*) (1968) 20825.
4 W. D. Basson, R. G. Böhmer and D. A. Stanton, *Analyst (London)*, 94 (1969) 1135.
5 W. D. Basson, P. P. Pille and A. L. Du Preez, *Analyst (London)*, 99 (1974) 168.
6 R. R. Willis, *Res. Rep. Br. Steel Corp., GS/RO/TECH/78/1/71/C.*
7 G. H. King and R. Wood, *Colloquium on the Application of the AutoAnalyzer for Metallurgical and Water Analysis, Bloomsbury Centre, April 1970.*
8 R. Di Pietro, C. Ronchetti, P. Pagano and L. Picconi, *Technicon Italy, Symposium April 1971*, p. 197.
9 L. J. Lionnel, *Analyst (London)*, 95 (1970) 194.
10 B. K. Afghan, P. D. Goulden and J. E. Ryan, *Water Res.*, 6 (1972) 1475.
11 P. Hulthe, L. Uppström and G. Östling, *Anal. Chim. Acta*, 51 (1970) 31.
12 L. Uppström, *Anal. Chim. Acta*, 43 (1968) 475.
13 R. H. A. Crawley, *Analyst (London)*, 89 (1964) 749.
14 B. Åberg, *Nord. Med.*, 80 (1968) 1284.
15 L. Uppström, *Modern Kemi*, 11 (1970) 34.
16 H. Oldenziel, *Medizinal-Markt/Acta Medicotechnica No 7*, 1973, p. 230.
17 F. Esser, A. Jahn and C. Beck, *Medizinal-Markt/Acta Medicotechnica No. 1*, 1971, p. 6; *No 2*, 1971, p. 36.
18 G. Östling, *Chem. Instr.*, 5 (*1*) (1973–74) 1.
19 I. Hansson, *Acta Chem. Scand.*, 27 (1973) 934.
20 G. S. Spicer and J. D. Strickland, *J. Chem. Soc., London*, (1952) 4650.

Analytica Chimica Acta, 78 (1975) 513–520

BOOK REVIEWS

O. G. Koch and G. A. Koch-Dedic, *Handbuch der Spurenanalyse*, Springer–Verlag, Berlin, Zweite Auflage 1974, xxiv+750 pp. (pt.1), xiii+847 pp. (pt.2), Gebunden, DM 498,— ($191.80).

Trace analysis is such an important part of analysis at the present time, that a comprehensive, critical, authoritative hand-book on the subject is extremely desirable. Yet the proliferation of techniques and matrices, as well as the continually increasing range of species that have to be determined at the trace level, would make such a hand-book very large, and almost beyond the capability of any single author to produce sufficiently quickly for it to be of value to practising analysts. Yet this two-volume book goes a long way to achieving the impossible. It provides a comprehensive, fluent account of the methods of trace analysis that the authors know to be suitable for the determination of most elements in a wide variety of samples. It also includes a far-ranging discussion of the techniques and chemical processes involved.

The book is in two parts. The first (172 pages) deals briefly with principles of trace analysis, scales of working and statistics, and includes concise but well-referenced descriptions of the various techniques used, including comparisons of their effectiveness for each element. This is followed by short descriptions of separation and concentration of trace elements, and of other means of enhancing sensitivity. This section is also extensively referenced, and leads to a more detailed discussion of macro and micro working techniques, including reagent purity and purification, instrumental methods (spectrophotometry, spectrofluorimetry, emission spectrography, x-ray spectrometry, coulometry and polarography). Evidence of hurried preparation in parts of this section is the insertion of "a" and "b" after some reference numbers, whereas other reference numbers are unused, and appear in the lists of references with just a hyphen after the reference number.

The second, and much the larger, part deals first in some detail with pretreatment of samples and with concentration processes, especially solvent extraction systems (199 pages). Then follows an account (1003 pages) of the determination of traces of each element (in alphabetical order of the symbols for each element). Each element is treated in the same way: comparison of sensitivity and determination limits for the various methods; separation procedures; spectrophotometric (and some spectrofluorimetric) procedures; other procedures; references. Full procedures for applications to different types of samples are usually given, but there is an undue emphasis on spectrophotometry at the expense of other techniques, which, with a few exceptions, are restricted to flame and spark emission spectrometry and atomic absorption spectrometry. All elements are not treated. The halides, nitrogen, oxygen, hydrogen, rubidium and caesium are not included. The treatment of the metals and metalloids is better than that of the non-metals. There is relatively little information on the determination of the non-metals as their various simple compounds. Naturally, organic compounds are not discussed.

Also included in the second part is a valuable section on multi-element trace analysis of a wide variety of matrices (79 pages), and a fairly detailed account of the microbiological determination of trace elements (52 pages). Although the latter is an interesting technique, it is out of place in a book on established procedures. The book concludes with various appendices (formula-weights, properties of solvents, absorbance–transmittance conversion, maximum working limits for toxic substances) and author and subject indexes occupying 73 pages.

The two volumes are superbly produced and contain a wealth of information for all who practice, or wish to learn about, trace inorganic analysis. Their extraordinarily high price, however, will almost completely rule out purchase by individuals and will even make institutions think twice before acquiring this useful book.

A. Townshend

The Infrared Spectra of Minerals, edited by V. C. Farmer, Mineralogical Society, London, 1974, x + 539 pp., price £16.00.

This substantial volume is a most useful addition to the literature. The first reaction of the reviewer was one of surprise that vibrational spectroscopy should be of such wide use in the study of apparently rather intractable substances, but the book presents a very good case for the general use of the technique both in routine identification and in detailed mineralogical analyses.

There is a proper concentration on collecting together material which is not readily available elsewhere. In a book which will be used for reference for many years it is a relief to find no attempt to describe the workings of commercial infrared spectrometers. However, there is a detailed description of those techniques of sample handling which have been found to be of particular use with mineral specimens. Three chapters are devoted to brief expositions of the theory of vibrations in crystalline solids and the interaction of radiation with crystals, and a fourth chapter gives an account of the modifications introduced by disorder. Although written by different authors, these four chapters have been well linked together so that they provide a useful introduction to the subject which is certainly adequate for an understanding of the later chapters. A collection of correlation tables from factor group to site group is included as an appendix and the mechanics of handling such tables are explained clearly. No attempt is made to explain group theory in detail but the references given will enable those unfamiliar with this essential equipment to fill in the background for themselves. Although the title only mentions infrared spectroscopy there is also a brief chapter on Raman spectroscopy, and the later chapter on carbonates makes considerable use of this complementary technique; both these chapters suggest a great potential for Raman work, particularly for single crystals.

The larger part of the volume gives compilations and analyses of the infrared spectra of naturally occurring crystalline substances. These make it clear that analytically important information is immediately available from the spectra of minerals which contain units which are vibrationally almost isolated, particularly protons, and anions such as carbonate or sulphate. Also with these units it is easiest

to derive some structural information. However, considerable attention is also given to the spectra of infinitely linked structures, oxides, borates, and in considerable detail, silicates. For these systems the complex spectra are well illustrated and the book becomes very useful as a manual for identification of unknown substances, but also indicates that structural information can sometimes be obtained. The final chapters discuss spectra of cements, ceramics and glasses; for cements, details are given for quantitative analyses by infrared spectroscopy for which precisions of a few percent or better are claimed.

The publishers and printers are to be congratulated on an elegant presentation. Unlike many recent expensive productions this is a book which handles well and lies open on the desk and in which both paper and type are of a pleasing quality. For a specialist work of this size the price, apparently somewhat subsidised, is by no means unreasonable. The book should be in the libraries of all institutions where spectroscopic or mineralogical work is carried out, and in laboratories where mineral specimens are examined routinely it will need to be continuously available. The analyst who meets mineral specimens occasionally will also find this in invaluable work of reference.

D. R. Lloyd

Annual Report on Analytical Atomic Spectroscopy, 1973, Vol. 3, edited by C. Woodward, Society for Analytical Chemistry, London, 1973, x+324 pp., price £6.00.

This third volume continues to provide a timely and valuable account of world-wide developments in analytical atomic spectroscopy. The number of papers discussed has increased to 1698, 50% more than in the previous year, yet the same high standard and speed of publication has been achieved. This series provides an excellent service to analytical chemists, and should be a mandatory companion to all concerned with the subjects discussed.

L. R. Snyder and J. J. Kirkland, *Introduction to Modern Liquid Chromatography*, Wiley, New York, 1974, XV+534 pp., price £9.00.

This is an excellent book which can be recommended to experienced chromatographers and also to students, since interesting introductory information is given in each chapter. By "Modern Liquid Chromatogrphy" the authors mean high-pressure liquid chromatography in all its modes; liquid–liquid, liquid–solid, ion-exchange, and gel chromatography. In addition to chapters on each of these, there are chapters on basic concepts, selecting and developing a chromatographic method, control of separation, equipment, detectors, and columns. There is also a chapter on large-scale separations, contributed by J. J. DiStefano.

This book, based on the American Chemical Society's short course on modern liquid chromatography which Snyder and Kirkland developed and presented to 800 studients over a period of two years, gives the essential background to the subject with a finely balanced blend of essential theory and practical details. The

authors' own background and continuing experience in chromatography make them eminently suitable to write a book such as this. They advise, completely justifiably, that the practical worker must know what he is doing if he is to get the optimum results in modern liquid chromatography; theory and experience, principles and practice must be suitably balanced.

The diagrams and reproductions of chromatograms are excellent, as is the general standard of this book. Unfortunately the main text, in which the direct reproduction of typescript has been used, involves an excessive blackness and thickness of line which makes it the least acceptable example of this type of printing seen so far.

D. M. W. Anderson

Jan Michal, *Inorganic Chromatographic Analysis* (translated by Julian Tyson), Van Nostrand–Reinhold, London, 1974, 218 pages, price $24.95 (£9.00).

Despite the implied comprehensiveness of its title, this translation of the work by Jan Michal published originally in Czech in 1970 is essentially a review devoted largely to the paper chromatographic separation of cations and anions in polar systems with lesser coverage of adsorption and partition methods in thin layer and column chromatography. Within this admitted limited framework the coverage is exhaustive and arranged for ready access in terms of inorganic species and qualitative analysis of minerals, metals, alloys and other inorganic materials.

After introductory chapters on methodology, chemical and physical detection methods and a survey of qualitative analysis systems involving chromatographic modifications of classical schemes, the organization is in terms of individual cation and anion separations and qualitative and quantitative analysis in real systems. An extensive appendix of separations in various solvent systems is included with appropriate R_f values, but only paper chromatographic procedures are included. The style of the book is that of a reference source rather than a descriptive study or critical review. The bulk of the subject matter involves investigations from the 1950s and early 1960s, and there are few references more recent than 1968, so that much of the material is dated.

While thin layer chromatographic applications are reviewed, relatively little space is devoted to metal complex separations or classical adsorption column separations. Since the text predates the development of high-pressure liquid chromatographic methods, the increasing applicability of this technique to inorganic separations is not included. Most importantly, two extensive areas of inorganic chromatography are absent: there are no ion-exchange methods and no mention of the wide use of gas chromatography of metal complexes.

In summary, this must be a book of limited appeal to the analytical chemist. While specialized monographs continue as important features in scientific information exchange, the general value of dated limited reviews of this type must be doubted.

P. C. Uden

G. J. Moody and J. D. R. Thomas, *Practical Electrophoresis*, Merrow, Watford, 1975, vii + 104 pp., price £2.50 ($8.30 overseas).

This paper-back, the fifth volume in the Merrow Technical Library of Practical Science, is a competent, concise review of the basic practical methods and main applications of all the variants of electrophoresis such as immunoelectrophoresis, isoelectric focusing, isotachophoresis, electrophoresis on paper, cellulose acetate, and gels (starch, agar, polyacrylamide). There are 87 pages of text; the rest is taken up by a good subject index, an appendix (9 pp.) giving details of apparatus available commercially, and the presentation of 104 key references, marred by a mis-spelling of Tiselius.

This will serve as a good introduction to the practical aspects for students and others who have not used electrophoretic methods before. There has been no attempt to cover theoretical detail nor to give an up-to-date review for the separation scientist.

W. Klyne and J. Buckingham, *Atlas of Stereochemistry*, Chapman and Hall, London, 1974, pp. xvi + 311, price £15.00.

This is the first extensive compilation of absolute configurations: it covers over 3.000 compounds. These compounds are mainly organic, although organometallics of group 4B are included. A large section is devoted to chiral molecules of low molecular weight and this is followed by sections on natural products—carbohydrates, terpenes and steroids, alkaloids and others. All these sections will be invaluable for natural product and biological chemists. Then follow sections on compounds which owe their chirality to isotopic substitution, chiral axes and planes etc. A final section deals with compounds of nitrogen, phosphorus, sulphur, silicon and organometallics.

All compounds are represented by their stereochemical formulae and are portrayed in a diagrammatic form which shows the evidence on which the presently accepted absolute configuration of a given compound is based. All information is referenced and indexed. As is essential for a work of this kind, stereochemical formulae and the general formåt of the book are first class. It is a fine addition to the list of reference works that a chemical library should contain.

E. J. Forbes

Selective Ion-Sensitive Electrodes, Cardiff, 1973, Edited by G. J. Moody, Butterworths, London, 1974, 80 pp. price £2.30.

This slim volume contains the plenary lectures which were presented at the International Symposium on Selective Ion-Sensitive Electrodes in 1973, and has been reprinted from *Pure and Applied Chemistry*.

The first lecture by R. G. Bates, deals with the development of ionic activity scales. The scale for hydrogen ion activity is now well accepted, but analogous scales

for other ion-selective electrodes are still in process of development, and the problems involved are authoritatively discussed here. In the second lecture, W. Simon describes the use of carrier antibiotics and model compounds in electrodes selective for mono- and di-valent cations. This paper, co-authored by W. E. Morf, D. Ammann and E. Pretsch, is important not only for information on electrodes of the antibiotic type but for the discussion on the vexatious problems of selectivity factors. Precipitate-based electrodes are then discussed by E. Pungor and K. Toth who concentrate on recent applications of electrodes prepared from precipitates in a supporting matrix, single crystals or pressed pellets. Mechanistic aspects of liquid, glass and crystal membrane electrodes are considered by G. A. Rechnitz, who stresses the importance of reconciling mechanistic models and experimental data, and outlines the attempts that have been made to elucidate the mechanisms responsible for selectivity. Finally, J. W. Ross describes potentiometric gas-sensing electrodes, discussing both the theory and development of a range of viable electrodes for ten different gases.

The topics have been well selected to emphasize the areas of growth and problems in this field, and this is a text which no one interested in ion-selective electrodes can afford to miss.

Rolf K. Freier, *Wasseranalyse–Chemische, Physiko–Chemische und Radiochemische Untersuchungenverfahren wichtiger Inhaltstoffe*, 2. Aufl., de Gruyter, Berlin, 1974, S.216, Gebunden DM 65,—.

This new edition of a book which was first published ten years ago, demonstrates the long time that elapses between the development of new, fast, and apparently reliable, techniques of analysis and their application in practical laboratories. Procedures are given here for forty-nine water analyses, but the most advanced instrumentation needed is a spectrophotometer, as it was ten years ago. For each analysis, details are given of the procedure, the principle of the method, the possible interferences, and the reagents needed. There are no frills, no general discussions, and no indication that in many water laboratories many procedures have now been automated, and techniques other than spectrophotometry used.

The principal departure from the first edition is a new section on radiochemical analysis for reactor cooling water, which has been prepared in conjunction with Dr. K. H. Neeb; sixteen simple radiochemical methods are described.

This is a practical handbook, clearly laid out and admirably produced. But one would like to believe that those responsible for our water supplies had a deeper understanding of the frailties of analytical methods than could be gained from this text.

Analysis Instrumentation Vol. 12, Edited by W. V. Dailey, J. F. Coombs, and T. L. Zinn, Instrument Society of America, Pittsburgh, Pa., (distributed by Wiley, New York), 1974, vi + 175 pp., price £7.25.

This unlovely production contains twenty-four of the papers read at the 20th

Annual ISA Analysis Instrumentation Symposium held in Pittsburg in May, 1974; the other thirteen papers read were not submitted within the required deadline. The papers are grouped under the headings: Air quality; Electrochemical and chemical; Sampling and Calibration systems; Combustibles analyzers; Water quality; Physical methods; Liquid chromatography; Analytical computer systems; and Radiation methods.

The contents illustrate well the sorry dichotomy between analytical chemists and the developers of instrumentation for routine environmental and industrial control work. Only in the papers on sampling and calibration is much heed paid to the real meaningfulness of the results produced. An end to this state of affairs will not be helped by Proceedings such as these, a thought which may have occurred also to the authors of the unsubmitted papers. It is a pity that these interesting papers were not released for publication in appropriate journals, for they are unlikely to be widely read in their present format.

J. C. Leclerc and A. Cornu, *Neutron Activation Analysis Tables*, Heyden, London, 1974, 64 pp., price £5.00.

This slim volume contains tabulated data on atomic weights, natural isotopes and their abundances, the origins of radionuclides, radionuclides classified by their half-lives and energies, radionuclide interferences, and saturation sensitivities. The text—in French and English—comprises brief introductory material, and short descriptions of personal research on peak interferences, calculation of weights of standards and saturation sensitivities. Most of the data are taken from reliable published sources, and are collected here in convenient form.

British Steel Corporation, *Methods of Chemical Analysis of Iron and Steel*, Corporate Development Laboratory, British Steel Corporation, Sheffield, S3 7EY, 1974, xi+161 pp., price £4.00 (post free).

This book is an up-dated version of Part I of the 1961 edition of Standard Methods of Analysis of Iron, Steel and Associated Materials. The sixty-seven procedures given for the determination of twenty-eight elements are mainly conventional colorimetric and titrimetric methods, and have of course been thoroughly checked by collaborative testing. Two polarographic methods (for copper and lead) are given. No atomic spectrometric procedures are described, and it is dismaying to learn from the preface that, although these techniques are in use in individual steel laboratories, collaborative testing has not even begun. Other widely accepted instrumental techniques are not mentioned at all.

Fifth Ceramic Chemists Conference on Silicate Analysis, Special Publication No. 86, British Ceramic Research Association, Stoke-on-Trent, England, 1974, vi+158 pp., price £5.00.

This paperback contains the proceedings of a conference held in Llandudno

in May, 1974. It includes papers on wet chemical methods, x-ray fluorescence analysis, atomic absorption spectrometry, electron microscopy, mass spectrometry, surface analysis, and the role of University research. Discussions are also printed in full.

Vacuum Manual, Edited by L. Holland, W. Steckelmacher and J. Yarwood, Spon, London, 1974, x+425 pp., price £10.75.

The proliferation of types of vacuum techniques and equipment makes it difficult for workers—whether in industry or in research—to establish just what is available and most appropriate for their purposes. This manual is designed to provide a ready source of comprehensive information. Part 1 provides basic data on the evolution and permeation of gases from and through different materials, on gas flows in vacuum systems, and on pump fluids and greases. In Part 2, which forms the bulk of the book, detailed information is given on the performance and characteristics of commercially available equipment, listed under vacuum pumps, valves, accessories, instrumentation, process plant and systems. The products of some 180 manufacturers, mainly in America and Western Europe, are listed. Part 3 contains brief superficial descriptions of recent developments in vacuum technology, such as new pump designs, instruments for surface analysis, and ion impact sputtering.

The manual will clearly save much time and energy for anyone responsible for setting up or remodelling vacuum equipment.

Wesley W. Wendlandt, *Handbook of Commercial Scientific Instruments Vol. 2: Thermoanalytical Techniques*, Dekker, New York, 1974, xii+234 pp., price $14.75.

This series is based on the well-founded idea that few research workers or organisations have the time to obtain and scrutinize the literature from all manufacturers of a particular type of instrument, so that they can be sure their final purchase will correspond to their real needs. The first volume dealt with atomic absorption spectrometry, and this second one deals with the instruments for all varieties of thermal analysis which were available in the U.S.A. at the time of writing; naturally these include many European and Japanese products, so that the book is of more than local interest.

Twenty-two manufacturers of thermobalances and differential thermal analyzers are listed. The specifications and vital statistics of the instruments have been taken from the manufacturer's literature, with introductory comments from the author. In most cases, sufficient information is given for calm assessment of what each instrument can and cannot do; there is no sales talk.

A major problem with this series will be in keeping it up-to-date, but anyone who does wish to buy a thermoanalytical instrument within the next two years or so should regard the price of this volume—apparently high for a lithographed typescript—as money well spent.

Analytica Chimica Acta, 78 (1975) 521

ANNOUNCEMENT

Summer School on Interfacial Charges, Fundamental Aspects and Applications

This summer school will be organized from the 1st to the 12th September 1975 near Montpellier (France) under the auspices of the French section of the International Society of Electrochemistry (I.S.E.). Papers will be given and discussions held in French. The number of participants will be limited to 50.

Sessions will be devoted to papers on fundamental aspects: the different modern approaches to the double layer at metallic electrodes and semi-conductors will be treated. This will be followed by extensions to other types of interfaces (membranes, ionic crystal, liquid–liquid and liquid–air). Seminars on experimental methods, and round-table discussions will be held on applied subjects of interest to the participants.

For further information those interested are invited to write to Dr. D. Schuhmann, Physico-Chimie des Interfaces, C.N.R.S., B.P. 5051, 34033 Montpellier cedex, France.

ANALYTICA CHIMICA ACTA, VOL. 78 (1975)

AUTHOR INDEX

ANALYTICA CHIMICA ACTA, VOL. 78 (1975)

SUBJECT INDEX

(Continued from page 4 of cover)

CONTENTS

(Continued on inside page of cover)